The influence of processing on properties of injection-moulded and lomolded components

by

B.A Johnson

Thesis presented in partial fulfilment for the
degree Master of Science
at the University of Stellenbosch

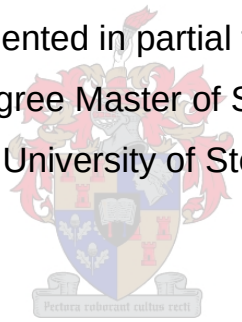

Promotor: Dr A.J. van Reenen

Copromotor: Prof A.H. Basson

April 2006

Declaration

I, the undersigned, hereby declare that the work contained in this thesis is my own original work, and have not previously, in its entirety or in part, submitted it at any university for a degree.

Signature: _____ Date: _____

B.A. Johnson

Abstract

Rectangular components were produced by both standard injection moulding and by a process called Lomolding. Both moulding grade polypropylene homopolymer and glass-filled polypropylene were used. The effect of processing parameters on material properties, as measured by tensile and impact strength, and warpage were determined for both injection moulding and lomolding, for both unfilled and glass-filled polypropylene materials. Sampling of the components allowed for critical evaluation of processing parameters' effect on material properties at points close to and distant from the injection point, as well as in the direction of materials flow and transverse to material flow.

Glass-filled components were also evaluated in terms of glass fibre length and fibre distribution (post-injection). Overall conclusions could be drawn with respect to the 2 different processes and the materials used. It was seen, inter alia, that the specimen orientation had no effect on the mechanical properties when using unfilled polypropylene, but that the orientation of the glass fibres in the testing direction resulted in an increase in the tensile strength and the impact strength for the injection moulded samples. Similar results were seen for lomolded samples, except that the fibre orientation effects were different. In the same vein, other notable differences could be observed for samples produced by lomolding and injection molding. Fibre length and distributions obtained by polymer burn-off experiments served to help explain differences in properties of glass-filled products produced by the two processes.

Uitreksel

Reghoekige komponente is met beide 'n standaard plastiekinspuitgietproses en 'n proses genaamd lomoldering, vervaardig. Beide inspuitgietgraad polipropileen homo-polimeer en glasgevulde polipropileen is gebruik. Die invloed van prosesveranderlikes op die meganiese eienskappe, gemeet in terme van treksterkte, impaksterkte en verwringing, is bepaal vir beide inspuitgiet en lomoldering, vir beide ongevulde en glasgevulde polipropileen materiale. Monsters van die komponente is gekies om 'n kritiese evaluering van die prosesveranderlikes se invloed op die materiaaleienskappe naby en ver van die inspuitpunt, asook in die rigting van die materiaalvloei en loodreg daarop, moontlik te maak.

Glasgevulde komponente is ook beoordeel in terme van die glasvesellengtes en die verselverspreiding (na inspuit). Oorkoepelende gevolgtrekkings is gemaak met betrekking tot die twee prosesse en die materiale wat gebruik is. Dit het onder andere getoon dat, wanneer ongevulde propileen gebruik is, die monsteroriëntering geen invloed op die meganiese eienskappe gehad het nie, maar dat oriëntering van die glasvesels in die toetsrigting gelei het tot toenames in die treksterkte en impaksterkte van die inspuitgiet monsters. Soortgelyke resultate is vir lomolderingsmonsters waargeneem, behalwe dat die invloed van veseloriëntasie anders was. Net so kon ander merkbare verskille tussen monsters wat met insluitgiet en wat met lomoldering gemaak is, waargeneem word. Vesellengte en –verspreidings wat verkry is deur die polimeer weg te brand, het gehelp om die verskille tussen die eienskappe van glasgevulde produkte wat deur die twee prosesse gemaak is, te verduidelik.

Dedication

To my parents

and to my late cousin who died tragically
on 1 January 2006,
his 18th birthday

Acknowledgements

The author would like to thank the following people and companies (in no particular order) who have made a valuable contribution to this thesis (in any way):

- to my Lord Jesus Christ from whom all things are made possible;
- to my parents and brother for their continued support and help in the final stages of the thesis;
- to Lomold for their initial financial support;
- to my promoter (Dr Albert van Reenen) for the guidance and for recommendations made during proof-reading;
- to Prof Anton Basson for his insight, recommendations, proof-reading and guidance during the last four years of the projects' duration;
- to Cobus Zietsman, Ferdi Zietsman and Lukusa Kababula of the Mechanical Engineering Department, Stellenbosch University, for the assistance rendered in the laboratories;
- to George Treurnicht and SMD for the manufacture of jigs and mould components for the machine;
- to Charl Goussard and Christiaan Bowes for their assistance;
- to Piet Bezuidenhout, Philemon Dlongolo and Rishi Madho of Sasol Polymers for their knowledge and willingness to characterise materials;
- to Sonja Oosthuizen at Sasol Polymer Distributors for the words of encouragement and for always being willing to assist with material;
- to Pierre Jurgens and the rest of the staff at Engel SA for the technical assistance when problem-solving was needed on the injection moulder;
- to Anthony Addison, Darryl Tucker and to Plastamid for allowing me the use of their materials testing equipment;
- to Stellenbosch Refrigeration & Air-conditioning for the loan of the prototype humidifier system, as well as a generator during power failures;
- to Barloworld Plascon Laboratories for the use of the optical microscope;
- to Victor Bauer of Flexoline for the machining of the sprue and sprue seat;
- to Dr Johan Fourie from the Cape Technikon for assistance in the interpretation of the results;
- to Teo Laine from Ticona GmbH for the assistance rendered in product literature and numerical codes;

- to Jim Thomason for the assistance with critical fibre lengths and fibre-related issues;
- to Prof Gunter Mennig for his assistance in articles regarding fibre attrition;
- to IMP for the loan of the materials testing software;
- to Advanced Lab Supplies for rheological work done on the components by their principal Anton Paar;
- to TA Instruments for the rheological work done on the raw materials;
- to Nico Laubscher for the guidance while using Statistica, and for the experimental design verifications that were done;
- to all my examiners for their time and valuable comments they passed;
- and last but not least, to all those who prayed for me and were thinking of me during the last few months while writing up this thesis.

Table of Contents

List of Figures

List of Tables

Nomenclature

η_o	fibre orientation factor
σ_{uc}	composite ultimate stress
σ_f	the fibre strength
D	average fibre diameter
L_c	critical fibre length
τ	the interfacial shear strength
σ_R	compressive radial stress
η	fibre effectivity
X	x-axis
Y	y-axis
Z	z-axis
μm	microns
m	gradient of a line
xp	midpoint co-ordinate (x)
yp	midpoint co-ordinate (y)
mp	gradient of line perpendicular to tangent
xc	intersection point of radii (x)
yc	intersection point of radii (y)
R	radius of a circle
Mw	molecular weight
MWD	molecular weight distribution
GMT	glass mat thermoplastics
PP	polypropylene
GFRPP	glass fibre reinforced polypropylene
LFT	long fibre thermoplastics
CMM	co-ordinate measuring machine
DOE	design of experiment

Chapter 1. Introduction

Injection moulding was first used in the early 1900s on metal die casting before being used in the plastics industry in the 1930s. The flow of thermoplastic material from an orifice is suggested in the earlier patents of the Hyatt brothers who processed cellulose nitrate. [1] A number of various machine designs have resulted in more efficient utilization of injection moulding machines designed for mass production methods.

The first commercially successful injection-moulding machine had a plunger at the injection end. [4] The plunger was a round steel bar that pushed the cold material towards the direction of the nozzle that was threaded into one end of a large steel tube. The outside of the nozzle had a radius which fitted into the reverse radius of the sprue bushing of the mould and melt was forced through a small hole (typically between 3 – 9mm) into the cavity.

The first revolution in machine design was separated the two functions of melting and moulding to separate cylinders. The first cylinder was a standard cylinder used for melting and was connected to the second moulding cylinder by means of a valve. The moulding cylinder was charged with molten material, and was injected into the cavity by means of the plunger. This resulted in better mixing of the plastic, a more even temperature distribution and better speed and pressure control.

This type of machine is called a pre-plasticizing machine and represents 95% of equipment in use today, either with a reciprocating screw or a screw-pot as mentioned above. [4] The reciprocating screw was seen to be the second revolution in machine design as the screw was an excellent mixer and was rapidly to make the plunger machine obsolete.

1.1 Injection Moulding

A schematic of a conventional (reciprocating screw) hydraulically-operated injection-moulding machine can be seen in Figure 1.1. The process permits the manufacture of very small parts that are almost impossible to fabricate in quantity by other methods. In 1987 5% of the injection moulding machines in the United States were plunger machines. [4] These were considered the first commercially successful injection-moulding machines.

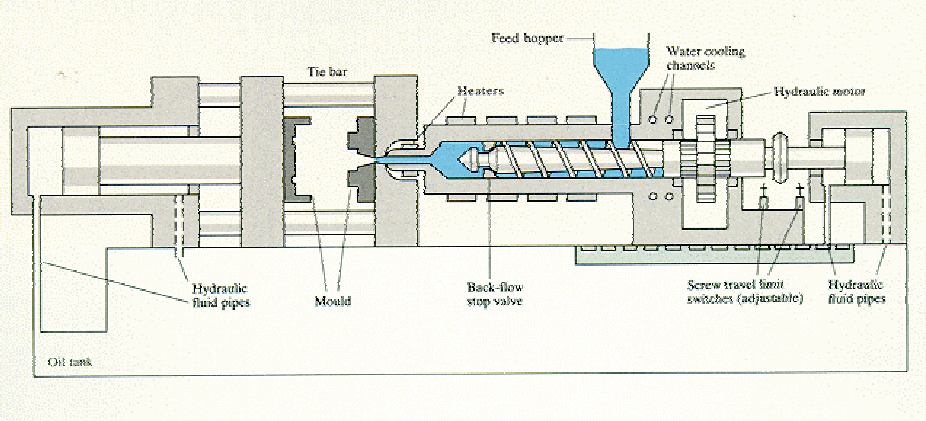

Figure 1.1: Schematic of a hydraulically-operated injection-moulding machine [3]

Thermoplastic materials are fed into a reciprocating injection screw within an electrically-heated barrel and are melted by means of convection as well as by friction generated between the screw and the barrel of the plasticizing unit. The injection screw is driven by either an electric or hydraulic motor, during which time the molten material is moved to the front of the plasticizing unit, thereby creating a backward force on the screw known as the back pressure.

The back pressure exerted on the screw forces the screw backwards to a pre-determined stroke length, allowing molten material to fill the void that was formed in the front of the screw. The injection unit then moves forward until the nozzle comes into contact with the mould applying a contact pressure so as to seal the nozzle to the mould.

Injection of the melt into a cooled mould through a nozzle with a small diameter (around 4 mm) occurs when the injection screw moves forward with a set speed until such a time or point that it reaches the switch-over point at which the forward movement of the screw is governed by the control of pressure and not speed as before. It can be seen that the injection screw acts as a ram plunger, driving the melt into the mould at high injection pressures (usually a few hundred bar).

The injection of the polymer is characterised by high melt deformation rates with typical shear rates of $10^5 s^{-1}$ near the injection gate with high temperature gradients and high cooling rates near the mould walls. [2] The molecules become stretched, resulting in some orientation that gets partly frozen in near the cooled cavity walls.

During the post injection pressure stage, otherwise known as packing pressure, material is forced into the mould as long as the injection sprue is not “frozen” (solidified). This is to compensate for any shrinkage that has occurred as a result of cooling and normally requires much higher pressures (sometimes 1000 bar) than that of the injection phase due to the increase of the materials viscosity with a decrease in temperature. This results in large pressure gradients in the mould even at low flow velocities. It is mainly during this stage that thermal as well as pressure-induced residual stresses are formed as a result of the inhomogeneous cooling and the presence of high pressures in the mould. Minor flow during packing can still induce molecular orientation that is partly frozen in.

Packing pressure can be released as soon as material in the injection gate has solidified, allowing the rest of the component to cool and to dominate the cycle time due to the low thermal conductivity of plastics. This makes injection moulding ideally suited for thin wall components so as to keep the cooling times as short as possible.

During the cooling of the component, the cavity pressure is seen to reduce due to the shrinkage of the material from the mould cavity wall. The graphs obtained from these sensors can be used to indicate when the material has cooled sufficiently. It is at this point that the component can be demoulded, yielding any sample imperfections such as warpage, shrinkage, as well as surface defects such as weld lines and differences in colour and gloss.

The moulds are mounted on platen, of which one is held stationary by the machine frame while the other can move forwards or backwards on machined tie bars or linear bearings mounted on the machine’s frame. The clamping force is supplied either mechanically or hydraulically to the clamping unit and is maintained during injection of the melt.

Many different materials can be processed via conventional injection moulding, including those that are filled to reduce cost or improve properties, as well as those that are reinforced by means of fibres. Glass fibre reinforced materials are commonly used in injection moulding of automotive components and an enormous amount of work has been done on obtaining better properties of the materials. One-way of increasing the properties is to limit the amount of fibre attrition that occurs in the processing stages of the injection moulder. This has attracted the interest of many companies.

1.2 Lomolding

A South African entrepreneur formed a company called Lomold Ventures, in order to investigate the possibility of using low-pressure injection moulding technology to obtain longer fibres in the component. He hoped to obtain better properties than that of short fibre materials. Postgraduate students, seen standing in front of the Lomolder in Figure 1.2, are involved in the research project (between Lomold and Stellenbosch University) to exploit the full technology of this process. This project has been initiated by Lomold and the Stellenbosch University.

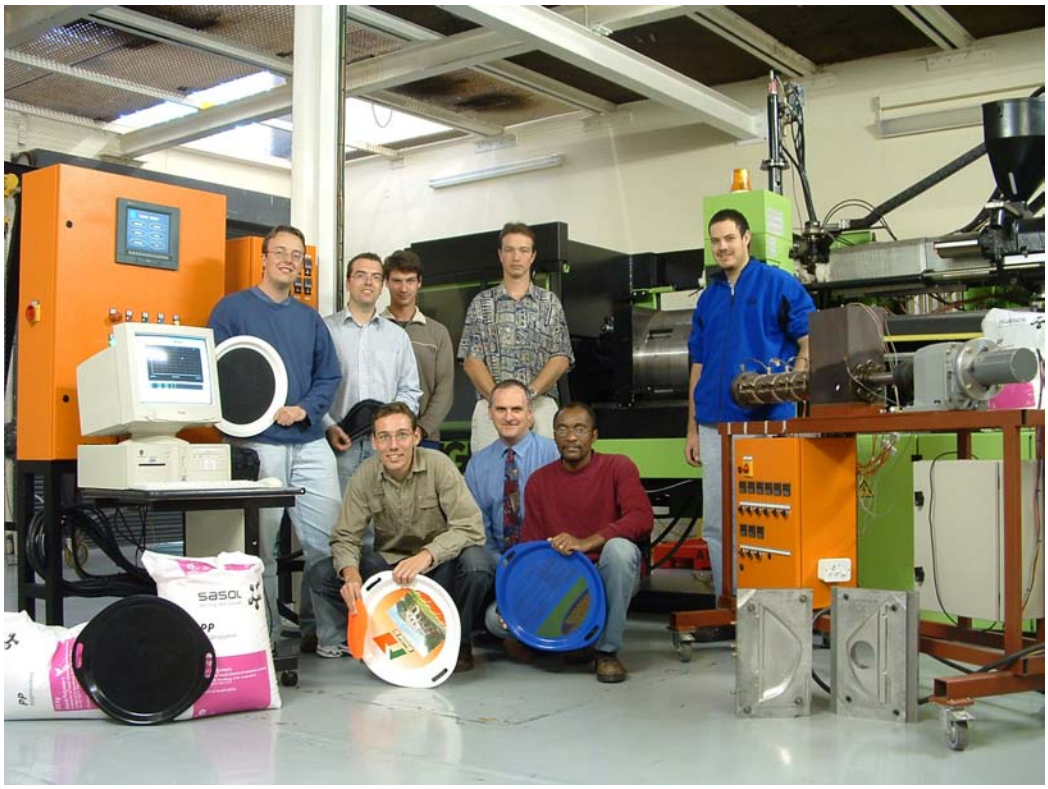

Figure 1.2: Team members involved with the development of the lomolder, which is seen in the background.

Lomolding is seen to be somewhat similar to the injection moulding technology that was first used in the early 1900s (as discussed earlier), and differs only in the control of the machine and the front of the moulding cylinder. The Lomold machine used for the project and for this thesis was based on a conventional injection-moulding machine that was modified to contain the Lomold hardware referred to hereafter as the “Lomold unit”.

The Lomold unit, is comprised of a metering unit connected to a moulding cylinder by means of hot runners and a shutoff valve as indicated in a computer-generated model of the Lomold experimental machine seen in Figure 1.3.

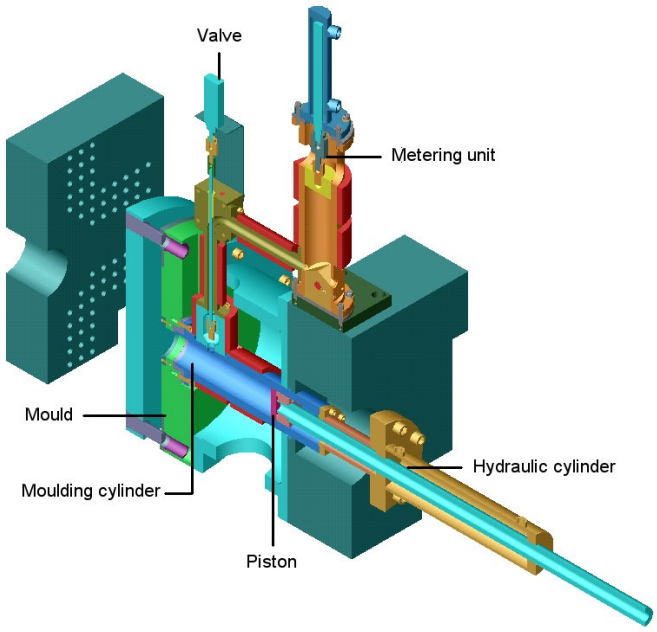

Figure 1.3: Computer-generated model of experimental Lomold unit

The injection unit was lifted to allow for the moulding cylinders' hydraulic cylinder and to enable the molten material to flow through a rotary shut off valve that was actuated by compressed air. The Lomold unit was bolted to the platen of the injection moulder, reducing the daylight (opening width) of the machine substantially.

A typical cycle in Lomold comprises of the following actions: the mould is closed, whereupon the in-feed valve situated between the injection unit and metering unit is opened. This allows for the reciprocating injection screw to operate in an intrusion manner, pushing molten material into the metering unit against a set back pressure lower than that of the injection screw back pressure. This continues until such time that the desired volume is obtained in the metering unit.

The in-feed valve is closed, at which point the out-feed valve can be opened pneumatically. The hydraulic cylinder on the metering unit applies a force on the material to transfer it to the moulding cylinder via a series of hot runner pipes with an internal diameter of 20 mm. During transfer in the hot runner pipes, the materials are subjected to a change in flow direction and velocity of flow. As in the last hot runner pipe the area of flow is reduced by the out feed valve activation rod thereby causing a

change in velocity. These hot runner pipes are heated electrically with heater bands as well as with cartridge heaters to ensure the material remains molten enough to flow.

As the metering plunger reaches the zero point in the metering unit the outfeed valve is closed. The moulding piston, with a diameter of 80 mm, moves towards the mould cavity forcing the molten material in the mould cavity, until such time as the piston face is flush with the mould cavity wall. It is because this piston is flush to the mould cavity wall that differentiates Lomolding from injection moulding that was done in the early 1900s.

This process iss made possible due to the developments in control system technology, as it was imperative that the piston was controlled within very tight tolerances to avoid it overshooting the set values and damaging the mould cavity of the moving mould half. The desired zero point of the moulding piston was the point at which the face of the piston was flush with the mould cavity.

The moulding cylinder was electrically heated to try and keep the temperature of the cylinder above the melt temperature of the material being processed so as to prevent any thickening and solidification of melt occurring. This would cause “skinning” to occur as was seen in previous work. However, the front section of the moulding cylinder could not be heated as it formed part of the mould which was continually cooled.

The moulding piston was cooled continuously and was kept a distance from the melt during the transfer into the moulding cylinder so as to prevent the premature solidification of material on the piston face. Failure to keep the piston in the forward position until the component had cooled sufficiently and had been demoulded would result in the piston causing a vacuum under the piston area. This would deform the component.

The moulds used in the Lomold process formed an integral part of the Lomold unit in that they were specifically manufactured for that unit. They are much more difficult to change than those in conventional injection moulding practices. It was also perceived that, due to Lomold having lower cavity pressures than that of injection moulding, moulds of a lesser strength could be made which will substantially reduce the costs for the manufacture.

Cycle time was largely dependent on the sequential execution of the individual tasks in the process due to the manner in which the Programmable Logic Controller (PLC) had been programmed. Through the use of the PLC connected to a Human Machine Interface (HMI) the operator was able to set the zero points as well as the speed and pressure profiles of the moulding piston. Data acquisition was also done through the PLC connected to a computer.

The area of the component under the moulding piston could have been seen as having undergone compression moulding, whereas the rest of the component would be subjected to normal flow as in injection moulding. This would result in material experiencing low shear rates and it was hence perceived that this as well as the large areas of flow, would result in minimised breakage of the fibres. It would therefore, give better properties than those of injection moulding.

Low-pressure moulding can be seen as an optimized extension of conventional injection moulding. The major benefits of low pressure injection moulding include a significant reduction of the clamp force tonnage required, less expensive moulds and presses and lower moulded in stresses. [6]

The project team seen in Figure 1.2 was responsible for the development of the Lomold technology and focused on the areas that were originally perceived as the advantages of Lomolding. One student is currently working on the life cycle assessment of the technology for his doctorate, while other masters degree students focused on some of these areas, including topics such as the numerical flow analysis of material in Lomolding; the use of rapid tooling in the Lomolding process; the effect of processing on the mechanical properties of injection moulded and Lomolded components. The latter was the focus for my masters degree in polymer science.

1.3 Objectives

The overall objective of the thesis is to determine the influence of processing parameters on the characterisation of components produced by, injection moulding and lomolding respectively.

The parameters that are considered are:

- specimen orientation

- distance from injection point or periphery
- temperature of barrel and lomold unit
- hydraulic pressure during moulding and packing

The characterisation of the components are expressed in terms of:

- tensile strength
- flexural modulus
- impact resistance
- warpage
- cavity pressures
- the resultant fibre lengths

1.4 Motivation

The influence of processing temperature and processing pressures on the mechanical properties of any technical component can be seen to be extremely important when it comes to, not only to the automotive industry, but to any industry where the components are to be put in service. Numerous studies have been directed towards injection moulding as it is one of the most used converting methods for the plastics industry. At this point Lomolding has not nearly received the same amount of attention due to it being a different concept. A study of this nature is then of importance as it aims to try and see the advantages as well as the disadvantages of both processes when producing a component, such as that which was selected for this thesis.

1.5 Outline

A design of experiments was used (in order to obtain results) at various combinations of the two main variables, pressure and temperature. Experiments were first conducted on lomolding, whereafter they were repeated using the same injection moulder. This had been rebuilt to its original configuration and the results were compared analytically to see the influence of temperature, pressure, specimen direction, sampling distance, fibre length, and materials on mechanical properties as well as the warpage and resultant fibre lengths within the components tested.

The specifications of the materials used will be discussed, after which the required machinery and equipment will be dealt with. The chosen design of experiments will then be discussed in depth so as to give the reader the understanding of why designed experiments are used in studies such as these.

The preparation of specimens for the mechanical tests are seen to be important. They did not have any influence on the results due to the way in which they were machined or conditioned. Hence thy form a standard by which all specimens were controlled.

The results for injection-moulded polypropylene (PP) will first be presented as a benchmark, whereafter glass fibre reinforced polypropylene (GFRPP) that was injection moulded will be discussed. Following these results, the results from lomolding will be given, whereafter the results for both processes will be compared to see what influence the process has on the results obtained. Due to the vast amount of information in the results, a full set of the graphical results can be found in the appendices and are summarized in the conclusion chapter. Recommendations for future research will also made.

The automotive industry has become more reliant on these fibre-reinforced composites, especially long fibre reinforced polypropylene. They can replace heavier materials within their fleet of vehicles thus making more efficient products. [18-24] This not only has an effect on the fuel economy, but also reduces exhaust emissions, assembly costs, etc.

Chapter 2. Historical and theoretical background

It is well known that the addition of fibres to high polymeric matrices improves the properties of the moulding. Short fibres are usually well below the critical length, thus falling short, compared to those above the critical fibre length. [14] The incorporation of long fibres is not that easy, as in injection moulding fibre attrition results in fibre lengths in the components that are almost independent of the starting length.

This chapter will seek to present the existing work done on special and emerging injection moulding processes and that of low-pressure moulding. The methods of fibre attrition will also be discussed, whereafter the influence of this attrition on resultant fibre lengths will be dealt with by looking at the interfacial shear stress instead of critical fibre lengths. Resultant fibre lengths also had an effect on the mechanical properties, not only from the fibre length, but also from the resultant orientation of fibres within the component. This will also be examined in this chapter.

2.1 Emerging injection moulding processes

New variations and emerging innovations of conventional injection moulding are being developed on a continual basis to extend the applicability, capability, flexibility, productivity and profitability of this mass production process. This brings about additional design freedom, new application areas and improved material properties, hence enhanced part strength, to name but a few.

In a paper by Turng [6], a general review of several special and emerging injection moulding processes were discussed, namely, co-injection moulding, fusible core injection moulding, gas assisted injection moulding, injection-compression moulding, in mould decoration, micro injection moulding, microcellular injection moulding and low pressure moulding. It was seen that PP was extensively used with low-pressure injection moulding due to the lower cost and improved physical and mechanical properties of these materials. It was also noted that generous gate sizes reduce the possibility of fibre breakage. [6]

The major benefits of low-pressure injection moulding include significant reduction of the clamp force tonnage requirement, less expensive moulds and presses and lower

molded-in stresses.[6] It was claimed by Hettinga, that low-pressure injection moulding generally allows materials to be moulded at a lower temperature, resulting in comparable cycle times, even if the filling was slower. [7] Low pressure injection moulding was based on material being injected into the cavity through a nozzle. The injection rate was set so that the melt front travelled at the same speed throughout the filling stage. This was also the basis for the patent that Hettinga filed in 1997. [22]

Low-pressure injection molding was seen to eliminate the need for packing, thereby reducing the required material by up to 5%. Moulded-in stresses were also reduced, thus permitting the overmoulding onto otherwise incompatible materials such as soft leather, delicate films and fabrics, and even thin paper and electronics. [51,52] Until recently, relatively long cycle times have restricted its acceptance, but new techniques developed by Hettinga and others promise to make it competitive with that of conventional injection moulding.

In October of 2002, Smorgon and Berelovich [28] were granted a US patent for the injection moulding of large plastic components using a similar concept as that which was used for lomolding. They sought to provide a method and apparatus for relatively low pressure injection moulding of large plastic articles in one shot, using post consumer recycled plastics which could still contain foreign matter. One of the many claims made is a method of injection moulding a plastics article, comprising feeding plastics material from an extruder into an accumulator, and displacing the extrudate from the accumulator into a mould via a valve leading into the mould cavity. The valve has a valve passage with a valve piston which, at the end of injection closes the mould cavity substantially at the mould surface of the article. The moulding is, therefore, formed without the presence of a sprue at the site of injection, etc.[28]

Dymond determined via numerical modelling of polymer flow that lomolding resulted in lower shear stresses [8] which would have an influence on the resultant fibre length within the part. This would affect the part properties as seen by Thomason in is his work of fibre-reinforced polypropylene. [9-13] The fibre damage or attrition is an important aspect when processing fibre reinforced polymers and is especially true during injection moulding where high shear stresses are present. [8,15] Yilamazer investigated the effects of processing conditions on fibre length degradation and showed that when the shear rate is increased through the alteration of the screw speed or feed rate, the average fibre length decreases. [36]

Coperion Werner & Pfleiderer used their expertise to develop processes for compounding and processing of long fibre reinforced thermoplastics. They used one heating operation which was developed in collaboration with Husky Injection Moulding Systems of Luxembourg. [37] Glass filaments (rovings) were pulled into the melt by means of the rotary screw motion which cut the fibres to length and dispersed them into the molten polymer matrix. The twin-screw extruder which can deliver a high torque, enabled re-starting of the filled machine under a full load, and dosed the prepared long glass fibre melt into the 'shooting pot' until the required shot volume was reached.

This direct processing technology gives cost advantages, as well as the option of simple modifications to the fibre content, fibre type and matrix material, for example in rapid response to market requirements. [37] Rüttgers Kunststofftechnik has been using such a plant for the manufacturing of fitting frames since 2000. [37]

2.2 Fibre attrition

The resultant fibre length within the part is very much dependent on the processing conditions of the material in all facets of the injection moulder. These have been seen to reduce the resultant fibre length in components substantially. It was found that fibre attrition predominantly occurs in the plasticization of the material which takes place in the injection unit. [14-16, 24, 38, 54, 62] It was found that when injection moulding a 10mm pellet various fibre lengths were found in the component, due to fibre attrition. The main part of fibre length reduction occured in the cylinder (55%), followed by the check ring valve (20%), nozzle (10%), gating (5%) and finally the mould (10%) when processed under optimized conditions. [54] This ratio will change dramatically if the gating or moulds are not optimised for long fibre thermoplastics (LFT).

Mennig and Wolf [14] studied the attrition of the fibres in the injection moulding process and found that the attrition was predominantly caused by melt circulation in the injection screw. The variation of processing conditions had a considerable influence on the nature of the resulting fibre length distributions. These results were obtained by removing helices of material from the screw [14,35] once the process was stopped suddenly and cooled rapidly. They found that there were six possible areas where fibres could be broken in the injection unit. These are briefly mentioned in the next few paragraphs.

Fibre attrition began with granule breakage of the polymer before melting could occur and was dependent on the channel depth in the feed zone and the pultruded pellets length. Granules could be squeezed between the barrel wall and the flight of the screw, resulting in the first mechanism for breakage. Additional breakage of the granules by interaction was not seen by Mennig and Wolf [14] and was confirmed in literature by others. [15][16] Further attrition was then seen to occur between the barrel and the screw flight where the cause could be seen as shear and friction (mechanism 3).

Fibre breakage induced by melt flow occured in the molten layers at the barrel surface (mechanism 4) and at the root of the screw (mechanism 5). [14] The former model considered a fibre which was anchored in solid polymer at one end while the other end was being subjected to the force of the polymer flow in the molten region as shown in Figure 2.1. In Figure 2.2, a large degree of fibre breakage was seen in the circulating melt compared to that of the previous mechanisms that were mentioned, and marginal damage was seen to occur in the mould cavity.

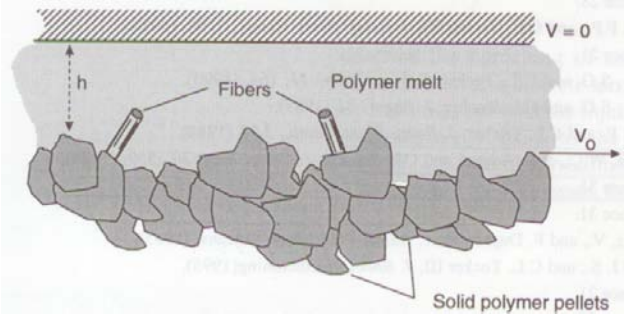

Figure 2.1: Solid and melt interface seen as fibre-breakage mechanism [15]

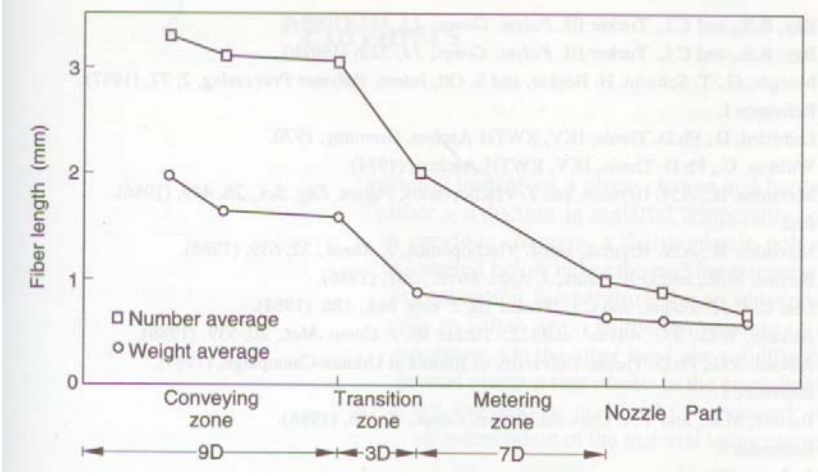

Figure 2.2: Fibre attrition measured in a plasticizing screw [15][16]

The residual fibre length appeared to be inversely proportional to fibre diameter in injection moulded composites. [17] However, the glass content also played a role in determining the residual fibre length in the final component as was seen by Thomason.[9-13] The most commonly used method for measurement of fibre lengths was direct measurement of the fibres after resin burn-off using a series of images. It was found that longer fibres could more easily intersect the photographs than shorter ones. [23]

It was seen by Hernandez [25], that the analysis of flow around solids can be done more accurately and efficiently using a boundary element method (BEM). This was compared with an existing approximate solution of fibre motion in a Newtonian fluid, developed by Burgers in 1938.

Fibre strength may be reduced significantly after fibre formation by the damage caused during processing. There is a growing body of indirect evidence which claims that the strength of glass fibres has been significantly reduced by the time they actually become the load-bearing component of a composite. [26]

The ability to transfer the stress across to the fibre through the fibre-matrix is often a function of 'adhesion' and relies on the length of the fibres. This is sometimes referred to as the critical fibre length, i.e. the length of fibre at which point it is no longer pulled out of the polymer matrix. Thomason [13] pursued those techniques, having found little enthusiastic support in the industrial product development environment. This was due to other methods being much more labour intensive, complex, inefficient and very costly as well as not being representative of the components produced. Thus Thomason followed up on an older method for deriving values for τ (the interfacial shear strength) and η_o (a fibre orientation factor) from a simple combination of the composite tensile stress – strain curves and the fibre length distribution. One of the generally accepted manifestations of this 'adhesion' is in the mechanically measured value of the interfacial shear strength (IFSS). [26]

2.3 Interfacial shear stress

Many methods of determining the IFSS exist and there is no real consensus in industry as to which method is best. This is because the sample preparation thereof is not optimised for use with thermoplastic matrices. This was also seen in previous attempts

by myself to embed single fibres with varying lengths in a polymer matrix by using an adjustable impregnation jig. The latter was heated in a press. A similar concept was used with greater success by Thomason [26] to investigate the effect of coupling agents on the interfacial shear stress.

The development of thermoplastic composites will routinely require the mechanical properties such as tensile strength and residual fibre length to be measured. Despite this development of micro-mechanical test techniques there has been little follow-up to the work originally done in the early seventies by Bader and Bowyer. [26]

Thomason [26] presented an improved version of the method and illustrated its use in glass fibre reinforced thermoplastics. The method could also be extended to obtain other important micro-mechanics parameters such as the average fibre stress σ_{uf} at composite failure. Bowyer and Bader's method was based on the Kelly – Tyson model for the prediction of the strength (σ_{uc}) of a polymer composite reinforced with discreet aligned fibres. It could be simplified as:

$$\sigma_{uc} = \eta_o (X + Y) + Z \tag{2.1}$$

$$L_c = \frac{\sigma_f D}{2\tau} \tag{2.2}$$

Here Z is the matrix contribution, X is the sub-critical fibre length contribution, and Y is the super-critical contribution with reference to the critical fibre length defined by equation 2.2. Bowyer and Bader extended the original Kelly – Tyson concept that assumed all fibres to be aligned in the direction of loading, to model the stress – strain curve of the composite prior to failure. The basis of their argument was that there is a critical fibre length obtained using equation 2.2 at any strain value (ε_c). The relative simplicity and cost effectiveness of this approach makes it ideal as an industrial screening tool for product developers.

Composites with fibres that are shorter than the critical length, L_c are said to be short fibre composites. Similarly, fibre lengths exceeding the critical fibre length are said to be long fibre composites. [15,26] For glass reinforced polypropylene a critical fibre length

of 3.1 mm is generally published, but can be reduced to 0.9 mm with chemically modified polypropylene. [29] Thomason found that the addition of a coupling agent resulted in a drop in polypropylene modulus and had a significant increase in the strength of the GFRPP specimens. [26]

The role of shrinkage stresses contributing to the transfer of stress at the interface has being widely discussed by many authors. This is because thermoplastic composites are moulded at temperatures above the melting point of the thermoplastic and are then cooled resulting in a compressive radial stress (σ_R) at the interface. [26] This compressive radial stress is as a result of the difference in thermal coefficients of the thermoplastic polymer compared to that of the reinforcement fibres. These frictional forces can make up a large fraction of the apparent IFSS when little or no chemical bonding across the interface is present, as seen with polyolefins. [26,30] Crystallization from the melt can lead to a further increase in the shrinkage and compressive frictional binding to the fibres

The properties and structure of the fibre – polymer interface region play a major role in determining the structural performance of the composite. A surface coating applied to the fibres by the manufacturer can have a large influence on the interface region. This, in turn, increases the interaction between the fibre and the polymer via two mechanisms. [30]

Firstly, the level of fibre / matrix contact, also referred to as the degree of wet-out, determines to what extent adhesion can take place between the reinforcing fibre and the polymer. Secondly, the interaction between the fibre and the polymer determines the nature and level of the actual adhesion, i.e. whether it is chemical, physical or mechanical. The non-reactive apolar nature of polyolefins tends to result in poor wet-out as well as the formation of fewer bonds of an intrinsically weaker nature. Although the adhesion of the polar glass fibre surface to the apolar polypropylene is a technical challenge, polypropylene is still attracting increased interest as a matrix material.

2.4 Influence of processing on mechanical properties

As mentioned previously, processing of fibre-filled materials results in the attrition of the fibres which will inherently affect the properties of the fibre filled polymer matrix. In a series of papers relating to the influence of fibre length (0.1 – 50 mm) and fibre

concentration (3 – 60% w/w) Thomason, Vlug, and Groenewald did a vast amount of work on the properties of glass fibre reinforced polypropylene.

In the first part of their study it was seen that the laminate stiffness increased linearly with fibre concentration up to 40% w/w whereafter higher concentrations of fibres resulted in fibre packing problems. This led to a reduction in modulus. [9] The stiffness was seen to be virtually independent of the fibre length above 0.5 mm. [9] This increase in fibre concentration or fibre length made processing of the materials much more difficult and it was seen that there was very little data or work done on this specific aspect of composites processing. Thomason [30] postulated the idea that, due to the mild preparation conditions of these samples prepared via a wet deposition method, it is not the aspect ratio that is reduced but the void content that is increased when the maximum fibre volume fraction is exceeded i.e. when insufficient polymer is able to fill the gaps between the fibres.

Fibre length is not that easy to control, as is the fibre volume fraction. This is principally due to thermoplastic composite preparation routes leading to significant uncontrolled degradation of the fibre length. [9, 14-16, 24] Many composite production processes result in test samples with a complex, unknown fibre orientation function. These could further complicate the data analysis, and with the comparison of model predictions. [39]

It was also seen that the probability of fibres crossing each other and thus being orientated out of plane, increases as the fibre length and concentration are increased. This results in a lower stiffness in the testing direction. The tensile stress in the fibre can be seen to be zero at the ends and a maximum in the middle. This maximum can never exceed the tensile stress in the matrix, thus resulting in the efficiency of stress transfer never reaching 100%. [9]

In Thomason's second paper on the influence of fibre length and fibre concentration on the thermal properties done in conjunction with Groenewoud, it was found that the heat deflection temperature of the materials are dependent on both fibre length and concentration. [10] A lower concentration of longer fibres was required to attain the maximum plateau level which was observed to be close to the melting point of polypropylene. Higher fibre lengths and fibre concentrations also enhanced the elevated temperature stiffness retention. [10]

It is important for designers to have a clear understanding of what influence temperature has on composite properties. These properties tend to experience extremes of temperatures as well as numerous temperature cycles. A complex thermal expansion behaviour resulting from the intrinsic in-homogenous anisotropic nature of the material can also result in the presence of large internal stresses in composite products, thus being able to contribute towards the warpage.

Further work by Thomason [11] found that the laminate tensile strength increased linearly with fibre concentration up to 60% w/w as well as with an increase in fibre length. At high fibre loadings the tensile strength reached a plateau level that was directly dependent on the fibre content. It was also found that the glass fibre sizing compatibility had a strong effect on the tensile strength of the laminates.

The results presented from the final part of their study showed that the charpy, tensile and high speed impact properties increased directly with an increase in fibre length up to 6 mm or with an increase in fibre concentration. Impact was shown to correlate directly with the tensile strength. [12] Impact strength at short fibre lengths approaches that of unreinforced polypropylene and increases until a plateau level is reached at around 6 mm. This was seen with the modulus and the tensile properties.

It was noted that doubling of composite impact strength could be obtained with the optimization of the fibre sizing compatibility as well as lower levels of impact strength resulting from higher levels of fibre-matrix adhesion. The effect of fibre length is different depending on the orientation distributions; therefore the fibre effectivity η (expressed as a fraction of the fibre failure) is a much easier parameter to rate material strength because it is independent of the actual fibre orientation. [38] At the critical fibre length, the effectivity can be seen to be around 0.5 which meant that of all of the glass present in the composite, only 50% of the potential strength is used.

Fibre efficacy for strength and stiffness as a function of fibre length is shown in Figure 2.3 and it can be seen that for stiffness, much shorter fibre lengths already yield near optimum results. Similarly, it can be seen that longer fibres are needed to achieve the same fibre efficacy when using glass mat thermoplastics (GMT). Schijve drew the conclusion that longer fibres are not always better and that critical fibre length is just a point where fibre efficacy for strength is seen to be 50%.

It is known that GFRPP materials exhibit high levels of impact strength that can often be attributed to the energy-dissipating mechanisms of fibre debonding and pullout which, as mentioned, is dependant on the fibre length. In real composite materials there is not just one fibre, but many with their fibre ends at different locations. This results in fracture which crosses some fibres in the middle but others near the ends of the fibre as seen in Figure 2.4. Even with relatively long fibres, some of them will cross the fracture surface near the fibre ends and fibre pullout will occur for those fibres. [38] This explains that even for material systems with an excellent fibre-matrix adhesion, a hairy fracture surface can still be seen.

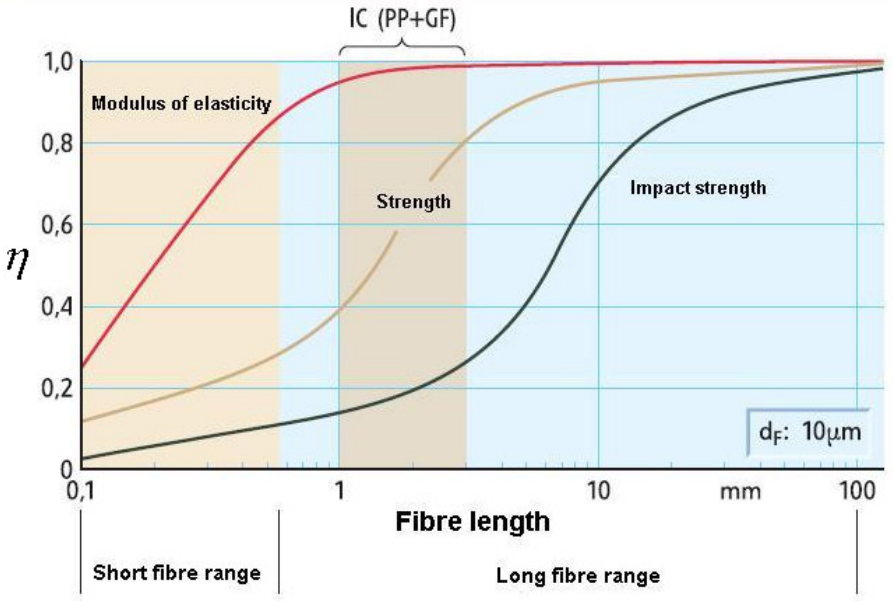

Figure 2.3: Fibre effectiveness for composite stiffness and strength [34,38]

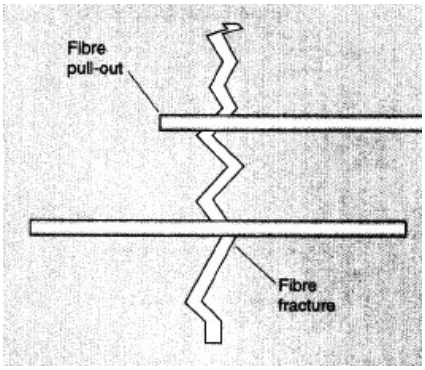

Figure 2.4: Failure modes for random fibre positions [38]

A step by step comparison of the mechanical performance of injection moulded 'long' and 'short' glass fibre polypropylene compounds was done by Thomason. [13] He saw that, at the same fibre diameter and the same fibre content, the long fibre

polypropylene material gave significant improvements in room temperature tensile and flexural strength, as well as that on impact resistance.

In many studies of injection-moulded composites it has been shown that the composites have a complex layered structure with very different average fibre orientations and thicknesses of the various layers. These vary with that of fibre length. This is discussed in the following few paragraphs.

2.5 Fibre orientation

As the mechanical properties of injection moulded short fibre reinforced thermoplastic components depend on flow induced fibre orientation, there was considerable interest by Vincent [33] in establishing relationships between flow and orientation. This interest was also in numerically predicted fibre orientation to mechanical properties. This flow induced orientation results in a number of fibre orientations at different layers in the component, seen in Figure 2.5. These seven layers can be described as:

- two thin outer layers with biaxial orientation, random in the plane of the disk, no distinct pattern; [15,31,32]
- two thick layers next to the outer layers with a main orientation in the flow direction, exposed to high shear rates; [15,31,32]
- two thin randomly orientated transition layers next to the centre layer, exposed to medium shear rates; [15,31,32]
- one thick centre layer with orientation mainly in the circumferential direction as was exposed to very low shear rates. [15,31,32]

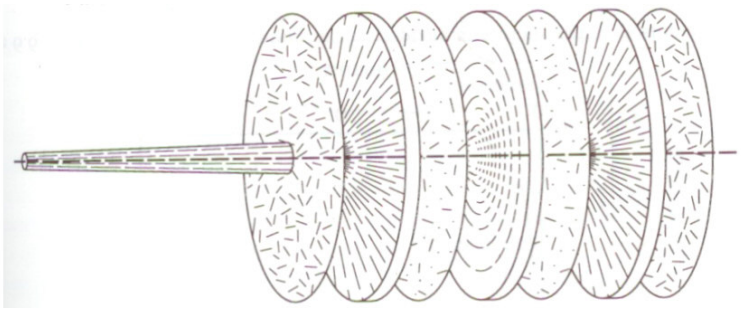

Figure 2.5: Fibre orientation in seven layers of a centrally injected disk [15,32]

Osswald and Menges [15] describe three mechanisms that lead to high degrees of orientation in injection moulded parts, the first being the effect of fountain flow. This is caused by the no-slip condition on the mould walls, forcing material from the centre of the flow towards the mould surfaces where it solidifies upon contact with the cooler mould walls.

The second mechanism that was described was that of radial flow which often leads to orientation perpendicular to the flow direction in the central layer of an injection-moulded part. This occurs when material that enters through the gate is stretched transversely while the melt expands radially as it flows away from the gate. Finally, the last mechanism that can influence the orientation is that of the flow induced by the holding pressure as solidification occurs.

In a paper discussing the influence of push-pull injection moulding on the fibres in a matrix, Waschitschek [46] noted that an increase of injection pressure increases the degree of fibre alignment in the component. It was also seen that the influence of pressure on the orientation of short fibres is just as significant for short fibres as it is for long fibres which resulted in a higher degree of orientation. [46] The orientation could also be enhanced by the increase in volume fraction which would increase the viscosity of the material that was seen to increase orientation. [31]

Shrinkage will therefore be affected not only by the direction of flow, but also by whether or not the flow is dominated by shear or extensional flow effects. [32] This also enables it to be able to contribute to the warpage of such a component as shrinkage is restricted in the direction of the fibre's orientation.

Work was also conducted on the determination of the three dimensional orientation of the glass fibre within the matrix. McGrath [45] did one such study which was based on imaging tracer fibres in index of refraction matched composites. A limitation on this method is the need to work with fibre/matrix combinations with matching indices of refraction, as well as that higher fibre densities are desirable, but often results in a decreased penetration depth.

Chapter 3. Materials

Commercially available materials with known properties were used in order to minimise variables in the experimental design. This was particularly important when it came to the use of reinforced materials. This is because the properties of these materials can vary considerably depending on the additives or processing aids that have been incorporated into the matrix in order to enhance the overall properties.

A Sasol Polymers polypropylene homopolymer with a melt flow index of 12 g/10 min was used and is referred to as PP1100N hereafter. It is an easily flowing general-purpose injection-moulding grade suitable for use in products that require rigidity and short cycle times. [1] The typical material properties for PP1100N can be seen in Table 3.1.

			Test method	
	Value	Unit	ISO	DIN
Physical properties				
Mass density	0.91	g/cm^3	1183	53479A
Melting point DSC	163	°C	3146	–
Melt flow index MFI 230/2.16	12	g/10min	1133	53735
Mechanical properties				
Tensile strength at yield (50mm/min)	36	MPa	527	53455
Elongation at yield (50mm/min)	9.0	%	527	53455
Ultimate elongation (50mm/min)	>50	%	527	53455
Modulus of elasticity in tension (1mm/min)	1550	MPa	527	53457
Izod notched impact resistance 23°C	3.0	kJ/m^2	180/1A	–
Charpy impact resistance 23°C	110	kJ/m^2	179/1eU	53453
Charpy impact resistance 0°C	25	kJ/m^2	179/1eU	53453
Charpy impact resistance -20°C	14	kJ/m^2	179/1eU	53453
Ball indentation hardness H 358/30	76	MPa	2039-1	–
Shrinkage	1.4	%	*	*
Thermal properties				
Heat distortion temp HDT/A (1.8 MPa)	54	°C	75	53461
Heat distortion temp HDT/B (0.45 MPa)	85	°C	75	53461
Vicat softening point A/120 10N	155	°C	306	–

* Sasol Polymers method

Table 3.1: Typical properties of PP100N at 23 °C for uncoloured products [42]

Typical applications of injection moulded PP1100N include items such as domestic items and closures; bottle closures and caps; multi-cavity mouldings; household

articles and outdoor furniture, to name but a few. PP1100N is not just limited to use in injection moulding but can also be used in extrusion of yarns and fibres.

Fibres, especially those made from E-glass, are often used to improve the material properties of the base polymer. This cannot be done successfully in polypropylene without the incorporation of additives to enhance the bond between the polar and non-polar particles in the plastics matrix. There is a continuous drive to improve properties of materials so as to allow it to compete with metals in the automotive and building industries.

Ticona produces pellets containing fibres, with known fibre lengths, that are fully wetted and homogenously dispersed in the plastic. The difference between short fibre pellets, a wire coated pellet, and a pellet made by a special patented pultrusion process can be seen in Figure 3.1.

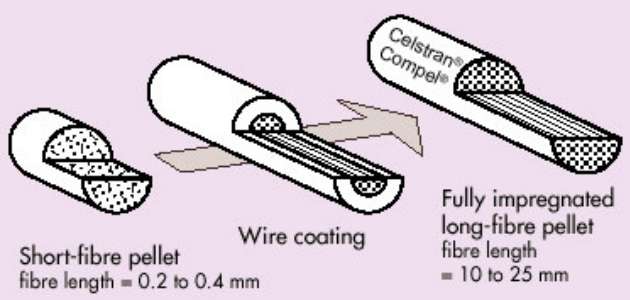

Figure 3.1: Diagram of a fully impregnated long fibre pellet (right) compared with wire coated (centre) and short fibre pellets (left) [43]

These pultruded pellets formed the base for the experimentation with glass fibre reinforced materials, and PP1100N was blended with Compel PP-GF30-0403P25/10 in a 50/50 ratio so as to dilute the long fibre matrix down to a 15% glass fibre loading. Compel PP-GF30-0403P25/10 has a 30% glass fibre loading in polypropylene, is chemically coupled, heat stabilised, and has increased flow ability. The pultruded pellet has a 25mm length and was pigmented black by the manufacturer as this material finds itself widely used in the automotive sector.

Appendix A includes information and test reports on the characterisation of the polymers used and were used for analytical purposes as well as for verification of information that was supplied by the various manufacturers of the materials.

Chapter 4. Equipment

Injection moulded samples were manufactured according to a designed experiment using an Engel injection moulder (Machine # 41200) that had a tie-bar-less clamping unit and a clamping force of one hundred and ten tonnes. The moulder was fitted with a 45 mm diameter screw and was fully controlled by the machines' own PLC (Programmable Logic Controller). A dual-purpose mould with interchangeable inserts housed a series of cavity pressure sensors, cooling channels and thermocouples.

The same Engel injection moulder had been retrofitted to incorporate a Lomold unit with metering units and valves, and was controlled via its own PLC with some functions still being used on the Engel's PLC. A separate temperature control unit was installed to control the temperature of the hot runner system of the Lomold unit.

A 19 kW Compact Cool TC15 chiller supplied chilled water at 12 ^{o}C. The chilled water was used for the machine as well as the mould cooling. A separate re-circulation cooling circuit comprising a pump, taps, and manifold, were used on the moving platen mould half to regulate the temperature to that of the fixed mould half.

Three different types of pressure sensors were located in the mould in order to measure the pressure drop within the cavity of the mould, as well as to verify the results that were previously obtained. A Gefran melt pressure transducer (model: M31-6-H-B35D-1-4-D) with a range from 0 - 350 bars was connected to a full bridge Clip AE301 amplifier to amplify the recorded pressure from the sensor that was located next to the injection point in the mould.

The remainder of the pressure sensors were piezoelectric cavity pressure sensors manufactured by Kistler in Switzerland. A type 6153C sensor had a 0 - 2000 bar range and was located directly under the injection point in the mould. It was connected to a type 5039A212 miniature charge amplifier. The remainder of the cavity pressure sensors (type 6157BD) were placed in a line from the centre of the mould outwards to enable pressure readings to be taken at more than one fixed point. Type 6157BD sensors were connected to type 5039A211Y36 miniature charge amplifiers and the signal generated was recorded by means of a data acquisition programme that was specifically written in Labview and C++ for this application. [55]

All recorded pressures and positions were recorded by means of low cost high precision Eagle PCI-730 and PCI-730E data acquisition boards that slot into the PCI slots of a desktop computer. They are multi function I/O boards which feature both analog and digital I/O on the same board. The PCI-730 features 16 single-ended or 8 differential 14-bit analog input channels with an overall sampling speed of 100 kHz. Unlike the PCI-730 board (serial #: 1000003650), the PCI-730E board (serial #: 1000004597) had 16-bit analog input channels. Boards are used for many other uses besides that of analog and digital data logging.

The MicroDAQ USB-73-T (serial #: 1000005427) is a data acquisition product for thermocouple temperature measurement, and can connect up to 16 thermocouples with a 14-bit resolution. Type T as well as Type J thermocouples, supplied by Unitemp, were supported providing temperature accuracy better than 1 degree. A special cold-junction compensation module was provided with each unit to ensure accurate temperature measurements. WaveView for windows (ver 2.0.4.7) was supplied by Eagle technologies for the data recording of the streaming temperatures through the USB port of a desktop computer.

4.1 Specimen preparation

Mounting holes were drilled and the v-notch of the impact specimens were cut on a Kent KTM-2VS turret mill using a drill chuck with a HSS drill bit and a v-notch cutter mounted on a tool holder.

A three flute tungsten carbide end mill was used in a Leadwell VMC-40 (model: Meldas M50, serial #: MA783640157) CNC machine for the cutting of the specimens from the component that had being bolted onto a jig in the machine. The CNC machine was located in an environmentally controlled laboratory set at 23°C, and it was seen that the humidity varied within the laboratory. A spindle speed of 5000 rpm was used and at a low feed-rate to avoid the specimen being deformed during cutting. The cutting path was supplied to the machine via a computer connected to it.

Specimen dimensions were determined with either a digital Mitutoyo vernier calliper (Model 500-172, serial #: 0037127) or a digital micrometer, and dimensions were entered directly into the data acquisition programmes or were recorded in a test sheet.

Impact specimens were shadow-graphed using a Mitutoyo shadowgraph (type 312-101) with a set magnification of 10 x (ten times) and a movable stage to check the dimensions of the v-notch.

A venturi based humidifying nozzle was connected to a supply air pressure of 6 bars and was activated by a solenoid connected to a Dixell humidistat and controller. Upon activation, the solenoid valve opened, allowing the compressed air to pass through. This created a vacuum and sucked the water up into the nozzle where it created mist which was then sprayed into the conditioning room.

4.2 Tensile tests

The tensile test equipment used was in accordance with the ASTM D638-02a [49] test method by using a Lloyds LR10K ***Plus*** 10 kN tensile tester (serial #: 104502), fitted with a Lloyds 10 kN load cell (serial #: 015201), with straight cut faces on the wedge action grips that were supplied. The equipment is calibrated on an annual basis and was last calibrated in August 05 by an approved SANAS agent. A data-sampling rate of 8 kHz could be obtained and was captured using materials testing software called Nexygen™ MT (Batch - Version 4.5 Issue 31) running on a desktop based computer. This was connected to the tensile tester by means of a RS232 cable which allowed full control of the machine from the computer's side.

4.3 Flexural tests

A Lloyds tensile testing machine (serial # 104657), fitted with a Lloyds 2.5 kN load cell (serial # 013908), as well as a 3 point flexural jig as stipulated in the ASTM D790-02 [48] test method, was used for testing the flexural properties of the specimen. The equipment is also calibrated annually and was last calibrated in December 04 by an approved SANAS agent. The Nexygen™ MT (Batch - Version 4.5 Issue 31) software was used to do the data capturing via a RS232 cable from the machine to the desktop computer, just like that of the tensile strength measurements.

4.4 Impact testing

A Zwick (serial #: 121390) impact tester, as stipulated by the ASTM D256-02 [27] international test method for determining the Izod Pendulum impact resistance of

plastics, was used. A pendulum with a capacity of 2.75 J was used alongside test method A which is a cantilever beam test.

For the first set of experiments, those being the Lomolded samples, the impact tester was connected to a dot matrix printer. It was then connected to a desktop computer running Test-Xpert (version 9.01), which is a data capturing programme supplied by Zwick. The last calibration took place in January 05 by an approved SANAS agent. A metal jig, machined to the correct size, was used for the correct positioning of the specimens in the clamping unit to ensure the correct depth. The specimens were perpendicular to the top face of the clamping unit.

4.5 Glass fibre content and orientation

Components containing glass fibre reinforcements were placed in a Gallenkamp muffle furnace (CAT Nr: FR550) at 650 ^{o}C for 1 hour to burn the base polymer away. This was to reveal the glass fibres in their skeletal structures and to allow the measurement of the fibre lengths.

An Olympus SZX12 – ILLK200 Optical microscope (serial #: 4G15276), fitted with an Olympus Plato 1x pf lens as well as a colour view soft imaging camera (serial #: 34473931), was used in conjunction with a soft image analysis programme called analySIS 5.0 (Build 1045). The purpose of this was for the dimensioning of the glass fibres and for the capturing of microscope images.

4.6 Warpage

A Mitutoyo Bright 710 co-ordinate measuring machine (CMM) was used for measuring the components coordinates in the X, Y and Z direction. Components were supported by three points on a jig that was bolted to the work surface of the machine.

Chapter 5. Design of experiment

By consciously planning some limited course of action to learn about what affects a process and how much of an effect it has on the process, one has, in a sense, designed an experiment. Effective scientists and technologists have been able to plan and carry out experiments carefully so as to efficiently generate a good set of data that can be used to reveal how things really work. This has often meant they had to work through the experimentation in a series of small steps where each time one factor was changed or a different level was used. This strategy can work, but involves a lot of care in order to make sure that only one factor or level of use is changed each time.

Simple experiments can take a very long time to fully explore complicated processes and results may also depend largely on skill and past experience. The more complicated the process being investigated is or the subtler the effects on the process are, the more likely it is for some experiments not to yield the desired results.

Statistica, in conjunction with Design-Expert, were used for the analysis of the experimental design and for the randomisation of the experimental runs. This was in order to prohibit any possible trends or effects of processing from influencing the results.

Designed experiments are much more efficient than one factor at a time (1-FAT) experiments whenever more than one factor is thought or known to have an influence on the process. They also detect and quantify special relationships in which two or more factors act differently in how they affect the process together than if they affected the process separately. Such relationships are known as interactions.

The final design of the experiment for the components produced in the Lomold process was a central composite design between moulding temperature and hydraulic system supply pressure. The designs' central point was the point at which a better component, assessed visually for warpage, and overall appearance was achieved. The central composite design starts with a 2-level factorial design in the two factors (2^2 design) to which a centre-point is added. The 2^2 design is then augmented by adding four axial runs (star points) as shown in Figure 5.1.

The star points were selected to lie the same distance from the central point as that of the original design points. This makes it a rotatable design that is desirable in that equally precise predictions will be obtained at any location equally distant from the centre point. The star points were made to lie in areas outside of the common processing limits to see the effect they had on the results.

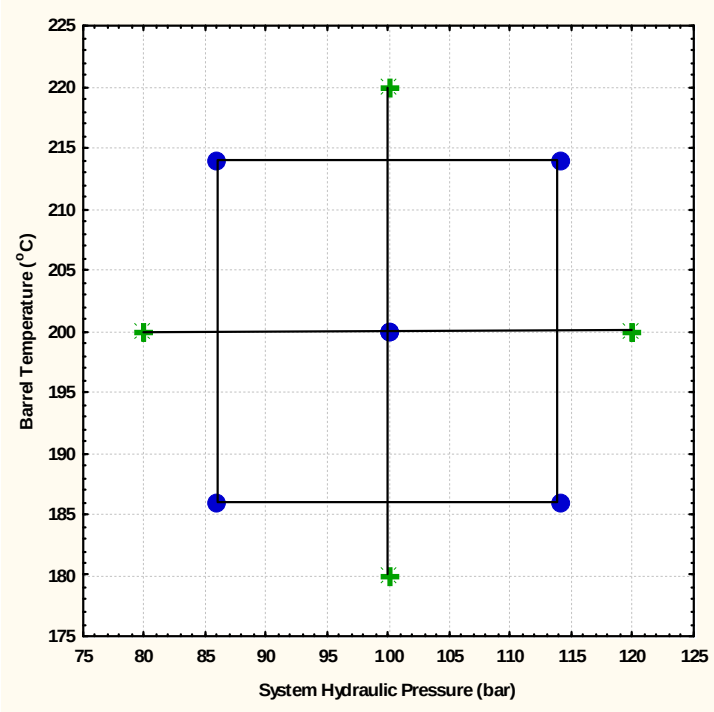

Figure 5.1: Centralised experimental design for Lomold

In injection moulding, flashing of the component was produced if either the melt temperature was higher than 220 °C or if the packing pressure was greater than 50 bars. It was clearly evident that, for the injection moulding comparisons, it was pointless to try and mould components in the upper regions of the set points and that only a certain part of the factorial design could indeed be used as illustrated in Figure 5.2. The centre node was once again the point at which a component was produced with low warpage and good finishes which was assessed on a visual basis. The five remaining points lay towards the lower part of the design and were not all exactly all same distance away from the centre point as with the central composite design.

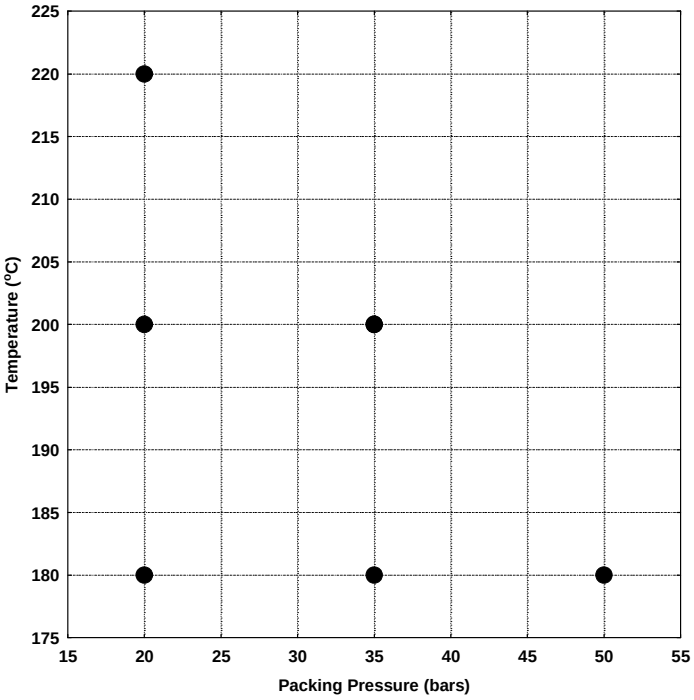

Figure 5.2: Half factorial experimental design for injection moulding

Both experimental designs discussed can be expressed in a table incorporating other information such as the order in which they were executed, the experiments run nomenclature, materials used etc. Table 5.1 gives a good overall picture of the experimental design for Lomolding as well as for Injection Moulding and shows the amount of experimental runs that needed to be done.

The initial design of experiments for Lomolding allowed certain runs to be omitted in order to reduce the number of experiments and are shown in Table 5.1 in the blue rows. Due to time available during experimentation, it was decided to include these runs that were first omitted so as to obtain more data. This would create a better understanding of the process.

The repeatability of the experimental results was verified by repeating the runs in the green rows in Table 5.1. Experiment L11, L12, and L13 were repeats of experiment L1, L2, and L3 respectively, due to browning of the material near the centre of all the components. It was thought to have originated from degraded material leaking past the piston in the moulding barrel and was referred to as piston leakage.

Table 5.1: Overview of experimental design for Lomold and Injection Moulding

Experimental set points & sample nomenclature								
Run order	Temp (°C)	Press (bar)	Material		Experiment #	Volume (ml)	Date: 2005	
1	200	100	PP	Rep	L1 / L11	233	26/4 & 3/5	LOMOLDING
2	214	86	PP		L2 / L12	232	28/4 & 4/5	
3	220	100	PP		L3 / L13	234	28/4 & 4/5	
4	180	100	PP		L4	228	28/4	
5	200	80	PP		L5	229	29/4	
6	200	120	PP		L6	235	30/4	
7	186	114	PP		L7	233	30/4	
8	200	100	PP	Rep	L8	233	2/5	
9	214	114	PP	Omit	L9	235	2/5	
10	186	86	PP	Omit	L10	229	3/5	
1	200	100	GFPP	Rep	GFL1	229	5/5	
2	214	86	GFPP	Omit	GFL2	228	6/5	
3	220	100	GFPP		GFL3	230	9/5	
4	180	100	GFPP		GFL4	224	9/5	
5	200	80	GFPP		GFL5	225	9/5	
6	200	120	GFPP		GFL6	231	10/5	
7	214	114	GFPP		GFL7	231	10/5	
8	186	86	GFPP		GFL8	225	11/5	
9	200	100	GFPP	Rep	GFL9	229	11/5	
10	186	114	GFPP	Omit	GFL10	229	12/5	
1	200	35	PP	Rep	I1	n/a	22/9	INJECTION MOULDING
2	200	20	PP		I2	n/a	22/9	
3	220	20	PP		I3	n/a	23/9	
4	180	20	PP		I4	n/a	23/9	
5	180	50	PP		I5	n/a	24/9	
6	180	35	PP		I6	n/a	24/9	
7	200	35	PP	Rep	I7	n/a	24/9	
1	200	35	GFPP	Rep	GFI1	n/a	24/9	
2	200	20	GFPP		GFI2	n/a	24/9	
3	220	20	GFPP		GFI3	n/a	24/9	
4	200	35	GFPP	Rep	GFI7	n/a	25/9	
5	180	35	GFPP		GFI6	n/a	26/9	
6	180	50	GFPP		GFI5	n/a	26/9	
7	180	20	GFPP		GFI4	n/a	26/9	

Chapter 6. Sample preparation for testing

Rectangular components of 301mm x 201mm x 3.5mm resembling a “bread cutting board” were produced on a Lomold configured injection moulder at various moulding conditions according to the design of experiment.

Figure 6.1: Rectangular components produced resembling “bread cutting board”

Material in the form of pellets was placed in the hopper of the injection moulding screw and allowed to flow freely into the feed throat, as was the case with PP. Due to the long pellet length of the GFRPP, it would form a bridge in the hopper feed throat. The material was mixed by hand during the plasticizing stage, which was also seen to alleviate the possibilities for phase separation to have occurred.

Processing of the materials in the plasticizer was done at the relatively low screw speed of approximately 128 rpm, which represented 40% of the machine’s capability. Similarly, the backpressure was kept at 10 bars to minimize fibre breakage occurring in the screw. Fibre breakage has been found to occur at higher screw speeds and high back pressures. [16] Appendix B contains a summary page of set points and resultant pressures recorded for each of the design of experiment runs in Lomold.

6.1 Lomolding

The melt passed through a shut-off valve and entered into the metering unit On reaching the desired set point the in-feed valve closed. The desired set point was 228 ml to 235 ml for unfilled PP, and between 224 and 231 ml for GFRPP. Values were dependent on the materials' pVT data as supplied by the manufacturer and were verified by weighing the initial few components after manufacture.

The out-feed valve opened via a pneumatic system and a rod, allowing the material to be discharged into the moulding barrel. At the point of this valve closing, the moulding piston with a diameter of 80mm then moved forward according to a profile that could be set in the PLC.

Cavity pressures were recorded using Kistler piezoelectric cavity pressure sensors that were placed in the moving half of the mould. In order to verify the pressures recorded, a melt pressure transducer, made by a different manufacturer using strain gauge technology, was inserted in the mould. This was at exactly the same distance away from the centre as that of one of the piezoelectric sensors. The pressures measured by this melt pressure transducer were seen to be the same values as that of the piezoelectric sensor.

The cavity pressure sensor located directly under the injection point could only be used in calculations involving the mechanical aspects of the machine design. As it will be directly influenced by the hydraulic pressure in the injection unit and is clearly illustrated in Figure 6.2 along with that of other sensors located elsewhere in the component. It was noted that the shape of the pressure curve became more rounded the further the sensor is located from the injection point.

At the point where the moulding piston started moving, the pressure transducers were activated so as to see the increase of pressure in the mould. This indicated the presence of melt passing the sensor. At a distance of 7 mm away from the zero position relative to the mould cavity wall, the moulding piston changed from a speed profile to a pressure profile taking position into account. The piston was set to obtain the same desired zero point, at which point the PLC maintained the piston's position.

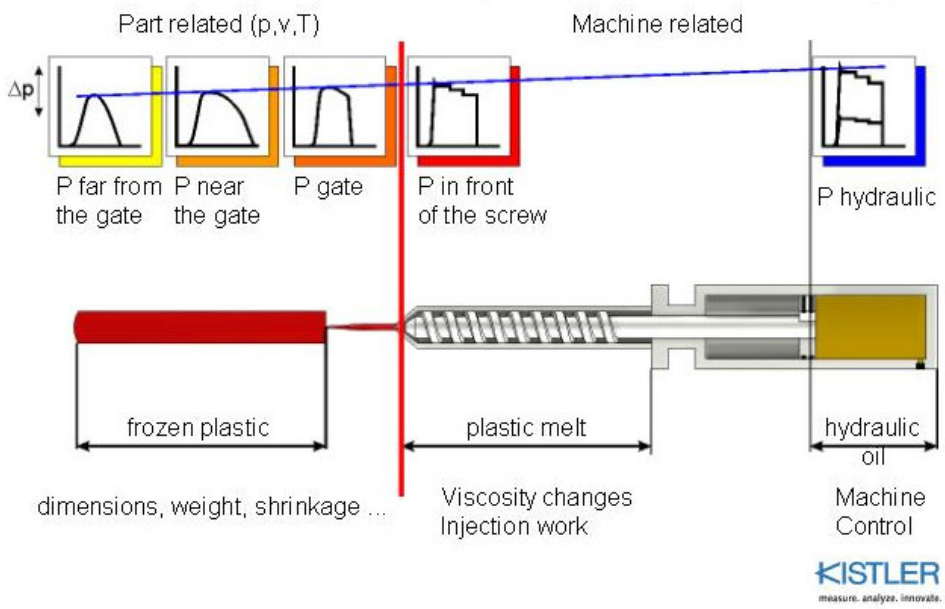

Figure 6.2: Injection Moulding Pressures [56]

During this time, the material in contact with the mould cavity walls cooled and shrank away from the mould cavity walls, thereby reducing the cavity pressure readings as time progressed. Figure 6.3 shows a typical graph obtained from Kistler melt pressure transducers like those used. It shows how the pressure curve fits the various filling stages of the cavity when comparing pressure versus time. These points can also be seen on the graphs obtained from all the pressure sensors used in the mould. They can relay important information about the processing of the material in that particular component.

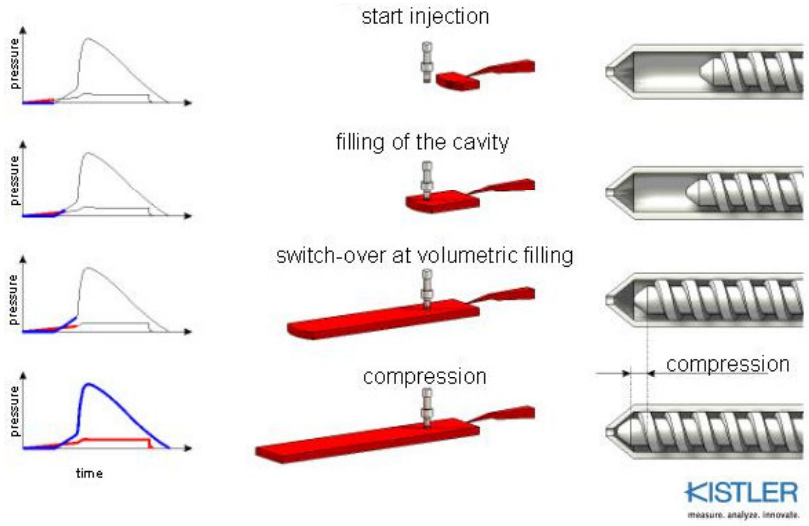

Figure 6.3: Cavity pressure at various mould filling stages [56]

In order to obtain results without having the cooling time influencing them, the cooling time was set at 90 s for all experiments. This was in excess of what was needed before de-moulding could occur. No ejector pins were present in the mould for this component and the component had to be removed by hand.

The moulding cycle was repeated each time with a great emphasis on keeping the moulding times as constant as possible. The data analysis and the sampling were only started once it was seen that the mould and machine were fully stabilised. Thirty components of each material were recorded for each experimental run.

Components were laid on a flat surface and were clearly marked with a permanent felt tip pen with the experiment number, component number, and the date of manufacture. After this they were placed together to store until the specimens were to be cut.

Various specimens were required for impact, tensile, and flexural tests, and the ASTM methods were used for the dimensioning of the specimens. In the case of the tensile tests, various size specimens could be used for certain materials, and in the case of PP and GFRPP, the recommended specimen size was according to Type I in the standard. Type V specimens were used where only limited material having a thickness of 4mm or less was available for evaluation, or where a large number of specimens are to be exposed in a limited space. [49] In the case of this design of experiments at least two specimens for each mechanical test were required from the same sample.

To be able to machine the specimens from the sample, a drawing and layout of the test pieces had to be made. This was then converted to a cutter path file containing all the co-ordinates, speeds, etc. needed to machine the samples. As part of this study, the influence of distance and flow direction of sampling on mechanical properties was of interest. Specimens were laid out in such a way as to incorporate all positions. As well as to keep to the minimum number of specimens as required by the ASTM methods used.

The above resulted in five different cutting programmes, of which the first two could be rotated to yield the same results. This led to a need for only three cutter paths to be drawn. The cutter paths were named LOM1 (R), LOM2 (R), and LOM3 as seen in Figure 6.4, Figure 6.5, and Figure 6.6 respectively, to yield 3 tensile specimens, 3 impact specimens, and 2 flexural specimens per component. The resultant number of

specimens for tensile and impact strength per experimental run were 15 and were grouped as seen in Table 6.1 for tensile specimens.

Two wooden jigs were made before the specimens could be machined. The first jig was used on the milling machine for the drilling of pilot holes whereby the sample could be bolted on the second jig using protruding bolts with nuts, which was to be used in the CNC machine to mount the sample.

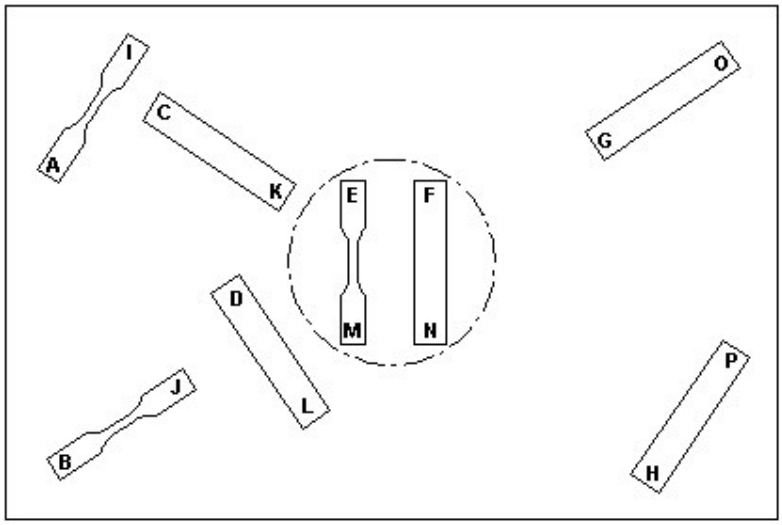

Figure 6.4: Layout of specimens according to cutter programme LOM1

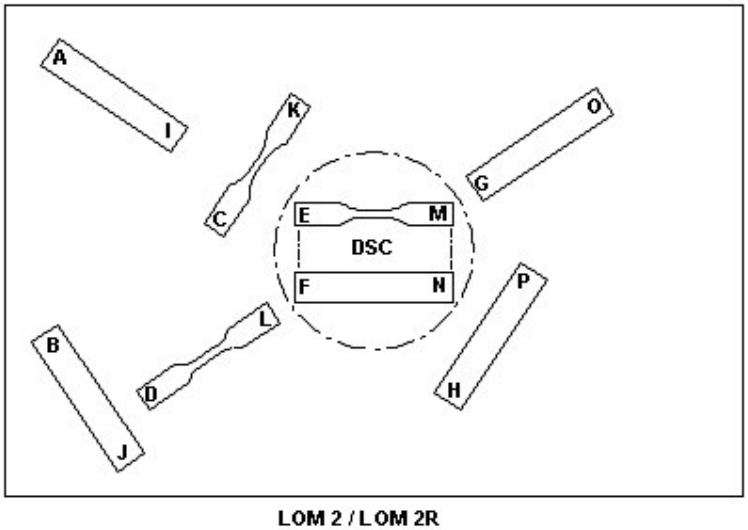

Figure 6.5: Layout of specimens according to cutter programme LOM2

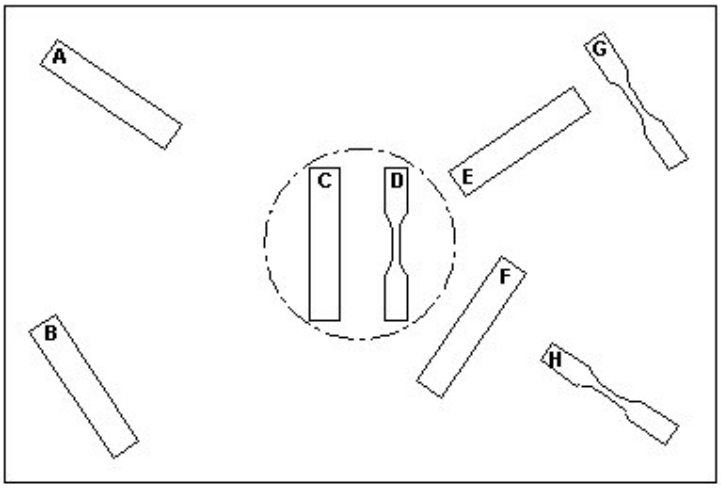

Figure 6.6: Layout of specimens according to cutter programme LOM3

Table 6.1: Tensile specimens resulting from different cutting programmes

Programme	Parallel	Perpendicular	Random
LOM1	1 x Far (B)	1 x Far (A)	1 x Centre (E)
LOM 1R	1 x Far (J)	1 x Far (I)	1 x Centre (M)
LOM 2	1 x Near (D)	1 x Near (C)	1 x Centre (E)
LOM 2R	1 x Near (L)	1 x Near (K)	1 x Centre (M)
LOM 3	1 x Near (G)	1 x Near (H)	1 x Centre (D)

Once the sample was secured, the cutter programme was sent to the CNC machine via a desktop computer, and was first run in step mode to ensure the programming was correct. The speeds as well as the number of cuts that were programmed on the CNC machine for cutting the samples can be seen in Table 6.2. Final cutter speeds used were 60% of the original set speeds and were manually overridden on the control panel of the CNC machine when it was seen that the specimens in the test run were being stressed at high feed rates. The feed down speed, as seen in Table 6.2, was 3000 mm/min. This was found to be too fast and resulted in broken cutters caused by insufficient reaction time to stop the feed of the machine if an error had been made with either mounting of the specimen or with uploading the cutting programme to the machine.

Compressed air was used to remove the waste material from the cutter, as cutting fluid could have affected the GFRPP specimens. It might also have caused the wooden jig to swell and distort, resulting in difficulty in mounting the samples.

Key	Value
Feed down speed (mm/min)	3000
Feed across speed (mm/min)	4000
Spindle speed (rpm)	5000
Z safe (mm)	10
Z 1st cut (mm)	2
Z 2nd cut (mm)	-0.5
Z 3rd cut (mm)	-2.5
Depth of final cut (mm)	0.5
Number of cuts	2

Table 6.2: Programmed cutter speeds

Specimens were labelled with a unique number comprising of the experimental run, sample number, cutter programme, and specimen position, as seen in Figure 6.4 to Figure 6.6. This was done using either a permanent overhead transparency pen or a silver paint marker dependent on the material. Specimens were demoulded from the sample by using a 45° bevelled wood chisel and a ball-peen hammer after which the burrs were be removed with a carpet knife blade. Great care was taken so as to not cause a nick in the sample, thus creating a stress concentration in that area and influencing the results.

As required by the ASTM test method D618 (procedure A), samples were required to be conditioned in a controlled environment at 23 $\pm$ 2°C and 50 $\pm$ 5% relative humidity for not less than 40 hours prior to testing, unless otherwise specified by the relevant ASTM material specification. A room fitted with a split unit air conditioner and which had no windows except for those in the door, was used as a conditioning area. Boiling water was initially used to try and increase and maintain humidity, but this proved unsuccessful.

The humidity was then controlled using a prototype humidification system which comprised of a humidistat and a controller that activated a solenoid valve when the humidity was below the set point. This allowed compressed air to flow through a nozzle. This flow through the nozzle created a venturi and drew water into the flow path of the air, creating a very fine mist which increased the humidity steadily until it reached the set point on the controller.

The humidity values were verified by constantly measuring the wet and dry bulb temperatures and then using those values on a psychrometric chart. This was to

obtain relative humidity values which could then be compared to those obtained from the humidistat controller. An example of the typical readings obtained every second from the humidistat and thermocouples can be seen in Figure 6.7. It can be seen that the samples were indeed conditioned within the limits as set out in the ASTM [50] methods.

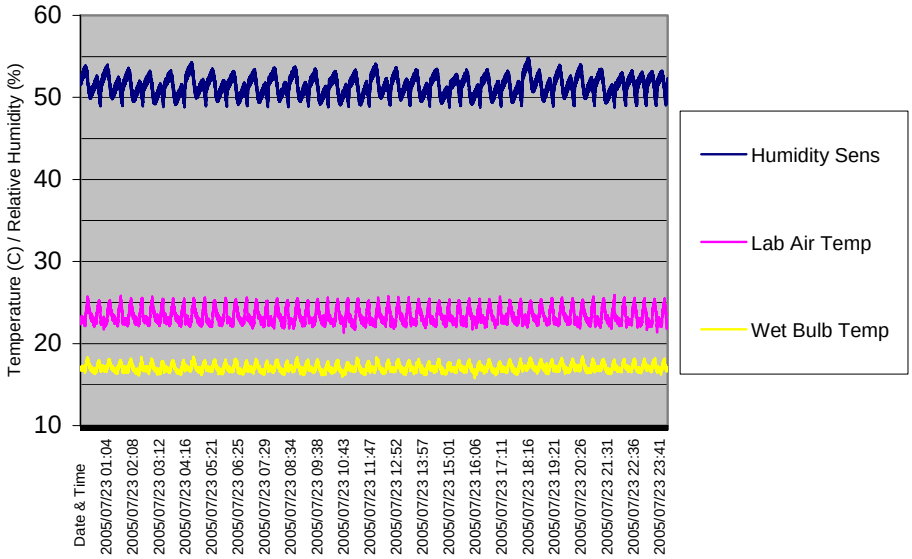

Figure 6.7: Verification of conditioning temperatures and humidity

The dimensions of each impact specimen were measured while conditioning and recorded. The v – notch of each specimen had to be shadow graphed to verify the notch depth, the inclusive angle of the notch, and the radius of the notch tip. The cutter which was used was specially manufactured and it is known that the notch dimensions have a great effect on the impact properties. [27]

A drawing of the minimum and maximum v – notch dimensions were printed to a representative scale on a transparency film, and mounted on the shadowgraph. The specimens were placed on the stage of the microscope and the shadow was portrayed on the screen, at which point it could be seen if the v-notch was within the set limits.

Specimens were left in the environmentally controlled room to condition until testing could commence. These conditions needed to be maintained as best as possible, including during transportation. To ensure that the temperature and humidity remained constant, three two litre bottles were filled with water and placed in a rigid cooler box and left in the environmentally controlled room until needed. These water bottles act

as buffers for any change in temperature during transportation and the sealed cooler box did not allow any replacement of air. This maintained the humidity for a limited period of time.

Tensile tests were conducted using a Lloyds LR10K Plus tensile tester in accordance with ASTM D638-02a test method for un-reinforced and reinforced plastics in the form of standard Type V dumbbell-shaped test specimens. It is important that where directly comparable results are desired, all samples should be of the same thickness.

A sample was placed in each wedge grip and the cross head was adjusted until the distance between the grips was 25.4 mm apart. This point was taken to be the zero point of the crosshead for all the tensile tests conducted. A Test speed of 50 mm/min was used. The specimen's thickness and width were measured, and were entered in the materials testing software along with the specimen nomenclature. It was then placed in the wedge grips, taking care to align the long axis of the specimen with an imaginary line joining the points of attachment of the grips to the machine.

After the grips had been tightened, the load cell value could be zeroed, and the test was initiated, pulling the sample at a constant crosshead speed while measuring the force and displacement exerted on the specimen. Depending on the specimen's properties and orientation, it could either undergo cold drawing giving rise to a high elongation at break, or could break without necking and hence have a very low elongation at break.

Once the specimen had fractured and had been removed, the crosshead was returned to the zero position, and the next specimen could be inserted after entering its data. The data from each specimen was recorded with the Nexygen materials testing software and the graphs could be opened at a later stage for further analysis.

The settings were changed on a Zwick impact tester to measure the impact resistance in J/m. A 2.75 J pendulum hammer was attached to the impact tester, as required by the ASTM D356-02 test method. At least five free swings, not having any specimen present, were made to check the friction or effect of the airflow on the pendulum. The average of these five swings was taken as the friction and windage of the pendulum, and was subtracted from the results obtained to obtain true impact strengths of the materials.

Specimens had been previously measured and values were recorded in a separate test sheet. A standard value of 3.2 mm was used for the thickness in the calculations and was re-calculated after completion of the tests to produce an impact strength per specimen notch length or impact strength with original sample dimensions.

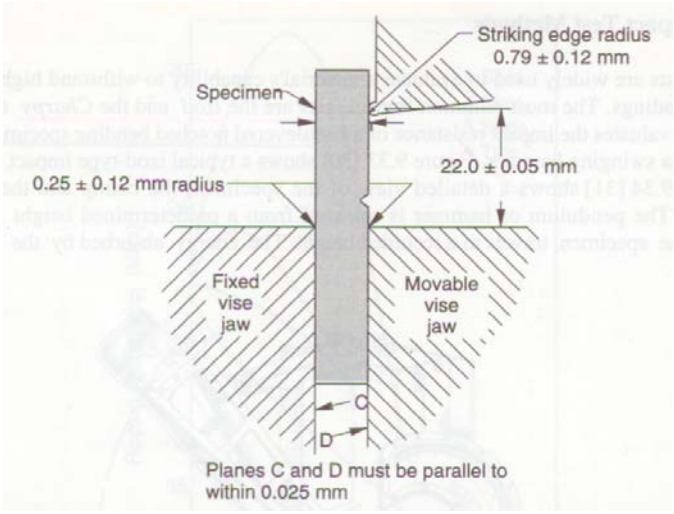

Figure 6.8: Mounting of impact specimen in clamping unit. [15, 27]

A jig was used for the alignment and mounting of the specimens in the clamping unit as shown in Figure 6.8. The pendulum was released and hit the specimen face on, causing it to break and continue to travel forward until a certain point. The height of the pendulum at this point or the angle of the pendulum was used by the impact tester to calculate the energy that was lost due to the specimen. This is called the impact strength. The hammer was returned to the starting point before the fractured sample could be removed. The results were printed on a dot matrix printer after each test was completed. Results were then entered into a spreadsheet to enable further calculations to be done.

The flexural tests were conducted on a Lloyds Flexural tester fitted with a three point flexural jig and a 2.5 kN load cell. The width and the thickness of the specimen were captured along with the specimen's details in the materials testing software before the specimen was placed in the flexural jig with a 50 mm span between the supports.

The top support was lowered to the point just above the specimen and the machine was then zeroed. The test was started and the top support was lowered at a rate of 1.3 mm/min until it reached a displacement of 6.5 mm. The test then stopped and returned the top support to the zero position, so as to be able to enter the next specimen. The

same materials testing software that was used with the tensile tester was used for the flexural tests, except that it had been set up differently.

6.2 Injection moulding

Once the results had been obtained for those components produced via the Lomold process, the Lomold configured injection-moulder was rebuilt to the original Engel injection moulder.

Tests were conducted to ensure the machine was working correctly as an injection moulder. After this further modifications were necessary to the mould, for example the manufacture of a mould mounting plate, injection sprue insert, mounting flange, pressure plug and mould cavity insert.

The mould mounting plate was the interface between the machine and the mould that was used in the Lomolding experiments. To enable the mould to be used for injection moulding, an injection sprue bush was machined to fit the previous piston barrel and bolted to the mould with eight allen cap screws. This proved to be insufficient in the first moulding trials. The pressure exerted in the mould and on the 80 mm diameter insert exceeded that of the materials strength and started to yield. This caused the insert to buckle. After the second such failure, a mounting flange manufactured from tool steel was used to hold the insert in place after it was skimmed down to remove the buckled regions.

The sprue bushing had a nozzle seat with a radius of 40 mm and an initial sprue diameter of 5.7 mm enlarging to 6.5 mm over a distance of 26 mm. This resulted in a draft angle of approx 1° on each side that was polished to remove any nicks or burrs in the material. The length of the insert was adjusted by surface grinding the cavity end of the insert until the desired length was obtained and left a good surface finish on the insert.

Higher cavity pressures than those of Lomold were expected in injection moulding which would cause damage to the Gefran melt pressure transducer as it had a range from 0 – 350 bars. A plug, manufactured from mild steel, was used to seal the cavity after the melt pressure transducer had been removed.

It was shown that for thick parts, a higher packing pressure than that of injection pressure was needed to produce a good part. [5] Calculations indicated that the clamp force required to mould the “bread cutting board” was in excess of the machines capacity and that it would not be possible to obtain high pressures in the cavity as the mould would be forced open. By manufacturing a mould cavity insert and mounting it in the present cavity by means of a press fit, thus enabled the testing of a smaller component that was 100 x 150 x 3.6 mm thick. However, it proved to be too small for sampling and would differ from the previous components tested. The decision was made to stay with the original component dimensions of 301 x 201 x 3.5 mm.

An extended standard injection nozzle was manufactured to use instead of the shut-off valve supplied. It was known that these valves result in large fibre attritions and hence the mechanical properties would be affected.[47] The nozzle had a 12mm bore diameter and tapered to a 4mm diameter hole near the end of the nozzle so as to render as little fibre attrition as possible.

The set-up on the injection moulder was done as close as possible to that of the Lomold settings. Important factors were: injection speed, injection pressure, packing pressure, and packing time which would affect the fill rate and weight of the component. The injection speed was calculated by taking the stroke of the plasticizer and dividing it by the required fill time (approx 2s) that was the same as that of Lomold. It resulted in the required velocity of the injection screw being calculated as 70mm/s.

The plasticizer stroke was adjusted until the material had just filled the cavity without the aid of any packing pressure. The packing pressure was increased until a good component was achieved. An injection-moulding expert [44] who had set the machine up in exactly the same way verified these settings as being correct. The set cooling time remained the same as with Lomold, as with all other set points on the machine. This can be seen in Appendix B1 and B2.

Components were produced at various settings according to the design of experiment used and were demoulded by hand. Some proved to be more difficult in removing than others. Great care had to be taken so as not to further deform the sample. The sprue was removed by using a pair of side cutters, marked with a paint pen and then left to cool on a flat surface for at least half an hour before being stacked until they were demoulded.

Specimens were machined, marked, conditioned and tested in exactly the same procedure as those produced via the Lomold process. There was an exception, namely, in testing the impact strength, the results were captured by a desktop computer instead of being printed on a dot matrix printer as before.

In order to measure the resultant glass fibre length in the GFRPP components, samples had to be cut from the injection point / piston centre towards the edges along the two centre lines. This was so as to render a specimen that contained one quarter of the total sample area. These specimens were placed in stainless steel trays, weighed, and then placed in a muffle furnace for 1hr at a temperature of approximately 650 °C. The polymer was burnt off to reveal a skeletal structure comprising of fibres alone.

A 2 mm glass plate that was 75 x 75 mm was used for mounting the fibres on the stage of the optical microscope. Fibres were removed from the skeletal structure with fine point tweezers and were disentangled by shaking the tweezers slightly in mid air. This allowed the individual fibres to fall and land on the glass plate. The fibre density on the glass plate was reduced by gently blowing on the plate until such a time as the samples were separated enough and could be seen clearly in the microscope. Care had to be taken so as not to blow all the fibres away or blow them in bunches that would make it impossible to see the individual fibres clearly.

The stage was moved until a good image containing a maximum amount of individual fibres could be seen. The magnification was kept constant and the image on the computer was focused until a clear, sharp image was obtained. This image was then stored prior to measurements being taken. This was done by clicking on the start of the fibre and the end of the fibre giving a resultant fibre length. A minimum of 300 fibres per experiment were measured.

The warpage of the components was measured using a co-ordinate measuring machine that would measure the X, Y, and Z co-ordinates of the component that was supported by three adjustable machined bolts in a wooden jig. The warpage seen visually could be quantified by either using the standard deviations of the components, or by calculating the radii of curvature. The resultant data can be seen in appendix D.

In the first instance, the standard deviation of all the points seen in Figure 6.9 was used to show the maximum amount of deviation that occurred between the samples. A

higher value thus rendered a component that had more warpage than that with a lower standard deviation. This method fell short in that a person could not obtain any information regarding the shape of the component.

Warpage of a component or, in this case, a sample almost always results in a change of shape due to uneven stresses within the component. This shape can be quantified in the latter method, and it was seen to overcome the shortfall of the first method used. The co-ordinates from three measured points were to be used so that a circle with a radius R could be plotted through the three points. This was done by first plotting a line, using equation 6.1, between the first and second point, which became a tangent to a circle with an unknown radius R.

$$m_{12} = \frac{(y_2 - y_1)}{(x_2 - x_1)} \tag{6.1}$$

Similarly, the gradient of the line between the second and the third point can be calculated using the same formulae with a change in denotation. The midpoints of these tangents were then determined by

$$xp_{12} = x_1 + \frac{(x_2 - x_1)}{2} \tag{6.2}$$

$$yp_{12} = y_1 + \frac{(y_2 - y_1)}{2} \tag{6.3}$$

where xp_{12} and yp_{12} are the midpoint co-ordinates of the tangent m_{12}. Similarly, the same was done for the midpoint of the tangent m_{23}. A line perpendicular to the tangent was calculated using equation 6.4 for both sets of tangents.

$$mp_{12} = -\frac{1}{m_{12}} \tag{6.4}$$

As the tangents are on the same circle, the perpendicular lines should intercept at a the centre of the circle. The intersection points of the radii, x_c and y_c were found by using the following two equations, respectively:

$$xc = \frac{(yp_{12} - mp_{12} * xp_{12} - yp_{23} + mp_{23} * xp_{23})}{(mp_{23} - mp_{12})} \tag{6.5}$$

$$yc = yp_{23} * mp_{12} + mp_{23} * mp_{12} * (xp_{12} - xp_{23}) - yp_{12} * mp_{23} \tag{6.6}$$

The radius of the circle, ***R***, could now be calculated using the centre co-ordinates, and the co-ordinates from the tangents to the circle by using equation 6.7;

$$R = \sqrt{(xp_{12} - xc)^2 + (yp_{12} - yc)^2} \tag{6.7}$$

An infinitely large radius would reflect no warpage on the component as the two perpendicular lines through the midpoint (mp_{12} and mp_{23}) would be parallel and would never intercept. Calculations of the curvature of the part were done lengthwise, as well as across the width of the component. For ease of use, the warpage of the component was expressed as the inverse of the radii, resulting in a lower figure representing low warpage, as opposed to the radii that were very large.

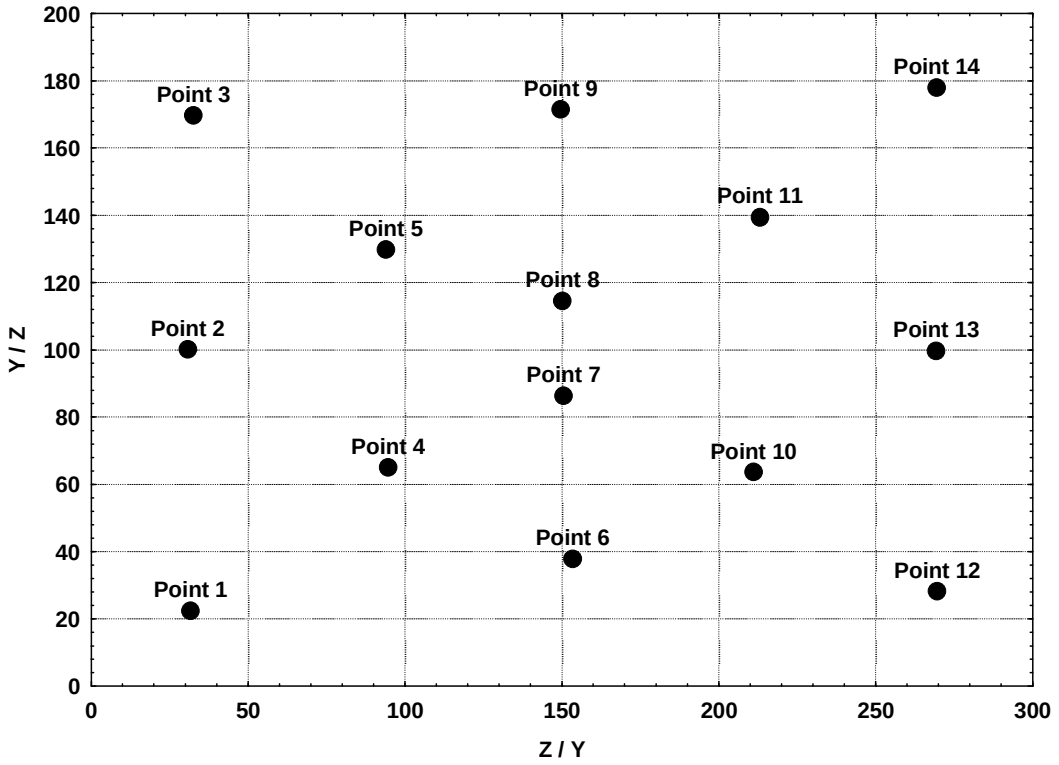

Figure 6.9: Measured points of component for warpage calculations

Chapter 7. Results and discussion

The results will first be presented in sub-sections for each combination of process and material, containing information relating to the tensile strength, flexural modulus, impact resistance, as well as the warpage of the component. Further results obtained from characterisation will then be presented. Statistica (version 7.0 AG), a computer-based data analysis programme, was used for the statistical analysis of the results obtained. Only graphs that showed trends or tendencies were selected to be displayed in this chapter due to the amount of graphs obtained. A full set of graphical results for each mechanical test mentioned above can be seen in appendix D of this thesis.

Various means of representing the data were examined and two types of plots were found to relate a great amount of information about the data, namely 2D scatter plots and 2D box and whisker plots. The latter one consisted of a box containing 50% of the data in the box, and the whiskers on each side of the box contained 25% of the data and also ignored any outlying or extreme results. Three-dimensional surface plots were also used in some instances. However, great care had to be taken as a quadratic equation was fitted to the surface plot, leading to a roundness of the plot and hence resulting in values near the edges of the plot that could be skewed.

7.1 Injection Moulding

Mechanical properties of injection moulded components can be directly, as well as indirectly, affected by processing conditions such as processing temperature. This would directly affect the flow ability of the melt and indirectly affect the fibre length in glass reinforced materials. Results portrayed in this section are for unfilled polypropylene and glass fibre reinforced polypropylene with only the post injection pressure and barrel temperature being changed according to the afore-mentioned design of experiments. Tests were conducted as a benchmark to compare to the Lomold results in order to do a direct comparative analysis later on in the thesis.

7.1.1 Polypropylene (PP)

It was seen from the results obtained that the barrel temperature had no influence on the tensile strength of the specimens, except that more scatter was found with those specimens that were produced at lower temperatures. Similarly, the post injection pressure had a high amount of scatter at higher pressures as seen in Figure 7.1. However, it had no real effect on the mechanical properties of the specimens as the median was similar to those at a lower pressure.

Injection pressure was responsible for the filling of the cavity and it was only when the cavity was full that the machine switched over to post injection pressure, hence not affecting the flow characteristics during filling. Post injection pressure was used to force material into the cavity to compensate for the shrinkage that occurs during the solidification of the melt. Too high a post injection pressure as that seen in Figure 7.1, may lead to over packing (higher density of solidified material) of the component that would then result in a large variance in the results.

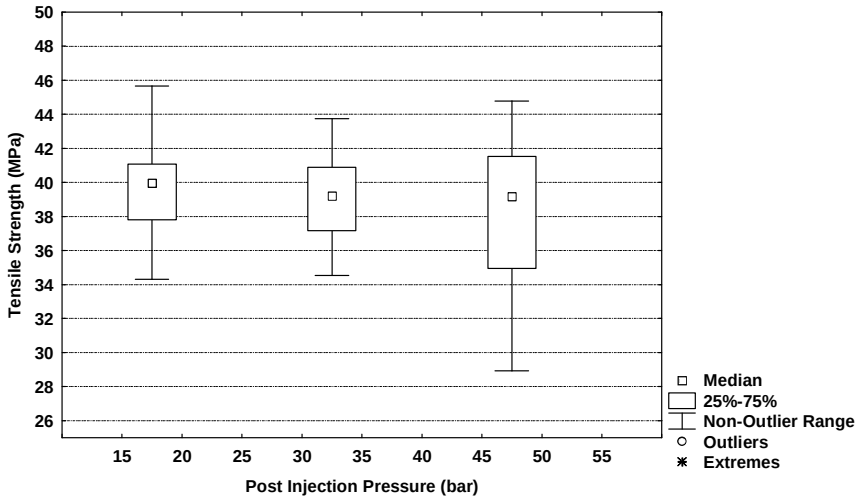

Figure 7.1: Influence of post injection pressure on tensile strength

The specimens taken from the area around the injection point (specimen 1E, 1M, 2E, 2M, and 3D) were seen to have an increase in tensile strength when compared to the other samples taken further away. This was also true for those samples taken parallel or perpendicular to the flow. In Figure 7.2 it was of interest to see that the specimens taken parallel as well as perpendicular to the flow direction, did not seem to have any

change in the tensile strength. They did have a very slight effect on the amount of scatter between the sampling directions.

The increase in tensile properties of specimens located around the injection point (comparable to those under the piston area in lomold) can be seen to have more orientation than those situated elsewhere in the component. This orientation occurs due to stress exerted on the molecules in the direction of melt flow. These molecules were not allowed to relax before the melt solidified due to cooling, thus resulting in a higher amount of orientation in that particular region. This does not mean that the crystallinity of the material in that region will be less than other regions, but that the material will be more isotropic, i.e. less aligned in one direction.

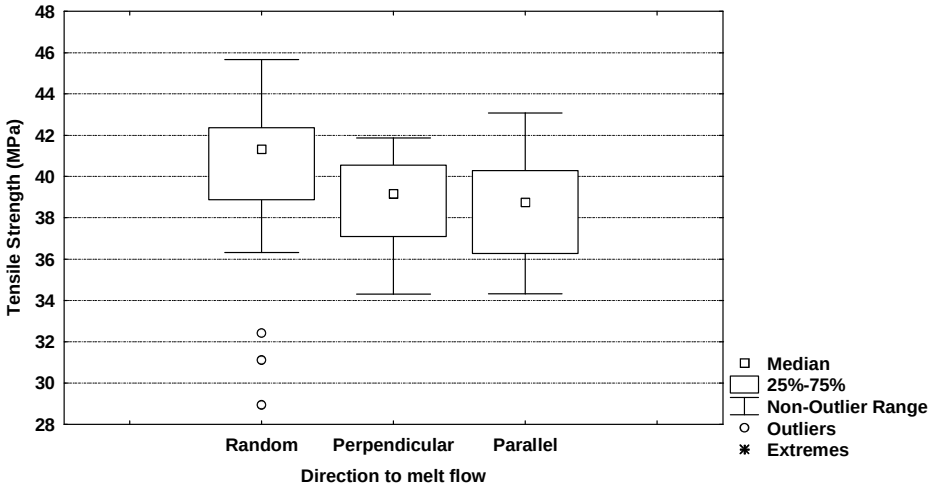

Figure 7.2: Influence of direction on tensile strength

The secant modulus or stiffness of the specimen was derived from the flexural tests that were conducted on two specimens from each sample. No flexural tests were conducted on specimens from directly around the injection point due to a lack of space to incorporate another specimen in that area. The modulus values are far more indicative of the properties than that of the tensile strength.

It was seen that the secant modulus of the specimens that were taken furthest away from the injection point (2A, 2B, 2I, 2J) showed a 3.5% decrease compared to those specimens taken midway in the sample (1C, 1D, 1K, 1L, 3E, 3F) between the injection point and the furthest corner of the sample. This decrease in modulus cannot be seen as significant as the standard deviation was higher than the difference between the

specimen locations. This was brought about by a decrease in molecular orientation at the furthest specimen locations.

Perpendicular, as well as parallel, specimens in relation to the direction of melt flow had no significant influence on the modulus. It was seen that the medians were equal, unlike those of the post injection pressure which was seen to have a significant effect on the secant modulus. The modulus in Figure 7.3 can be seen to have a decrease with an increase in post injection pressure, which was brought about by the change in orientation that occurred during the packing phase. During this stage, the molecules undergo an alignment in the flow direction in the middle (of cross section) of the component that has not yet solidified.

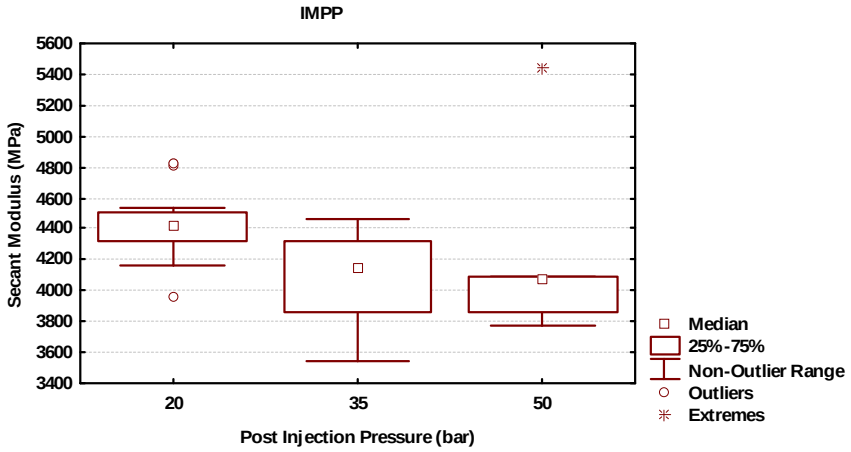

Figure 7.3: Influence of post injection pressure on secant modulus in injection moulding

When looking at the effect that the barrel temperature had on the modulus, significant variances could be seen, but no trend or tendency could be found in the results. It was seen that the modulus initially reduced with increasing temperature. However, with a further temperature increase the modulus was found to also increase much higher than the initial value at a lower temperature as seen in Figure 7.4. It must be remembered that only one set of data was used for the plotting of the points at the higher temperature and that those at the lower temperature had three sets of data.

At a processing temperature of 180 ^{o}C the material will be more difficult to process due to its increase in viscosity as seen in the flow curves of Figure 7.5. This will result in a larger amount of shear heating which will increase the temperature of the material as well as immediately lower the viscosity again. This is because polymer melts are seen to be shear sensitive with respect to viscosity. This increase in temperature will lead to

more relaxation of molecules which was seen to increase the overall stiffness of the specimens.

Fewer effects of shear heating were seen with an increase in temperature, resulting in a higher modulus. This was because of better stress relaxation that could occur at a lower melt viscosity due to a longer time for stress to be reduced resulting in less orientation. Orientation of molecules can be seen as “preferred” alignment in one direction.

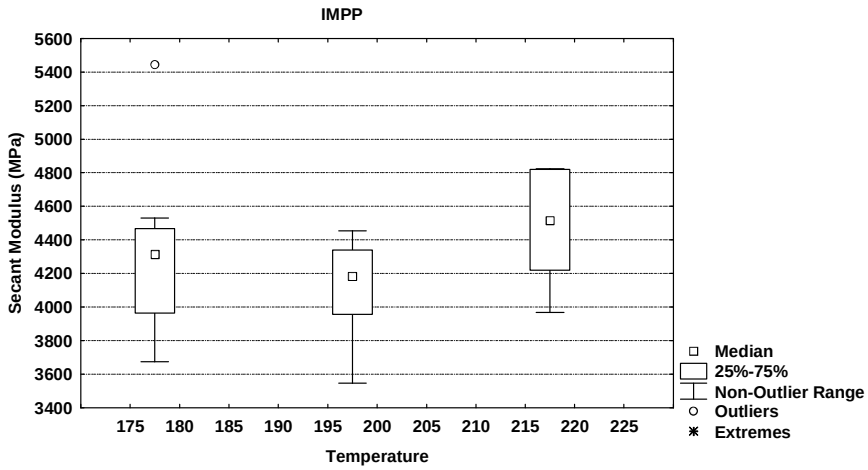

Figure 7.4: Influence of temperature on secant modulus in injection moulding

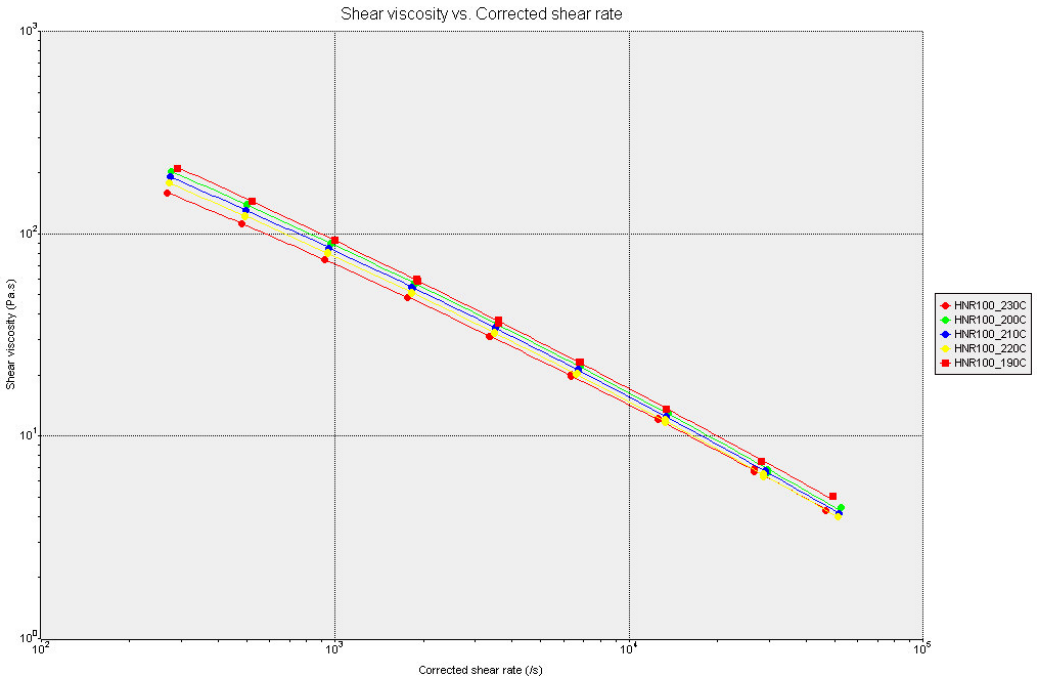

Figure 7.5: Flow curves of PP1100N (HNR100) at various temperatures [57]

Specimen sampling distances were not seen to have any increase in impact resistance for specimens further away from the injection point. However, they did indeed result in a lower impact resistance for specimens located directly next to the injection point (1F, 1N, 2F, 2N, 3C). Lower impact values were seen in this area due to the high amount of orientation of molecules being perpendicular to the specimens' length. This indicated that the materials had a greater amount of stress. A great amount of scatter could also be seen in the results of those specimens located midway between injection point and furthest point of the sample.

Direction of specimen sampling was seen to have a significant effect on the impact resistance. Those specimens parallel to the melt flow were seen to have the highest impact resistance as was expected. A higher value than those obtained in the area directly surrounding the injection point were found for the specimens that were perpendicular to the melt flow.

It can be seen in Figure 7.5 that the impact resistance of injection moulded polypropylene increases with the orientation of the specimen to the flow length. Thus those specimens with the highest amount of molecular orientation which, as mentioned before, were located in the area around the injection point, were seen to have a lower impact resistance. This was because the molecules which were perpendicular to the specimen length thereby allowing the crack to propagate easier through the specimen.

As mentioned earlier, the samples directly surrounding the injection point (random) were seen to have a high amount of orientation perpendicular to the specimen length, thereby allowing easier propagation of the crack. This orientation is due to the packing of the material as well as the material solidifying before relaxation of the molecules could occur. The orientation of molecules in those specimens that were perpendicular to the melt flow were thought to be at an angle somewhere between that of perpendicular and parallel to the specimen length. Specimens parallel to the melt flow had the highest impact resistance as the molecules were orientated parallel to the length of the specimen. This made it more difficult for the propagation of the crack as it had to break through these molecular chains.

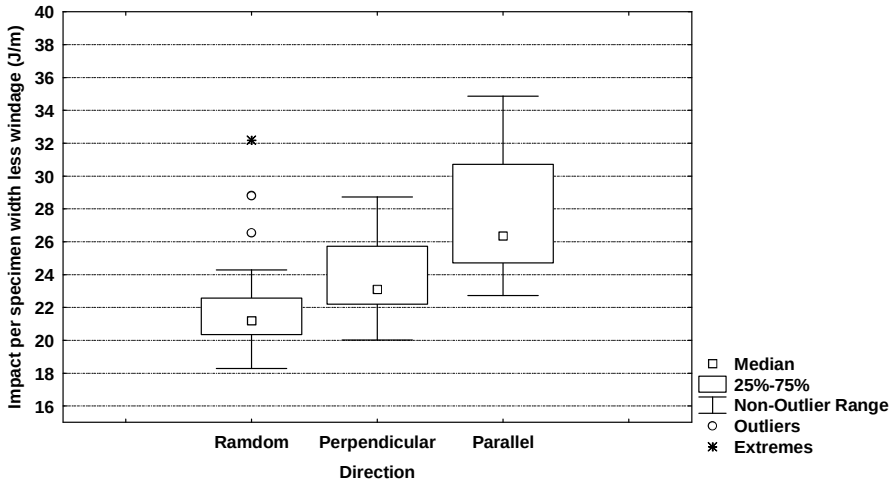

Figure 7.5: Influence of direction from injection point on impact resistance for IMPP

Similarly, it was seen in Figure 7.6 that an increase in post injection pressure resulted in an increase in impact resistance and a decrease in the amount of scatter of the results. At lower post injection pressures the molecules will not be as tightly packed as those specimens produced at the higher post injection pressures. This results in a large variance in the results due to the lower density of packing as well as that of enormously different orientations as the results were based on all specimens no matter what the distance from the injection point or the direction of the specimen to the melt flow.

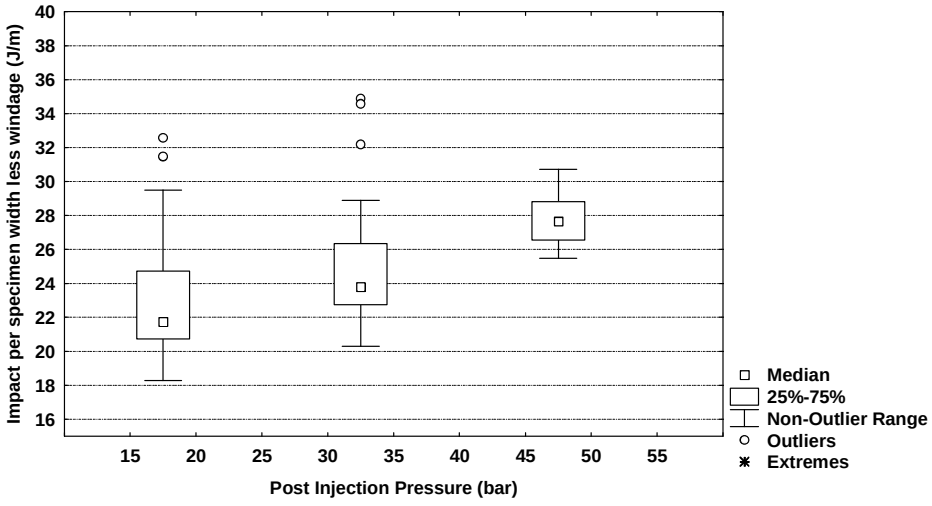

Figure 7.6: Effect of post injection pressure on impact resistance of specimens

A higher packing density causes materials to be less stressed. This makes the specimen more ductile than those at lower post injection pressures and hence is more difficult to break. At the pressures used in the experimentation, no over packing of the

cavity was seen. This was because over packing would result in flashing. It was originally perceived that the higher the packing the higher the bulk density and crystallinity would be, due to more molecular chains as a result of the crystallinity, that would need to be broken in the sample. Notched specimens were used, resulting in most of the applied energy only being used for crack propagation and not for crack formation.

Warpage was seen not to be significantly influenced by a change in post injection pressure. However, it did indeed show a large decrease in the amount of warpage and scatter when compared with an increase in barrel temperature, seen in Figure 7.8. A greater force is required to fill the mould at low melt temperatures. This inherently results in moulded-in stresses caused by orientation of molecules which can be one of many contributing factors towards the warpage of components. Warpage is caused by non-uniform shrinkage in the component which occurs as a result of the crystallisation of the orientated or stressed molecules.

The viscosity is dependent on the molecular mass of the material and can be seen to decrease with an increase in melt temperature which will reduce the moulded in stresses and scatter. Hence the warpage of the sample will be less. This effect could also be seen if an extrusion grade with a low MFI as well as an injection-moulding grade with a medium MFI were moulded at the same temperatures and conditions. The low MFI extrusion grade is expected to yield more warpage on the component due to it experiencing higher moulded in stresses.

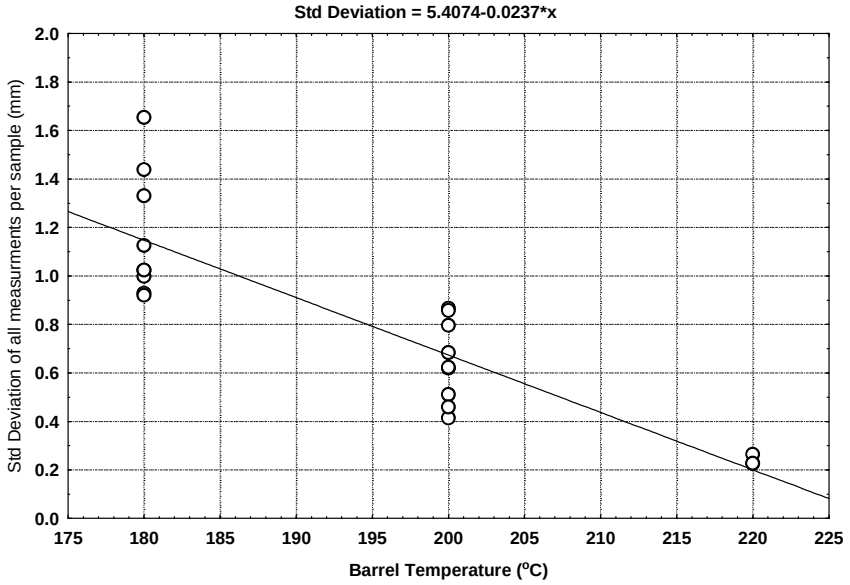

Figure 7.7: Influence of Barrel Temperature on sample warpage

The results obtained for the warpage based on standard deviation were seen to compare well with those that were based on the fitting of a circle to three points of the sample. An infinitely large radius meant that the perpendiculars to the tangent i.e. the radii, were parallel. The data points measured at corresponding X and Y values across the length and width of the sample can be seen in Table 7.1, along with the inverse of the radii. The smaller the inverse of the radii, the lower the warpage was for that sample.

Table 7.1: Inverse of radii of curvature for injection-moulded polypropylene

Sample Number	Y1 (L) @ X=30.78	Y2 (L) @ X=150.20	Y3 (L) @ X=269.27	(1/R (L)) Exp 8	Y1 (W) @ X=37.86	Y2 (W) @ Y=86.36	Y3 (W) @ X=171.48	(1/R (W)) Exp 8
I1-15	25.11	26.39	25.18	**92**	26.63	26.32	26.94	**69**
I1-22	25.05	26.59	25.06	**140**	26.39	26.43	27.48	**16**
I1-25	25.13	26.29	25.30	**68**	26.79	26.36	26.44	**12**
I2-15	25.00	26.45	25.12	**114**	27.20	26.53	27.53	**242**
I2-20	24.92	26.56	25.08	**145**	27.51	26.69	27.56	**255**
I2-26	25.09	26.23	25.14	**73**	26.93	26.32	27.23	**198**
I3-22	25.06	24.85	25.51	**8**	25.59	25.00	25.39	**81**
I3-26	25.22	24.77	25.52	**20**	25.31	24.91	25.25	**50**
I3-30	25.03	25.17	25.42	**2**	25.84	25.28	25.82	**108**
I4-24	24.74	27.80	24.54	**596**	27.32	27.40	29.34	**56**
I4-29	24.62	27.72	24.71	**558**	28.21	27.65	28.76	**221**
I4-30	24.61	27.37	24.71	**437**	27.81	27.24	28.70	**301**
I5-21	25.92	27.35	25.39	**166**	27.89	27.53	27.07	**61**
I5-22	25.87	27.24	25.37	**153**	27.62	27.36	27.23	**12**
I5-27	25.84	27.20	25.35	**151**	27.65	27.26	27.29	**3**
I6-23	25.43	27.32	24.92	**269**	27.11	27.22	27.74	**19**
I6-24	25.56	27.24	25.05	**218**	27.06	27.20	27.19	**0**
I6-29	25.57	27.24	25.00	**223**	27.15	27.16	27.37	**1**
I7-19	25.24	26.04	25.26	**38**	25.94	25.96	26.40	**3**
I7-21	25.32	25.96	25.29	**25**	25.38	25.74	26.45	**91**
I7-25	25.27	26.12	25.25	**43**	26.12	26.09	26.33	**3**

7.1.2 Glass Fibre Reinforced Polypropylene (GFRPP)

From the data sheets obtained as well as from the verification tests conducted on moulded test pieces, it was seen that glass fibre reinforced polypropylene showed a substantial improvement in properties to that of unfilled polypropylene. An increase in the glass fibre content was also seen to improve the properties, but could lead to more fibre attrition through fibre-fibre interaction. [9 –13]

The barrel temperature was seen to have no effect on the tensile properties of the specimen as was seen for the unfilled polypropylene. Similarly, it was found that the post injection pressure had no effect on the tensile properties. It did, however, result in a lower Young's modulus at a higher post injection pressure which indicates that the material was more deformable. Glass fibre reinforced polypropylene underwent brittle failure and no yielding occurred in any of the specimens.

In Figure 7.8 and Figure 7.9, it can be seen that there is an improvement of tensile strength in those specimens located around the injection point compared to those that were taken from varying orientations or distances within the sample. The fibre orientation was seen to be parallel to the specimens' length in specimens located directly next to the injection point, thus resulting in improvements in tensile strength.

Specimens from other locations were seen to not have a significant influence on the tensile strength, just like that of the injection moulded polypropylene specimens. The tensile strength of specimens near as well as far from the injection point were not seen to vary greatly due to no change occurring in the flow properties. This could have had an effect on the results.

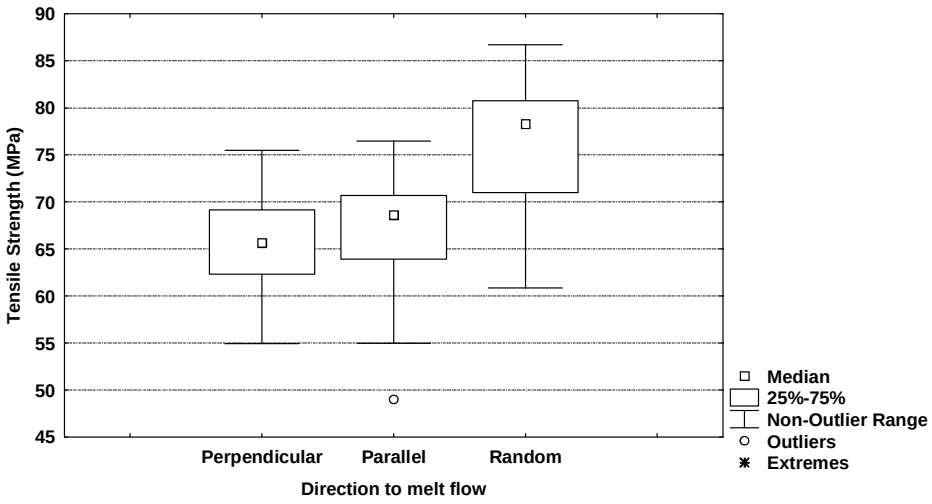

Figure 7.8: Effect of sampling direction to melt flow on tensile strength

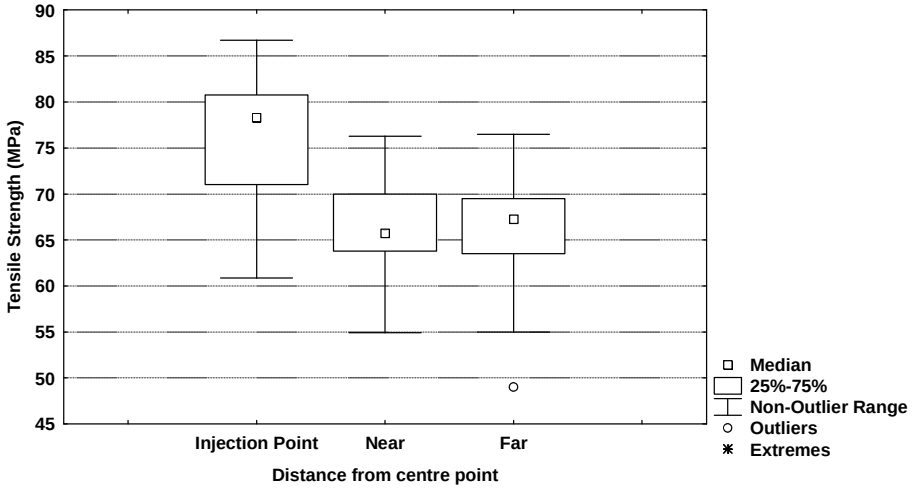

Figure 7.9: Influence of specimen distance on tensile strength

Injection moulded GFRPP gave a vast array of scatter in the results, more than that which was obtained with injection moulded PP. Besides the scatter, a 5% increase in the chord modulus was obtained with specimens that were perpendicular to the melt flow, greater than those that were parallel to the flow. Specimens that were taken from midway in the component, showed an 8% increase in the chord modulus compared to those taken from the furthest point of injection as seen in Figure 7.10.

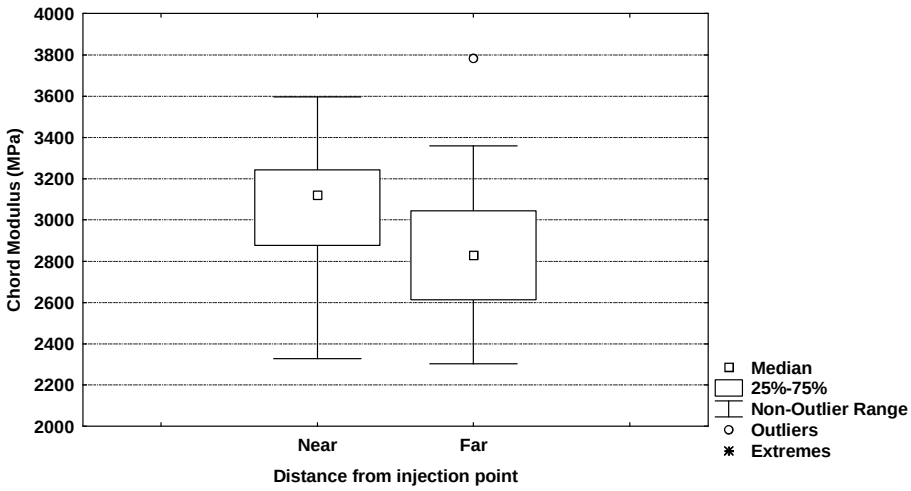

Figure 7.10: Specimens near the injection point yielded a higher Chord Modulus than those further away

An increase in the chord modulus could be brought about by an increase in fibre orientation parallel to the specimens' length, as was typically seen in Figure 7.10. The amount of orientation seems dependent on the amount of flow that had passed in that specific area. This was because fibre alignment was seen to be higher in areas subjected to a higher amount of flow that had passed.

A change in temperature was seen not to have any effect on the modulus and resulted in a large amount of scatter in the data at all temperatures. A decreasing trend in the secant modulus was seen with an increasing post injection pressure as illustrated in Figure 7.11. This decrease in the secant modulus could be due to the fibre as well as the molecular orientation being changed by the increase in post injection pressure also resulting in a potential change in crystallinity.

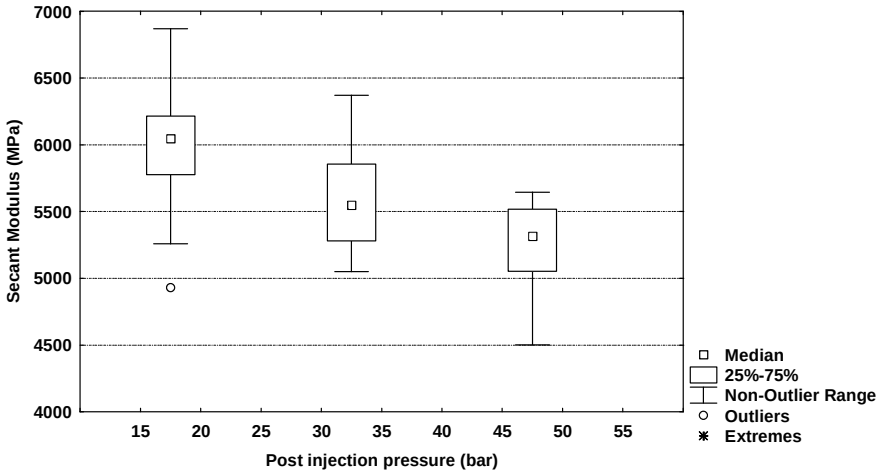

Figure 7.11: Effect of post injection pressure on secant modulus

Impact strength of the specimens produced, based on looking at the medians were seen not to be affected by a change in barrel temperature. However, it was an increase in pressure that resulted in an increase of the impact resistance which again indicates that maybe a lower crystallinity was an effect of a lower post injection pressure. There was a definite influence on the amount of scatter present at either low temperatures, or higher pressures.

In injection moulding of GFRPP the impact resistance increases with an increase in orientation of the fibres to the specimens length as shown in Figure 7.12. This was believed to be due to the alignment of the fibres in the same direction as the specimen length for those specimens located directly next to the injection point. The fracture surface of these specimens would be irregular and jagged due to the impact energy having to either break the fibres and for the crack to propagate around the fibres. Hence it can be said that the properties in this case were determined by the fibre orientation properties rather than the material properties.

Specimens located parallel to the melt flow direction were thought to have an orientation of fibres perpendicular to the specimens length. This resulted in a lower impact resistance as the crack would run parallel with the fibres which meant that no fibres would have be broken or fewer fibres were broken. The orientation of the specimens positioned perpendicular to the flow would have fibres orientated at an angle somewhere between those that were located next to the injection point and those parallel to the melt flow.

Polishing a cut section of the specimen and looking at the shape of the embedded fibres through an optical microscope, as seen in Figure 7.12, can be used to determine the angle at which they lie and hence relate important information about the fibre orientation to the researcher.

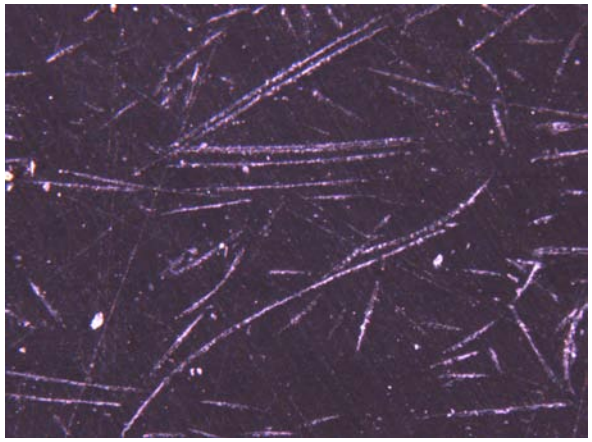

Figure 7.12: Magnification (10X) showing fibres in top layer of random specimen

It was also noted that the specimens in the area directly surrounding the injection point had a marginal increase of 5% in impact resistance. Specimens located midway and near the edge of the component remained fairly constant as was seen in the injection moulding of PP.

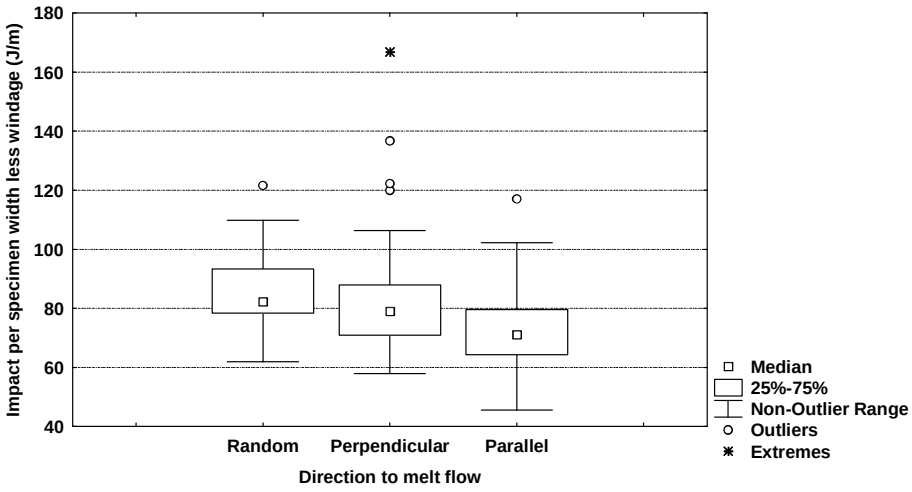

Figure 7.12: Influence of specimen direction on impact resistance

The resultant shape of the component due to warpage was saddle shaped, and it was seen that with GFRPP a large amount of scatter was produced. The quantification of the saddle shape can be found in appendix D. It was also seen that a reduction in warpage occurred with an increase in post injection pressure and is clearly seen in Figure 7.13.

The reduction in warpage seen can be related to the moulded-in stresses that were caused by the materials' viscosity and the pressures required for compensating the

shrinkage of material, even though the material had a processing aid added by the manufacturer. Temperature resulted in no trend seen in the warpage of the sample as that which was seen for injection moulding of PP.

A three dimensional graph could be used to portray the influences of temperature and pressure. However, one would need to be extremely cautious as the points are fitted to a quadratic equation that assumes certain information if no points have been plotted. This was the case with specimens that were injection moulded as only a part of a full factorial was used in the design of the experiment.

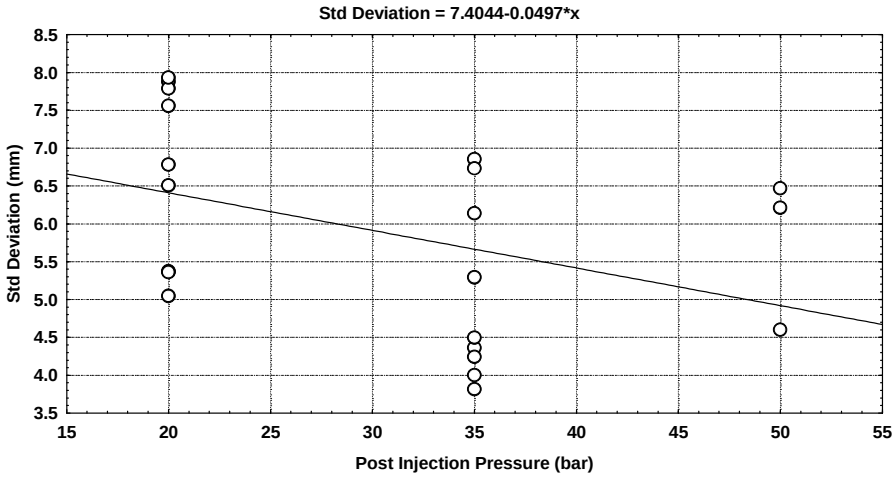

Figure 7.13: Influence of post injection pressure on standard deviation of samples

7.2 Lomolding

Specimens were expected to have a vast improvement in mechanical tests as mentioned previously. This is because one of the perceived advantages of Lomold would be minimised breakage of the fibres, resulting in a component containing a larger degree of long fibres (> 10mm) than would be obtained in a conventional injection moulding process. Unfilled, as well as glass fibre reinforced, polypropylene was once again used as a standard material to benchmark against that of the injection moulding. Post injection pressure could not be set on the Lomold unit as the correct amount of material was metered off beforehand. Thus the hydraulic supply pressure was varied.

7.2.1 Polypropylene (PP)

The tensile strength of the specimens was seen not to be affected by a change in barrel temperature, hydraulic system pressure, or even the distance and direction of the specimens in relation to the centre point and direction of melt flow respectively. A difference in tensile strength at break was seen between injection moulding and Lomold, in that the latter process had lower values.

Unlike that of tensile strength, the flexural properties of Lomolded polypropylene were affected by distance, direction and system temperature. It can be seen in Figure 7.14 that a greater increase in secant modulus was obtained for specimens located near the piston area in comparison to those that were located further away resulting in less deformation. This increase in secant modulus was due to the higher orientation of the molecular chains at specimens nearer the injection point than those further away. This was because the amount of flow passing through those particular areas resulted in the orientation of the molecules.

No real difference in medians was seen in orientation of specimens to melt flow, but it was noted that there was less scatter in the results for the specimens that were parallel to the melt flow. Hydraulic system pressure (i.e. moulding pressure) was seen to have no influence on the results. A temperature increase was seen to render less scatter of the results and had a slight trend in that the secant modulus median was also reduced slightly.

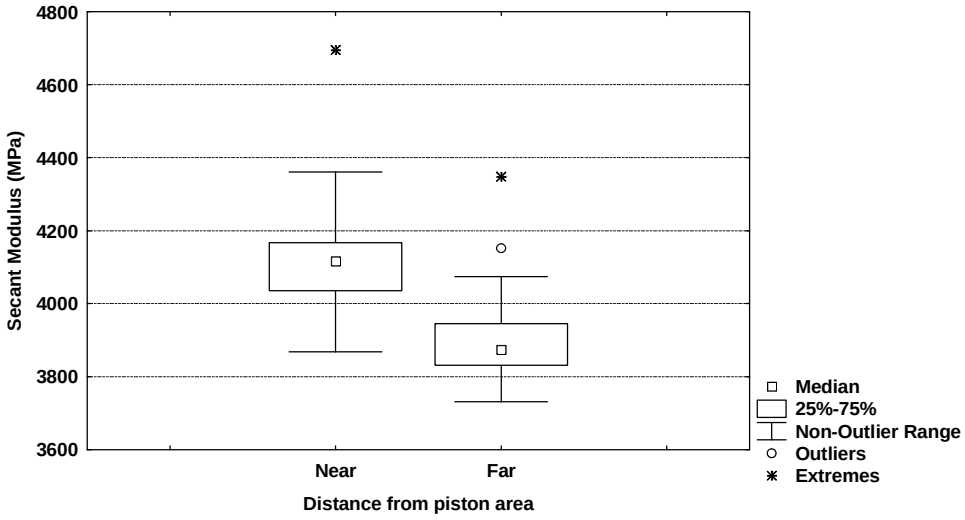

Figure 7.14: Effect of sampling distance on secant modulus

Although resistance to impact was found to increase with an increase in sampling distance, the results obtained were still lower than those obtained in the injection moulding trials with either of the materials. The increase in impact resistance in relation to sample distance can be seen in Figure 7.15.

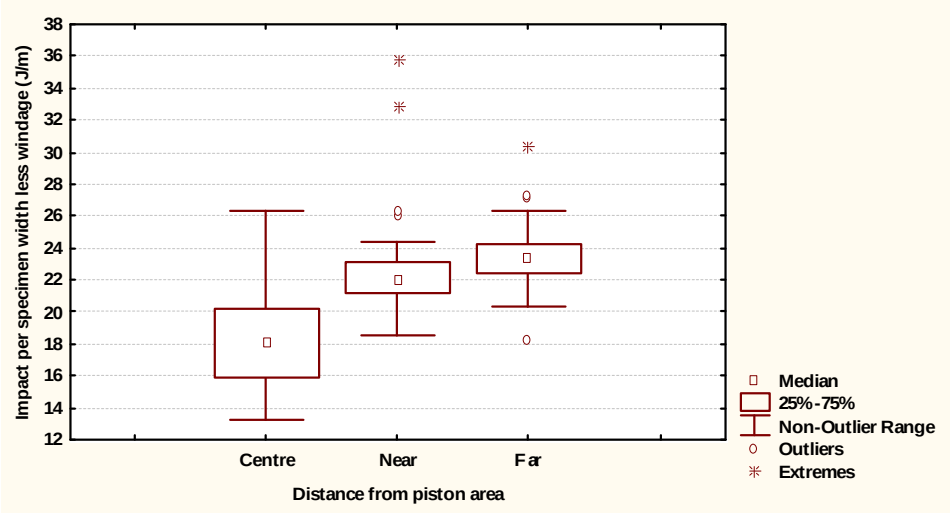

Figure 7.15: Effect of distance from piston area on impact resistance for PP

The area of the sample directly under the piston was seen to undergo some form of compression moulding, which resulted in very little orientation of molecules. However, it was more likely due to a slower rate of cooling under the piston area which allowed more relaxation of the molecules before solidification occurred, hence giving lower impact values with a large variance in results. Specimens further away from the

injection point were seen to have a slight increase in impact resistance due to an increase of orientation in specimens further away from the piston area. This was because the material was believed to experience a slow down of the melt front, thus allowing this orientation to occur.

Direction or orientation of specimens in relation to melt flow direction did not indicate any trends. It was seen that the specimens in the piston area had a lower impact resistance accompanied by a large amount of scatter. A change in barrel temperature was not seen to have any significant influence or trend on the results obtained.

When looking at the components that had been moulded, no warpage could be seen with the naked eye. The components were at first placed on a flat surface and tapped on the corners to verify that there was any movement which would indicate that warpage was present within the sample. It was seen that temperature had more of an influence on the warpage, as seen for injection moulding of PP, than that of the system hydraulic pressure. Warpage was seen to reduce with an increase in either the system hydraulic pressure or system temperature which would have an effect on the viscosity of the melt

Less scatter was seen in Lomolded polypropylene than with that of injection moulding and these components also had the lowest warpage from all the tests conducted thus far. The observations of warpage were quantified by plotting a circle through three points to find the radii of the circle as well as by looking at the standard deviation of all the measured points as seen in Table 7.2 and Figure 7.16 respectively.

The results were plotted on a three dimensional graph without too many assumptions having to occur as the rotatable central composite design for the experiments was used. Thus the graph area had sufficient data to plot the surface plot of the results as seen in Figure 7.17.

Table 7.2: Inverse or radii of curvature for Lomolded polypropylene

Board Number	Y1 (L) @ X=30.78	Y2 (L) @ X=150.20	Y3 (L) @ X=269.27	(1/R (L)) Exp 8	Y1 (W) @ X=37.86	Y2 (W) @ Y=86.36	Y3 (W) @ X=171.48	(1/R (W)) Exp 8
L4-12	25.50	25.47	25.03	**1**	26.31	25.55	25.50	**13**
L4-28	25.53	27.06	24.85	**202**	26.62	27.06	26.31	**120**
L4-26	25.52	26.15	24.87	**48**	26.52	26.07	26.33	**43**
L5-27	25.47	26.14	25.06	**43**	26.33	26.27	25.38	**21**
L5-22	25.45	25.73	25.11	**10**	25.92	25.81	25.20	**24**
L5-19	25.39	26.02	25.07	**35**	26.26	26.12	25.19	**47**
L6-28	25.52	25.45	25.21	**1**	25.81	25.44	25.42	**3**
L6-22	25.54	25.19	25.25	**1**	25.54	25.11	25.31	**31**
L6-17	25.51	24.99	25.24	**8**	25.53	24.93	25.22	**63**
L7-23	25.50	25.63	25.10	**4**	26.28	25.62	25.61	**1**
L7-19	25.48	25.65	25.12	**5**	26.20	25.68	25.55	**24**
L7-15	25.52	25.62	25.11	**3**	26.12	25.65	25.49	**27**
L12-24	25.41	24.99	25.14	**4**	25.49	24.96	25.02	**12**
L12-19	25.41	25.01	25.22	**5**	25.44	24.92	25.07	**29**
L12-17	25.38	24.84	25.23	**12**	25.38	24.81	25.00	**40**
L13-13	25.40	24.31	25.30	**63**	25.01	24.19	25.00	**241**
L13-23	25.35	24.18	25.30	**77**	24.88	24.02	25.02	**312**
L13-30	25.34	24.26	25.32	**68**	25.06	24.06	25.18	**399**
L8-14	25.55	25.59	25.19	**1**	26.05	25.66	25.15	**72**
L8-19	25.47	25.75	25.17	**10**	26.04	25.81	25.27	**43**
L8-27	25.49	25.62	25.17	**3**	26.09	25.68	25.30	**56**
L9-26	25.39	24.30	25.32	**66**	25.49	24.32	24.96	**271**
L9-23	25.37	24.34	25.31	**58**	25.34	24.31	24.98	**248**
L9-17	25.36	24.29	25.32	**65**	25.29	24.21	25.02	**315**
L10-27	25.53	26.84	24.96	**147**	26.38	26.76	26.04	**98**
L10-20	25.52	26.34	25.04	**62**	26.13	26.28	25.60	**39**
L10-14	25.51	26.18	25.07	**45**	26.12	26.15	25.48	**7**
L11-27	25.48	25.35	25.17	**1**	25.76	25.30	25.34	**7**
L11-24	25.43	25.30	25.20	**1**	25.60	25.24	25.38	**18**
L11-18	25.52	25.39	25.21	**1**	25.56	25.26	25.22	**4**

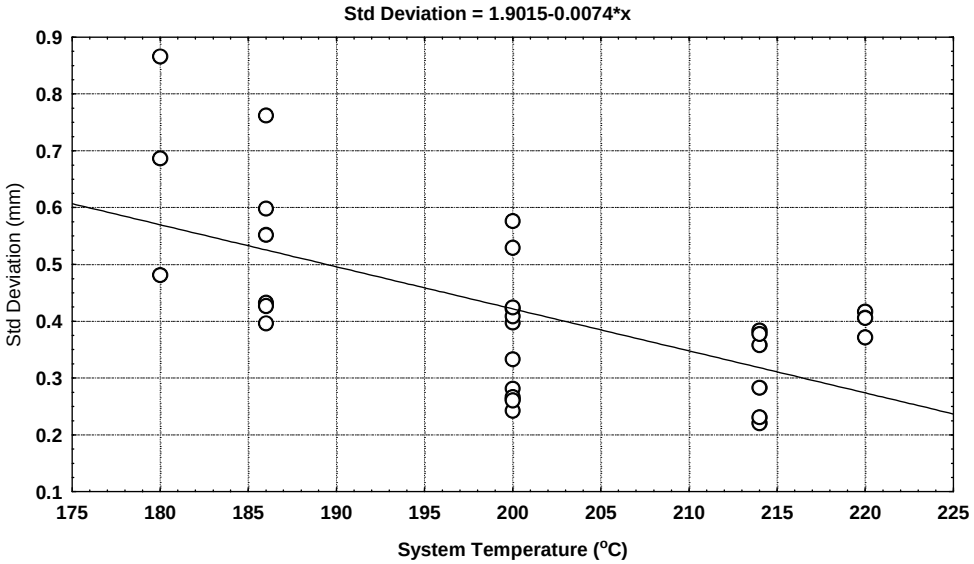

Figure 7.16: Influence of system temperature on standard deviation of warpage measurements

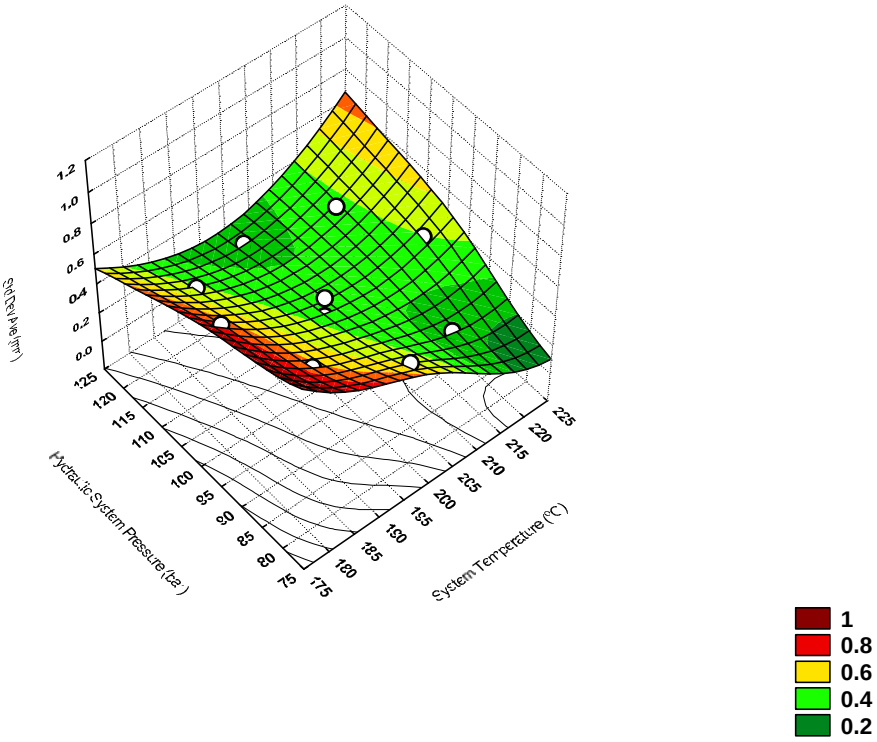

Figure 7.17: 3D Surface plot of Temperature vs Pressure vs Std Deviation

7.2.2 Glass Fibre Reinforced Polypropylene (GFRPP)

Temperature and pressure were seen not to have any affect on the increase of tensile properties of the GFRPP composites that had been Lomolded. Much more scatter was seen in these results than with those of Lomolded polypropylene or with that of injection moulding.

Specimens perpendicular to the direction of melt flow showed an increase in tensile strength compared to those specimens that were parallel or under the piston area. The latter yielded a vast array of scatter in the results as seen in Figure 7.18. The scatter in the specimens from the piston area can also be seen in Figure 7.19. This shows that the tensile results of those specimens near the piston area did not differ from those further away as the flow length was to short for substantial orientation to have occurred.

A higher orientation of fibres in the direction of specimen length was seen to increase the tensile properties of the GFRPP for specimens located perpendicular to the melt flow. Specimens parallel to the melt flow were seen to have fibres perpendicular to the specimens' length, resulting in the lower tensile properties seen. The specimens located under the piston area were seen to undergo compression moulding that would result in lower mechanical properties due to no orientation being present in the area.

Brittle failure was seen in the specimens when subjected to a tensile load, resulting in low elongation as was expected with fibre filled materials. The values observed for tensile strength of GFRPP were substantially lower than that of injection moulding.

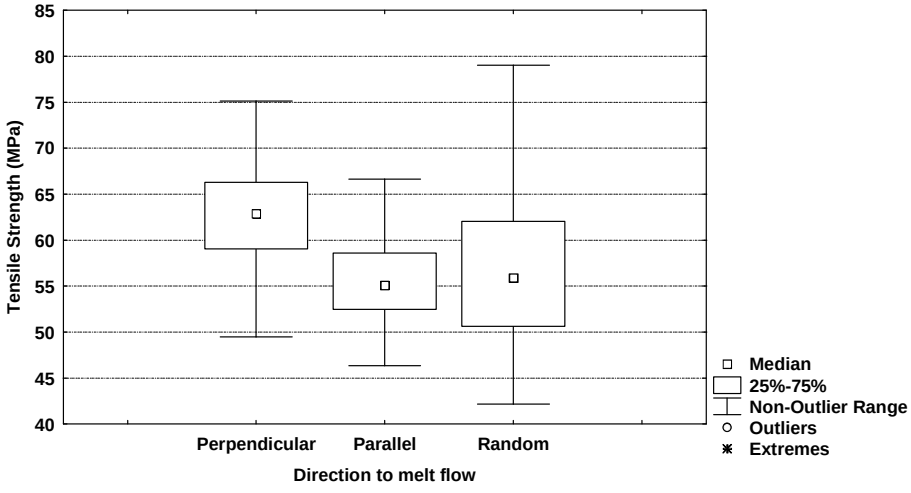

Figure 7.18: Effect of specimen distance on tensile strength

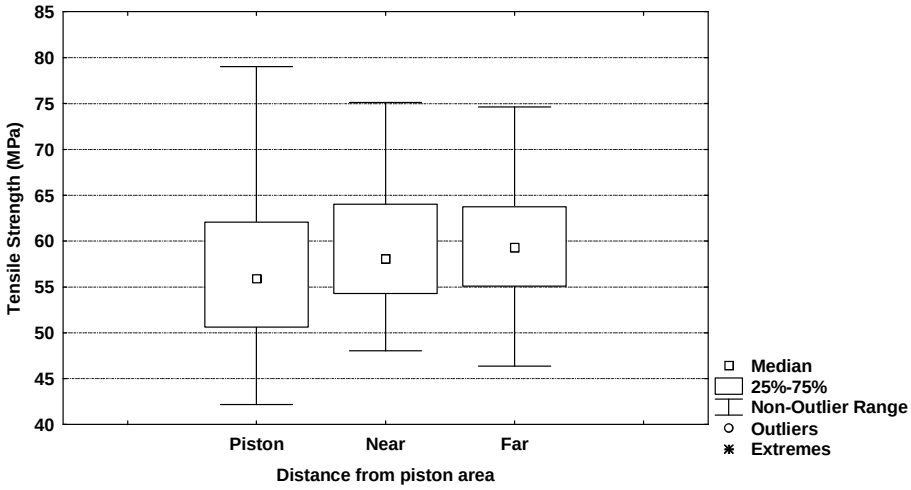

Figure 7.19: Effect of distance on tensile strength of Lomolded GFRPP

Neither the system hydraulic pressure, nor the system temperature, or the distance of specimen sampling was seen to have any affect on the secant or chord modulus on those samples that were manufactured via the Lomold process. It was, however, seen that specimen direction had a big influence on the chord as well as the secant modulus, with an increase of almost 9% and 18% respectively. The increase in the secant modulus can be seen in Figure 7.20.

Those specimens that were parallel to the melt flow had a corresponding fibre orientation that was seen to increase the secant modulus. This was unlike that experienced in the injection moulding of GFRPP specimens parallel to the melt flow. Specimens perpendicular to the direction of melt flow were thought to have fibres orientated across the width of the specimen, thereby resulting in a lower modulus.

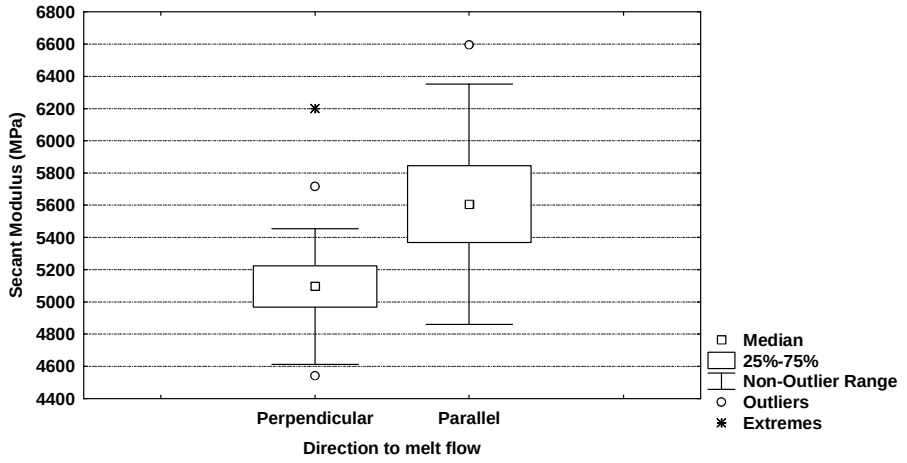

Figure 7.20: Specimen direction seen to influence the chord modulus

The impact resistance of the specimens was seen to be slightly lower than that of injection moulding. A three-fold improvement in impact resistance was seen between GFRPP and unfilled PP. Specimens located in the piston area, as mentioned earlier, either underwent some form of compression moulding (used more for moulding amorphous polymers at a temperature somewhere between the T_g and T_m of the material) or molecular stress relaxation due to the slower cooling of the melt in that area. This resulted in those specimens having a larger amount of scatter than those parallel and perpendicular to the melt flow. The latter had a constant amount of scatter, as well as the former one having a higher impact strength as seen in Figure 7.21.

This increase in impact strength appeared to be as a result of fibre orientation in the specimens' length increasing the amount of fibres to break as was seen for the secant modulus results. Sampling distance, system temperature and system hydraulic pressure were not seen to have any affect on the resistance to impact of the specimens.

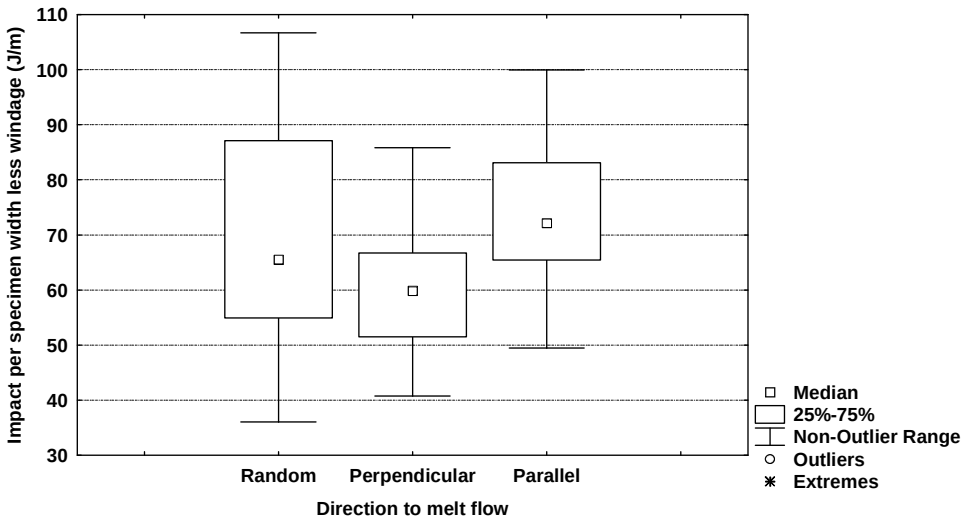

Figure 7.21: Specimen direction seen to influence impact resistance

Similarly, as seen for injection moulding, the warpage in the component was seen to reduce with an increase in system temperature as seen in Figure 7.22. System hydraulic pressure was seen to have no influence on the warpage as a vast array of scatter could be found within the data, much more than that of polypropylene.

The effect of system hydraulic pressure and system temperature combined can be seen in the three dimensional graph in Figure 7.23. It can be seen in the figure that warpage is fairly constant for most of the designed experiment. It tapers off to lower values at a combination of a higher temperature and higher hydraulic pressure. It was also seen that a change in system pressure had less of an effect on the warpage than that of a change in system temperature.

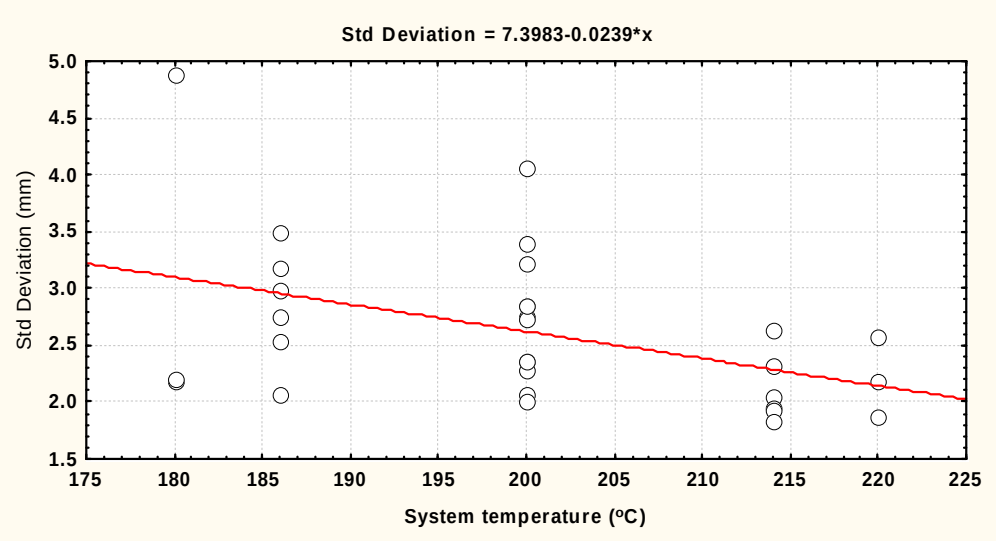

Figure 7.22: Effect of system temperature on standard deviation of warpage

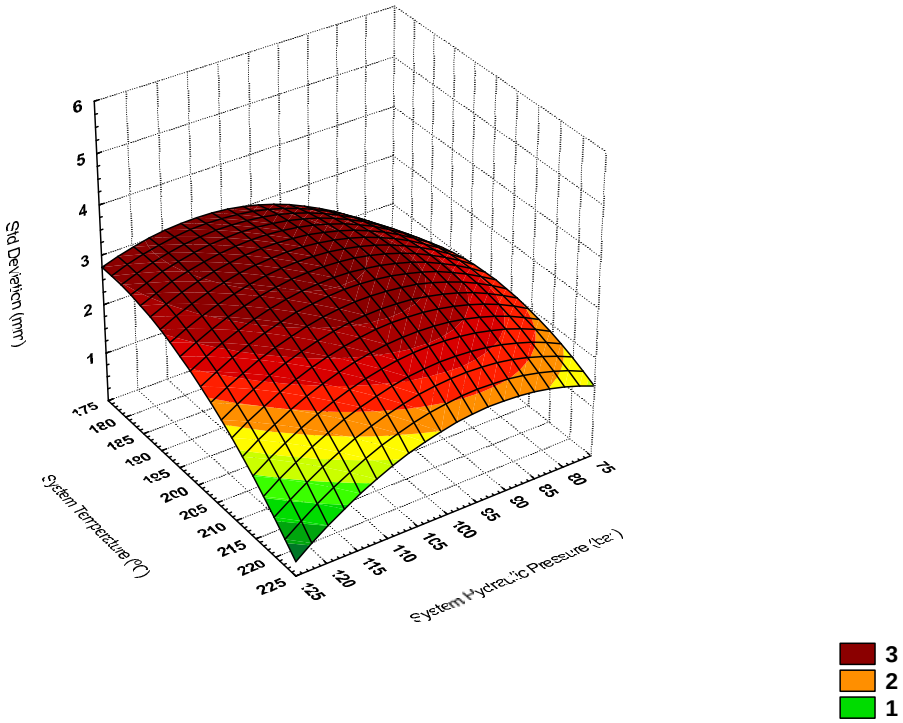

Figure 7.23: Effect of system temperature and pressure on standard deviation

7.3 Comparative process analysis

7.3.1 Mechanical properties

A vast amount of scatter in the tensile strength results was seen for injection moulding of polypropylene, ranging from approx 32.5 MPa to 45.5 MPa as seen in Figure 7.24. It can also be seen that specimens produced via the Lomold process were somewhat lower in tensile strength than those in injection moulding. This resulted in tensile strength ranging between 34 MPa and 37.5 MPa.

It was also seen that using GFRPP yielded the same amount of scatter in the results from the two processes, with a 16% increase in the median of the tensile strength being observed in those that were manufactured via injection moulding.

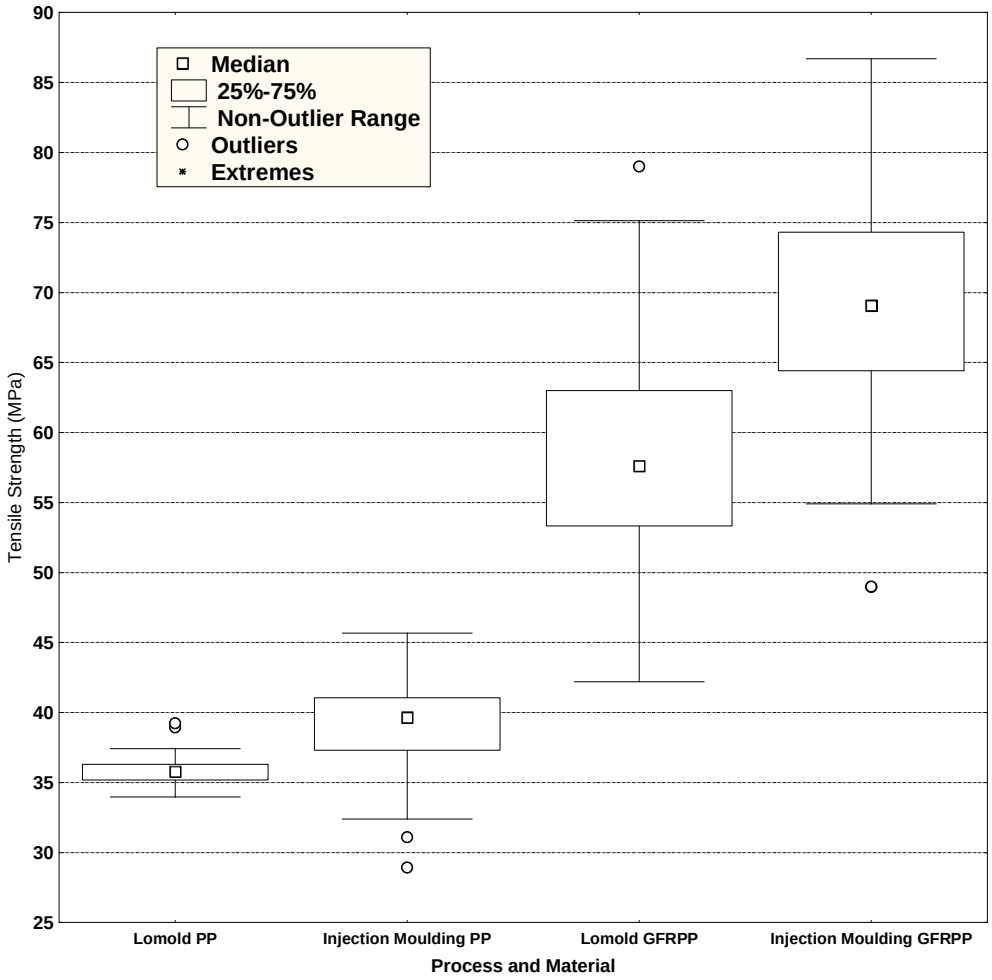

Figure 7.24: Influence of process and material on tensile strength of specimens

The same trends and tendencies that were seen with the tensile results were seen in the chord modulus of the flexural specimens as seen in Figure 7.25. GFRPP was seen to have a higher modulus, hence resulting in a stiffer component than was expected due to the fibre reinforcement within the polymer matrix.

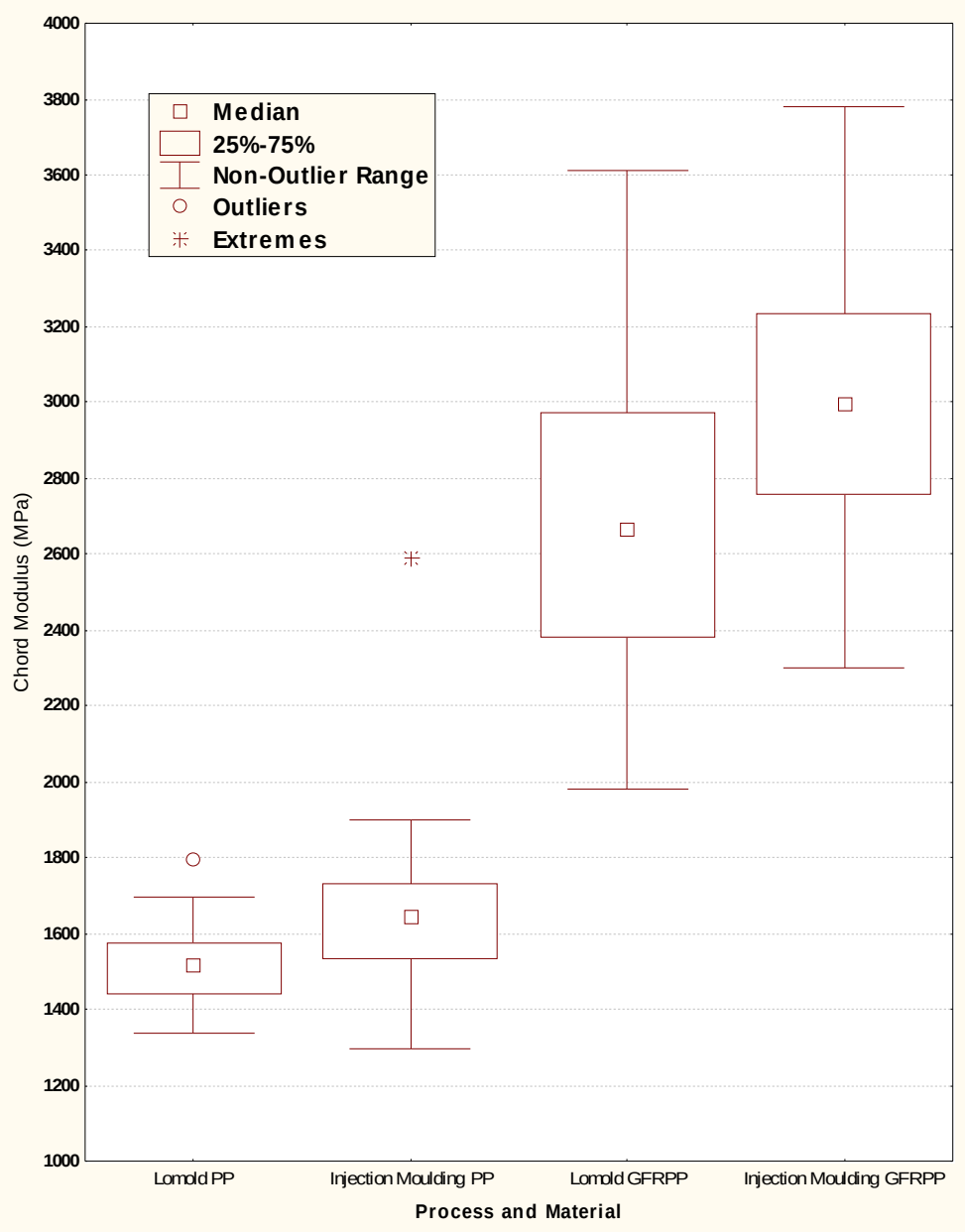

Figure 7.25: Effect of process and material on chord modulus

The impact resistance of injection moulded GFRPP was seen to exhibit a large range of data that was classified as outlying. The scatter seen in the GFRPP specimens was higher for the Lomolded components than for that of injection moulding. The

polypropylene results showed some outlying data with Lomolding, and the median was seen to be 12% lower than that of injection moulded polypropylene. Similarly, as seen in Figure 7.26, the injection moulded GFRPP had an impact resistance 16.5% greater than those samples produced via the Lomold concept.

Most of the specimens resulted in a complete break in the sample when tested. It could be seen that the GFRPP had better impact properties as it was thought the fibres could relay the impact forces to the fibre ends. This resulted in a distribution of forces. compared to that of unfilled polypropylene, resulting in a higher impact resistance.

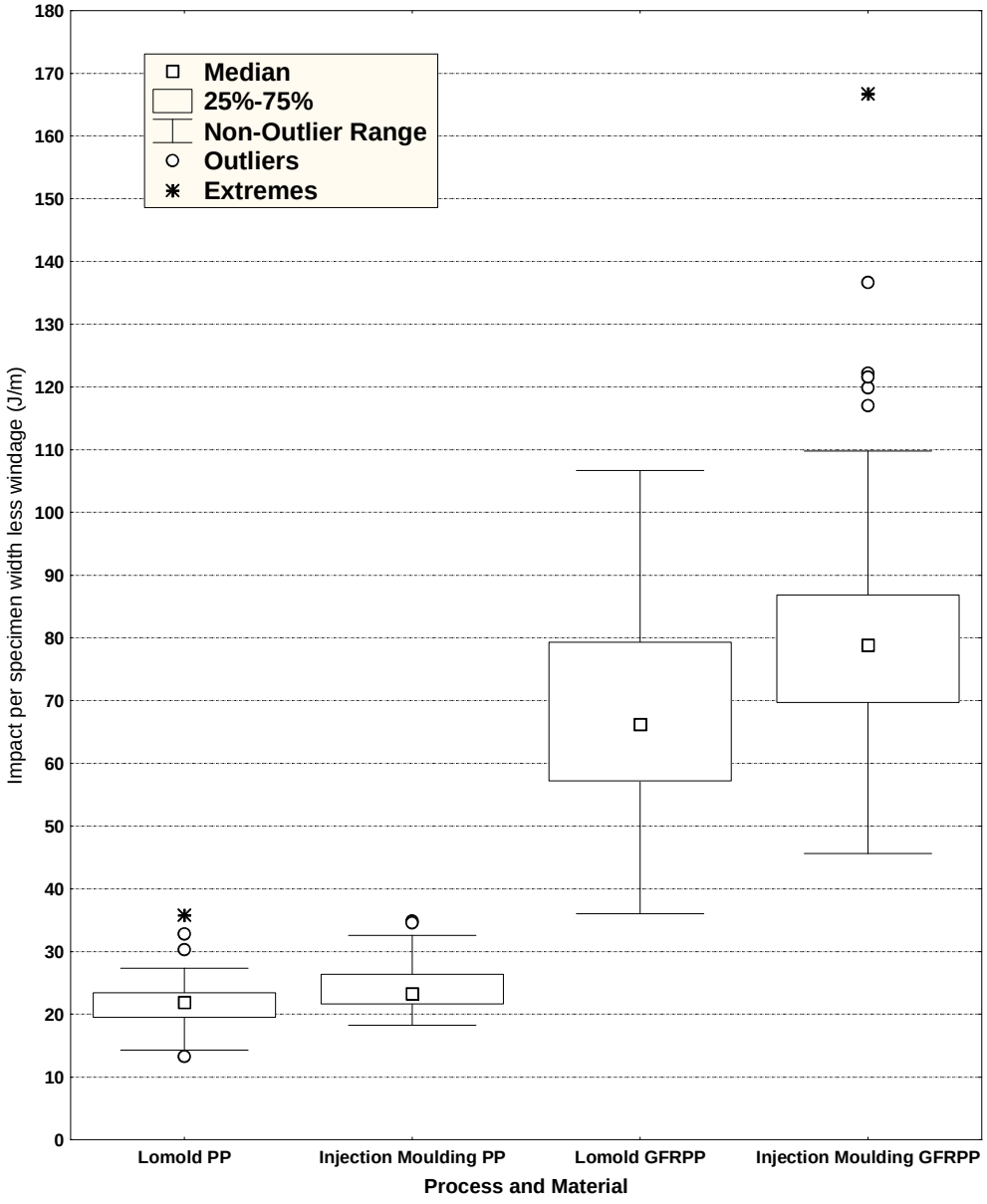

Figure 7.26: Effect of process and material on the impact resistance of specimens

7.3.2 Warpage

Warpage in injection moulding components was seen to be 50% greater than those components produced via the Lomold process, irrespective of the material used. This is evident in Figure 7.27 which shows the warpage of the components at each experimental run according to that of the original design. The reduction in component warpage can be shown easier in Figure 7.28 where it can be seen that, for injection moulded PP, the standard deviation is between 0 - 2 mm compared to that of Lomold produced components having a standard deviation of 0 – 1 mm. Similarly, it was seen that GFRPP resulted in a standard deviation of 4 – 8 mm and 2 – 4 mm for injection moulding and lomolding respectively.

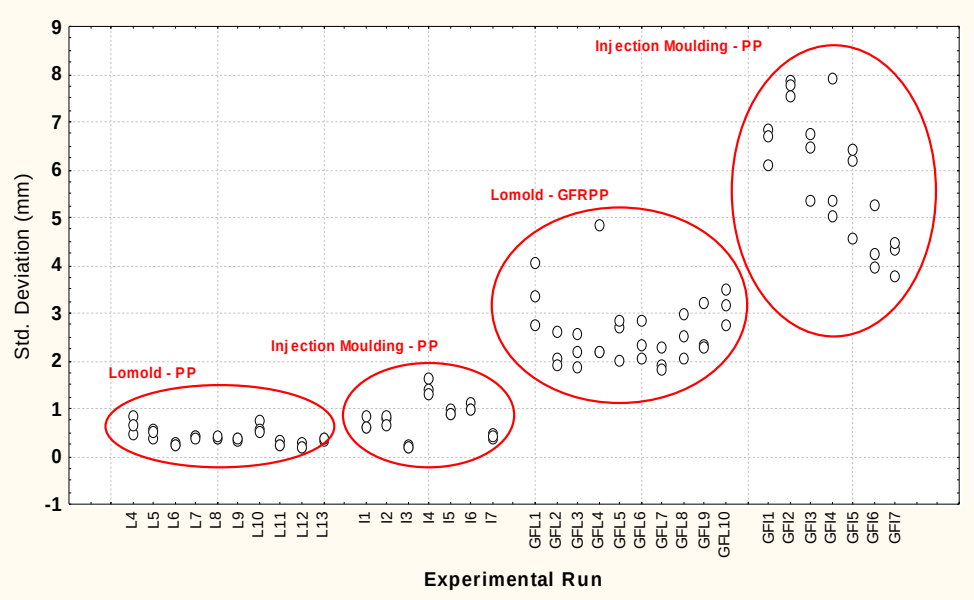

Figure 7.27: Variation of standard deviation due to experimental runs according to the DOE

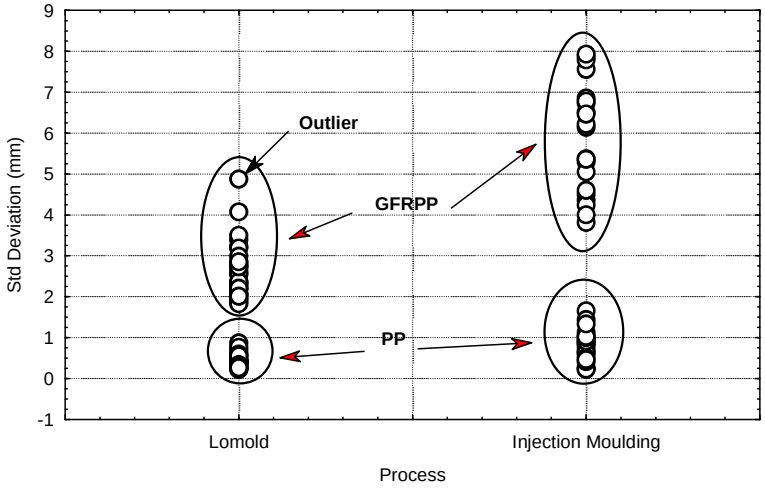

Figure 7.28: 50% Reduction in component warpage seen in Lomold

7.3.3 Resultant glass fibre lengths

The resultant fibre lengths within a component are known to influence the properties as mentioned previously. Many companies do not measure the resultant fibre lengths due to it being a time consuming and a costly exercise. Optical “fibre length analysis” after burning out the polymer from the matrix was preferred [29] as it gives an indication of what the processing was like for the long fibre thermoplastics (as shown in Figure 7.29).

This method was seen to be a quick, practical and easy way of seeing the influence of processing on the resultant fibre length. It was used in conjunction with optical microscopy to measure the resultant fibre lengths. Appendix B and C contains both photographs of the skeletal structure and of the fibres under the microscope for each experimental run that was executed.

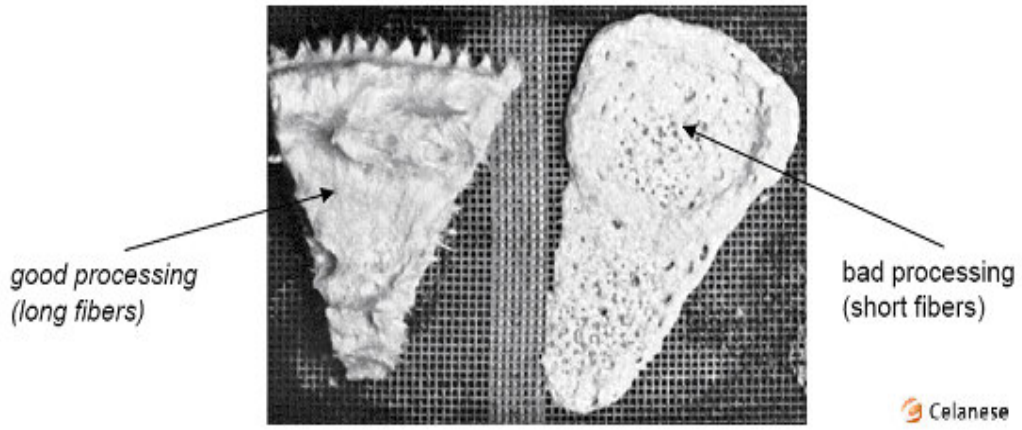

Figure 7.29: Examples of processing conditions on resultant skeletal structures [29]

Fibres from three injection moulded samples, as well as from three lomolded samples, were measured via optical microscopy to obtain the fibre distribution within the component. This can be seen in Figure 7.30 and Figure 7.31 respectively. Fibres were classified in 100 μm intervals up to a length of 3000 μm, whereafter the intervals were increased by 250 μm up to a fibre length of 5000 μm, and then every 1000 μm thereafter. The distributions were seen not to contain any fibres greater than 12 000 μm in length, less than half of the original starting fibre length.

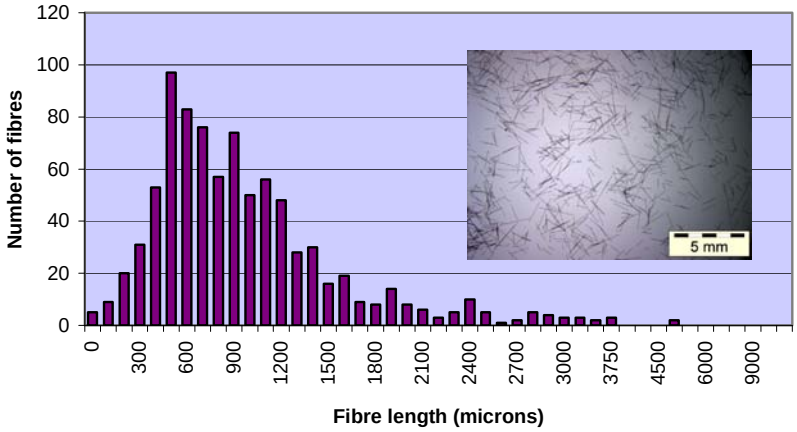

Figure 7.30A: Injection moulding fibre length distribution – component GFI1-24

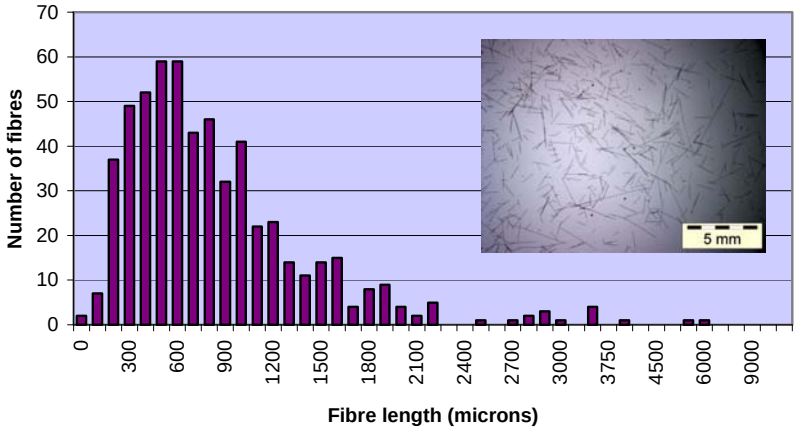

Figure 7.30B: Injection moulded fibre length distribution – component GFI2-27

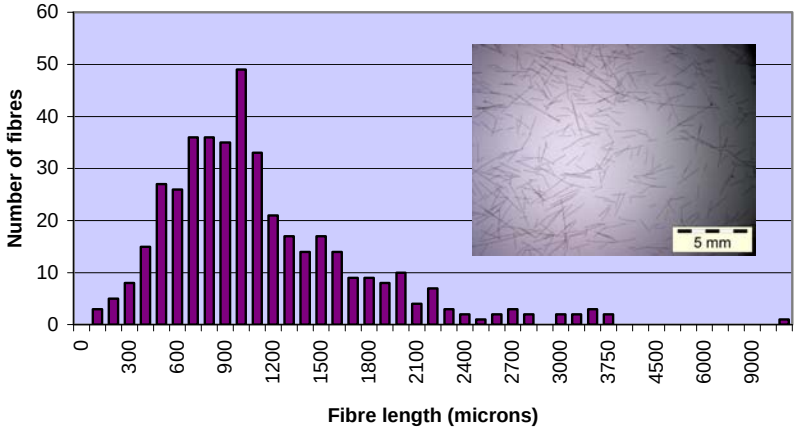

Figure 7.30C: Injection moulded fibre length distribution – component GFI7-21

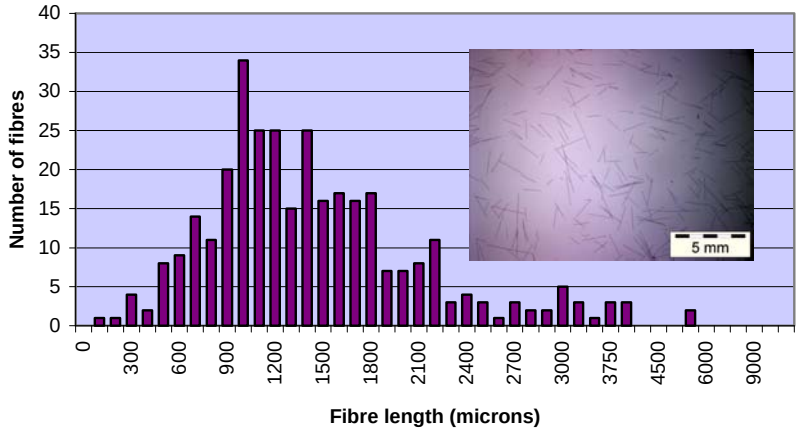

Figure 7.31A: Lomolding fibre length distribution – component GFL5-28

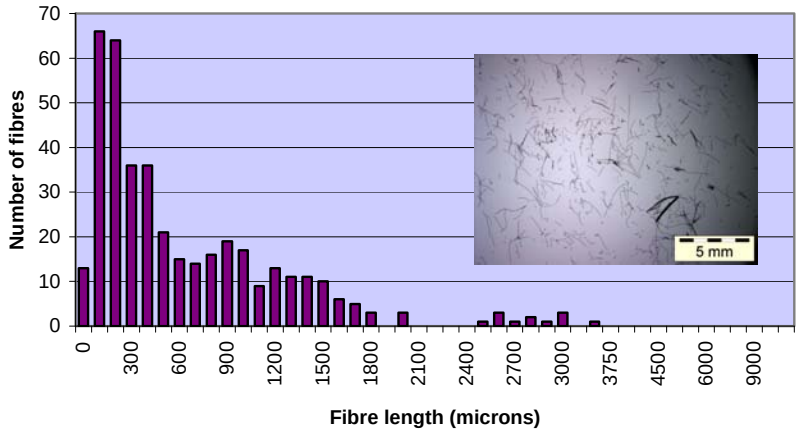

Figure 7.31B: Lomolding fibre length distribution – component GFL7-26

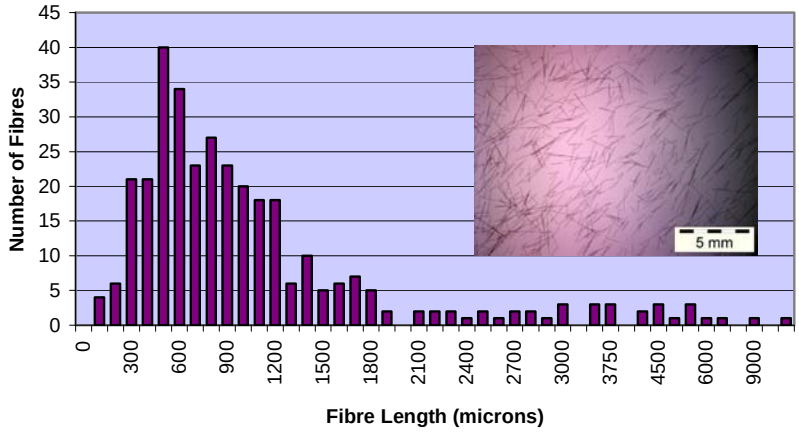

Figure 7.31C: Lomolding fibre length distribution – component GFL8-27

In the results obtained for components produced via injection moulding, it could be seen that the majority of the fibres were less than 2000 μm in length with only a few longer fibres being present within the matrix. It was also noted that this method of fibre length analysis could yield varying results between two samples that were processed under the same conditions that were purely repeated for seeing the repeatability of the measurements as was the case for Figure 7.30A and Figure 7.30C. These results suggest that a vast amount of data is needed to be able to have reproducible results, as it is largely dependent on how and where the samples were taken.

One of the originally perceived advantages of lomolding was that it could minimise fibre breakage thus resulting in a component with longer residual fibre lengths that would be stronger than that which was injection moulded. It is not known exactly where the fibre breakage occurred in the lomold process. However, it was seen that the residual fibre lengths were lower than those of injection moulding in some instances, with a few fibres being longer than 3 mm in length. Possible breakage of fibres in the lomolding process could have occurred in the hot runner system as the melt had to undergo changes in direction as well as a change in velocity in the region of the outfeed valve.

Critical fibre lengths ranging from 2 – 3 mm are often seen in literature, but can be reduced to 0,9 mm when using a chemically modified polypropylene. [29] If too high a percentage of the fibres are shorter than this, worse mechanical properties will result due to the fibre pullout effect. The fibre length alone does not define the material properties, as the critical fibre length is dependent on the diameter of the fibre, the tensile strength of the fibre, as well as the shear stresses between the fibre and polymer interface. [54] The latter has more of an effect in this work as the same materials were used for the analyses.

During microscopy it was noted that some fibres in certain experimental designs had been kinked and were very short, resulting in a very narrow fibre length distribution at lower fibre lengths, as that seen in Figure 7.30B. This can result in a high amount of fibre pullout. These and other microscopy images can be seen in Appendix B and C, along with photos showing the skeletal structure of the remaining fibres after burn off of the matrix resin. It can also be seen in the photos of the skeletal structure that certain experimental runs resulted in a finer structure. This made sampling of fibres much more difficult as they had seemed to adhere to one another even though the temperature in the furnace did not reach the temperature at which glass melts.

7.3.4 Cavity pressures

A better comparison between the two processes was made by recording the pressure within the cavity by means of a series of cavity pressure sensors in the mould that was connected to a data acquisition system. This was due to the post injection pressure in injection moulding being based on the pressure of the melt as opposed to that of the hydraulic pressure in lomolding. This resulted in two totally different sets of values which would not be comparable.

The cavity pressures were seen to vary greatly between the two processes and, in some cases, the cavity pressures in lomolding were seen to be higher than those in injection moulding, and visa versa. The recorded pressures for each experimental run can be seen in a graphical format in appendix B and C, along with that of the set experimental values. One such set of results for injection moulding and lomolding can be seen in Figures 7.32 and 7.33 respectively.

When looking at the graph obtained from injection moulding, it could be seen that the curve for pressure sensor 0 reflects that of the pressure in the injection unit. The latter is machine related, similar to that which was shown in Figure 6.2, and cannot be taken into account for any cavity pressure measurements. Pressure sensors 1 and 2 are seen to increase steeply, with a sudden decrease in pressure. After this it increases steeply once again, much like that of a heart beat on a heart rate monitor. This “beat” indicates the position where change-over occurred in the injection unit from speed to pressure control.

At the point where the mould cavity was totally filled, the pressure was seen to reach a maximum value for a short while and then started to decrease gradually with the solidification of the melt. A second “beat” could be seen in this area. This could be attributed to the plasticizing action of the screw. This only affected the pressure sensors that were located under or near the point of injection and not those that were located further away.

The resultant graphs seen from lomolding can be regarded as somewhat similar to those obtained from injection moulding. The pressure also increased steeply with a “beat” occurring in the region of increasing pressure due to the switch-over point between speed control and position control of the moulding piston. No second “beat” was seen due to the moulding piston sealing off the cavity and hence not allowing

anymore melt through. It was also seen that the pressure measured at sensors 0 and 1 remained constant during solidification of the melt, unlike that of pressure sensor 2. The latter was seen to decline gradually over a few seconds after reaching the peak pressure directly after injection as was experienced in the injection moulding process.

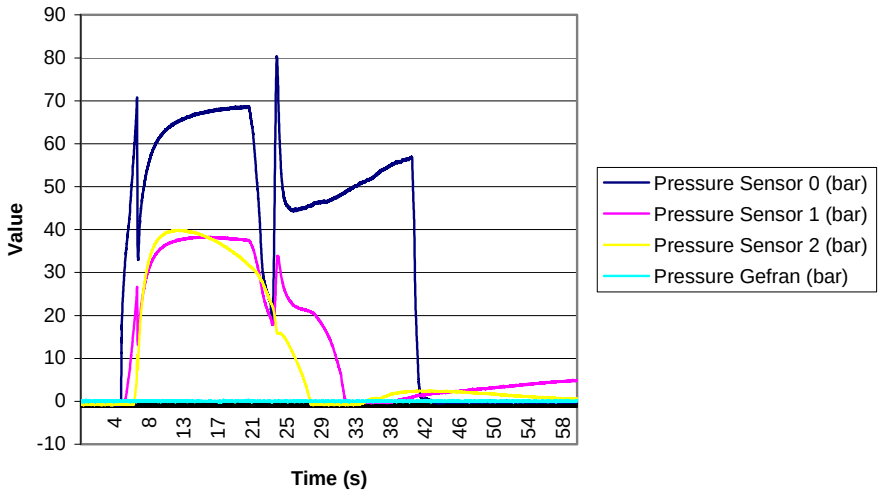

Figure 7.32: Cavity pressures recorded in injection moulding

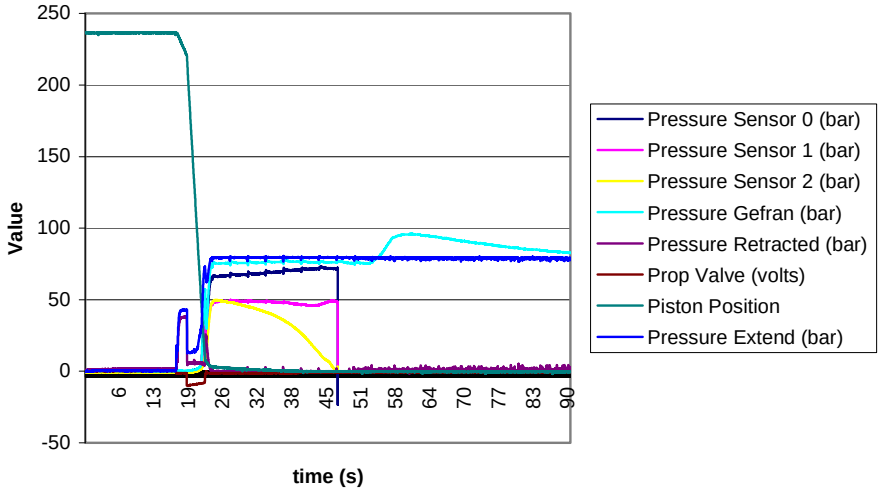

Figure 7.33: Cavity pressures recorded in lomolding

It can also be seen in Figure 7.33 that the previous concern of the pressure sensors giving much lower values than those that were computed numerically for lomolding [8], can be confirmed by the Gefran melt pressure transducer which was placed alongside that of pressure sensor 0, with a very little difference seen between them.

Chapter 8. Conclusion and recommendations

Research was done on two plastics moulding processes. One was conventional injection moulding through a nozzle and sprue, whilst the other was one of many emerging “low-pressure” injection moulding processes using a melt accumulator. The latter transfers melt to a moulding barrel and piston which then forms part of the mould cavity wall during moulding.

A design of experiments approach was taken to provide a set of experiments. These would enable the effect of specimen orientation, specimen distance, moulding temperatures and moulding pressures to be expressed in terms of the following: tensile strength; flexural modulus; impact resistance; warpage; cavity pressures, and the resultant fibre lengths when moulding unfilled polypropylene and glass fibre reinforced polypropylene.

8.1 Conclusions

It was seen that the specimen orientation had no effect on the mechanical properties when using unfilled polypropylene. This was compared to when glass fibre reinforced polypropylene was used in either of the processes. The orientation of the glass fibres in the testing direction resulted in an increase in not only the tensile strength, but also in the impact strength, as well as a 5% increase in the chord modulus in samples produced via injection moulding.

Similarly, for lomolded samples, the tensile strength of the specimen was seen to increase with specimens orientated perpendicular to the direction of melt flow. The secant modulus increased with fibre orientation. This was more so in those specimens orientated parallel to the melt flow unlike that seen in injection moulding. The impact resistance was also seen to increase in those specimens that were orientated parallel to the melt flow, as the increase of fibres resulted in more fibres having to be broken.

In injection moulding of polypropylene, it was seen that the tensile strength decreased with an increasing distance from the sprue. This was unlike that of lomolded components where no difference was seen. A higher tensile strength was seen in glass fibre reinforced specimens located directly next to the injection point than in those

located elsewhere in the component. With lomolding no differences could be seen between specimen sampling distances.

It was seen that the distance of sampling had no effect on the GFRPP components produced via lomolding. On the other hand that of unfilled PP for both processes and for lomolded GFRPP showed a decrease in the secant modulus with increasing sampling distance from the injection point or piston area.

The impact strength of unfilled PP specimens taken from both processes was seen to be lower in the piston area than elsewhere in the component, where it was seen to remain close together. With GFRPP the total opposite was seen in that the piston area resulted in a higher impact resistance.

Tensile strength, flexural modulus and impact resistance were seen not to be affected by a change in the moulding temperature of GFRPP components. The same is also true for polypropylene moulded by both processes except that the secant modulus in injection moulded polypropylene had varied in no particular trend. This was seen with those that were lomolded.

A change in moulding temperature also brought about a change in the amount of warpage that was seen, no matter which material or process had being used to manufacture the components. The increase in melt temperature resulted in longer cooling times. This allowed relaxation of the materials and fewer moulded in stresses, as well as a lower pressure difference between the injection point and the furthest point. This resulted in the lower warpage.

In lomolding PP or GFRPP, the hydraulic system pressure was seen to have no effect on the tensile, flexural or impact strengths of the specimens, as was seen in injection moulding. The increase of pressure resulted in a lower secant modulus and an increase of impact resistance in injection moulding of PP. Similarly, for injection moulded GFRPP, the Young's modulus was seen to decrease with the increase in pressures, while at the same time the impact was seen to increase.

Warpage was seen to be reduced either by, an increase in the moulding temperature or the hydraulic pressure, whether it was the post injection pressure in injection moulding or the system pressure in lomolding. It was also seen that warpage is influenced by many other factors that were not investigated in this thesis.

Injection moulding had a higher degree of molecular orientation resulting in the tensile strength and the chord modulus having higher values than those seen in lomolding. Similarly, for GFRPP the injection moulded specimens had a 16% increase above that of the lomolded specimens, with the same amount of scatter.

The warpage in injection moulding components was seen to be 50% greater than those components produced via the lomold process, irrespective of the material used. The lowest warpage observed in unfilled polypropylene components were those that were lomolded. Similarly, the same was found for the glass fibre reinforced components. The reduction of warpage observed can be attributed to a few factors, for example, lower shear stresses in the cavity resulted in less moulded-in stresses in the final component and thus resulted in lower warpage; an increase in temperature resulted in smaller pressure differences and thus reduced warpage.

The resultant fibre matrix obtained after polymer burn-off can give an indication of what the processing was like. This was seen to cause fibre attrition mainly in the screw of the plasticizer. Injection moulded and lomolded components were ashed to obtain glass fibres to be able to measure them on an optical microscope. This revealed that the fibre distributions obtained from the two processes were somewhat complex in that there was no definite trend. In general, it was seen that the resultant fibre lengths were shorter in lomolding, hence reducing the properties as was seen. Cavity pressures were seen to vary greatly between experiments as well as between processes, with no particular trend being seen in the results.

8.2 Recommendations for further work

There is scope for more work and improvements on this project and on the technology. The author will mention a few aspects that he feels would considerably improve the work and also improve the properties of the materials. These improvements would allow new products to be manufactured using this technology. Previously these products were somewhat difficult to manufacture with special reference to large industrial applications.

A large amount of work in future can be conducted on the fibre reinforcement of polypropylene and, more specifically, on the reduction of fibre attrition in the lomold

process by the incorporation of a twin screw compounder linked to the metering unit, thus eliminating a large portion of fibre breakage. Alternative fibres could also be investigated such as recycled polyester yarns, natural fibres, etc. in a PP matrix that can be lomolded.

A new machine design that is fibre-friendly needs to be investigated if long fibres are to be incorporated in the final component to increase the mechanical properties. This can only happen if the interfacial shear stress between the polymer and the matrix is maintained or improved. This would also involve the study on its microscopic properties.

References

[1] Delmonte, J., ***Plastics Molding***, John Wiley and Sons Inc, 1952

[2] Haagh, G.A.A.V., Phd Thesis: ***Simulation of gas-assisted injection moulding***, Eindhoven Technical University, 1998, ISBN: 90-386-0620-6

[3] ManTech, Manufacturing Technology Database, http://iprod.auc.dk/mantec/

[4] Rubin I.I., Handbook of Plastic Materials and Technology, Rubin I.I. (Ed.), John Wiley and Sons Inc, 1990

[5] Arburg, ***Practical guide to injection moulding***, (Edited by V. Goodship), Rapra Technology Limited, UK, 2004

[6] Turng, L., ***Special and emerging injection moulding processes,*** Journal of injection molding technology, September 2001, Vol 5, No. 3, pages 160 - 179

[7] Hettinga, S., Innovation in Polymer Processing – Molding, J.F. Stevenson (Ed.), Hanser, 1996

[8] Dymond, J.A.D., MEng Thesis: ***The simulation of the flow of polymer melt in lomolding,*** Stellenbosch University, 2004

[9] Thomason, J.L. and Vlug, M.A., ***Influence of fibre length and concentration on the properties of glass fibre-reinforced polypropylene: 1. Tensile and flexural modulus***, Composites: Part A 27A, 1996, pages 477 - 484

[10] Thomason, J.L. and Vlug, M.A., ***Influence of fibre length and concentration on the part properties of glass fibre reinforced polypropylene: 2. Thermal properties***, Composites: Part A 27A, 1996, pages 555 - 565

[11] Thomason, J.L. and Vlug, M.A., ***Influence of fibre length and concentration on the part properties of glass fibre reinforced polypropylene: 3. Strength and strain at failure***, Composites: Part A 27A, 1996, pages 1075 - 1084

[12] Thomason, J.L. and Vlug, M.A., ***Influence of fibre length and concentration on the part properties of glass fibre reinforced polypropylene: 4. Impact properties***, Composites: Part A 28A, 1996, pages 277 - 288

[13] Thomason, J.L. and Vlug, M.A., ***Influence of fibre length and concentration on the part properties of glass fibre reinforced polypropylene: 5. Injection moulded long and short fibre PP*** , Composites: Part A 33, 2002, pages 1641 - 1652

[14] Mennig, G. and Wolf H.J., ***Fibre attrition when processing filled thermoplastics in a screw / barrel system***, paper presented at PLASTKO '97 conference, Plasty a Kaucuk 34, 1997/10, pages 295 - 298

[15] Osswald, T.A., and Menges, G., ***Materials science of polymers for engineers***, Hanser publishers, 1995

[16] Steinbichler, G., Engel fibremelt brochure: ***Processing of long fibre thermoplastics***, Engel, 1998

[17] Thomason, J.L., Micromechanical parameters from macromechanical measurements on glass reinforced polypropylene, Composites Science and Technology, 2002, pages 1455 - 1468

[18] Zhang, G., and Thompson, M.R., ***Reduced fibre breakage in a glass-fibre reinforced thermoplastic through foaming***, Composite science and technology, 2005, pages 2240 - 2249

[19] Reinforced plastics magazine, ***LFT's for automotive applications***, February 2005, pages 24 - 33

[20] Reinforced plastics magazine, ***Car makers increase their use of composites***, February 2004, pages 26 - 32

[21] Reinforced plastics magazine, ***VW chooses long fibre PP for Golf***, December 2003, page 8

[22] Hettinga, S., ***Low pressure method for injection moulding a plastic article***, US Patent # 5,853,630, 1998

[23] Fu, S.Y., et al, ***Correction of the measurement of fiber reinforced thermoplastics***, Composites: Part A33, 2002, pages 1549 - 1555

[24] Joseph, P.V., et al, ***Effect of processing variables on the mechnical properties of sisal-fiber-reinforced polypropylene composites***, Composites Science and Technology 59, 1999, pages 1625 - 1640

[25] Hernandez, J.P., et al, ***Analysis of fiber damage mechanisms during processing of reinforced polymer melts***, Engineering Analysis with Boundry Elements 26, 2002, pages 621 - 628

[26] Thomason, J.L., ***Interfacial strength in thermoplastic composites – at last an idustry friendly measurement method?,*** Composites: Part A33, 2002, pages 1283 - 1288

[27] ASTM D256-02, Standard test methods of determining the Izod impact resistance of plastics, ASTM International, 2002

[28] Smorgon, S., and Berelovich, L., ***Injection moulding of large plastic components***, US Patent # 6,464,910 B1, 2002

[29] Littwitz, B., ***Fibre length - short,*** presentation sent via email, Ticona GmbH, 2004

[30] Thomason, J.L. and Schoolenberg, G.E., ***An investigation of glass fibre / polypropylene interface strength and its effect on composite properties***, Composites, Vol 25, Number 3, 1994, pages 197 - 203

[31] Neves, N.M., et al., ***Fiber contents effect on the fiber orientation in injection molded GF/PP composite plates***, Antec, 2002, pages 2089 - 2092

[32] Beaumont, J.P., et al., ***Successful injection moulding. Process, Design, and Simulation***, Hanser, 2002

[33] Vincent, M., et al., ***Description and modeling of fiber orientation in injection moulding of fiber reinforced thermoplastics***, Polymer volume 46, 2005, pages 6719 - 6725

[34] Bürkle, E., et al., ***Injection moulding of long-glassfibre-reinforced PP***, (Translated from Kunststoffe 3/2003, pp 47-50), Kunststoffe plast europe, Hanser, 2003, pages 17 - 19

[35] Singh, R., et al., ***Injection moulding of glass fiber reinforced phenolic composites. 2: Study of the injection moulding process***, Polymer composites Vol. 19 No. 1, February 1998, pages 37 - 47

[36] Yilmazer, U., and Cansever, M., ***Effects of processing conditions on the fibre length distribution and mechanical properties of glass fiber reinforced nylon-6***, Polymer composites Vol. 23 No. 1, February 2002, pages 61 - 71

[37] Coperion Werner & Pfleiderer, ***Long fibre thermoplastics: compounding and direct processing***, Plastics additives & compounding, February 2002, pages 20 - 21

[38] Schijve, W., ***High performance at medium fibre length in long glass fibre polypropylene***, Paper first presented at 3rd AVK-TV conference in Baden-Baden, Germany, 2000, pages 14 - 21

[39] Matsuoka, T., ***Fiber orientation prediction in injection moulding***, Chapter 3 of book 3 'Polypropylene:Structure, blends and composites', (Edited by J. Karger-Kocsis), Chapman & Hall, London, 1995

[40] Del Vecchio, R.J., ***Understanding design of experiments: A primer for technologists***, Hanser, Munich, 1997

[41] Dealy, J.M., and Wissbrun, K.F., Melt rheology and its role in plastics processing: Theory and applications, Kluwer academic publishers, 1999

[42] Sasol Polymers, ***Material Data Sheet for PP1100N***, July 2002

[43] Ticona GmbH, ***Celstran brochure (english)***, December 2000

[44] Tom du Toit, Managing Director, Qtec moulding, tom@qtec-moulding.com, personal communication.

[45] McGrath, J.J., ***Determination of 3D fiber orientation distribution in thermoplastic injection moulding***, Composite science and technology 53, 1995, pages 133 - 143

[46] Waschitschek, K***., Influence of push-pull injection moulding on fibre and matrix of fibre reinforced polypropylene***, Composites: Part A 33, 2002, pages 735 - 744

[47] ASTM D4101-02b, ***Standard specification for polypropylene injection and extrusion materials***, ASTM International, 2003, pages 648 - 663

[48] ASTM D790-02, ***Standard test methods for flexural properties of unreinforced and reinforced plastics and electrical insulating materials***, ASTM International, 2002, pages 146 - 154

[49] ASTM D638-02a, ***Standard test method for tensile properties of plastics***, ASTM International, 2003, pages 46 - 59

[50] ASTM D618-00, ***Standard practice for conditioning plastics for testing***, ASTM International, 2001, pages 36 - 39

[51] Hettinga, S., ***How low-pressure injection moulding differs from conventional molding***, Modern plastics international, June 1992, pages 60 - 63

[52] Plastiscope, ***Low-pressure injection molding gains from new technologies***, Modern plastics international, March 1990, pages 5 - 6

[53] Plastamid, Member of the Chemical Services Group, 43 Coleman street, Elsies river, SA

[54] Laine, T., Product Manager LFT, Ticona GmbH, Correspondence via email

[55] Kahr, F., Exchange student from Germany working on Thripp project, 2005

[56] Kistler Instruments, represented by Inher S.A. (Pty) Ltd, Correspondence via email

[57] Sasol Polymers, ***Laboratory results report RM148***, 2005

[58] Ticona, ***Materials data sheet*** from www.ticona.de

[59] Sasol Polymers, ***Laboratory results report RZ176***, 2004

[60] Chen, T., and Yao, M-l., ***Sample analysis report for University of Stellenbosch***, TA Instruments, Dec 2005, pages 14 - 28

[61] Rebolo, M., ***Report – Polymer samples, Ref # uni0912mr***, Advanced Laboratory Solutions, 2005

[62] Wolf, H.J., ***Screw plasticating of discontinuous fiber filled thermoplastics: Mechanisms and prevention of fiber attrition***, Polymer Composites, October 1994, Vol 15, No. 5, pages 375 – 384

Appendices

Table of Contents

Appendix A: Material properties

Appendix A1: Unfilled polypropylene (PP1100N)

Mechanical tests such as tensile, flexural, and impact resistance were executed using an unfilled homopolymer polypropylene for verification of material used and as a benchmark in which to compare other materials to. Samples were injection moulded into test pieces as seen in Figure A1 with an Engel 80 T injection moulder fitted with a standard 30 mm diameter screw. The Plastamid test reports follow;

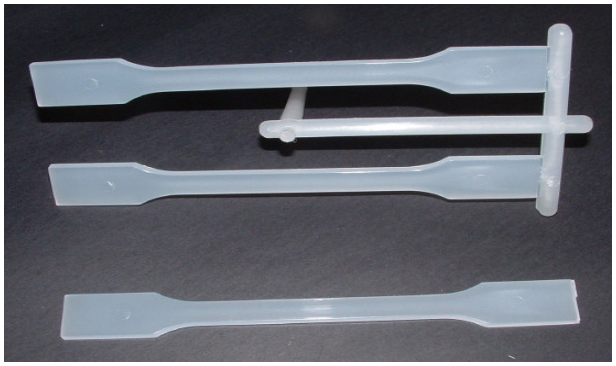

Figure A1: Moulded test pieces used for tensile and impact tests

Sample width: 10 mm
Sample thickness: 4 mm
Speed: 50 mm/min
Gauge length: 115 mm

PLASTAMID
ENGINEERING POLYMERS
Member of the Chemical Services Group

Sample reference	Stress at break MPa	Stress at yield MPa	Strain at yield %	Strain at break %
PP 1100N (NAT)	10.6	34.1	10.5	393.6
PP 1100N (NAT)	15.6	34.2	10.8	23.4
PP 1100N (NAT)	19.2	35.0	11.4	419.4
PP 1100N (NAT)	18.2	34.6	11.0	352.1
PP 1100N (NAT)	18.6	34.7	10.7	172.3
PP 1100N (NAT)	10.8	34.8	10.9	350.6
PP 1100N (NAT)	22.6	33.6	11.4	368.3
PP 1100N (NAT)	22.8	34.6	11.5	417.9
PP 1100N (NAT)	21.0	34.8	10.8	384.9
PP 1100N (NAT)	20.6	34.1	11.1	546.9

Statistics

Mean	18.0	34.5	11.0	342.9
Standard Deviation	4.4	0.4	0.3	145.1

Figure A2: Tensile test report – PP 1100N. [53]

Sample width: 10 mm
Sample thickness: 4 mm
Speed: 10 mm/min

PLASTAMID
ENGINEERING POLYMERS
Member of the Chemical Services Group

Sample reference	Flex Strength MPa	Flex Modulus MPa	Chord Modulus MPa
PP 1100N (NAT)	48.6	1639.7	1585.6
PP 1100N (NAT)	50.4	1615.9	1627.1
PP 1100N (NAT)	51.0	1591.0	1647.0
PP 1100N (NAT)	52.8	1598.3	1597.8
PP 1100N (NAT)	48.6	1613.3	1620.9
PP 1100N (NAT)	48.4	1640.6	1609.9
PP 1100N (NAT)	49.6	1611.2	1611.5
PP 1100N (NAT)	49.1	1652.5	1620.1
PP 1100N (NAT)	50.2	1591.1	1602.2
PP 1100N (NAT)	51.3	1613.9	1585.6

Statistics

Mean	499.9	16167.5	16107.7
Standard Deviation	1.4	20.2	18.1

Figure A3: Flexural strength report – PP 1100N. [53]

Zwick / Roell Standard protocol 03.11.2005

Parameter table:

Customer : PLAST
Tester : brett
Test standard : pp natural
Material :
Test device 1 :
Test device 2 :
Test device 3 :

Results:

Nr	Impact resistance kJ/m²	Impact resistance/Notch length J/m	Type of test, PIT	Work contents J
46	3.64	14.54	Izod	2.75
47	3.64	14.54	Izod	2.75
48	3.53	14.13	Izod	2.75
49	4.33	17.32	Izod	2.75
50	3.33	13.34	Izod	2.75
51	3.73	14.92	Izod	2.75
52	4.33	17.32	Izod	2.75
53	3.83	15.33	Izod	2.75
54	3.94	15.74	Izod	2.75
55	3.83	15.33	Izod	2.75

Statistics:

Series n = 10	Impact resistance kJ/m²	Impact resistance/Notch length J/m	Work contents J
x̄	3.81	15.25	2.75
s	0.32	1.29	0.00
v	8.44	8.44	0.00

Figure A4: Impact resistance report – PP 1100N. [53]

Appendix A2: 15% GFRPP

Mechanical tests such as tensile, flexural, and impact resistance were also done for 15% glass fibre reinforced polypropylene for verification purposes. Samples were injection moulded into test pieces as seen in Figure A5 with an Engel 80 T injection moulder fitted with a standard 30 mm diameter screw. The Plastamid test reports follow;

Figure A5: Moulded test pieces used for tensile and impact tests

Sample width: 10 mm
Sample thickness: 4 mm
Speed: 50 mm/min
Gauge length: 115 mm

PLASTAMID
ENGINEERING POLYMERS
Member of the Chemical Services Group

Sample reference	Stress at break MPa	Stress at yield MPa	Strain at yield %	Strain at break %
PP-GF15%	70.9			6.9
PP-GF15%	72.5			12.1
PP-GF15%	65.5			6.6
PP-GF15%	78.9			6.5
PP-GF15%	81.5			6.6
PP-GF15%	76.1			6.2
PP-GF15%	76.4			6.6
PP-GF15%	73.4			8.8
PP-GF15%	74.2			6.4
PP-GF15%	67.8			8.9

Statistics

Mean	73.7			7.6
Standard Deviation	4.9			1.9

Figure A6: Tensile test report – 15% GFRPP. [53]

Sample width: 10 mm
Sample thickness: 4 mm
Speed: 10 mm/min

PLASTAMID
ENGINEERING POLYMERS
Member of the Chemical Services Group

Sample reference	Flex Strength MPa	Flex Modulus MPa	Chord Modulus MPa
PP-GF15%	135.6	4792.2	4740.4
PP-GF15%	140.1	4779.1	4684.6
PP-GF15%	122.9	4136.3	4133.7
PP-GF15%	99.0	3151.3	3131.2
PP-GF15%	123.4	4100.7	4039.5
PP-GF15%	108.9	3510.7	3499.2
PP-GF15%	110.8	3517.2	3502.9
PP-GF15%	107.6	3467.0	3441.7
PP-GF15%	108.9	3387.2	3425.9
PP-GF15%	98.6	3105.8	3121.3

Statistics

Mean	1155.9	37947.5	37720.4
Standard Deviation	13.6	591.1	564.2

Figure A7: Flexural strength report – 15% GFRPP. [53]

Zwick / Roell Standard protocol 03.11.2005

Parameter table:

Customer : PLAST
Tester : brett
Test standard : pp 15% long glass
Material :
Test device 1 :
Test device 2 :
Test device 3 :

Results:

Nr	Impact resistance kJ/m²	Impact resistance/Notch length J/m	Type of test, PIT	Work contents J
57	9.18	36.71	Izod	2.75
58	4.43	17.74	Izod	2.75
59	5.45	21.79	Izod	2.75
60	4.43	17.74	Izod	2.75
61	7.71	30.83	Izod	2.75
62	9.60	38.40	Izod	2.75
63	9.60	38.40	Izod	2.75
64	9.39	37.57	Izod	2.75
65	6.37	25.47	Izod	2.75

Statistics:

Series n = 9	Impact resistance kJ/m²	Impact resistance/Notch length J/m	Work contents J
$\bar{x}$	7.35	29.41	2.75
s	2.22	8.87	0.00
v	30.17	30.17	0.00

Figure A8: Impact resistance report – 15%GFRPP. [53]

Appendix A3: 30% GFRPP (Compel PP-GF30-04)

Mechanical properties of the 30% GFRPP that was obtained for the analysis work was tested for verification purposes by moulding of test pieces as seen in Figure A12 on an Engel 80 T injection moulding machine. The injection unit was fitted with a standard 30 mm diameter screw and a heated mould (60 ºC). The test reports follow;

Figure A8: Moulded test pieces used for tensile and impact tests

Sample width: 10 mm
Sample thickness: 4 mm
Speed: 50 mm/min
Gauge length: 115 mm

PLASTAMID
ENGINEERING POLYMERS
Member of the Chemical Services Group

Sample reference	Stress at break MPa	Stress at yield MPa	Strain at yield %	Strain at break %
PP-GF30%	100.6			5.6
PP-GF30%	104.7			6.1
PP-GF30%	103.8			5.8
PP-GF30%	104.4			5.7
PP-GF30%	99.8			5.6
PP-GF30%	105.5			5.8
PP-GF30%	111.1			6.3
PP-GF30%	110.1			6.2
PP-GF30%	108.7			6.0
PP-GF30%	100.9			5.7

Statistics

Mean	104.9			5.9
Standard Deviation	4.0			0.2

Figure A9: Tensile test report – 30% GFRPP. [53]

Sample width: 10 mm
Sample thickness: 4 mm
Speed: 10 mm/min

PLASTAMID
ENGINEERING POLYMERS
Member of the Chemical Services Group

Sample reference	Flex Strength MPa	Flex Modulus MPa	Chord Modulus MPa
PP-GF30%	162.8	5891.3	5725.5
PP-GF30%	162.7	6000.8	5893.7
PP-GF30%	169.8	6274.4	6202.8
PP-GF30%	170.2	6021.9	5918.8
PP-GF30%	169.6	6050.9	5957.7
PP-GF30%	161.9	6121.2	6030.4
PP-GF30%	163.3	6161.9	5992.3
PP-GF30%	162.0	5891.1	5833.0
PP-GF30%	170.1	6249.5	6153.9
PP-GF30%	162.5	6043.8	5968.1

Statistics

Mean	1655.0	60706.8	59676.2
Standard Deviation	3.6	125.4	133.9

Figure A10: Flexural strength report – 30% GFRPP

Zwick / Roell Standard protocol 03.11.2005

Parameter table:

Customer : PLAST
Tester : brett
Test standard: pp 30% long glass
Material :
Test device 1 :
Test device 2 :
Test device 3 :

Results:

Nr	Impact resistance kJ/m²	Impact resistance/Notch length J/m	Type of test, PIT	Work contents J
67	12.50	49.98	Izod	2.75
68	14.34	57.37	Izod	2.75
69	16.33	65.31	Izod	2.75
70	17.56	70.23	Izod	2.75
71	13.15	52.59	Izod	2.75
72	22.17	88.69	Izod	2.75
73	16.89	67.55	Izod	2.75
74	16.00	64.01	Izod	2.75
75	15.67	62.67	Izod	2.75
76	18.00	72.02	Izod	2.75

Statistics:

Series n = 10	Impact resistance kJ/m²	Impact resistance/Notch length J/m	Work contents J
x	16.26	65.04	2.75
s	2.75	11.00	0.00
v	16.91	16.91	0.00

Figure A11: Impact resistance report – 30% GFRPP. [53]

Appendix A4: Material data sheets

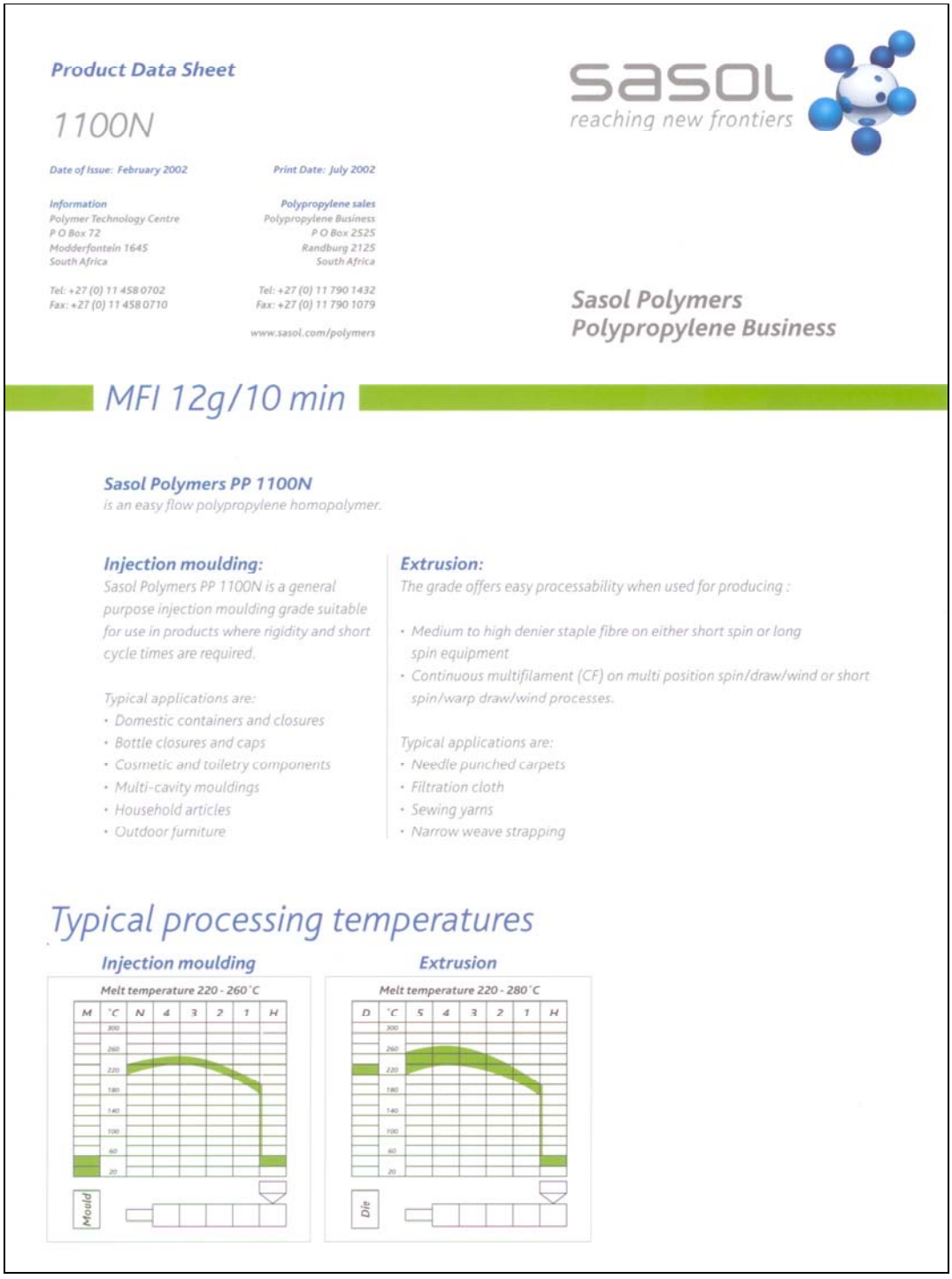

Product Data Sheet

1100N

sasol
reaching new frontiers

Date of Issue: February 2002

Print Date: July 2002

Information
Polymer Technology Centre
P O Box 72
Modderfontein 1645
South Africa

Tel: +27 (0) 11 458 0702
Fax: +27 (0) 11 458 0710

Polypropylene sales
Polypropylene Business
P O Box 2525
Randburg 2125
South Africa

Tel: +27 (0) 11 790 1432
Fax: +27 (0) 11 790 1079

www.sasol.com/polymers

Sasol Polymers
Polypropylene Business

MFI 12g/10 min

Sasol Polymers PP 1100N
is an easy flow polypropylene homopolymer.

Injection moulding:
Sasol Polymers PP 1100N is a general purpose injection moulding grade suitable for use in products where rigidity and short cycle times are required.

Typical applications are:
- Domestic containers and closures
- Bottle closures and caps
- Cosmetic and toiletry components
- Multi-cavity mouldings
- Household articles
- Outdoor furniture

Extrusion:
The grade offers easy processability when used for producing :

- Medium to high denier staple fibre on either short spin or long spin equipment
- Continuous multifilament (CF) on multi position spin/draw/wind or short spin/warp draw/wind processes.

Typical applications are:
- Needle punched carpets
- Filtration cloth
- Sewing yarns
- Narrow weave strapping

Typical processing temperatures

Injection moulding

Melt temperature 220 - 260 °C

M °C N 4 3 2 1 H

300 260 220 180 140 100 60 20

Mould

Extrusion

Melt temperature 220 - 280 °C

D °C 5 4 3 2 1 H

300 260 220 180 140 100 60 20

Die

Figure A12: Sasol 1100N product data sheet page 1. [42]

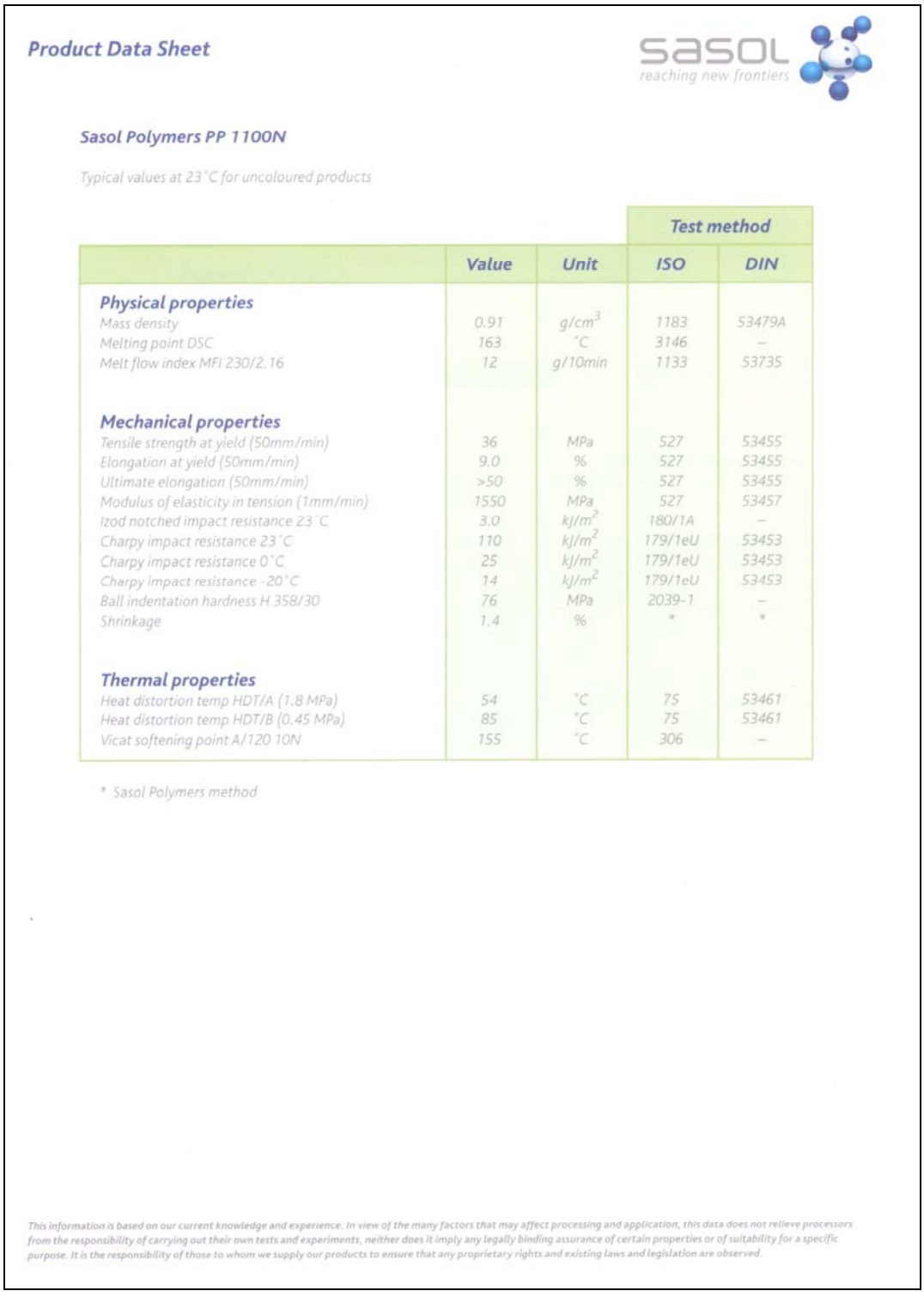

Product Data Sheet

sasol
reaching new frontiers

Sasol Polymers PP 1100N

Typical values at 23 °C for uncoloured products

	Value	Unit	Test method ISO	Test method DIN
Physical properties				
Mass density	0.91	g/cm^3	1183	53479A
Melting point DSC	163	°C	3146	–
Melt flow index MFI 230/2.16	12	g/10min	1133	53735
Mechanical properties				
Tensile strength at yield (50mm/min)	36	MPa	527	53455
Elongation at yield (50mm/min)	9.0	%	527	53455
Ultimate elongation (50mm/min)	>50	%	527	53455
Modulus of elasticity in tension (1mm/min)	1550	MPa	527	53457
Izod notched impact resistance 23 °C	3.0	kJ/m^2	180/1A	–
Charpy impact resistance 23 °C	110	kJ/m^2	179/1eU	53453
Charpy impact resistance 0 °C	25	kJ/m^2	179/1eU	53453
Charpy impact resistance -20 °C	14	kJ/m^2	179/1eU	53453
Ball indentation hardness H 358/30	76	MPa	2039-1	–
Shrinkage	1.4	%	*	*
Thermal properties				
Heat distortion temp HDT/A (1.8 MPa)	54	°C	75	53461
Heat distortion temp HDT/B (0.45 MPa)	85	°C	75	53461
Vicat softening point A/120 10N	155	°C	306	–

* Sasol Polymers method

This information is based on our current knowledge and experience. In view of the many factors that may affect processing and application, this data does not relieve processors from the responsibility of carrying out their own tests and experiments, neither does it imply any legally binding assurance of certain properties or of suitability for a specific purpose. It is the responsibility of those to whom we supply our products to ensure that any proprietary rights and existing laws and legislation are observed.

Figure A13: Sasol 1100N product data sheet page 2. [42]

Ticona

COMPEL PP-GF30-04 | PP | Glass Reinforced

Description

Heat Stabilized Polypropylene reinforced with 30% long glass fiber

Physical properties	Value	Unit	Test Standard
Density	1120	kg/m³	ISO 1183

Mechanical properties	Value	Unit	Test Standard
Tensile modulus (1mm/min)	7200	MPa	ISO 527-2/1A
Tensile stress at break (5mm/min)	95	MPa	ISO 527-2/1A
Tensile strain at break (5mm/min)	2.3	%	ISO 527-2/1A
Flexural modulus (23°C)	7000	MPa	ISO 178
Charpy impact strength @ 23°C	48	kJ/m²	ISO 179/1eU
Charpy impact strength @ -30°C	44	kJ/m²	ISO 179/1eU
Charpy notched impact strength @ 23°C	18	kJ/m²	ISO 179/1eA
Charpy notched impact strength @ -30°C	20	kJ/m²	ISO 179/1eA

Thermal properties	Value	Unit	Test Standard
DTUL @ 1.8 MPa	148	°C	ISO 75-1/-2

Disclaimer

NOTICE TO USERS: Values shown are based on testing of laboratory test specimens and represent data that fall within the standard range of properties for natural material. These values alone do not represent a sufficient basis for any part design and are not intended for use in establishing maximum, minimum, or ranges of values for specification purposes. Colorants or other additives may cause significant variations in data values.

Properties of molded parts can be influenced by a wide variety of factors including, but not limited to, material selection, additives, part design, processing conditions and environmental exposure. Any determination of the suitability of a particular material and part design for any use contemplated by the users and the manner of such use is the sole responsibility of the users, who must assure themselves that the material as subsequently processed meets the needs of their particular product or use.

To the best of our knowledge, the information contained in this publication is accurate; however, we do not assume any liability whatsoever for the accuracy and completeness of such information. The information contained in this publication should not be construed as a promise or guarantee of specific properties of our products. It is the sole responsibility of the users to investigate whether any existing patents are infringed by the use of the materials mentioned in this publication.

Moreover, there is a need to reduce human exposure to many materials to the lowest practical limits in view of possible adverse effects. To the extent that any hazards may have been mentioned in this publication, we neither suggest nor guarantee that such hazards are the only ones that exist. We recommend that persons intending to rely on any recommendation or to use any equipment, processing technique or material mentioned in this publication should satisfy themselves that they can meet all applicable safety and health standards.

We strongly recommend that users seek and adhere to the manufacturer's current instructions for handling each material they use, and entrust the handling of such material to adequately trained personnel only. Please call the telephone numbers listed listed (+49 (0) 69 30516299 for Europe and +1 908 598-4169 for the Americas) for additional technical information. Call Customer Services for the appropriate Materials Safety Data Sheets (MSDS) before attempting to process our products.

The products mentioned herein are not intended for use in medical or dental implants.

Figure A14: Product data sheet for Ticona Compel PP-GF30-04. [58]

Appendix A5: Rheological results

Rheology is the study of polymer flows during melt and can be used to obtain a vast amount of information on the materials themselves. Various samples, ranging from raw material pellets to components, were sent for analysis at various companies and rheometer manufactures throughout the world. The results obtained can be seen below along with a short introductory passage for each test. A full report may be requested from the author if needed.

Sasol Polymers were sent two PP samples, labelled ‘M’ and “S’ which were taken from the same batch of supplied material. Sample ‘S’ was taken from one bag whereas sample ‘M’ was taken from a mixture of ten bags so as to check for variability in the materials that were supplied. It was also important to see what the viscosity properties of this material were so as to be able to fit a Carreau viscosity model to it for the numerical modelling of the polymer flow in injection moulding using Cadmould. It was found that sample ‘S’ possessed a higher viscosity than sample ‘M’, although the difference was very small as seen in Figure A15, this could result in sample ‘M’ processing easier.

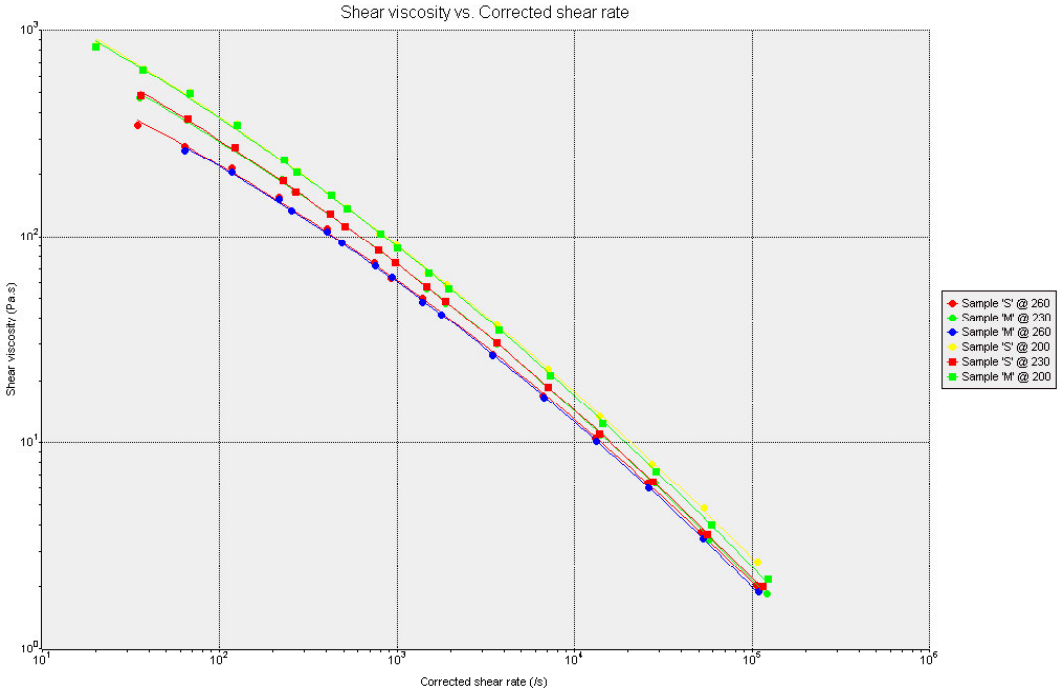

Figure A15: Shear viscosity vs corrected shear rates for PP1100N. [59]

As mentioned earlier, samples were also sent to the machine suppliers as part of a batch in order to test the equipment before the tenders were accepted, and TA Instruments, who are represented by AMS locally, presented the following results on two samples of material received by them, that being Sasol Polymers' PP1100N in pellet form and Ticona's Compel PP-GF30-04 in pultruded form. The results for the various tests conducted on these materials can be seen hereafter.

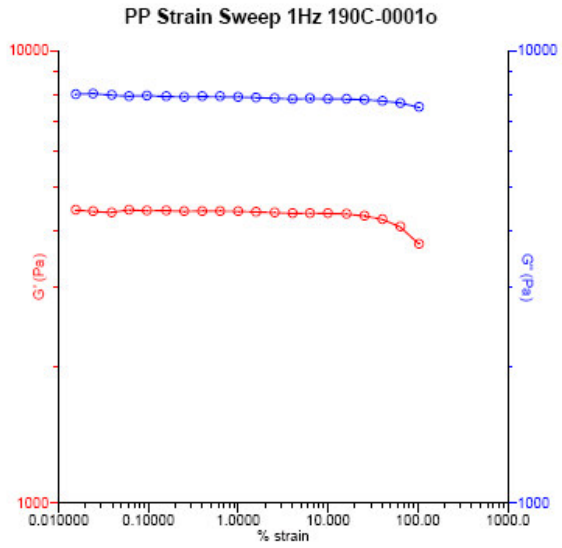

Figure A16: Dynamic strain sweep used to determine the linear viscoelastic region. [60]

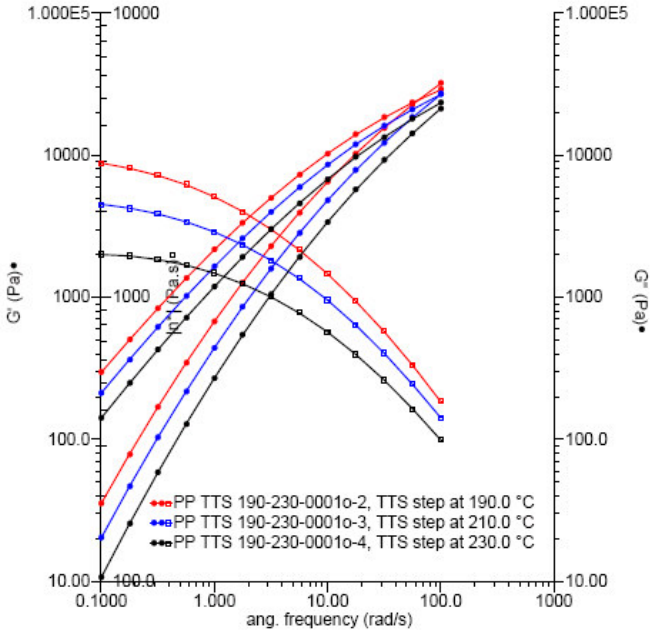

Figure A17: Frequency sweep used to conduct TTS (time temperature superposition) [60]

Various other tests were conducted which made it possible to calculate the molecular weight (Mw), as well as the molecular weight distribution (MWD) of the material as seen in Figure A18, but were not included due to space constraints.

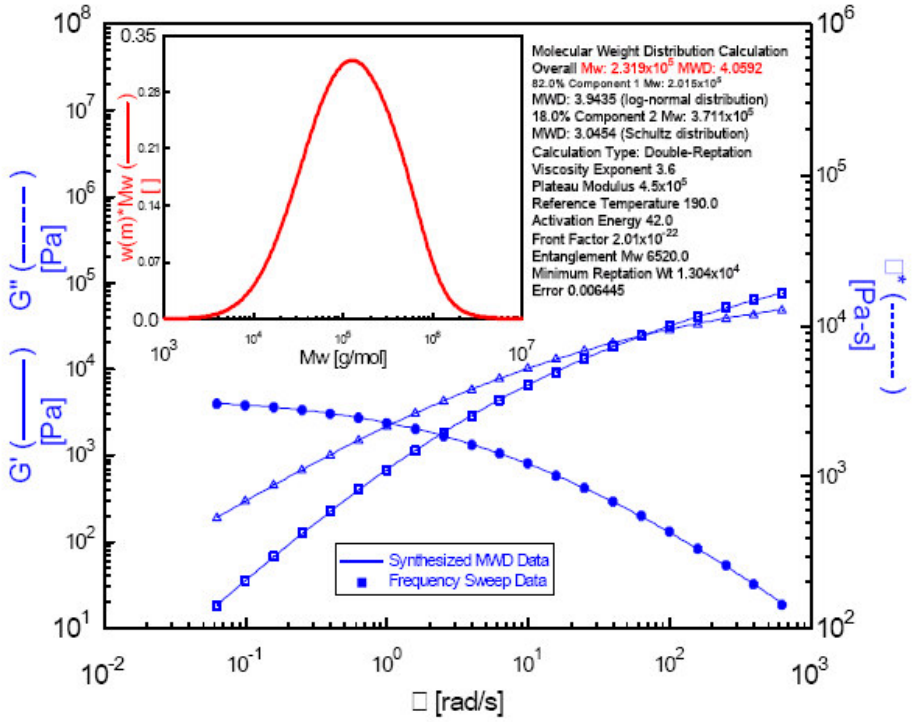

Figure A18: Mw & MWD calculation for PP using TA Orchestrator MWD software. [60]

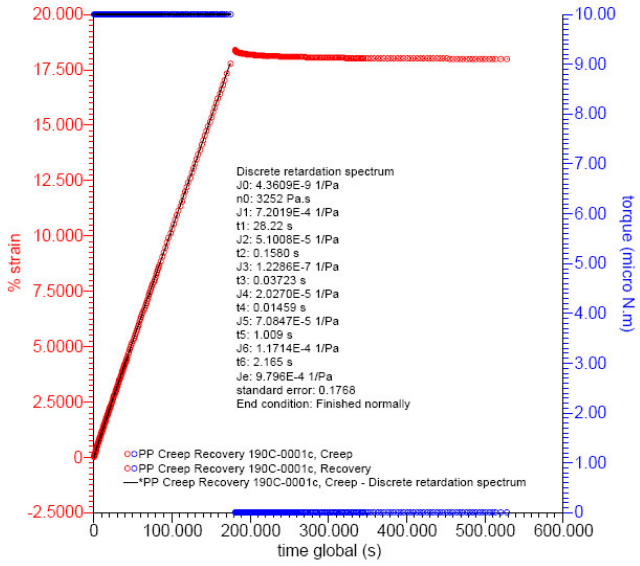

Figure A19: Creep recovery of PP. [60]

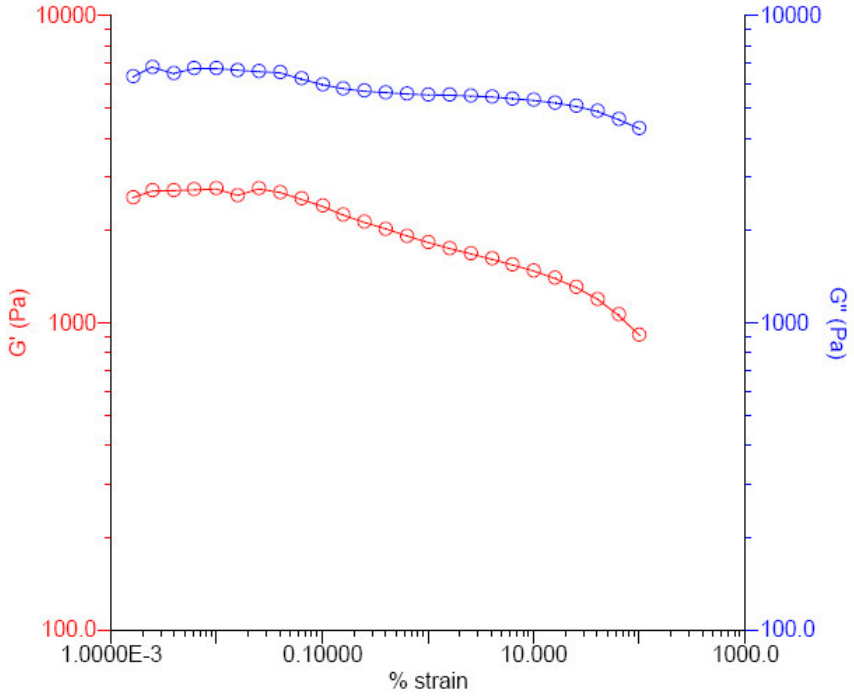

Figure A20: Strain sweep of glass fibre reinforced PP at 1Hz, 190 ºC. [60]

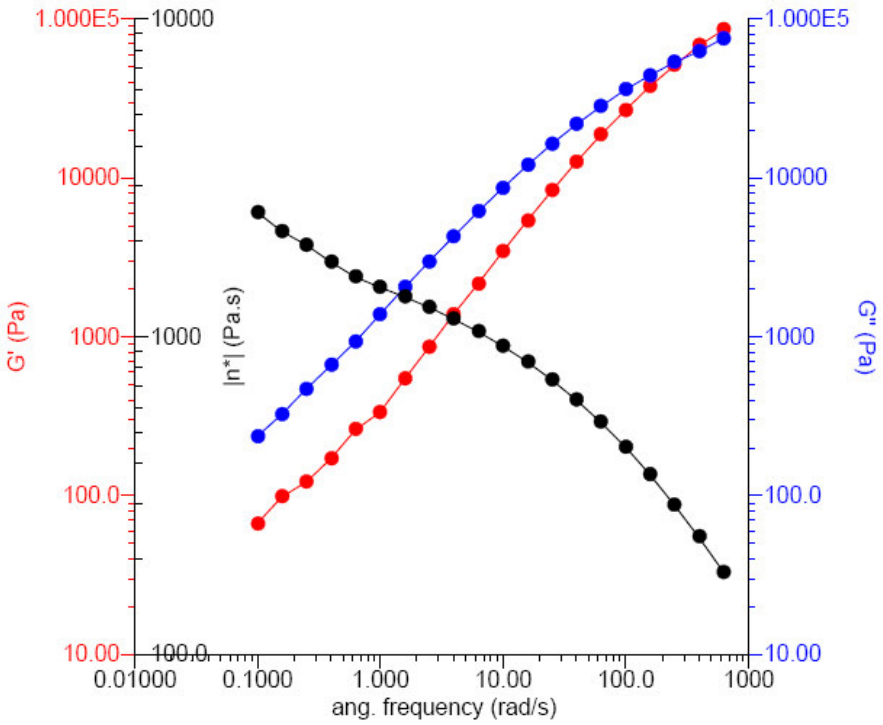

Figure A21: Frequency sweep of glass fibre reinforced PP @ 190ºC [60]

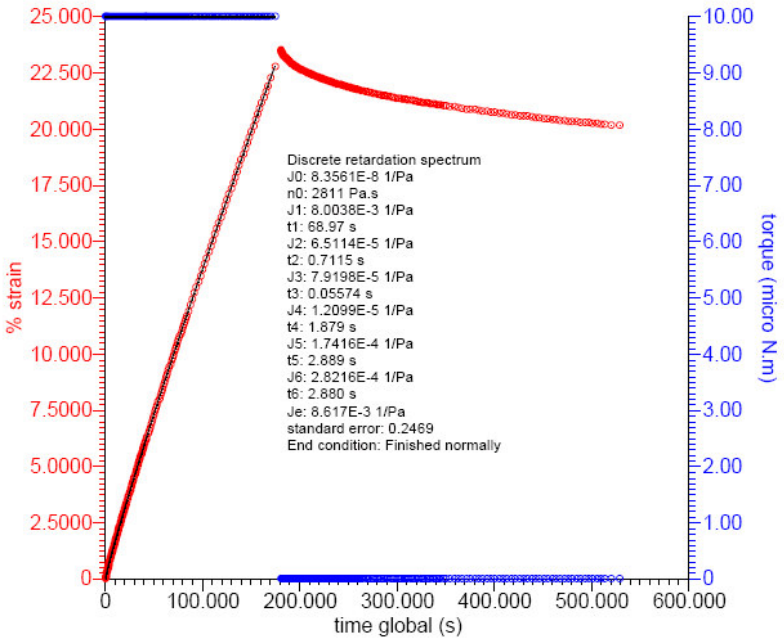

Figure A22: Creep recovery of glass fibre reinforced PP @ 190 ºC. [60]

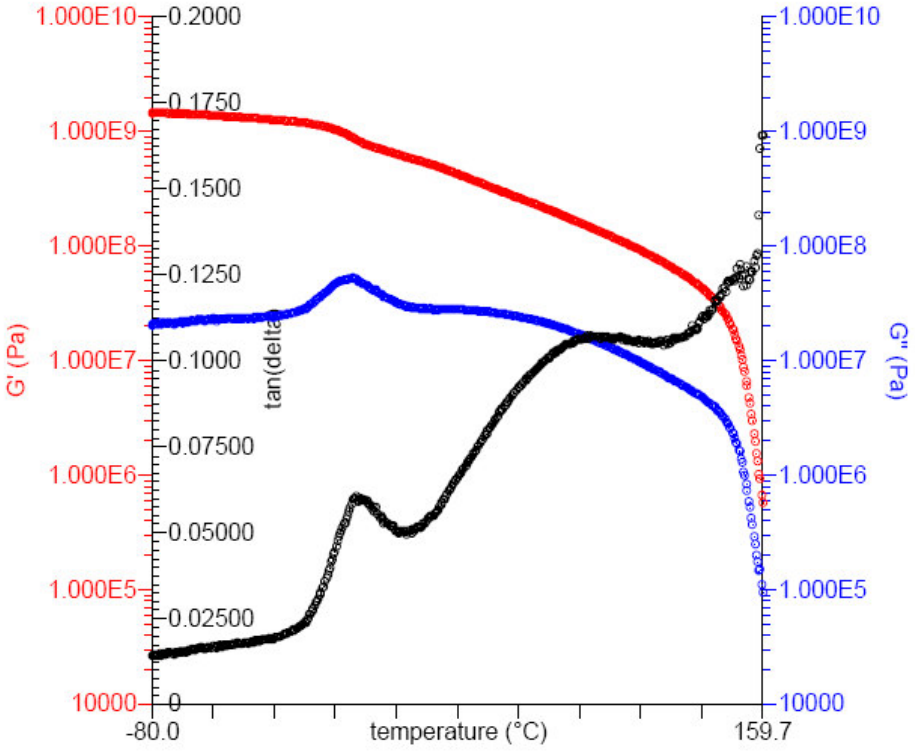

Figure A23: Temperature ramp test with glass fibre reinforced PP (1Hz, 3 ºC/min) [60]

Samples from components were also submitted for testing of unfilled PP (DOE L8 and L12) as well as GFRPP (DOE GFL1 and GFL10). A sole measuring system on a large temperature scale from very low temperatures, up to high temperatures, when the polymer begins to melt measured the rheological behaviour of the polymer samples as seen in Figure A24, Figure A25, and Figure A26.

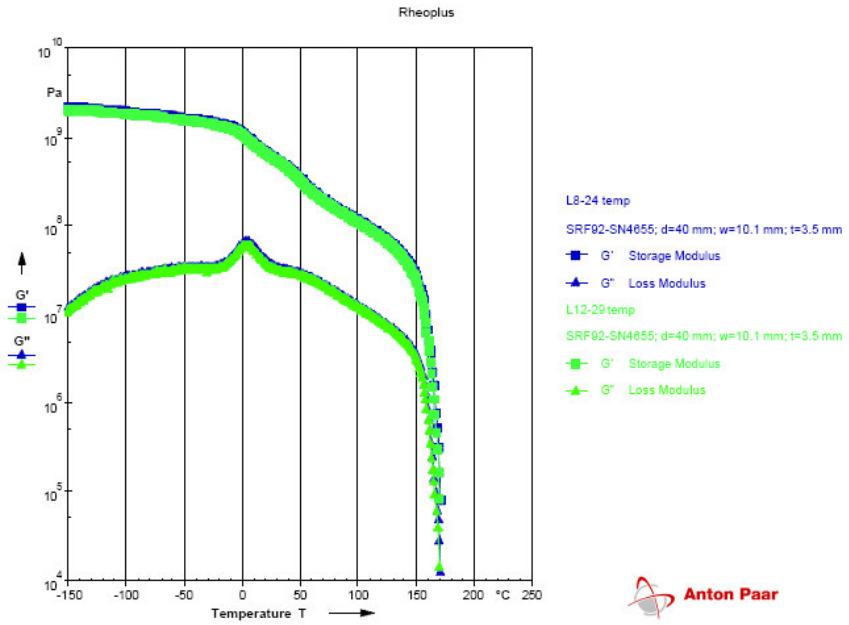

Figure A24: Curves of storage G', and loss G" modulus, of solid polymer bars (L8/L12) [61]

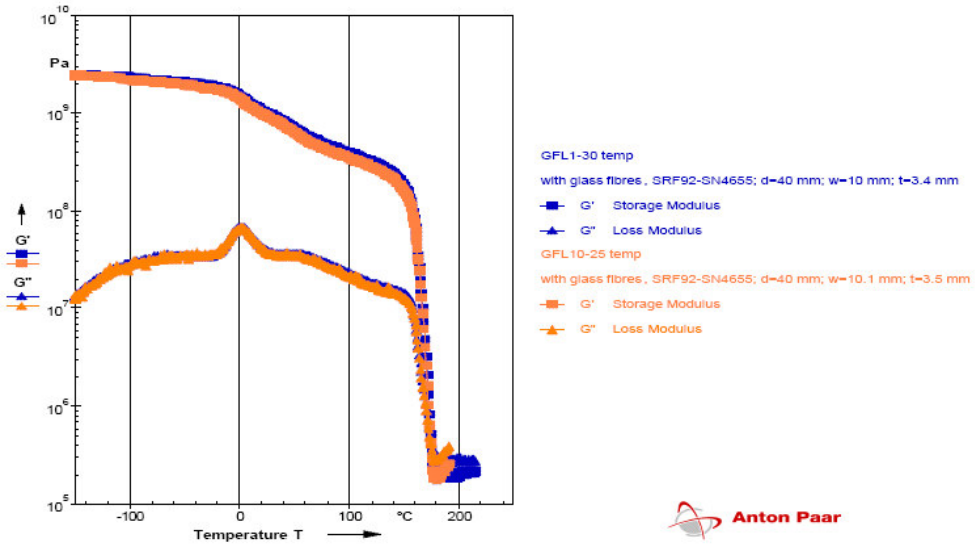

Figure A25: Curves of storage G', and loss G" modulus, of solid polymer bars (GFL1/GFL10) [61]

The storage modulus, G', and the loss modulus G", in Figure A24 and Figure A25, describes the elastic behaviour of the polymer samples. It was seen that there was no significant difference between L8 and L12, similar to that seen with GFRPP. The T_g (glass transition temperature) seen in Table A1 can be found as a maximum in G" or the peak value of tan(delta) depending on the method that was used.

Table A1: T_g of materials obtained via rheometry

Sample	G" (max)	Temperature (°C)
L8-24	6.60 E+7	4.5
L12-29	6.06 E+7	4.4
GFL1-30	6.89 E+7	2.4
GFL10-25	6.81 E+7	0.4

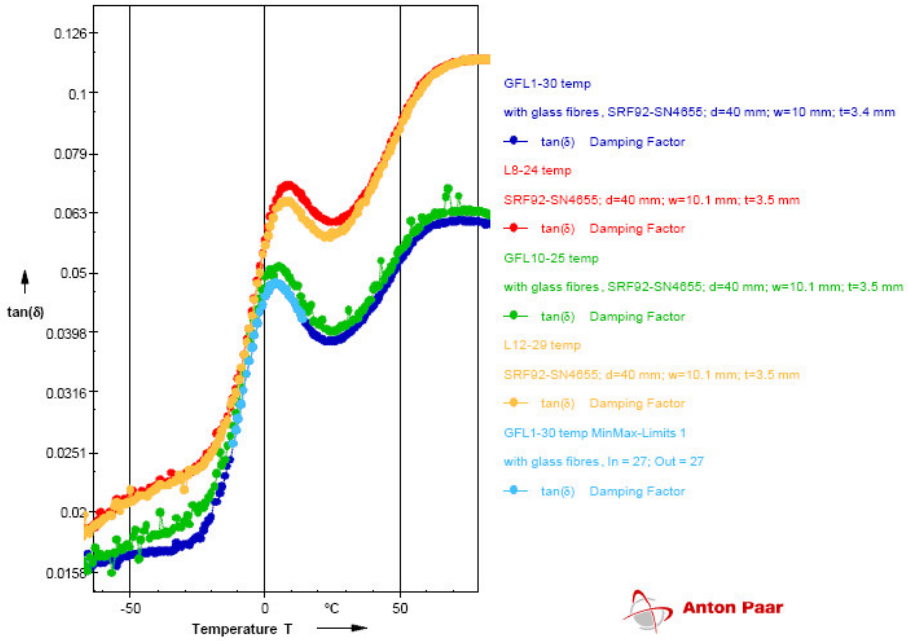

Figure A26: Damping factor curves of polymer bars, measured between 150 ºC – 215 ºC. [61]

As seen in Figure A26, and Figure A23, the shape of the material is stable until a critical temperature of about 150 ºC. At higher temperatures, the rectangular samples become deformed due to the temperature being very close to the T_m (melting point) of the material. The glass fibres were seen to keep the structure of the sample together, and can also be found in the plateau value of G' and G" at higher temperatures.

Appendix B: Injection moulding parameters

MOULD CLOSING

```
MOULD POSITION ACT.VAL.   SFx=   0.0 mm
OPENING STROKE            A  = 370.0 mm

1.CLOSING SPEED    A -W3  V1 =    25 %
2.CLOSING SPEED    W3-W1  V2 =    30 %
3.CLOSING SPEED    W1-G2  V3 =    10 %

START 2ND SPEED       V2  W3 = 300.0 mm
START 3RD SPEED       V3  W1 =  40.0 mm

MOULD PROTECTION STROKE   G1 =  15.0 mm
MOULD PROT.PRES.          P2 =    25 %
MOULD PROT. END           G2 =   0.1 mm
MOULD PROT.TIME ACT= 0.36 ZF =  2.00 s
```

CLAMPING FORCE

```
SET VALUE                 SK =  1100 kN
ACTUAL VALUE              SKx=  1070 kN

START 1ST M.PROT.PRESSURE G1 =  15.0 mm
1ST MOULD PROT.PRESSURE   P2a=    25 %
START 2ND M.PROT.PRESSURE G3 =   0.9 mm
2ND M.PROT.PRESSURE       P2e=     0 %
```

MOULD OPENING

```
1ST OPENING SPEED  G2-W4  V6 =     5 %
2ND OPENING SPEED  W4-W2  V7 =    40 %
3RD OPENING SPEED  W2-A   V8 =    20 %

START 2ND SPEED    V7     W4 =  50.0 mm
START 3RD SPEED    V8     W2 = 350.0 mm
```

HEATINGS UNIT 2

THE FOLLOWING TABLES CONTAIN THE VALUES FOR THE INJECTION UNIT HEATING

Description	Units	I1	I2	I3	I4	I5	I6	I7
Engel nozzle : Set	°C	200.0	200.0	220.0	180.0	180.0	180.0	200.0
: Actual	°C	198.5	201.0	220.2	180.8	180.2	180.5	200.2
Engel Plasticiser 1 : Set	°C	200.0	200.0	220.0	180.0	180.0	180.0	200.0
: Actual	°C	199.5	200.0	220.4	180.8	180.0	180.4	200.0
Engel Plasticiser 2 : Set	°C	200.0	200.0	220.0	180.0	180.0	180.0	200.0
: Actual	°C	199.8	200.1	220.0	180.8	180.1	180.6	199.9
Engel Plasticiser 3 : Set	°C	200.0	200.0	220.0	180.0	180.0	180.0	200.0
: Actual	°C	200.3	199.9	220.1	179.9	180.1	180.0	199.6
Engel Plasticiser 4 : Set	°C	200.0	200.0	220.0	180.0	180.0	180.0	200.0
: Actual	°C	199.6	199.9	219.9	179.9	180.0	180.0	199.9

Description	Units	GFI1	GFI2	GFI3	GFI4	GFI5	GFI6	GFI7
Engel nozzle : Set	°C	200.0	200.0	220.0	180.0	220.0	220.0	180.0
: Actual	°C	201.5	199.4	220.1	182.1	221.3	217.5	187.8
Engel Plasticiser 1 : Set	°C	200.0	200.0	220.0	180.0	180.0	180.0	180.0
: Actual	°C	200.0	200.0	220.1	180.8	180.0	179.9	197.3
Engel Plasticiser 2 : Set	°C	200.0	200.0	220.0	180.0	180.0	180.0	180.0
: Actual	°C	199.8	200.3	220.4	180.5	180.2	179.9	197.5
Engel Plasticiser 3 : Set	°C	200.0	200.0	220.0	180.0	180.0	180.0	180.0
: Actual	°C	199.9	199.6	220.2	180.1	180.3	180.0	198.5
Engel Plasticiser 4 : Set	°C	200.0	200.0	220.0	180.0	180.0	180.0	180.0
: Actual	°C	199.8	200.3	219.9	180.4	180.3	180.3	192.7

INJECTION UNIT 2

```
MAX INJECTION SPEED:            157 mm/s
INJECTION SPEED:   ACT= 73 mm/s  SET :
 70      70      70      70      70
 70      70      70      70      70
INJECTION PRESSURE LIMIT P6 = 150.0 bar
STOP INJECTION AT PRESSURE LIMIT   YES

INJECTION TIME MONITORING
MIN=  0.50   MAX= 20.00  ZSx=  2.05 s
```

SWITCHOVER MODE UNIT 2

```
STROKE-DEPENDENT                YES
SWITCHOVER SET VALUE     C3 =  60.0 mm
SWITCHOVER POSITION      C3u=  60.0 mm #
SCREW POS. ACT. VALUE    SSx= 199.6 mm

POST INJ.: PRESSURE: P7 TO P16  (bar)
```

Description	Units	I1	I2	I3	I4	I5	I6	I7
Post Injection Pressure	bar	35	20	20	20	50	35	35

Description	Units	GFI1	GFI2	GFI3	GFI4	GFI5	GFI6	GFI7
Post Injection Pressure	bar	35	20	20	20	50	35	35

PLASITCIZING UNIT 2

```
PLASTICIZING STROKE      C1 = 195.0 mm
PLASTICIZING SPEED :    %
    40      40      40      40      40
BACK PRESSURE : (bar)    PSx=   0.3 bar
  10.0    10.0    10.0    10.0    10.0

PLASTICIZING DELAY TIME  Z3 =   1.0 s
DECOMP.STROKE AFT.PLAST. C2 =   5.0 mm
DECOMPRESSION END        C2*= 200.0 mm
DECOMPRESSION SPEED      V24=    50 %
```

Appendix B1: Design of experiment I1

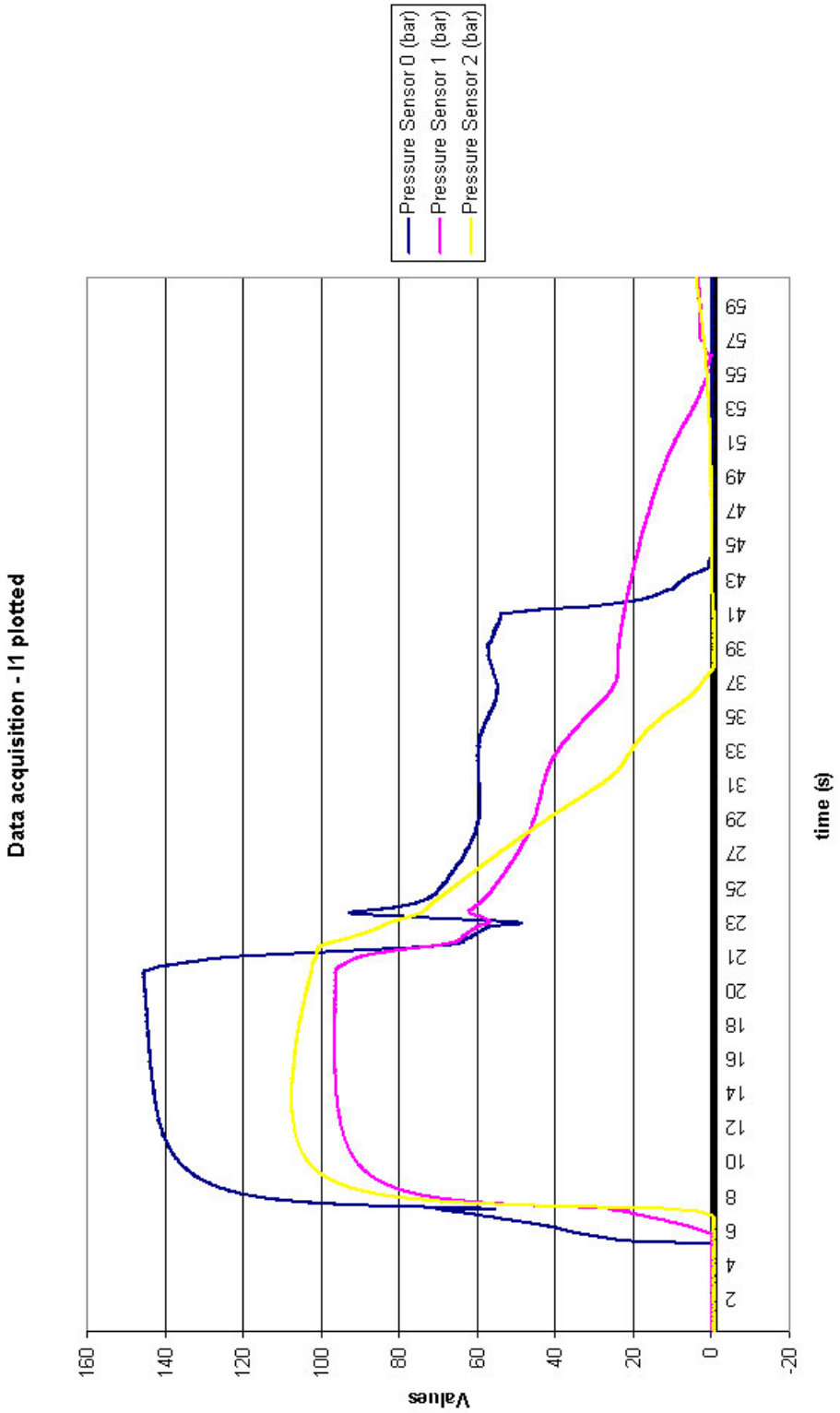

Figure B1a: Cavity pressures in injection moulding DOE I1

Appendix B2: Design of experiment I2

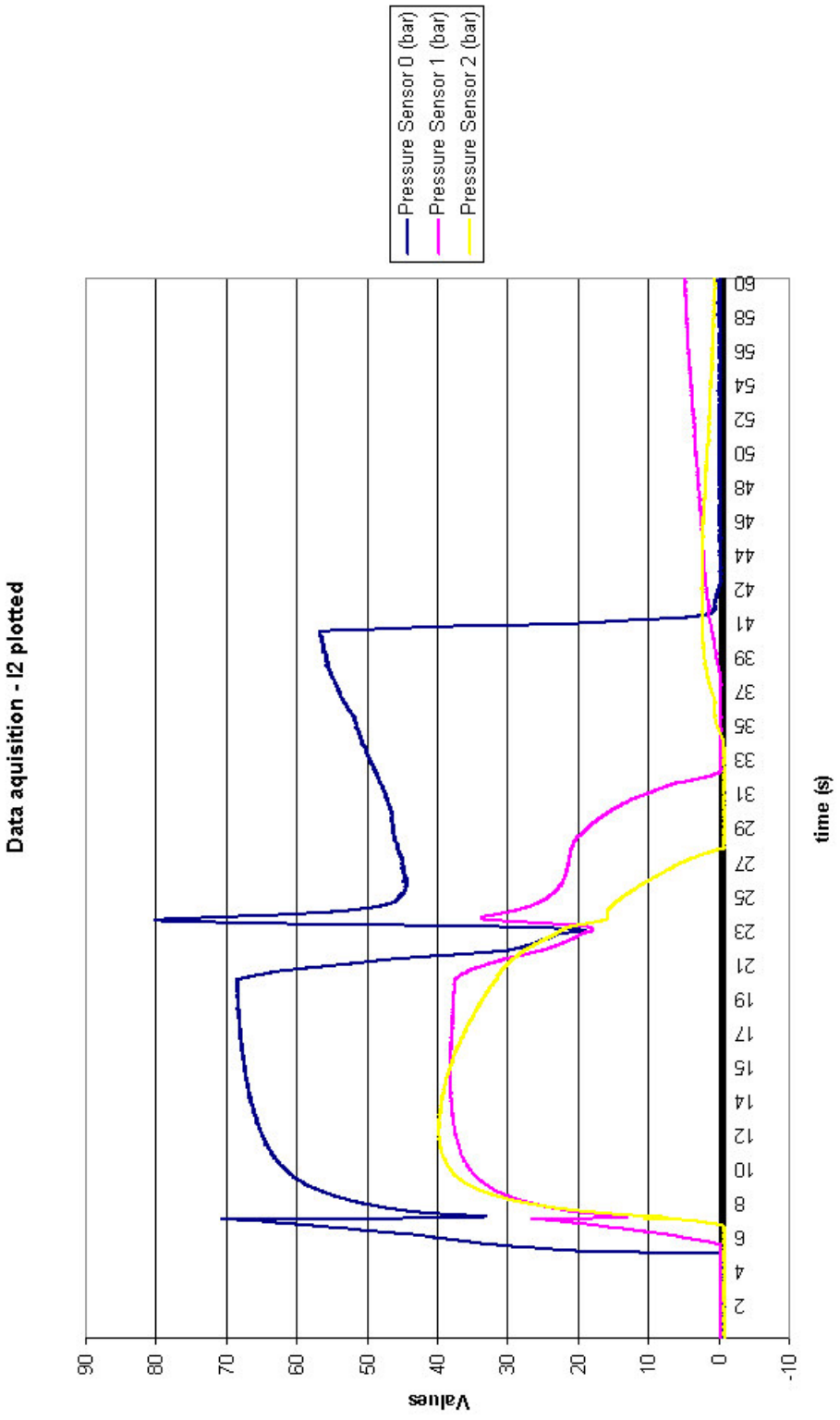

Figure B2a: Cavity pressures in injection moulding DOE I2

Appendix B3: Design of experiment I3

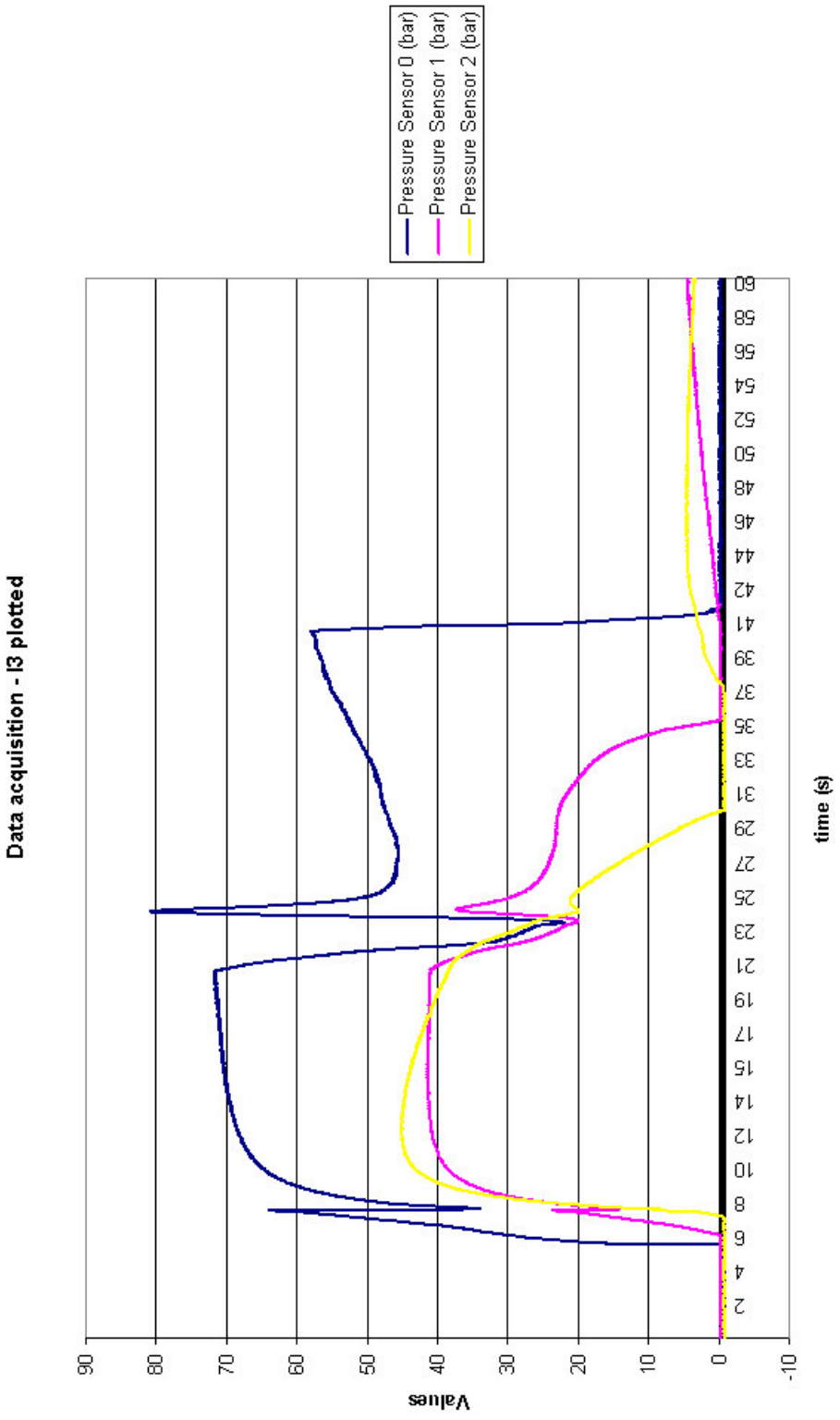

Figure B3a: Cavity pressures in injection moulding DOE I3

Appendix B4: Design of experiment I4

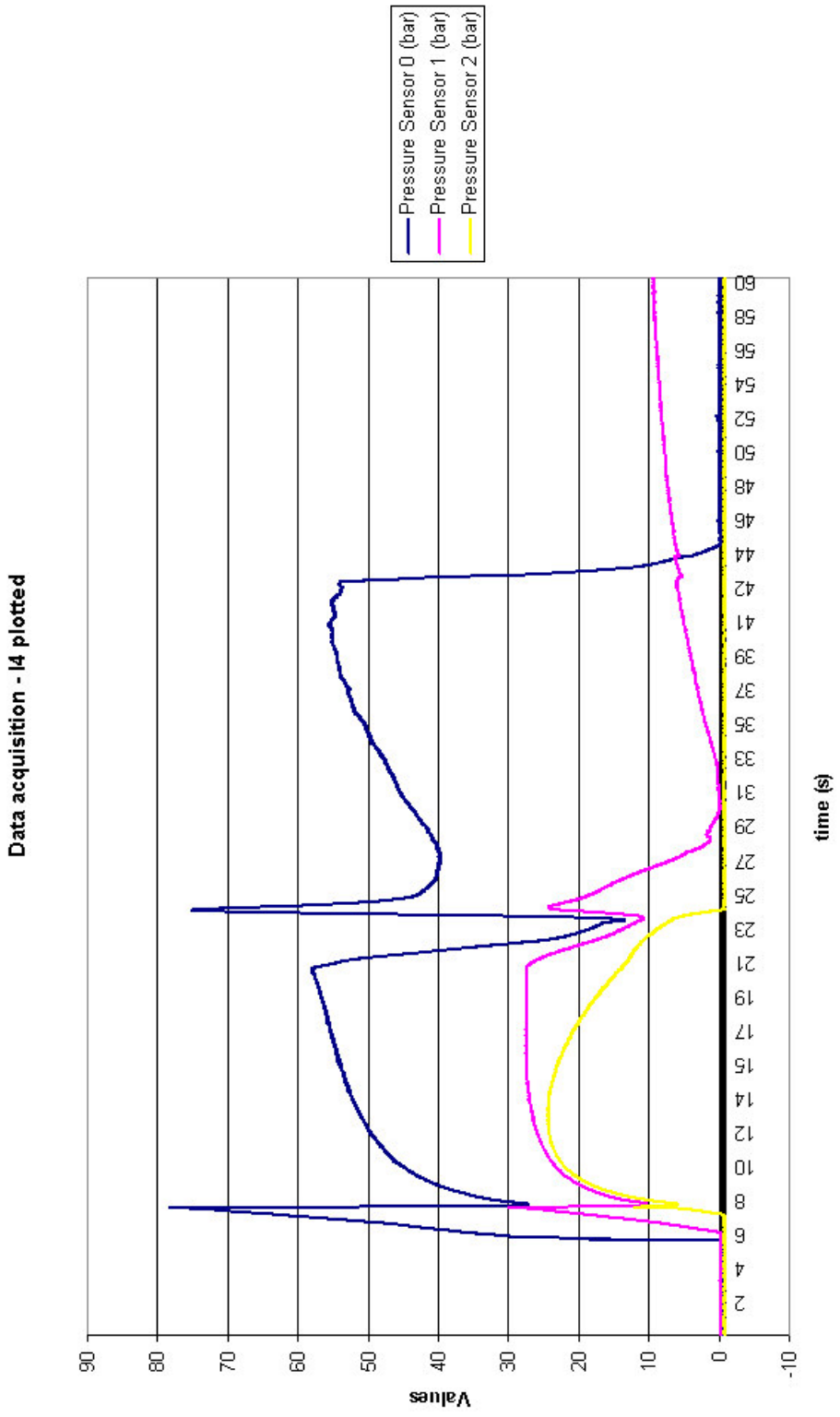

Figure B4a: Cavity pressures in injection moulding DOE I4

Appendix B5: Design of experiment I5

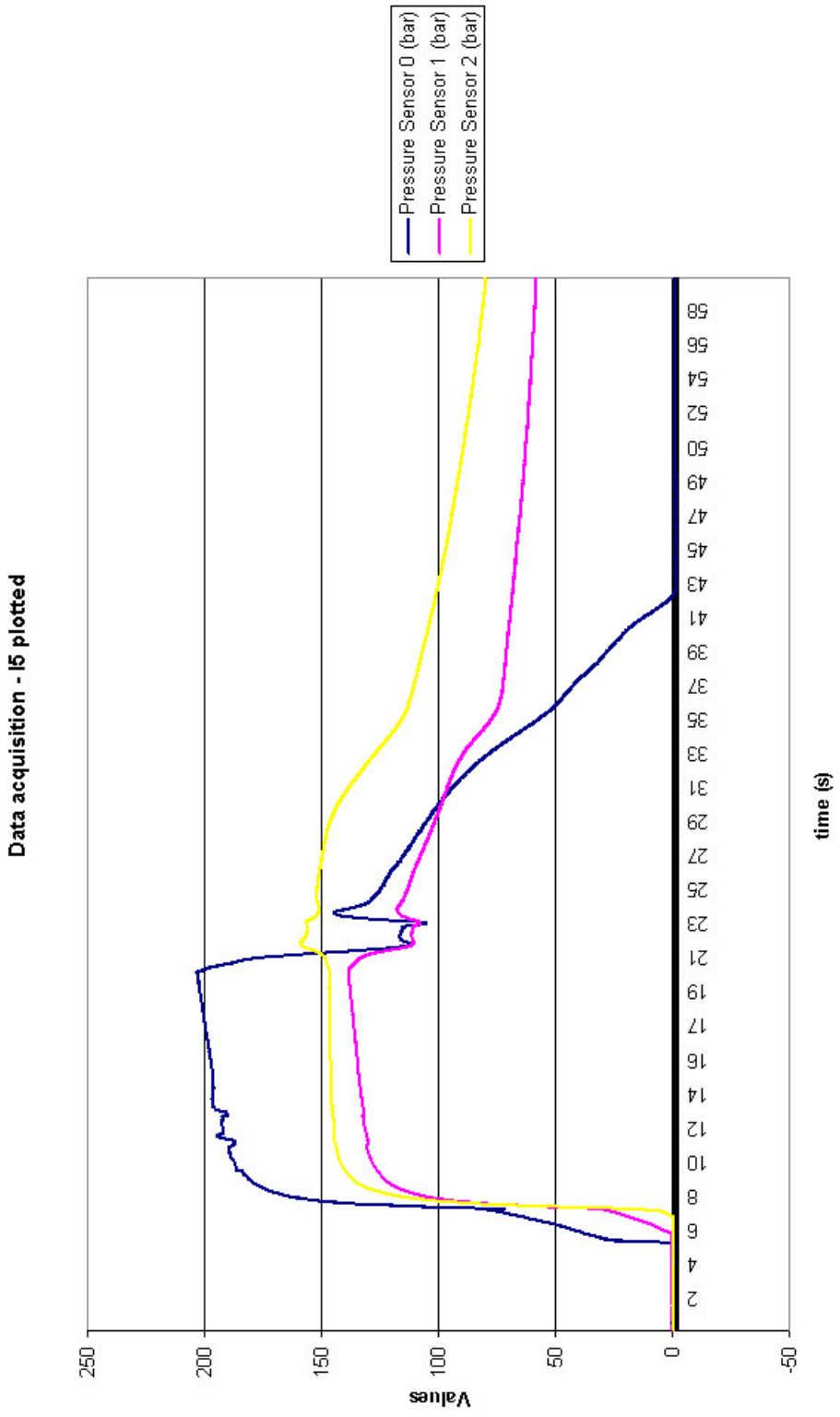

Figure B5a: Cavity pressures in injection moulding DOE I5

Appendix B6: Design of experiment I6

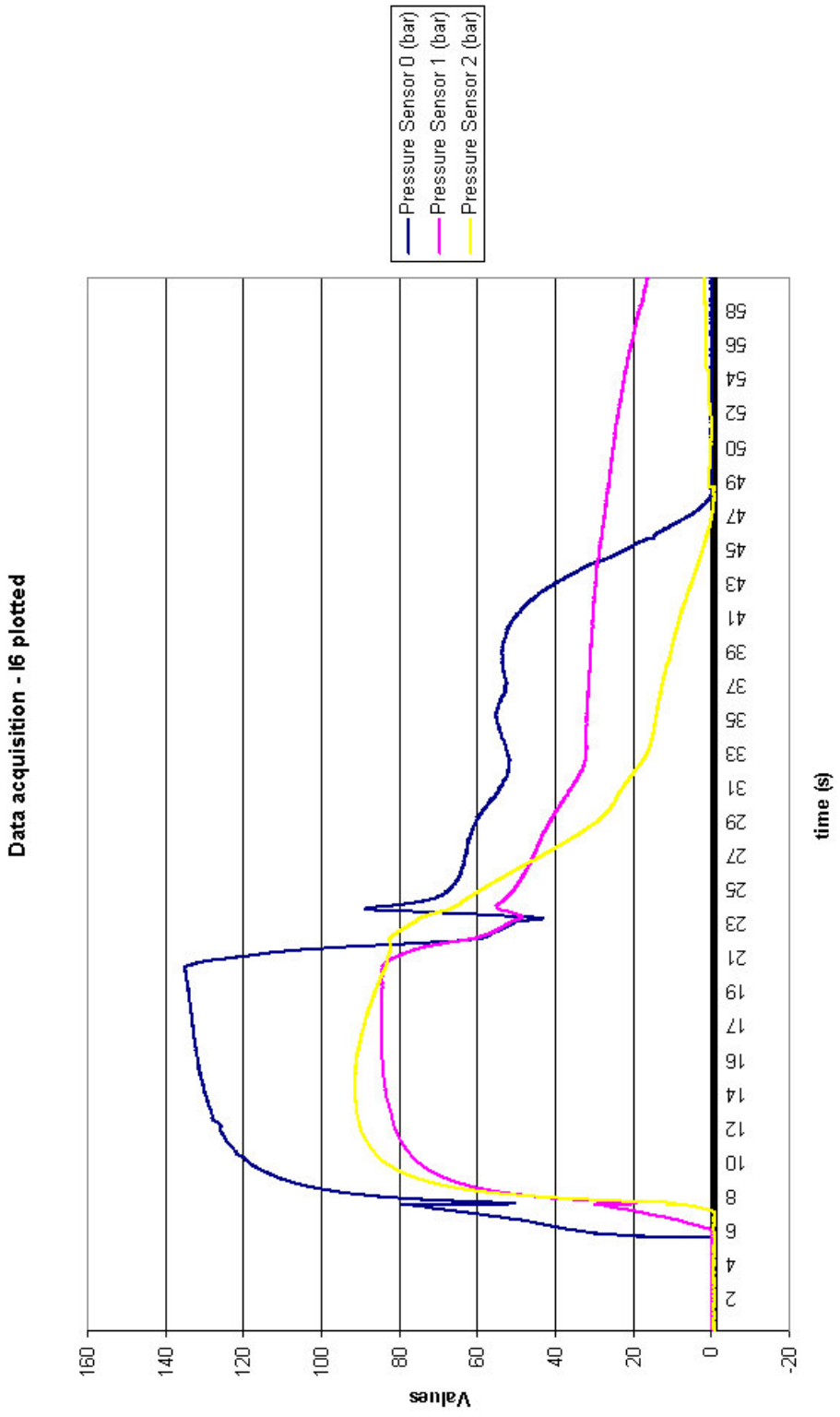

Figure B6a: Cavity pressures in injection moulding DOE I6

Appendix B7: Design of experiment I7

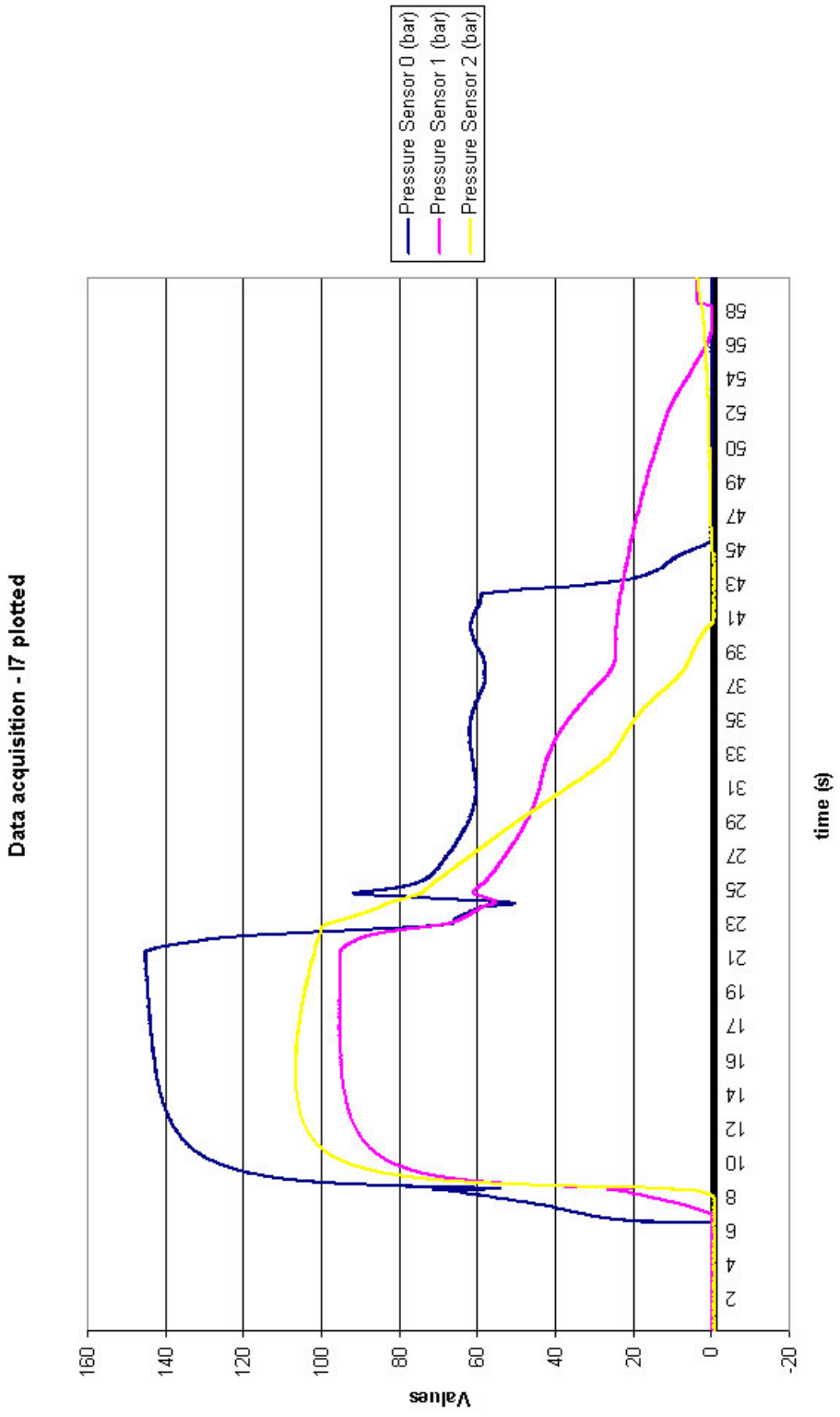

Figure B7a: Cavity pressures in injection moulding DOE I7

Appendix B8: Design of experiment GFI1

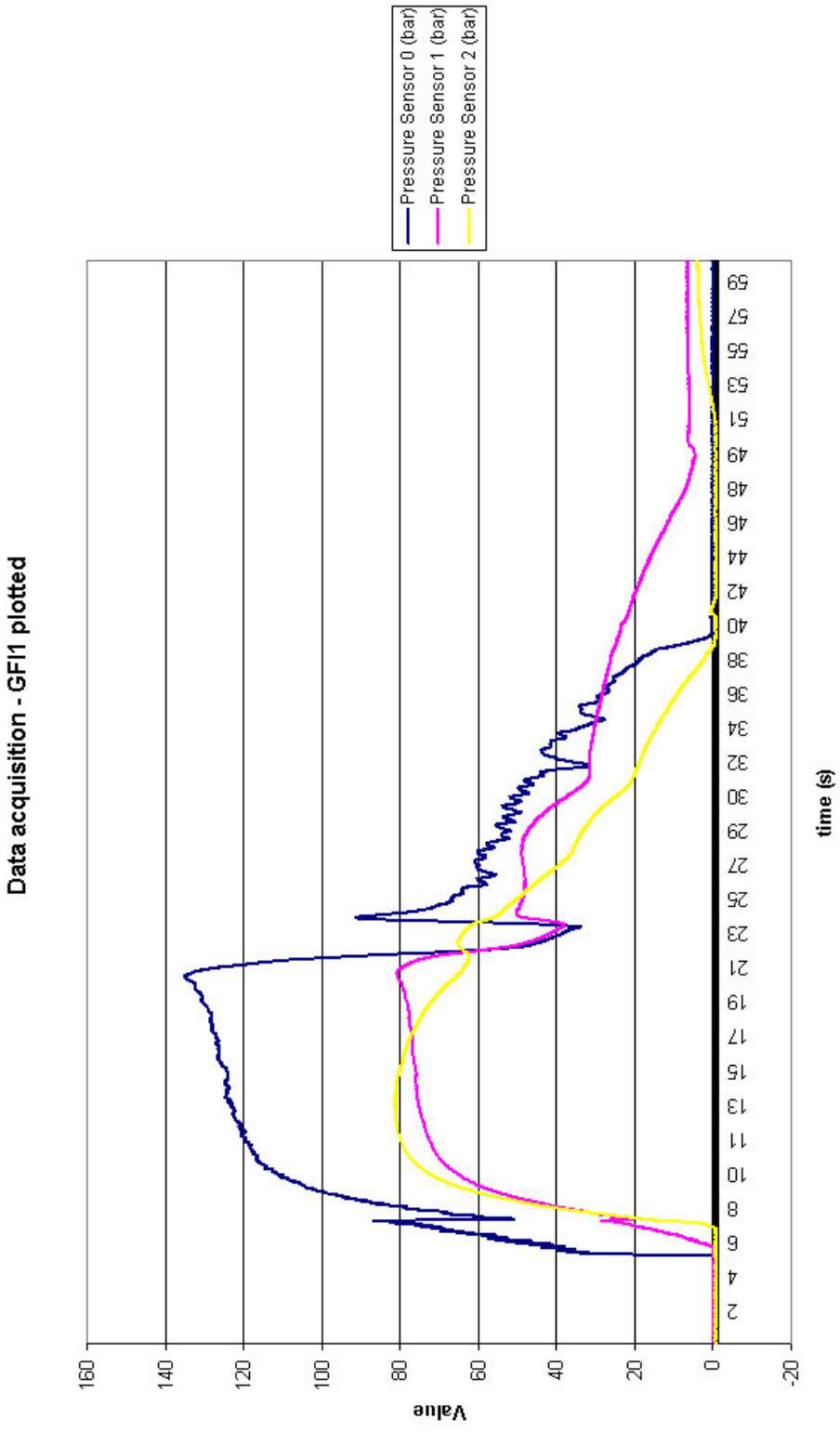

Figure B8a: Cavity pressures in injection moulding DOE GFI1

Figure B8b: Fibre skeleton remaining after burn off of GFI1-24

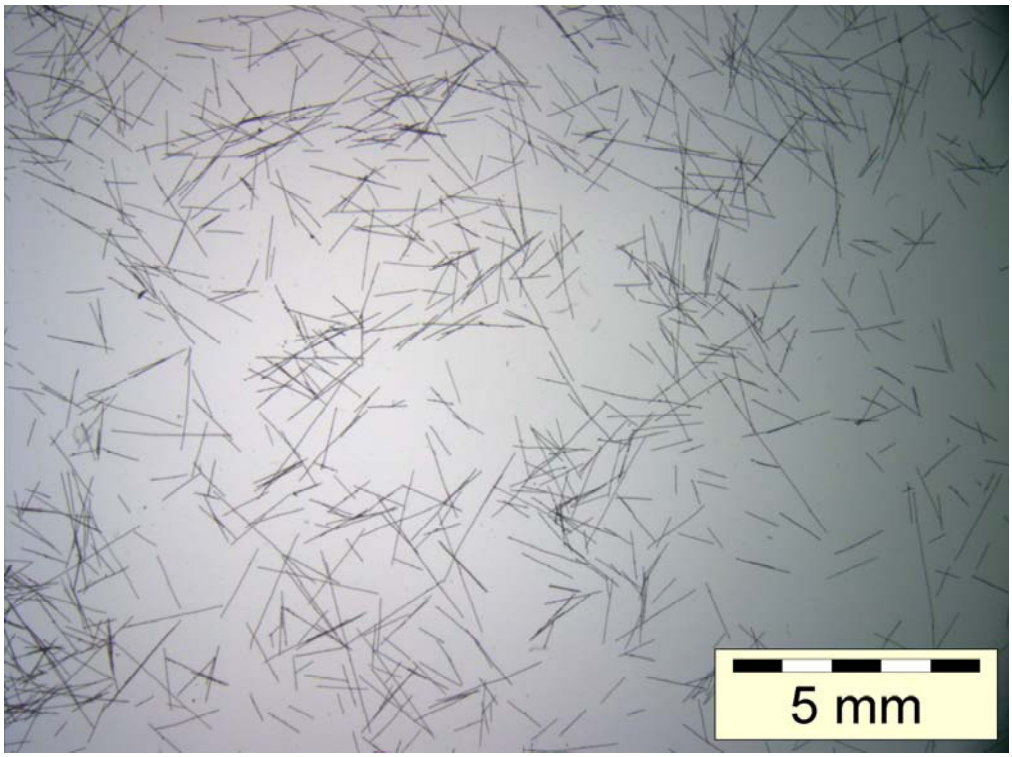

Figure B8c: Optical microscope photo taken with sample from GFI1-24

Appendix B9: Design of experiment GFI2

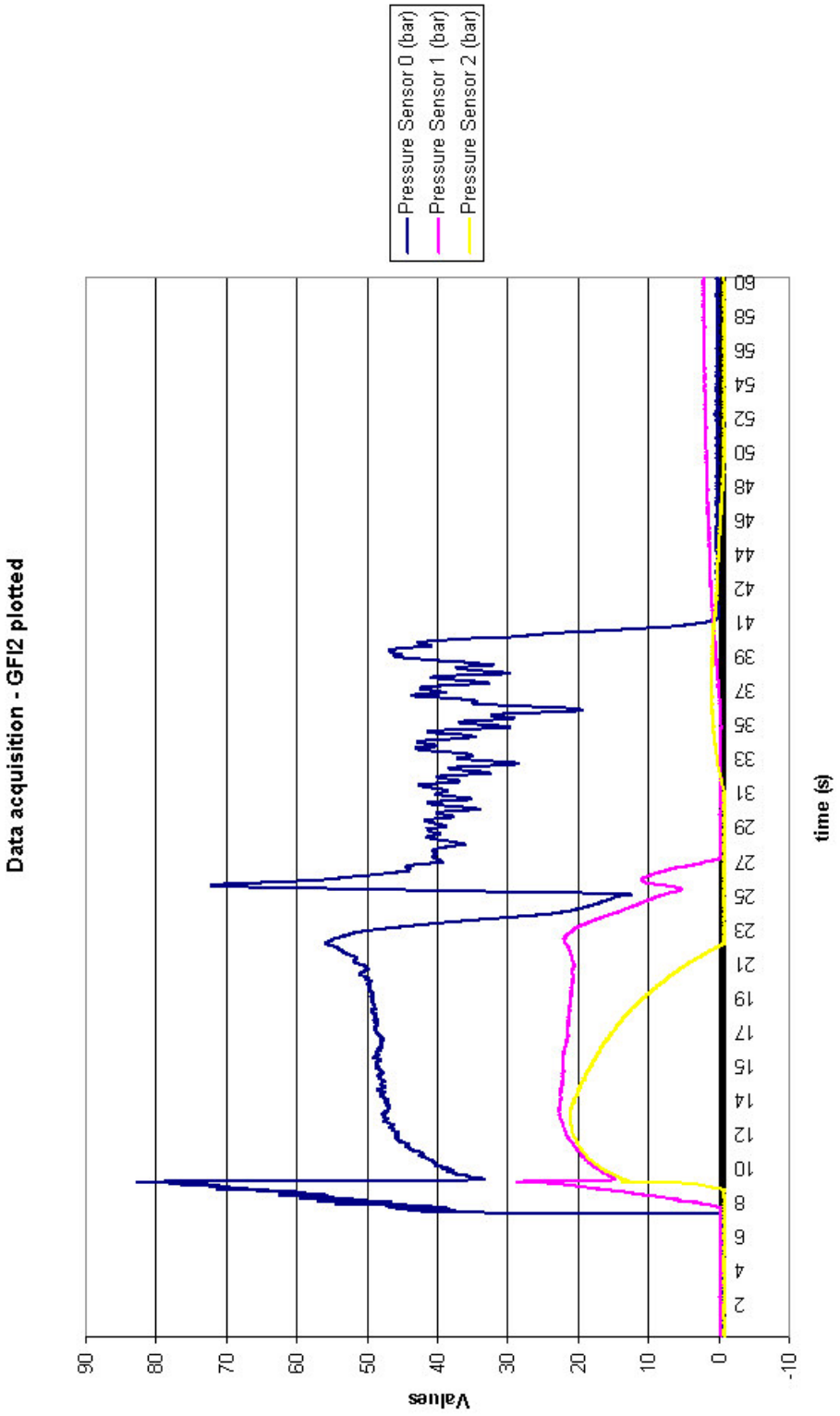

Figure B9a: Cavity pressures in injection moulding DOE GFI2

Figure B9b: Fibre skeleton remaining after burn off of GFI2-27

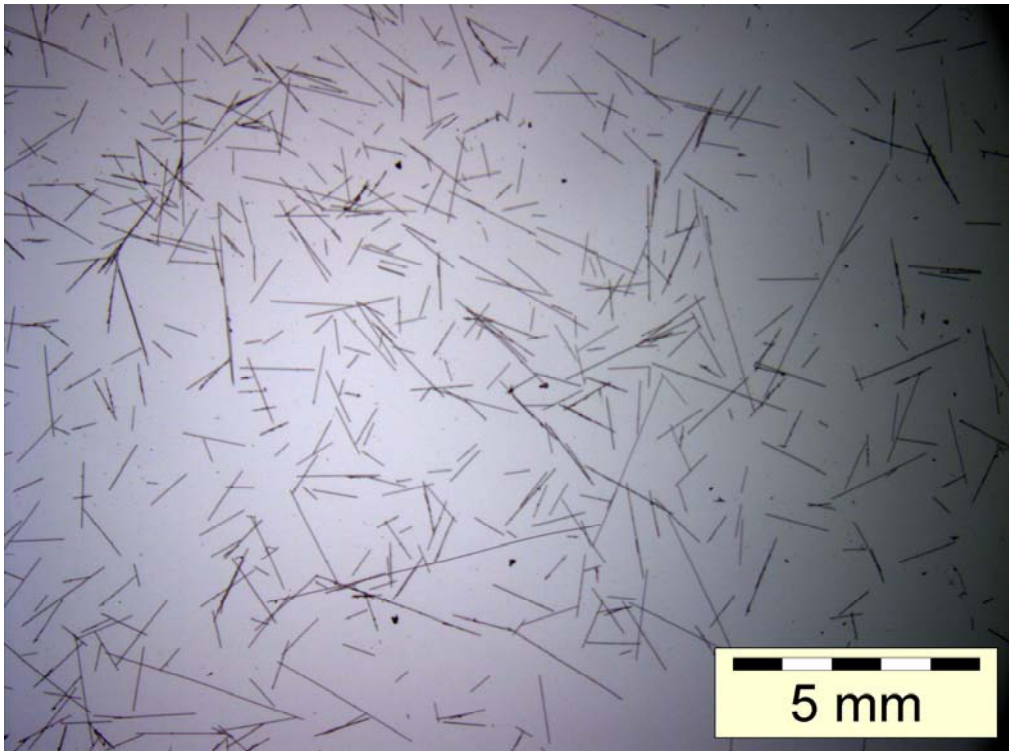

Figure B9c: Optical microscope photo taken with sample from GFI2-27

Appendix B10: Design of experiment GFI3

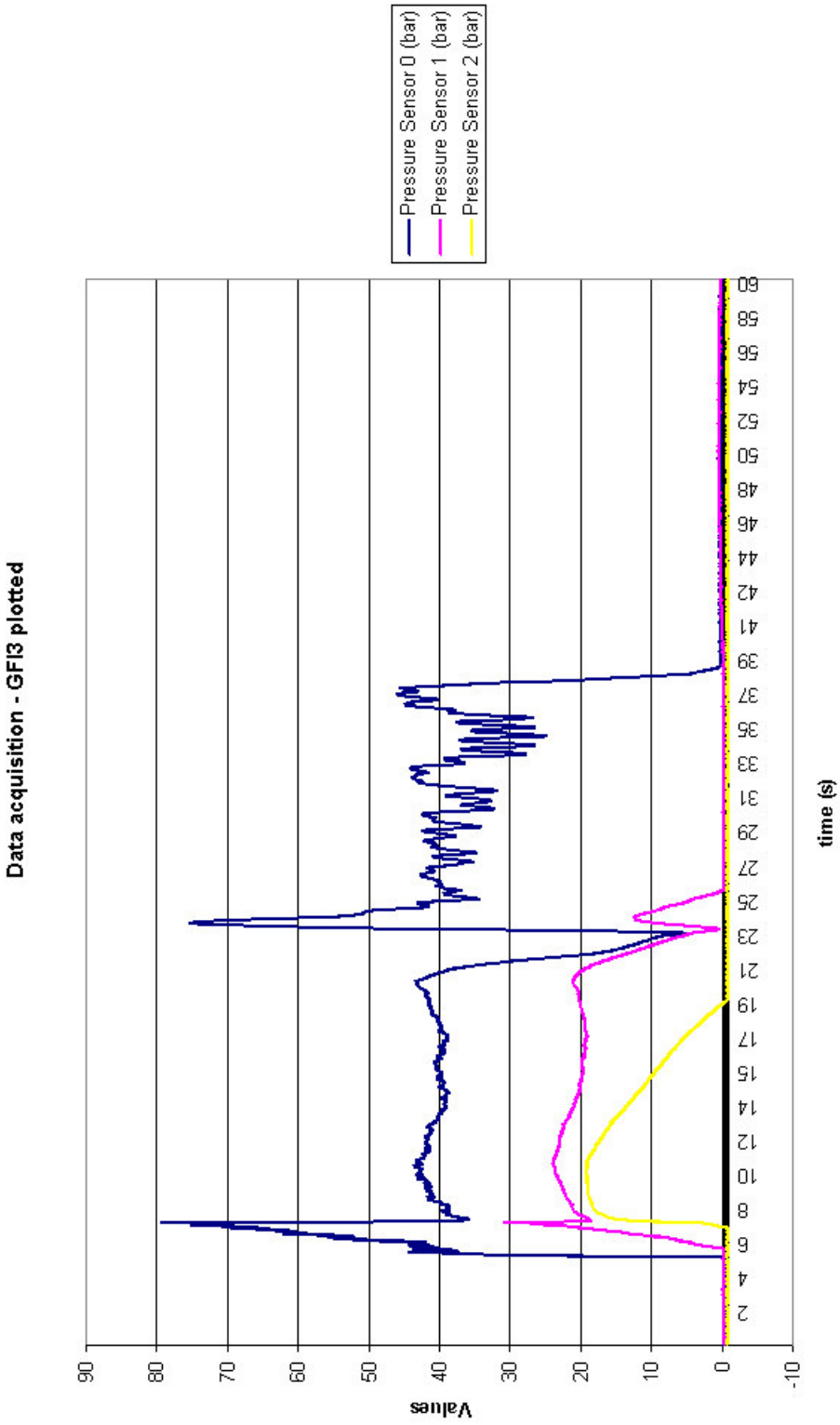

Figure B10a: Cavity pressures in injection moulding DOE GFI3

Figure B10b: Fibre skeleton remaining after burn off of GFI3-18

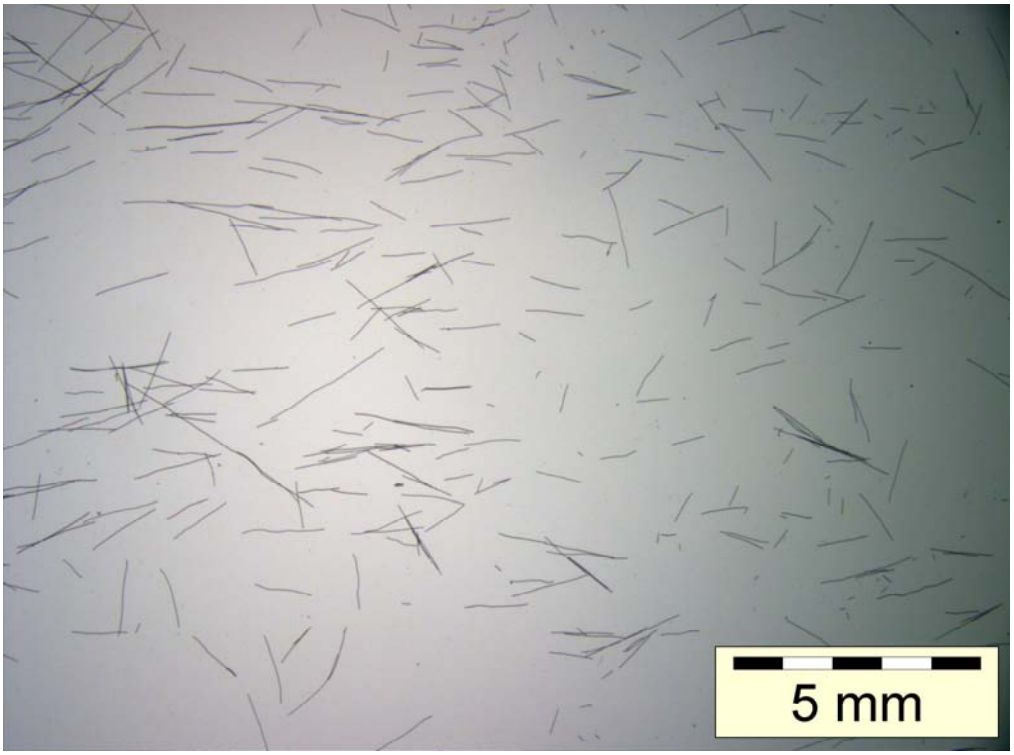

Figure B10c: Optical microscope photo taken with sample from GFI3-18

Appendix B11: Design of experiment GFI4

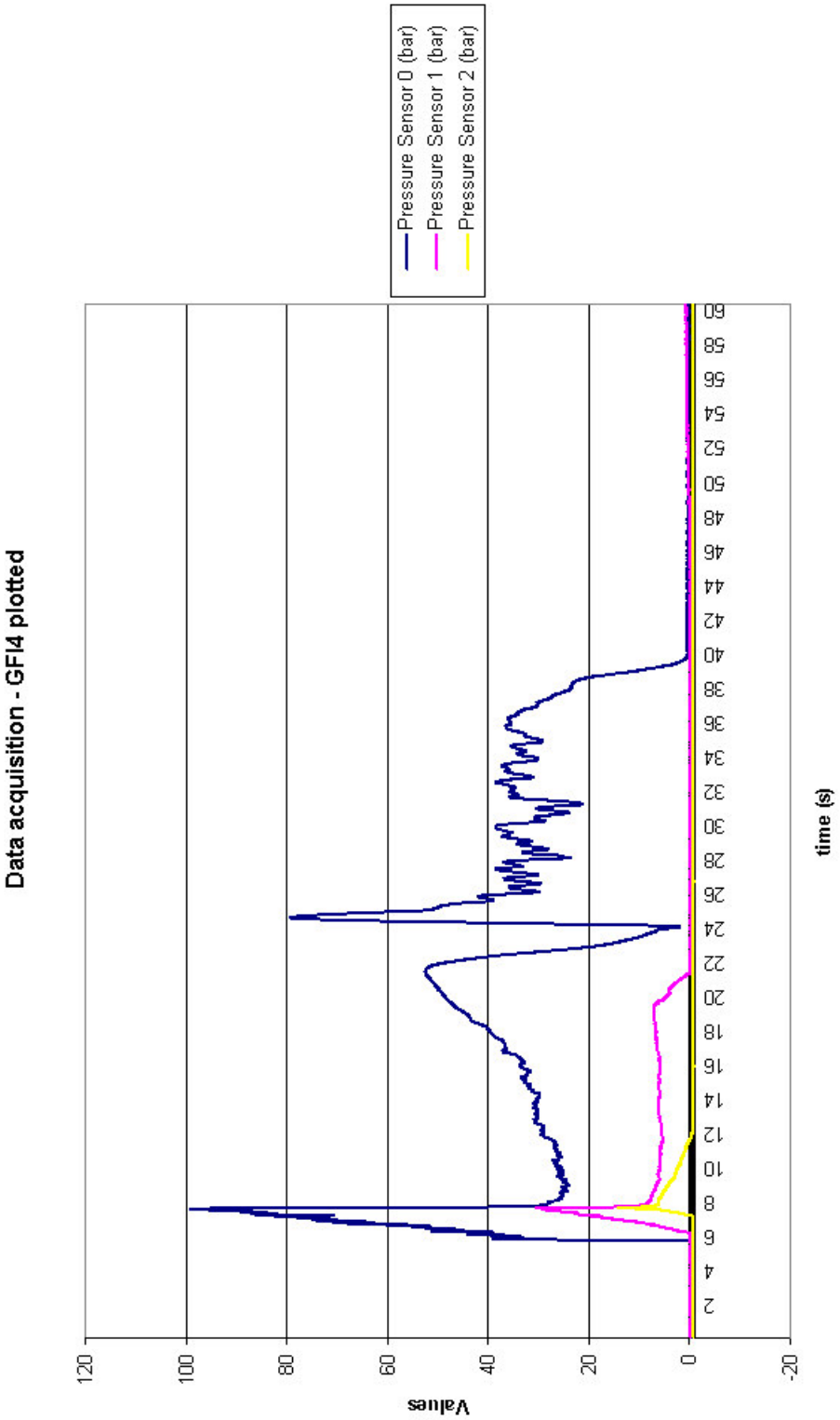

Figure B11a: Cavity pressures in injection moulding DOE GFI4

Figure B11b: Fibre skeleton remaining after burn off of GFI4-24

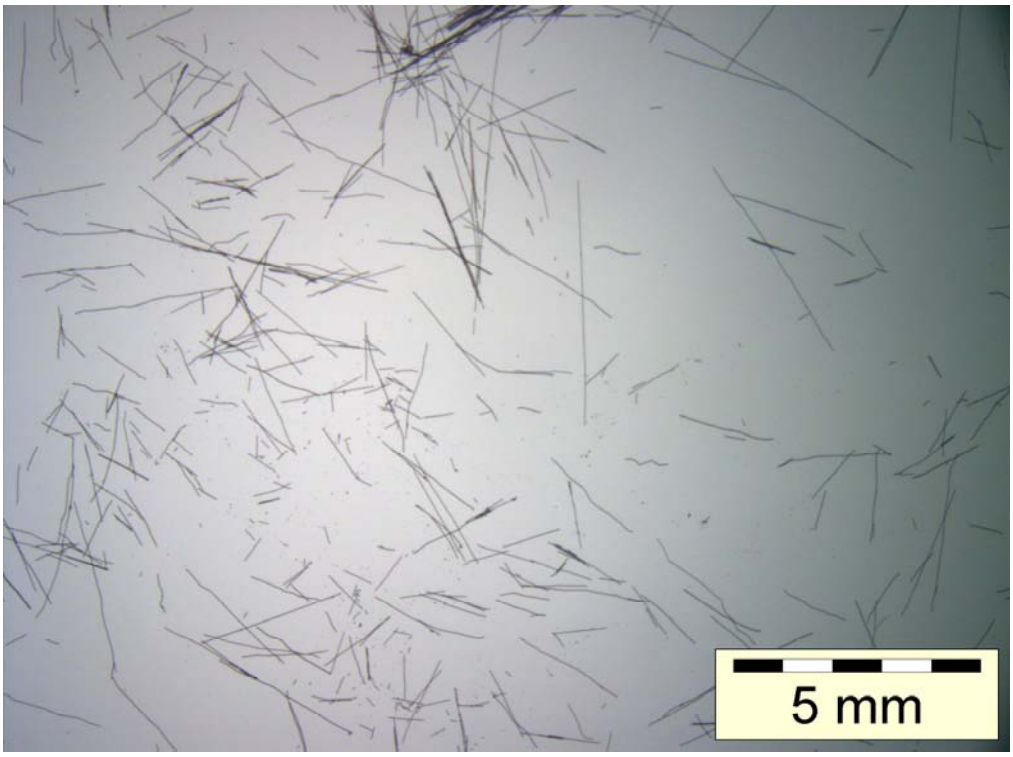

Figure B11c: Optical microscope photo taken with sample from GFI4-24

Appendix B12: Design of experiment GFI5

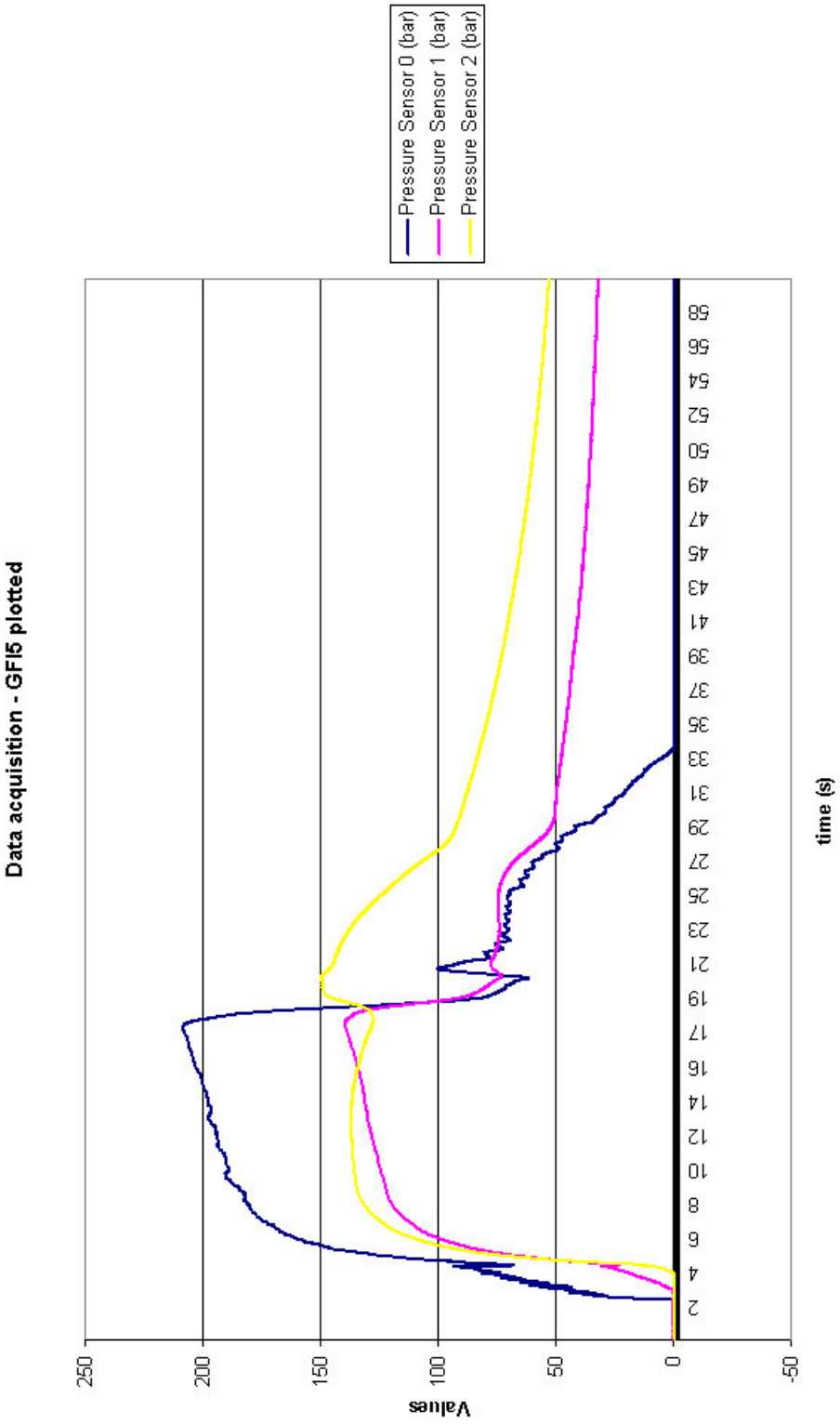

Figure B12a: Cavity pressures in injection moulding DOE GFI5

Figure B12b: Fibre skeleton remaining after burn off of GFI5-23

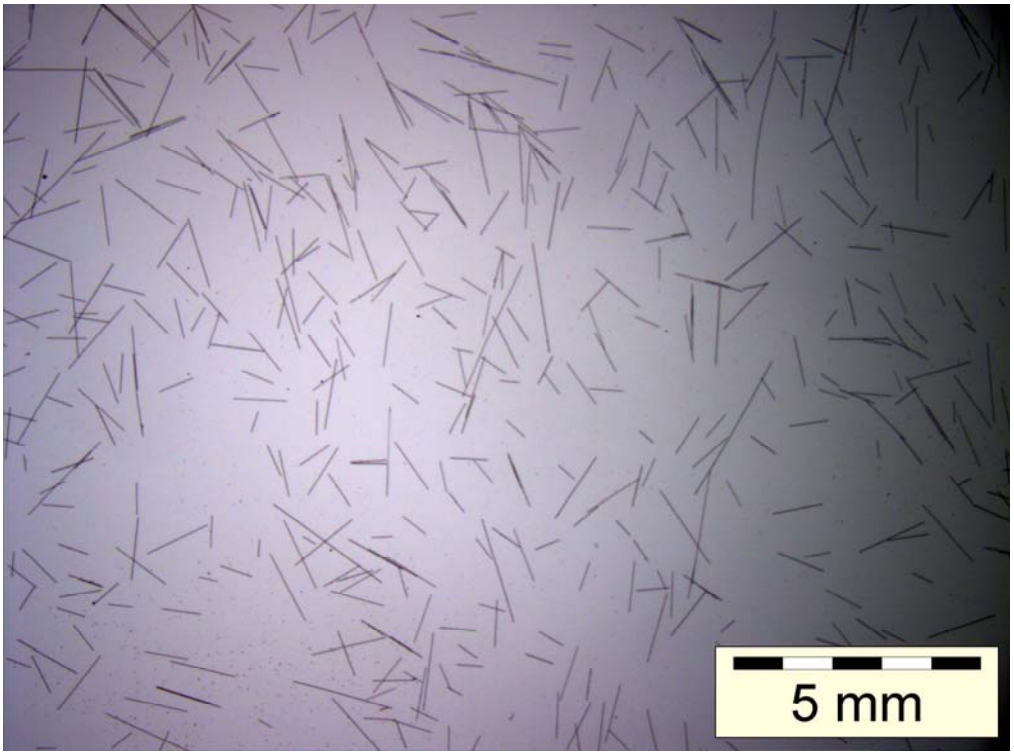

Figure B12c: Optical microscope photo taken with sample from GFI5-23

Appendix B13: Design of experiment GFI6

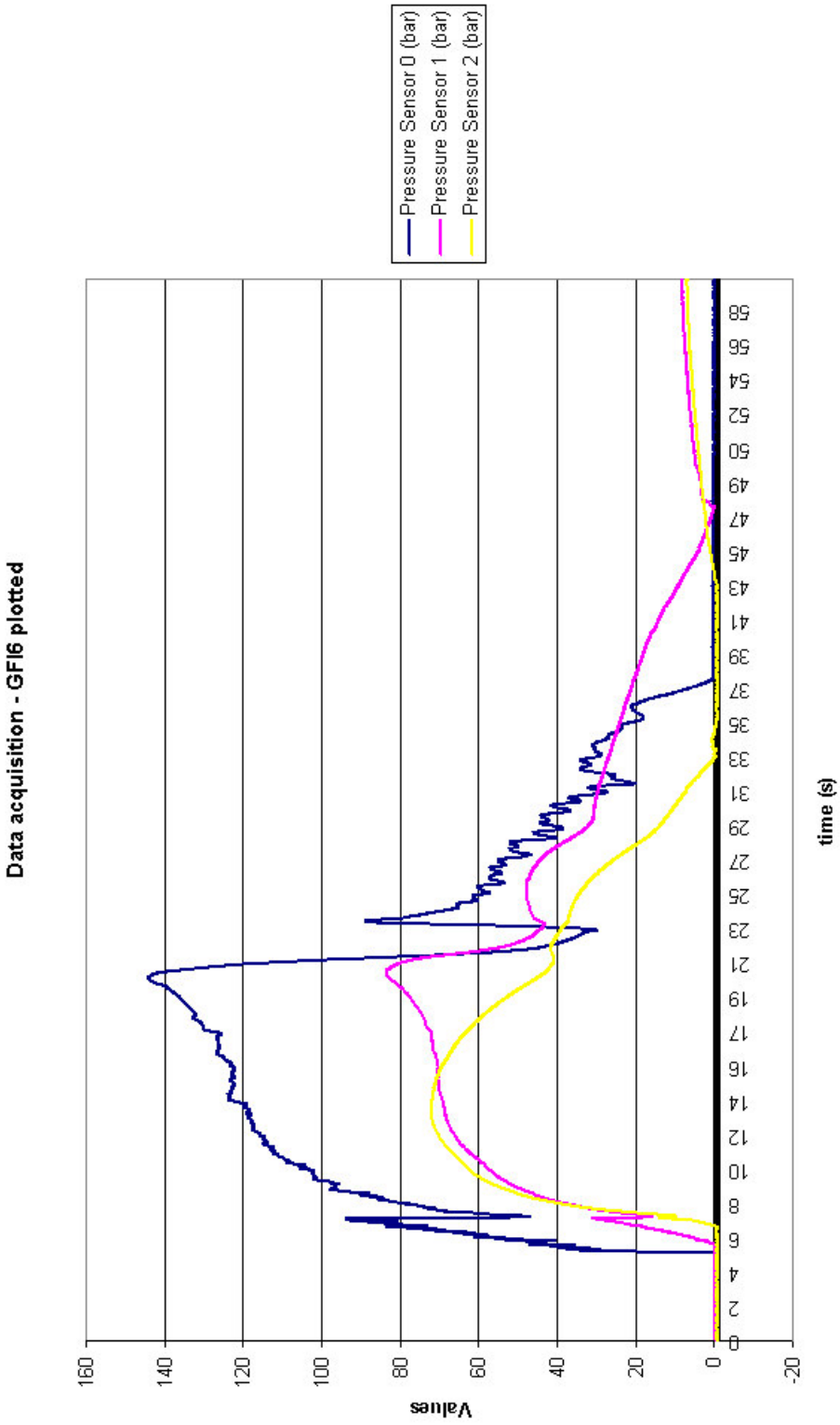

Figure B13a: Cavity pressures in injection moulding DOE GFI6

Figure B13b: Fibre skeleton remaining after burn off of GFI6-23

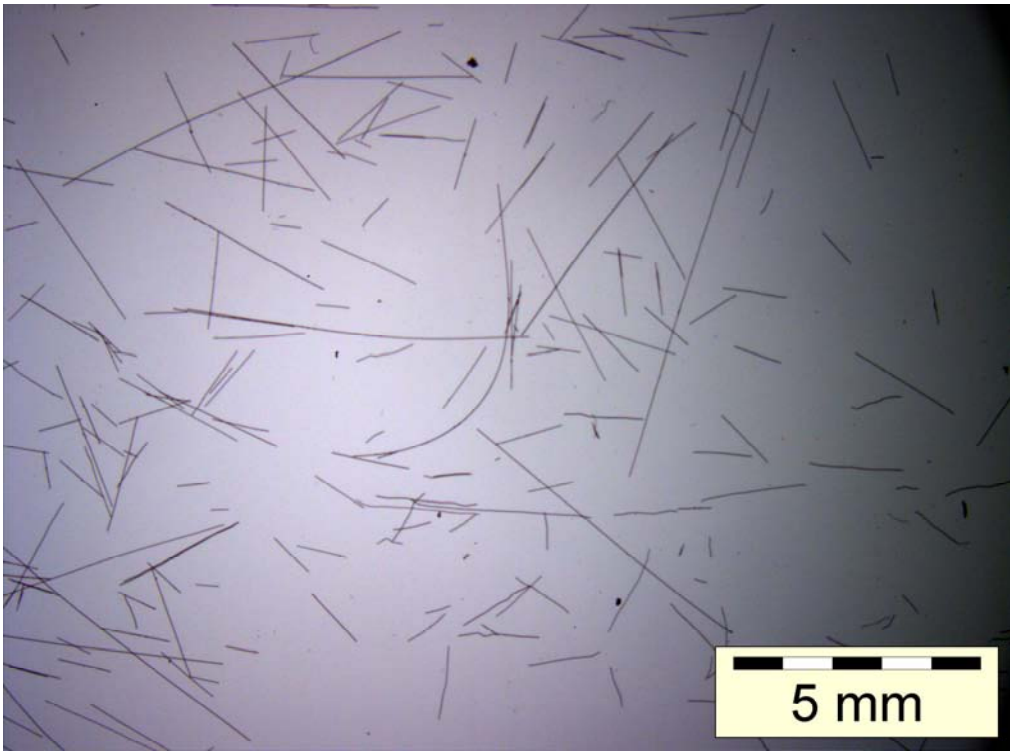

Figure B13c: Optical microscope photo taken with sample from GFI6-23

Appendix B14: Design of experiment GFI7

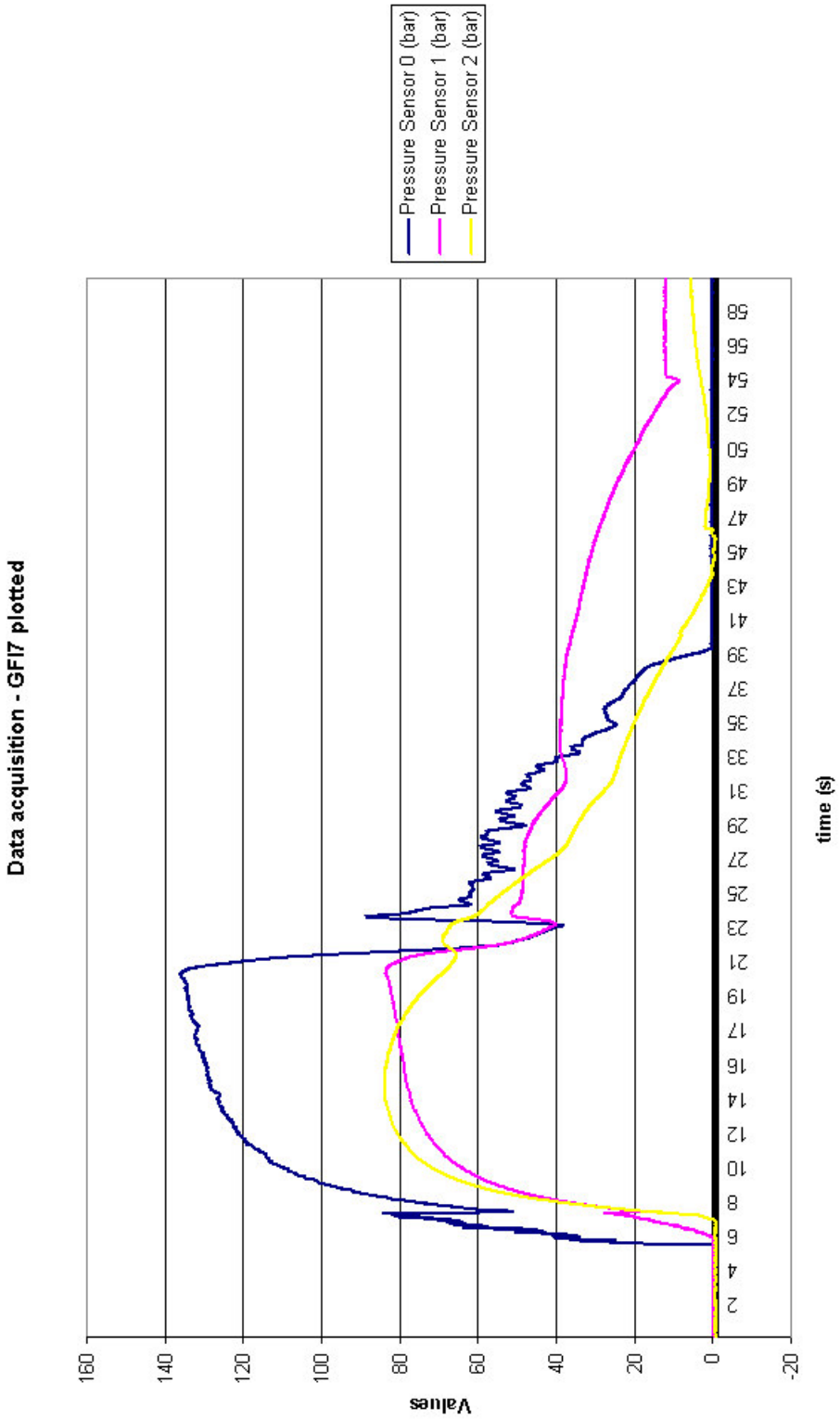

Figure B14a: Cavity pressures in injection moulding DOE GFI7

Figure B14b: Fibre skeleton remaining after burn off GFI7-21

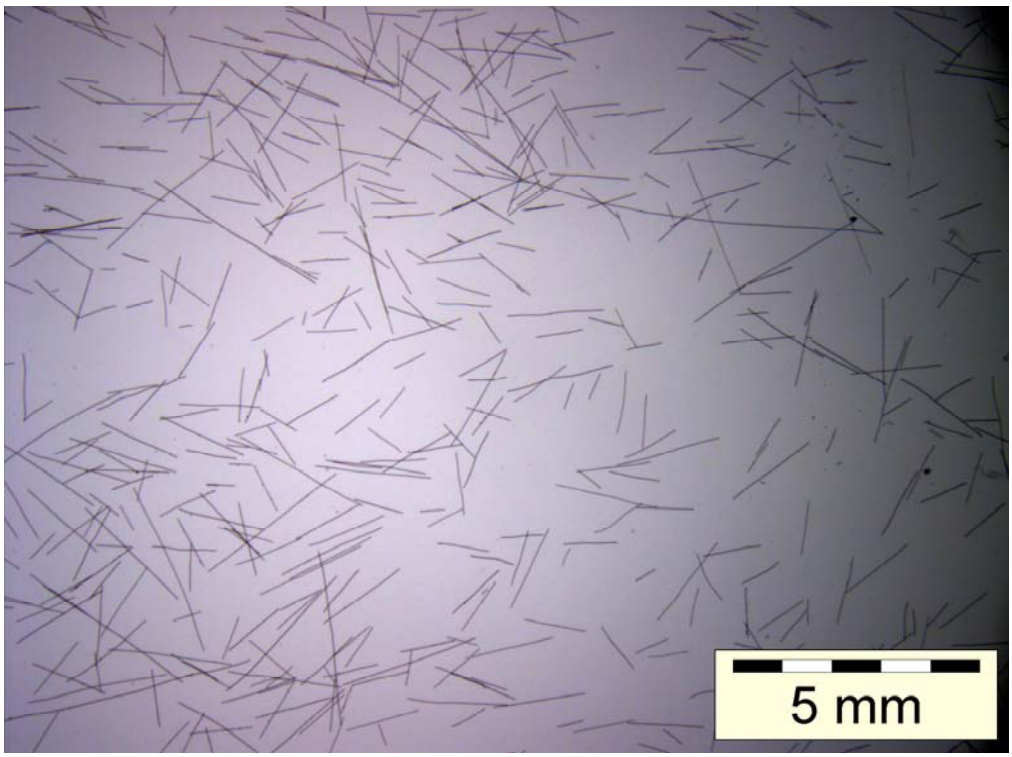

Figure B14c: Optical microscope photo taken with sample from GFI7-21

Appendix C: Lomolding parameters

Appendix C1: Design of experiment L1/L11

Materials used: Sasol PP1100N

COOLING SYSTEM:

Chiller set at 12 °C, 3.3 bar
Plasticiser: 20
Piston: 175
Fixed Mould 1: 170
Fixed Mould 2: 180
Moving Mould Cooling Circuit Pressure: 2.9 bar

BATCH SETUP (Critical Packing Pressure Control_

Volume: 233 ml
Change over pt: 7 mm
Cooling Time: 90 s

SPEED PROFILE

Position B: 224 mm @ 140 mm/s
Position C: 15 mm @ 100 mm/s
Position D: 10 mm @ 50 mm/s
Position E: 7 mm @ 20 mm/s

PRESSURE PROFILE

Injection: 120 bar
Packing: 120 bar for 15 s
Post Injection Pressure: 80 bar for 90 s

OVERVIEW:

Ambient Temp: 23 °C
Humidity: 59%

TEMPERATURES during stabilisation

Engel Plasticiser 1:	Set 200 °C	Actual 200 °C
Engel Plasticiser 2:	Set 200 °C	Actual 200 °C
Engel Plasticiser 3:	Set 200 °C	Actual 200 °C
Engel Plasticiser 4:	Set 200 °C	Actual 200 °C
Infeed Valve:	Set 200 °C	Actual 201 °C
Infeed Nozzle:	Set 200 °C	Actual 195 °C
MTC Middle:	Set 200 °C	Actual 199 °C
MTC Bottom:	Set 0 °C	Actual 167 °C
Horizontal Hot Runner:	Set 200 °C	Actual 199 °C
Hot Runner Bend:	Set 200 °C	Actual 199 °C
Vertical Hot Runner	Set 200 °C	Actual 200 °C
Outfeed Valve:	Set 200 °C	Actual 202 °C
MLC Right:	Set 200 °C	Actual 194 °C
MLC Left:	Set 200 °C	Actual 191 °C

ENGEL SETPOINTS

Metering Plunger Rear Pressure: 40%
Metering Plunger Rear Volume : 100%
Hydraulic Pressure Actual Value PHx: 100 bar approx

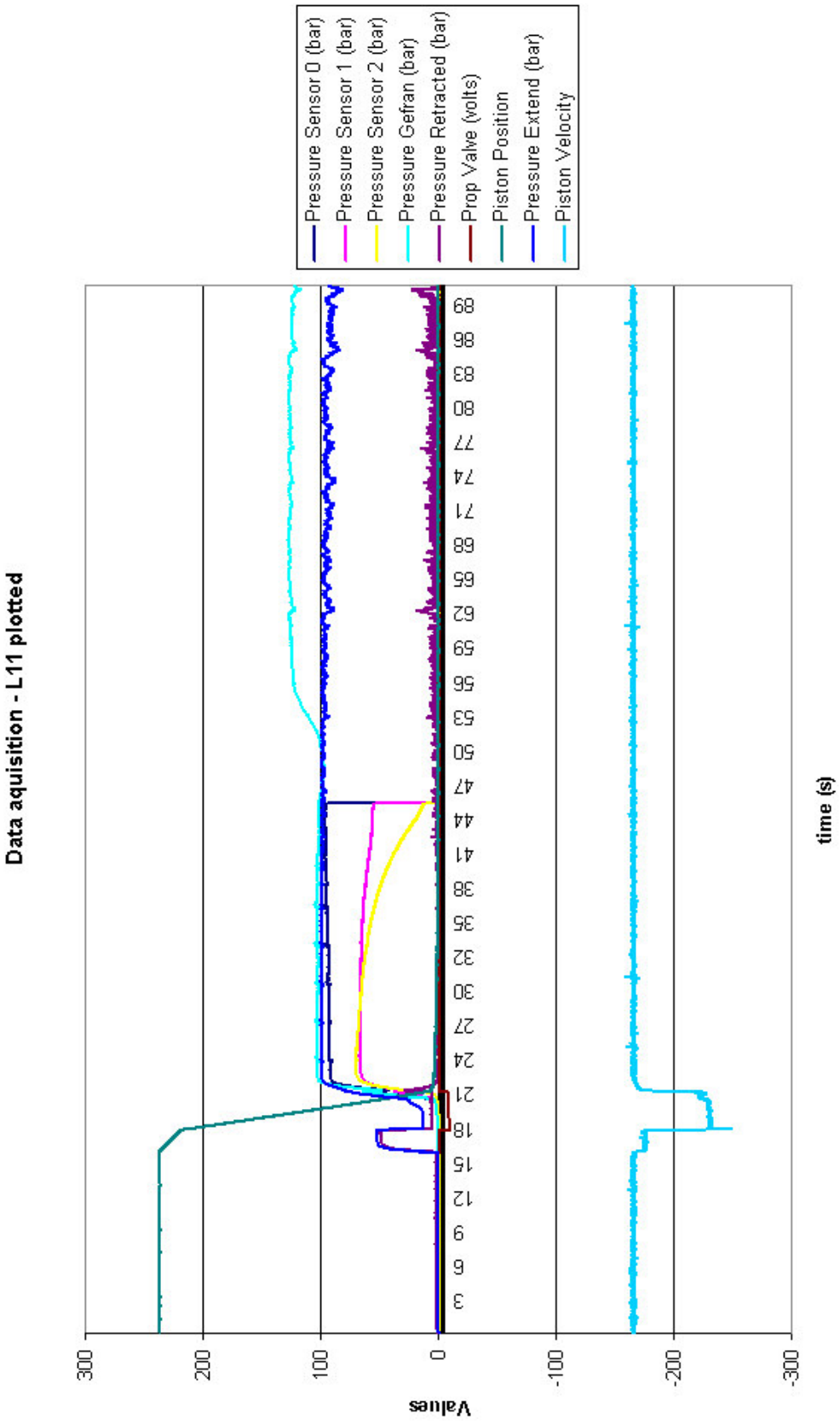

Figure C1: Cavity pressures in lomolding DOE L1/L11

Appendix C2: Design of experiment L2/L12

Material used: Sasol PP1100N

COOLING SYSTEM:

Chiller set at 12 °C, 3.3 bar
Plasticiser: 20
Piston: 175
Fixed Mould 1: 170
Fixed Mould 2: 180
Moving Mould Cooling Circuit Pressure: 2.9 bar

BATCH SETUP (Critical Packing Pressure Control)

Volume: 232 ml
Change Over pt: 7 mm
Cooling Time: 90 s

SPEED PROFILE

Position B: 224 mm @ 140 mm/s
Position C: 15 mm @ 100 mm/s
Position D: 10 mm @ 50 mm/s
Position E: 7 mm @ 20 mm/s

PRESSURE PROFILE

Injection: 120 bar
Packing : 120 bar for 15 s
Post Injection Pressure: 80 bar for 90 s

OVERVIEW:

Ambient Temp: 24 °C
Humidity: 60%

TEMPERATURES during stabilisation

Engel Plasticiser 1:	Set 214 °C	Actual 214 °C
Engel Plasticiser 2:	Set 214 °C	Actual 214 °C
Engel Plasticiser 3:	Set 214 °C	Actual 213 °C
Engel Plasticiser 4:	Set 214 °C	Actual 214 °C
Infeed Valve:	Set 214 °C	Actual 212 °C
Infeed Nozzle:	Set 214 °C	Actual 210 °C
MTC Middle:	Set 214 °C	Actual 214 °C
MTC Bottom:	Set 0 °C	Actual 178 °C
Horizontal Hot Runner:	Set 214 °C	Actual 214 °C
Hot Runner Bend:	Set 214 °C	Actual 211 °C
Vertical Hot Runner	Set 214 °C	Actual 214 °C
Outfeed Valve:	Set 214 °C	Actual 215 °C
MLC Right:	Set 214 °C	Actual 216 °C
MLC Left:	Set 214 °C	Actual 221 °C

ENGEL SETPOINTS

Metering Plunger Rear Pressure: 34%
Metering Plunger Rear Volume : 100%
Hydraulic Pressure Actual Value PHx: 86 bar approx

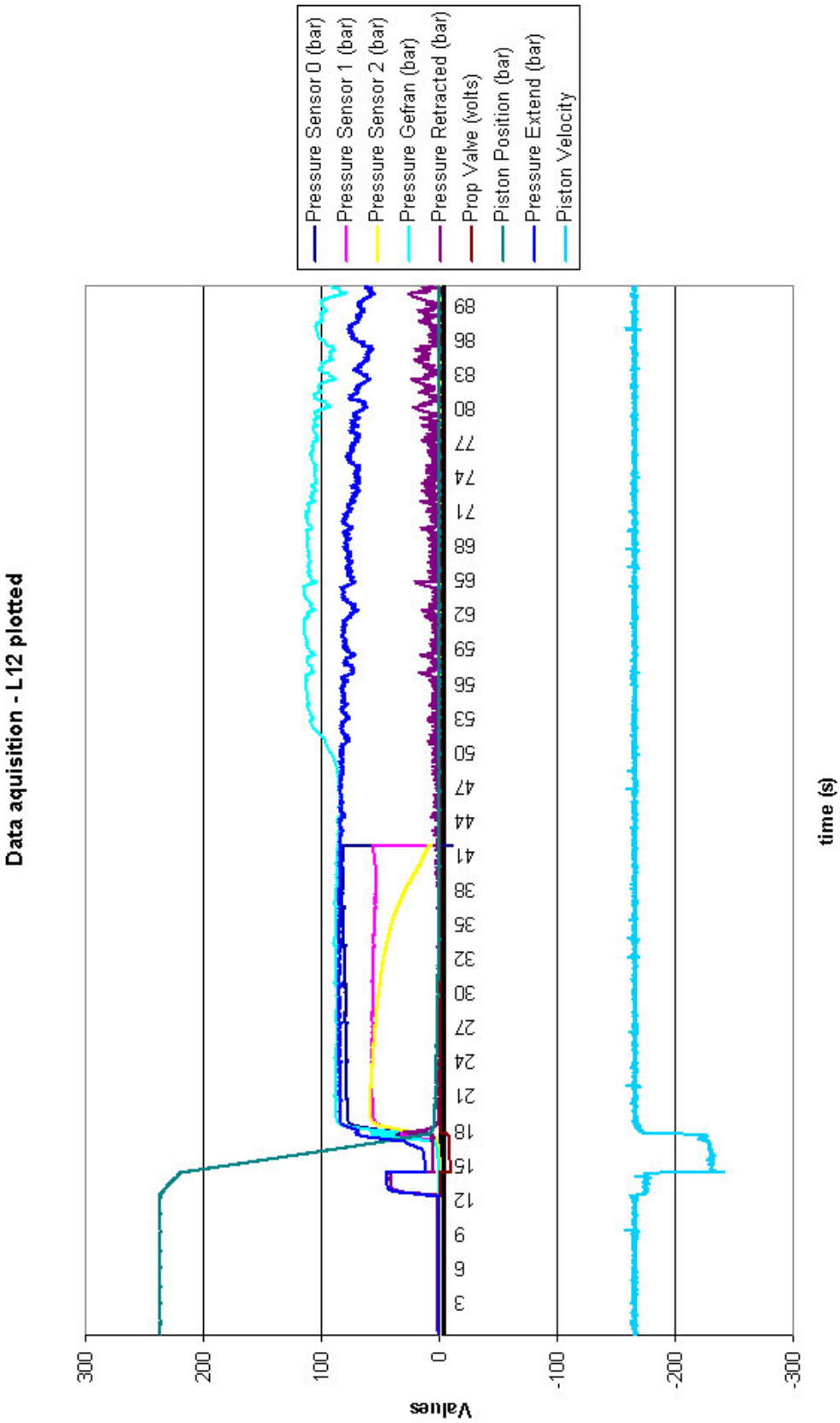

Figure C2: Cavity pressures in lomolding DOE L2/L12

Appendix C3: Design of experiment L3/L13

Materials used: Sasol PP1100N

COOLING SYSTEM:

Chiller set at 12 °C, 3.3 bar
Plasticiser: 20
Piston: 180
Fixed Mould 1: 170
Fixed Mould 2: 180
Moving Mould Cooling Circuit Pressure: 2.9 bar

BATCH SETUP (Critical Packing Pressure Control)

Volume: 234 ml
Change over pt: 7 mm
Cooling Time: 90 s

SPEED PROFILE

Position B: 224 mm @ 140 mm/s
Position C: 15 mm @ 100 mm/s
Position D: 10 mm @ 50 mm/s
Position E: 7 mm @ 20 mm/s

PRESSURE PROFILE

Injection: 120 bar
Packing : 120 bar for 15 s
Post Injection Pressure: 80 bar for 90 s

OVERVIEW:

Ambient Temp: 24 °C
Humidity: 61%

TEMPERATURES during stabilisation

Engel Plasticiser 1:	Set 220 °C	Actual 220 °C
Engel Plasticiser 2:	Set 220 °C	Actual 220 °C
Engel Plasticiser 3:	Set 220 °C	Actual 219 °C
Engel Plasticiser 4:	Set 220 °C	Actual 220 °C
Infeed Valve:	Set 220 °C	Actual 219 °C
Infeed Nozzle:	Set 220 °C	Actual 216 °C
MTC Middle:	Set 220 °C	Actual 220 °C
MTC Bottom:	Set 0 °C	Actual 185 °C
Horizontal Hot Runner:	Set 220 °C	Actual 219 °C
Hot Runner Bend:	Set 220 °C	Actual 219 °C
Vertical Hot Runner	Set 220 °C	Actual 220 °C
Outfeed Valve:	Set 220 °C	Actual 223 °C
MLC Right:	Set 220 °C	Actual 220 °C
MLC Left:	Set 220 °C	Actual 217 °C

ENGEL SETPOINTS

Metering Plunger Rear Pressure: 40%
Metering Plunger Rear Volume : 100%
Hydraulic Pressure Actual Value PHx: 100 bar approx

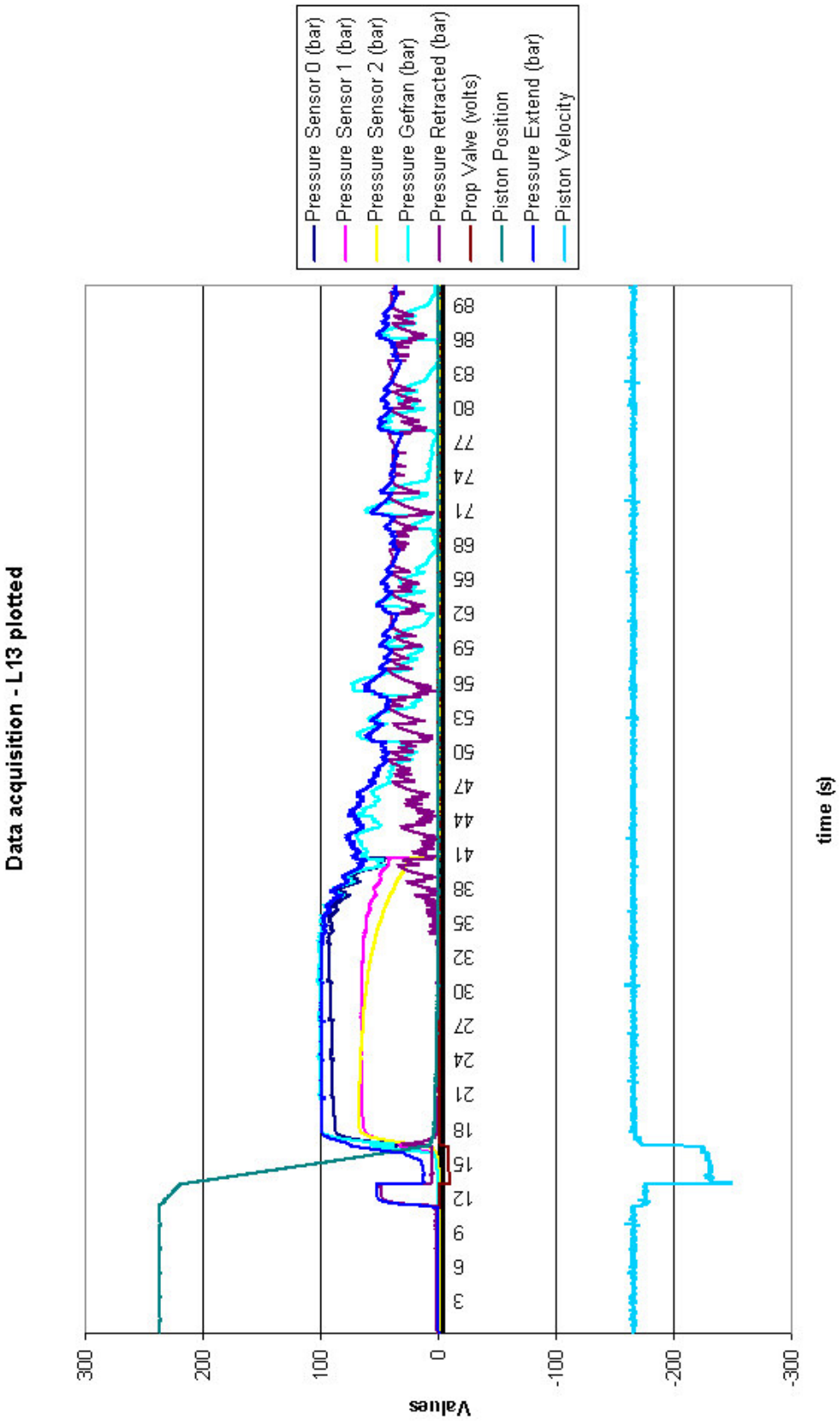

Figure C3: Cavity pressures in lomolding DOE L3/L13

Appendix C4: Design of experiment L4

Material used: Sasol PP1100N

COOLING SYSTEM:

Chiller Set at 12 °C, 3.3 bar
Plasticiser : 35
Piston : 170
Fixed Mould 1: 165
Fixed Mould 2: 180
Moving Mould Cooling Circuit Pressure: 2.9 bar

BATCH SETUP (Critical Packing Pressure Control)

Volume: 228 ml
Change Over pt: 7 mm
Cooling Time: 90 s

SPEED PROFILE

Position B: 224 mm @ 140 mm/s
Position C: 15 mm @ 100 mm/s
Position D: 10 mm @ 50 mm/s
Position E: 7 mm @ 20 mm/s

PRESSURE PROFILE

Injection: 120 bar
Packing : 120 bar for 15 s
Post Injection Pressure: 80 bar for 90 s

OVERVIEW:

Ambient Temp: 21 °C
Humidity: 53%

TEMPERATURES just before experimentation

Engel Plasticiser 1:	Set 180 °C	Actual 180 °C
Engel Plasticiser 2:	Set 180 °C	Actual 180 °C
Engel Plasticiser 3:	Set 180 °C	Actual 180 °C
Engel Plasticiser 4:	Set 180 °C	Actual 180 °C
Infeed Valve:	Set 180 °C	Actual 181 °C
Infeed Nozzle:	Set 180 °C	Actual 177 °C
MTC Middle:	Set 180 °C	Actual 184 °C
MTC Bottom:	Set 0 °C	Actual 152 °C
Horizontal Hot Runner:	Set 180 °C	Actual 180 °C
Hot Runner Bend:	Set 180 °C	Actual 181 °C
Vertical Hot Runner	Set 180 °C	Actual 182 °C
Outfeed Valve:	Set 180 °C	Actual 184 °C
MLC Right:	Set 180 °C	Actual 182 °C
MLC Left:	Set 180 °C	Actual 183 °C

ENGEL SETPOINTS

Metering Plunger Rear Pressure: 40%
Metering Plunger Rear Volume : 100%
Hydr Pressure Actual Value PHx: 100 bar approx

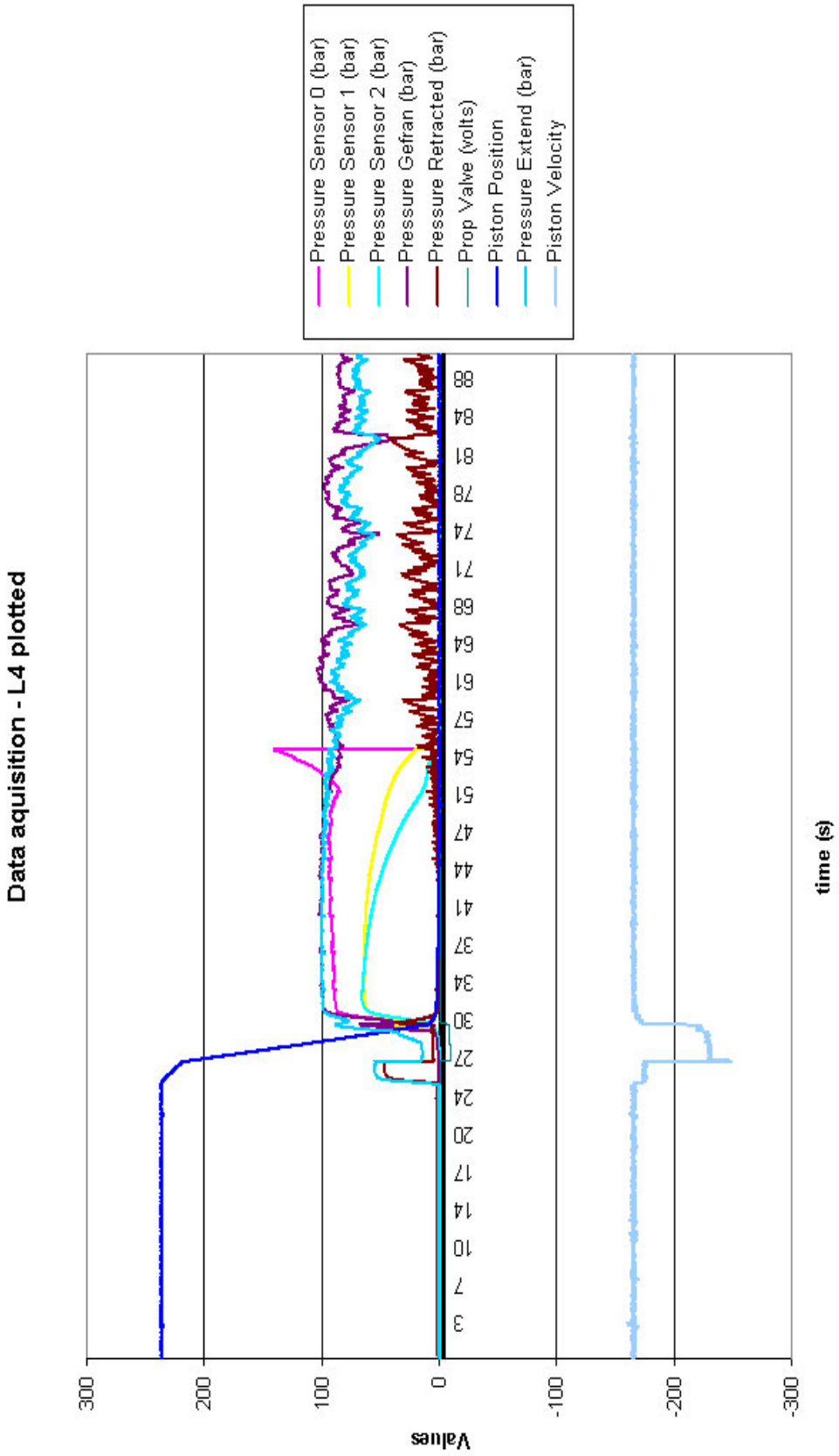

Figure C4: Cavity pressures in lomolding DOE L4

Appendix C5: Design of experiment L5

Material used: Sasol PP1100N

COOLING SYSTEM:

Chiller Set at 12 °C, 3.3 bar
Plasticiser: 35
Piston: 175
Fixed Mould 1: 170
Fixed Mould 2: 180
Moving Mould Cooling Circuit Pressure: 2.9 bar

BATCH SETUP (Critical Packing Pressure Control)

Volume: 229 ml
Change over pt: 7 mm
Cooling Time: 90 s

SPEED PROFILE

Position B: 224 mm @ 140 mm/s
Position C: 15 mm @ 100 mm/s
Position D: 10 mm @ 50 mm/s
Position E: 7 mm @ 20 mm/s

PRESSURE PROFILE

Injection: 120 bar
Packing : 120 bar for 15 s
Post Injection Pressure : 80 bar for 90 s

OVERVIEW:

Ambient Temp: 18 °C
Humidity: 47%

TEMPERATURES just before experimentation

Engel Plasticiser 1:	Set 200 °C	Actual 200 °C
Engel Plasticiser 2:	Set 200 °C	Actual 200 °C
Engel Plasticiser 3:	Set 200 °C	Actual 200 °C
Engel Plasticiser 4:	Set 200 °C	Actual 199 °C
Infeed Valve:	Set 200 °C	Actual 201 °C
Infeed Nozzle:	Set 200 °C	Actual 199 °C
MTC Middle:	Set 200 °C	Actual 204 °C
MTC Bottom:	Set 0 °C	Actual 168 °C
Horizontal Hot Runner:	Set 200 °C	Actual 198 °C
Hot Runner Bend:	Set 200 °C	Actual 201 °C
Vertical Hot Runner	Set 200 °C	Actual 202 °C
Outfeed Valve:	Set 200 °C	Actual 206 °C
MLC Right:	Set 200 °C	Actual 195 °C
MLC Left:	Set 200 °C	Actual 203 °C

ENGEL SETPOINTS

Metering Plunger Rear Pressure: 32%
Metering Plunger Rear Volume : 100%
Hydr Pressure Actual Value PHx: 80 bar approx

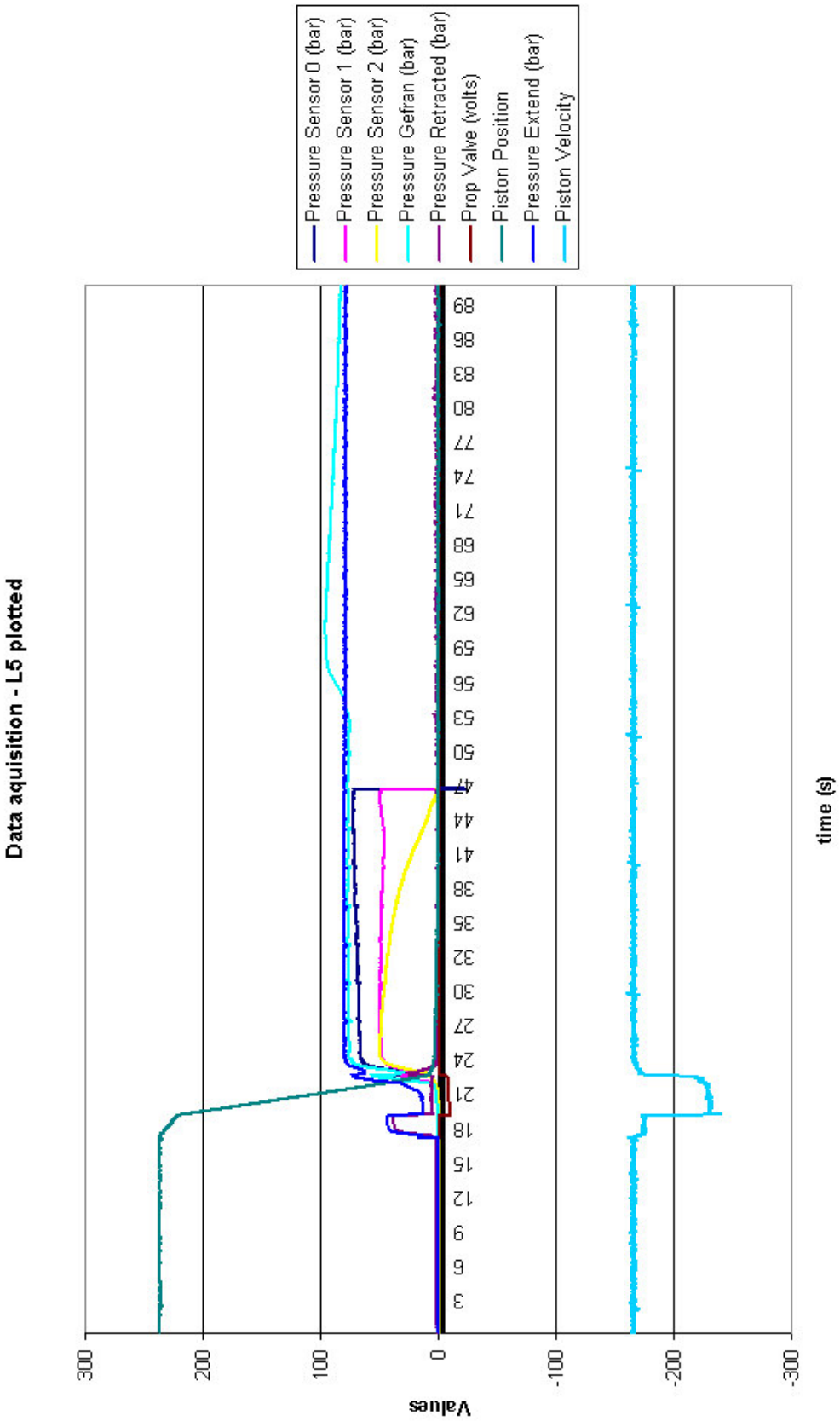

Figure C5: Cavity pressures in Iomolding DOE L5

Appendix C6: Design of experiment L6

Material used: Sasol PP1100N

COOLING SYSTEM:

Chiller Set at 12 °C, 3.3 bar
Plasticiser: 35
Piston: 175
Fixed Mould 1: 170
Fixed Mould 2: 180
Moving Mould Cooling Circuit Pressure: 2.9 bar

BATCH SETUP (Critical Packing Pressure Control)

Volume: 235 ml
Change over pt: 7 mm
Cooling Time: 90 s

SPEED PROFILE

Position B: 224 mm @ 140 mm/s
Position C: 15 mm @ 100 mm/s
Position D: 10 mm @ 50 mm/s
Position E: 7 mm @ 20 mm/s

PRESSURE PROFILE

Injection: 120 bar
Packing : 120 bar for 15 s
Post Injection Pressure: 80 bar for 90 s

OVERVIEW:

Ambient Temp: 23 °C
Humidity: 59%

TEMPERATURES during stabilisation

Engel Plasticiser 1:	Set 200 °C	Actual 200 °C
Engel Plasticiser 2:	Set 200 °C	Actual 200 °C
Engel Plasticiser 3:	Set 200 °C	Actual 200 °C
Engel Plasticiser 4:	Set 200 °C	Actual 199 °C
Infeed Valve:	Set 200 °C	Actual 199 °C
Infeed Nozzle:	Set 200 °C	Actual 199 °C
MTC Middle:	Set 200 °C	Actual 200 °C
MTC Bottom:	Set 0 °C	Actual 166 °C
Horizontal Hot Runner:	Set 200 °C	Actual 198 °C
Hot Runner Bend:	Set 200 °C	Actual 200 °C
Vertical Hot Runner:	Set 200 °C	Actual 202 °C
Outfeed Valve:	Set 200 °C	Actual 204 °C
MLC Right:	Set 200 °C	Actual 200 °C
MLC Left:	Set 200 °C	Actual 207 °C

ENGEL SETPOINTS

Metering Plunger Rear Pressure: 48%
Metering Plunger Rear Volume : 100%
Hydraulic Pressure Actual Value PHx: 120 bar approx

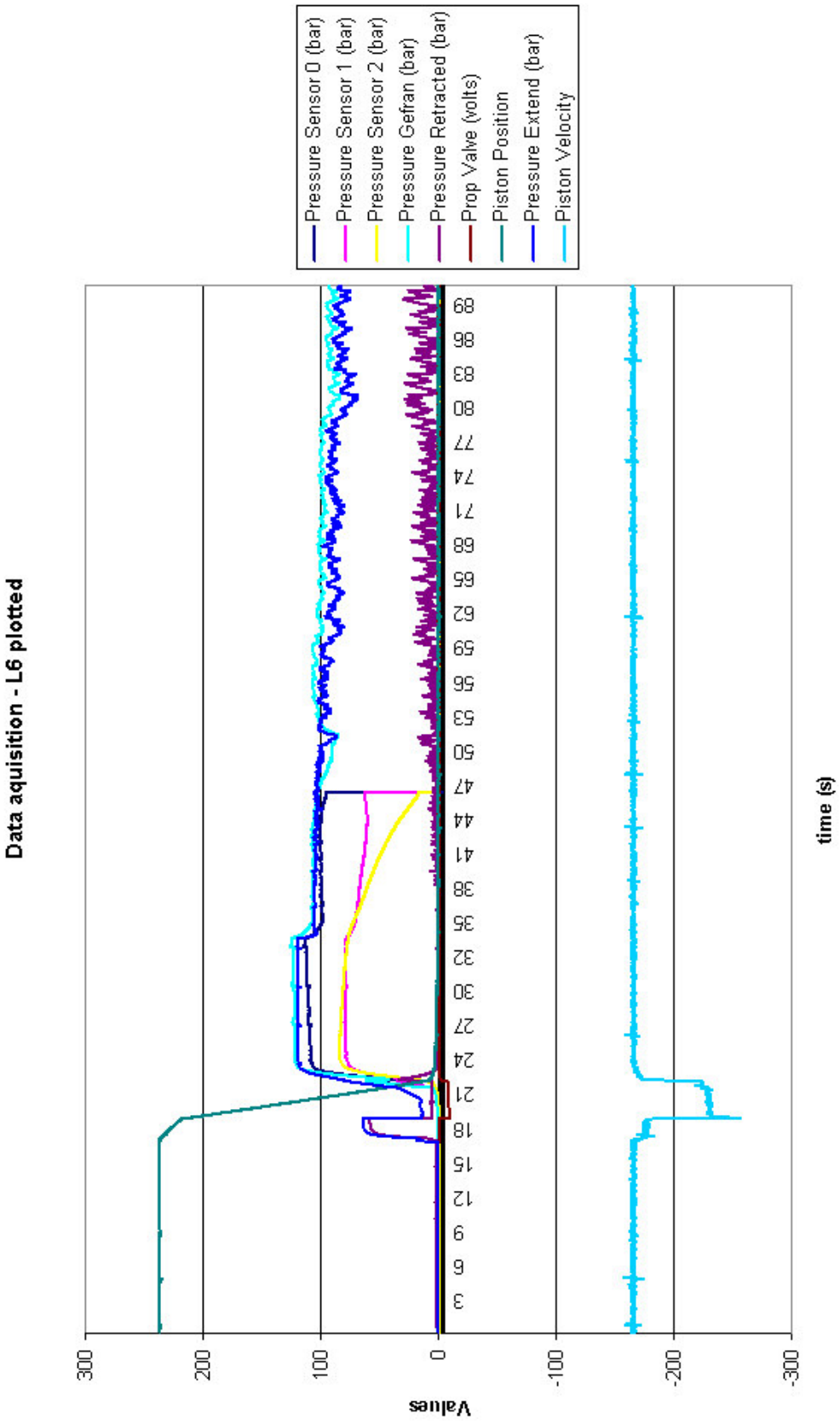

Figure C6: Cavity pressures in lomolding DOE L6

Appendix C7: Design of experiment L7

Material used: Sasol PP1100N

COOLING SYSTEM:

Chiller Set at 12 °C, 3.3 bar
Plasticiser: 35
Piston: 175
Fixed Mould 1: 170
Fixed Mould 2: 180
Moving Mould Cooling Circuit Pressure: 2.9 bar

BATCH SETUP (Critical Packing Pressure Control)

Volume: 233 ml
Change over pt: 7 mm
Cooling Time: 90 s

SPEED PROFILE

Position B: 224 mm @ 140 mm/s
Position C: 15 mm @ 100 mm/s
Position D: 10 mm @ 50 mm/s
Position E: 7 mm @ 20 mm/s

PRESSURE PROFILE

Injection: 120 bar
Packing : 120 bar for 15 s
Post Injection Pressure: 80 bar for 90 s

OVERVIEW:

Ambient Temp: 22 °C
Humidity: 57%

TEMPERATURES during stabilisation

Engel Plasticiser 1:	Set 186 °C	Actual 186 °C
Engel Plasticiser 2:	Set 186 °C	Actual 186 °C
Engel Plasticiser 3:	Set 186 °C	Actual 186 °C
Engel Plasticiser 4:	Set 186 °C	Actual 186 °C
Infeed Valve:	Set 186 °C	Actual 185 °C
Infeed Nozzle:	Set 186 °C	Actual 184 °C
MTC Middle:	Set 186 °C	Actual 189 °C
MTC Bottom:	Set 0 °C	Actual 157 °C
Horizontal Hot Runner:	Set 186 °C	Actual 187 °C
Hot Runner Bend:	Set 186 °C	Actual 184 °C
Vertical Hot Runner	Set 186 °C	Actual 186 °C
Outfeed Valve:	Set 186 °C	Actual 187 °C
MLC Right:	Set 186 °C	Actual 180 °C
MLC Left:	Set 186 °C	Actual 178 °C

ENGEL SETPOINTS

Metering Plunger Rear Pressure: 45%
Metering Plunger Rear Volume : 100%
Hydraulic Pressure Actual Value PHx: 114 bar approx

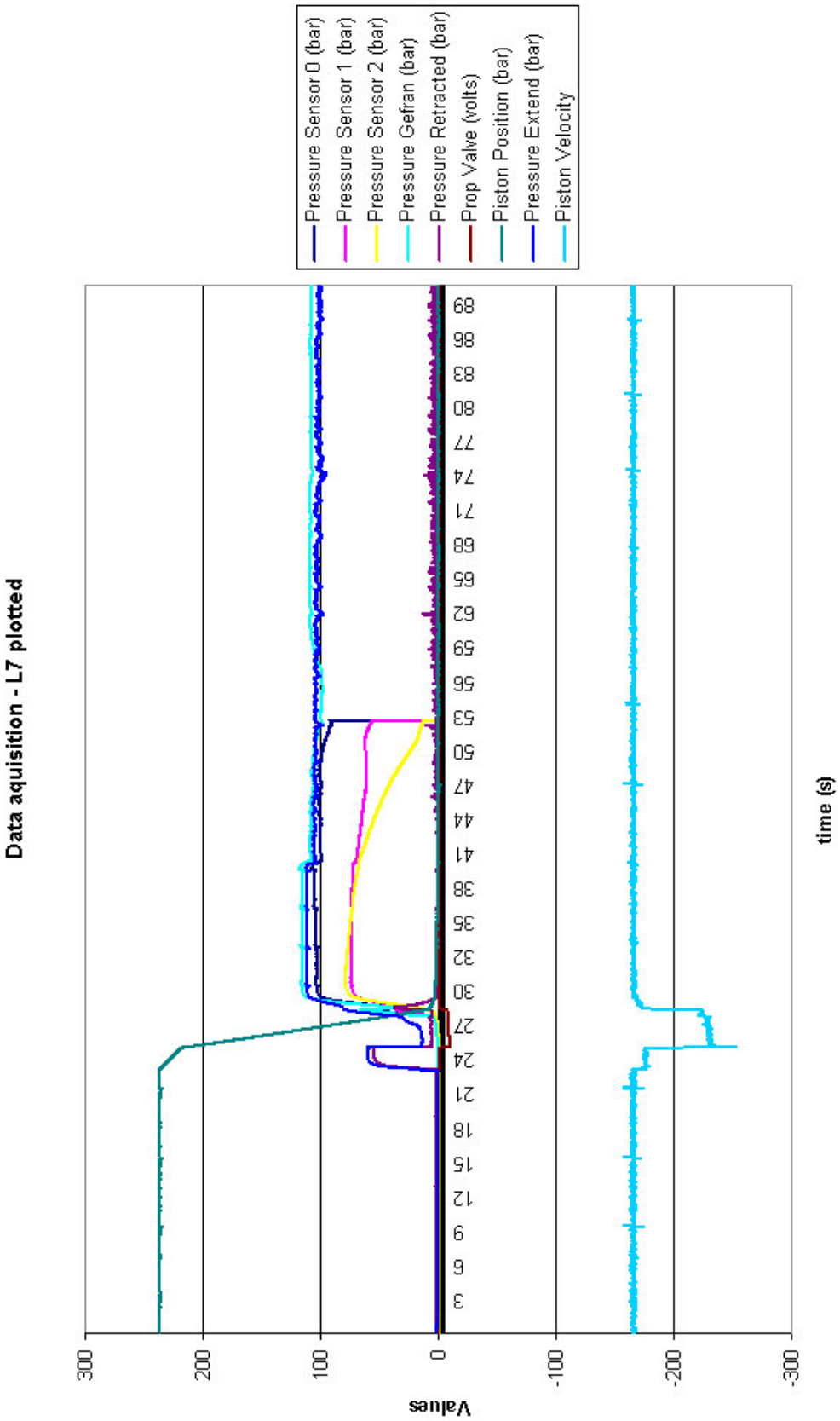

Figure C7: Cavity pressures in lomolding DOE L7

Appendix C8: Design of experiment L8

Material used: Sasol PP1100N

COOLING SYSTEM:

Chiller set at 12 °C, 3.3 bar
Plasticiser: 30
Piston: 175
Fixed Mould 1: 170
Fixed Mould 2: 180
Moving Mould Cooling Circuit Pressure: 2.9 bar

BATCH SETUP (Critical Packing Pressure Control)

Volume: 233 ml
Change over pt: 7 mm
Cooling Time: 90 s

SPEED PROFILE

Position B: 224 mm @ 140 mm/s
Position C: 15 mm @ 100 mm/s
Position D: 10 mm @ 50 mm/s
Position E: 7 mm @ 20 mm/s

PRESSURE PROFILE

Injection: 120 bar
Packing: 120 bar for 15 s
Post Injection Pressure: 80 bar for 90 s

OVERVIEW:

Ambient Temp: 20 °C
Humidity: 51%

TEMPERATURES during stabilisation

Engel Plasticiser 1:	Set 200 °C	Actual 200 °C
Engel Plasticiser 2:	Set 200 °C	Actual 200 °C
Engel Plasticiser 3:	Set 200 °C	Actual 200 °C
Engel Plasticiser 4:	Set 200 °C	Actual 201 °C
Infeed Valve:	Set 200 °C	Actual 201 °C
Infeed Nozzle:	Set 200 °C	Actual 198 °C
MTC Middle:	Set 200 °C	Actual 207 °C
MTC Bottom:	Set 0 °C	Actual 167 °C
Horizontal Hot Runner:	Set 200 °C	Actual 202 °C
Hot Runner Bend:	Set 200 °C	Actual 200 °C
Vertical Hot Runner	Set 200 °C	Actual 199 °C
Outfeed Valve:	Set 200 °C	Actual 203 °C
MLC Right:	Set 200 °C	Actual 200 °C
MLC Left:	Set 200 °C	Actual 192 °C

ENGEL SETPOINTS

Metering Plunger Rear Pressure: 45%
Metering Plunger Rear Volume : 100%
Hydraulic Pressure Actual Value PHx: 100 bar approx

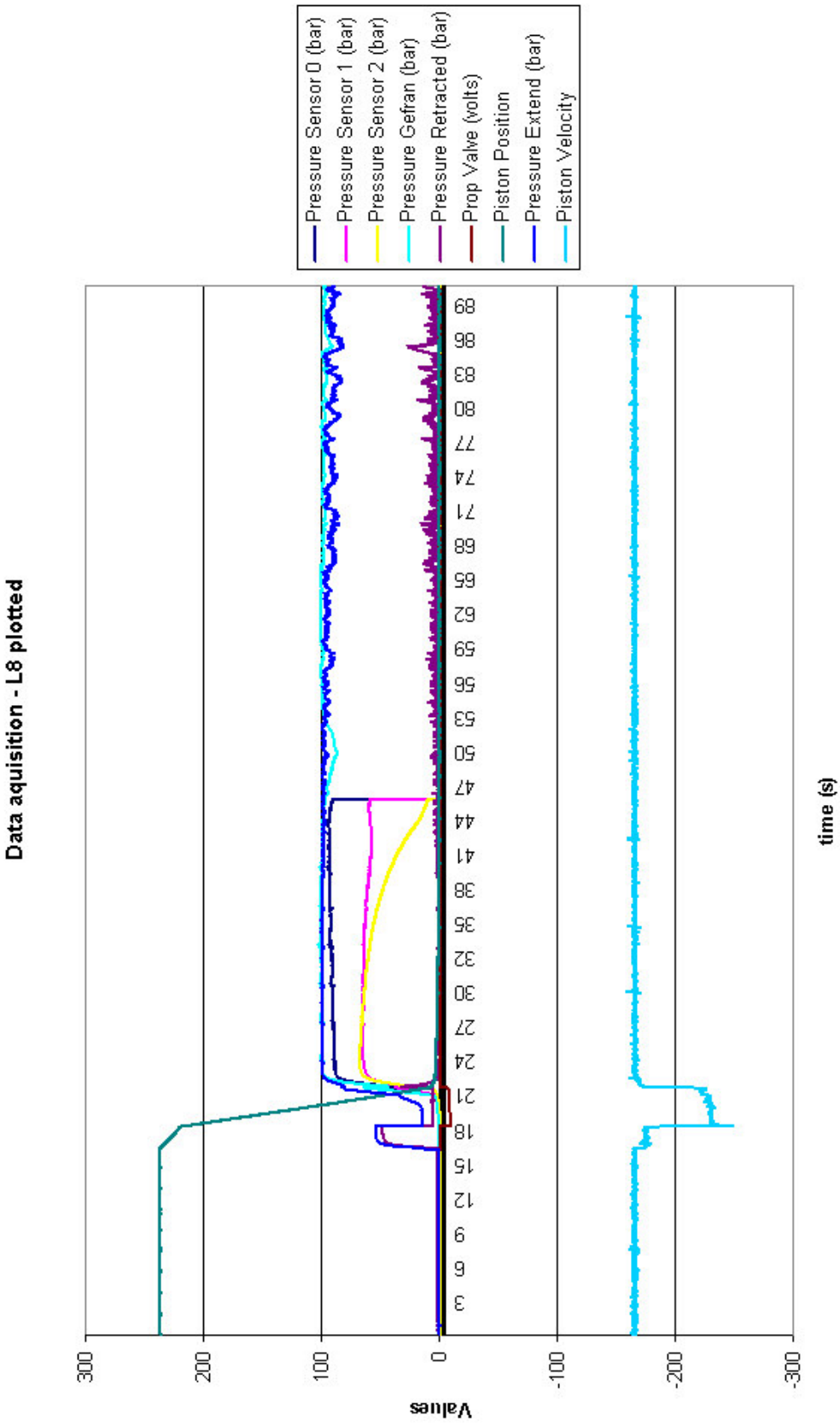

Figure C8: Cavity pressures in lomolding DOE L8

Appendix C9: Design of experiment L9

Material used: Sasol PP1100N

COOLING SYSTEM:

Chiller set at 12 °C, 3.3 bar
Plasticiser: 30
Piston: 175
Fixed Mould 1: 170
Fixed Mould 2: 180
Moving Mould Cooling Circuit Pressure: 2.9 bar

BATCH SETUP (Critical Packing Pressure Control)

Volume: 235 ml
Change over pt: 7 mm
Cooling Time: 90 s

SPEED PROFILE

Position B: 224 mm @ 140 mm/s
Position C: 15 mm @ 100 mm/s
Position D: 10 mm @ 50 mm/s
Position E: 7 mm @ 20 mm/s

PRESSURE PROFILE

Injection: 120 bar
Packing: 120 bar for 15 s
Post Injection Pressure: 80 bar for 90 s

OVERVIEW:

Ambient Temp: 20 °C
Humidity: 52%

TEMPERATURES during stabilisation

Engel Plasticiser 1:	Set 214 °C	Actual 214 °C
Engel Plasticiser 2:	Set 214 °C	Actual 214 °C
Engel Plasticiser 3:	Set 214 °C	Actual 214 °C
Engel Plasticiser 4:	Set 214 °C	Actual 214 °C
Infeed Valve:	Set 214 °C	Actual 215 °C
Infeed Nozzle:	Set 214 °C	Actual 210 °C
MTC Middle:	Set 214 °C	Actual 219 °C
MTC Bottom:	Set 0 °C	Actual 181 °C
Horizontal Hot Runner:	Set 214 °C	Actual 213 °C
Hot Runner Bend:	Set 214 °C	Actual 213 °C
Vertical Hot Runner	Set 214 °C	Actual 215 °C
Outfeed Valve:	Set 214 °C	Actual 216 °C
MLC Right:	Set 214 °C	Actual 215 °C
MLC Left:	Set 214 °C	Actual 221 °C

ENGEL SETPOINTS

Metering Plunger Rear Pressure: 45%
Metering Plunger Rear Volume : 100%
Hydraulic Pressure Actual Value PHx: 114 bar approx

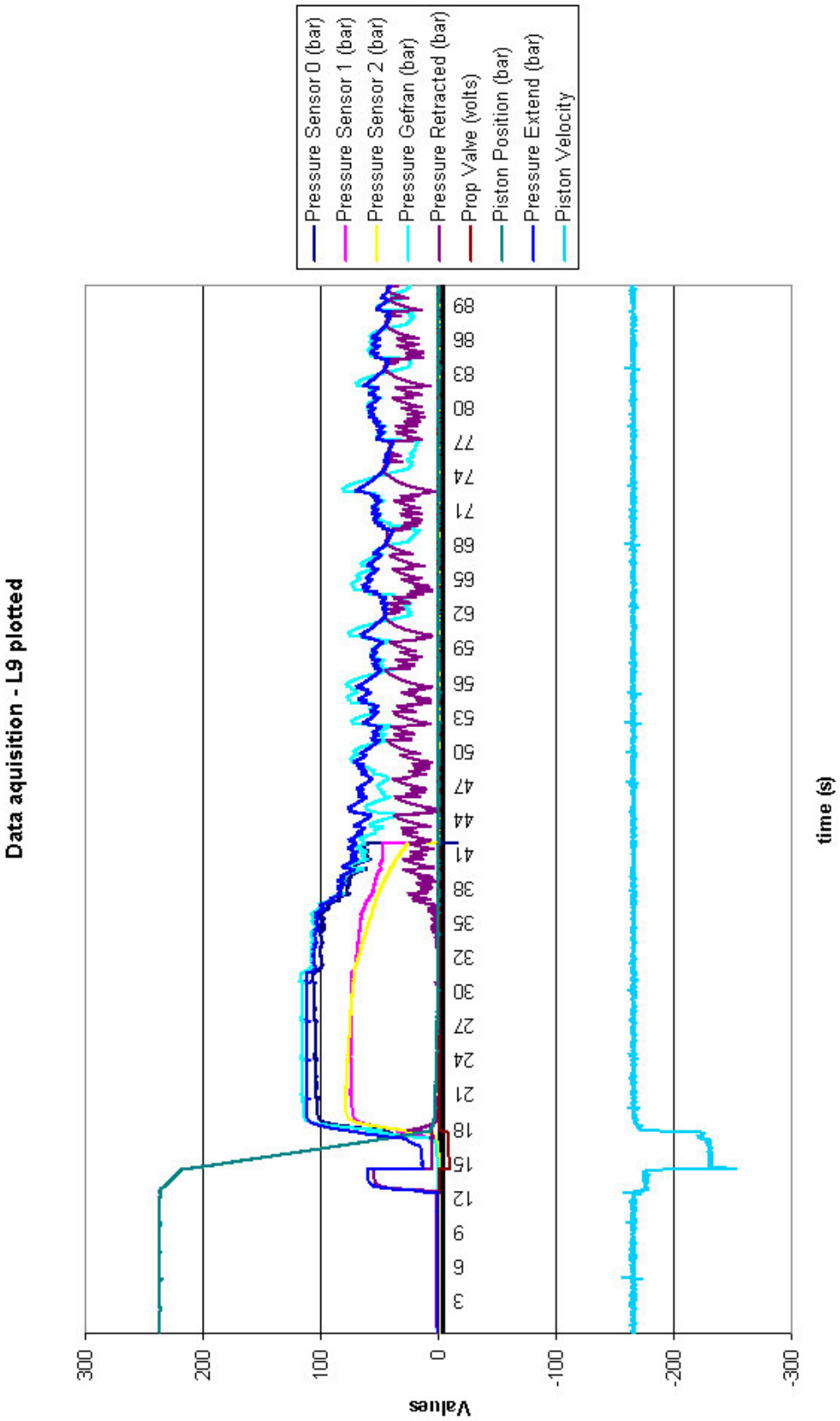

Figure C9: Cavity pressures in lomolding DOE L9

Appendix C10: Design of experiment L10

Material used: Sasol PP1100N

COOLING SYSTEM:

Chiller set at 12 °C, 3.3 bar
Plasticiser: 20
Piston: 175
Fixed Mould 1: 170
Fixed Mould 2: 180
Moving Mould Cooling Circuit Pressure: 2.9 bar

BATCH SETUP (Critical Packing Pressure Control)

Volume: 229 ml
Change over pt: 7 mm
Cooling Time: 90 s

SPEED PROFILE

Position B: 224 mm @ 140 mm/s
Position C: 15 mm @ 100 mm/s
Position D: 10 mm @ 50 mm/s
Position :   7 mm @ 20 mm/s

PRESSURE PROFILE

Injection: 120 bar
Packing: 120 bar for 15 s
Post Injection Pressure: 80 bar for 90 s

OVERVIEW:

Ambient Temp: 22 °C
Humidity: 57%

TEMPERATURES during stabilisation

Engel Plasticiser 1:	S186 A186
Engel Plasticiser 2:	S186 A186
Engel Plasticiser 3:	S186 A186
Engel Plasticiser 4:	S186 A186
Infeed Valve:	S186 A187
Infeed Nozzle:	S186 A183
MTC Middle:	S186 A187
MTC Bottom:	S0 A156
Horizontal Hot Runner:	S186 A189
Hot Runner Bend:	S186 A184
Vertical Hot Runner	S186 A186
Outfeed Valve:	S186 A186
MLC Right:	S186 A191
MLC Left:	S186 A195

ENGEL SETPOINTS

Metering Plunger Rear Pressure: 34%
Metering Plunger Rear Volume : 100%
Hydraulic Pressure Actual Value PHx: 86 bar approx

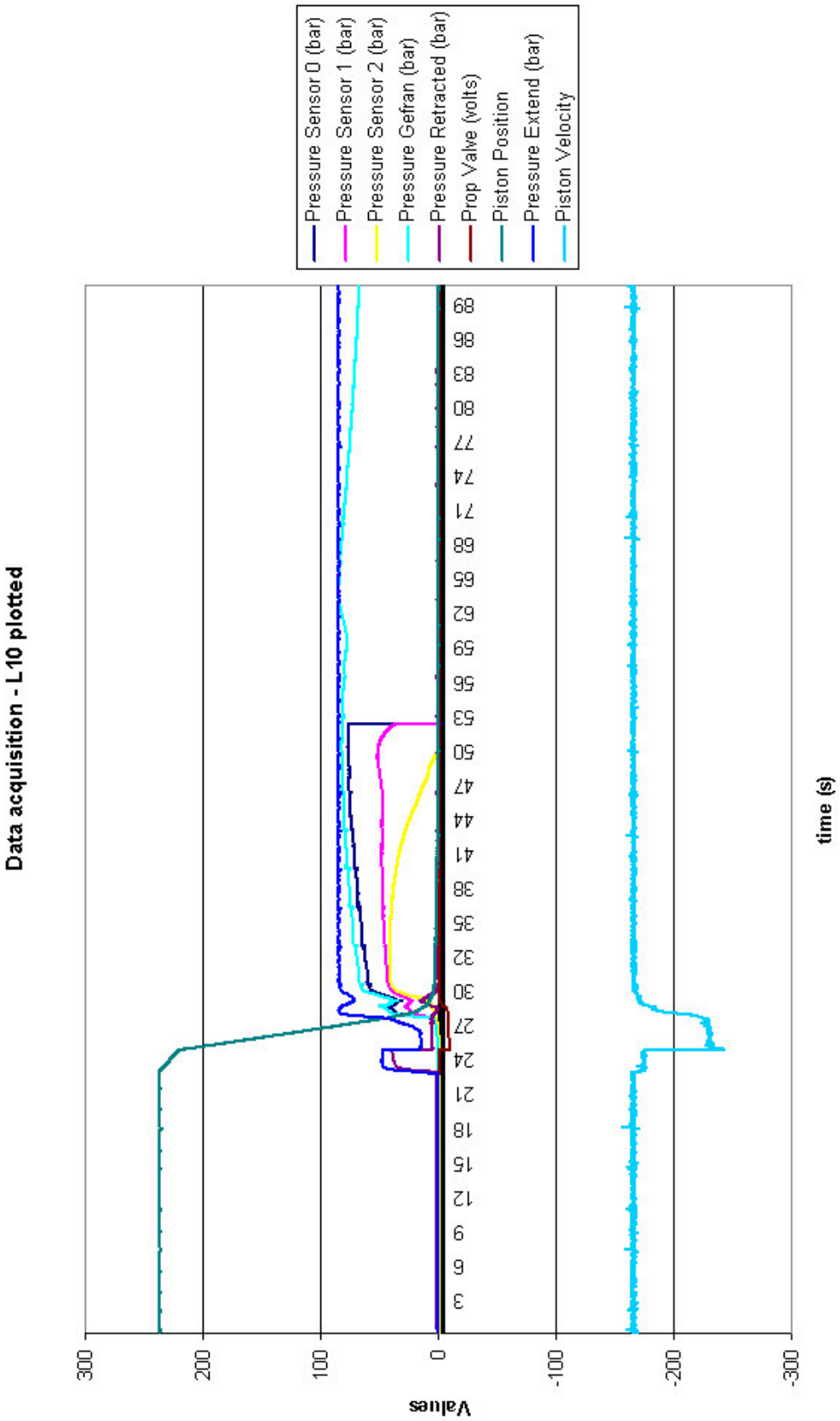

Figure C10: Cavity pressures in lomolding DOE L10

Appendix C11: Design of experiment GFL1

Material used: 50% Compel PP-GF30-0403P25/10 with Sasol PP 1100N

COOLING SYSTEM:

Chiller set at 12 °C, 3.3 bar
Plasticiser: 20
Piston: 180
Fixed Mould 1: 170
Fixed Mould 2: 180
Moving Mould Cooling Circuit Pressure: 2.9 bar

BATCH SETUP (Critical Packing Pressure Control)

Volume: 229 ml
Change Over pt: 7 mm
Cooling Time: 90 s

SPEED PROFILE

Position B: 224 mm @ 140 mm/s
Position C: 15 mm @ 100 mm/s
Position D: 10 mm @ 50 mm/s
Position E: 7 mm @ 20 mm/s

PRESSURE PROFILE

Injection: 120 bar
Packing : 120 bar for 15 s
Post Injection Pressure: 80 bar for 90 s

OVERVIEW:

Ambient Temp: 23 °C
Humidity: 59%

TEMPERATURES during stabilisation

Engel Plasticiser 1:	Set 200 °C	Actual 200 °C
Engel Plasticiser 2:	Set 200 °C	Actual 200 °C
Engel Plasticiser 3:	Set 200 °C	Actual 200 °C
Engel Plasticiser 4:	Set 200 °C	Actual 200 °C
Infeed Valve:	Set 200 °C	Actual 200 °C
Infeed Nozzle:	Set 200 °C	Actual 199 °C
MTC Middle:	Set 200 °C	Actual 207 °C
MTC Bottom:	Set 0 °C	Actual 169 °C
Horizontal Hot Runner:	Set 200 °C	Actual 199 °C
Hot Runner Bend:	Set 200 °C	Actual 197 °C
Vertical Hot Runner	Set 200 °C	Actual 200 °C
Outfeed Valve:	Set 200 °C	Actual 202 °C
MLC Right:	Set 200 °C	Actual 202 °C
MLC Left:	Set 200 °C	Actual 191 °C

ENGEL SETPOINTS

Metering Plunger Rear Pressure: 40%
Metering Plunger Rear Volume : 100%
Hydraulic Pressure Actual Value PHx: 100 bar approx

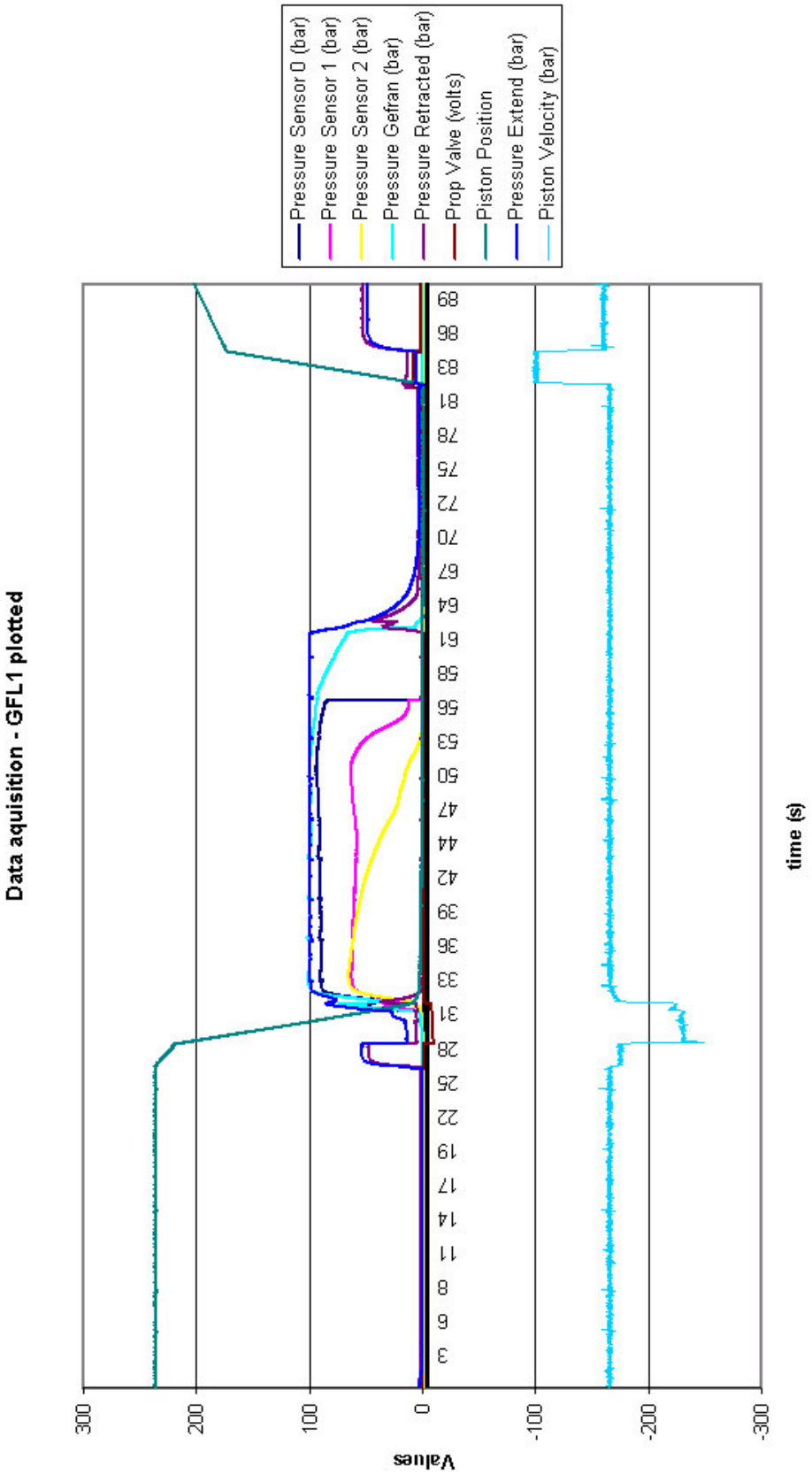

Figure C11a: Cavity pressures in lomolding DOE GFL1

Figure C11b: Fibre skeleton remaining after burn off of GFL1-23

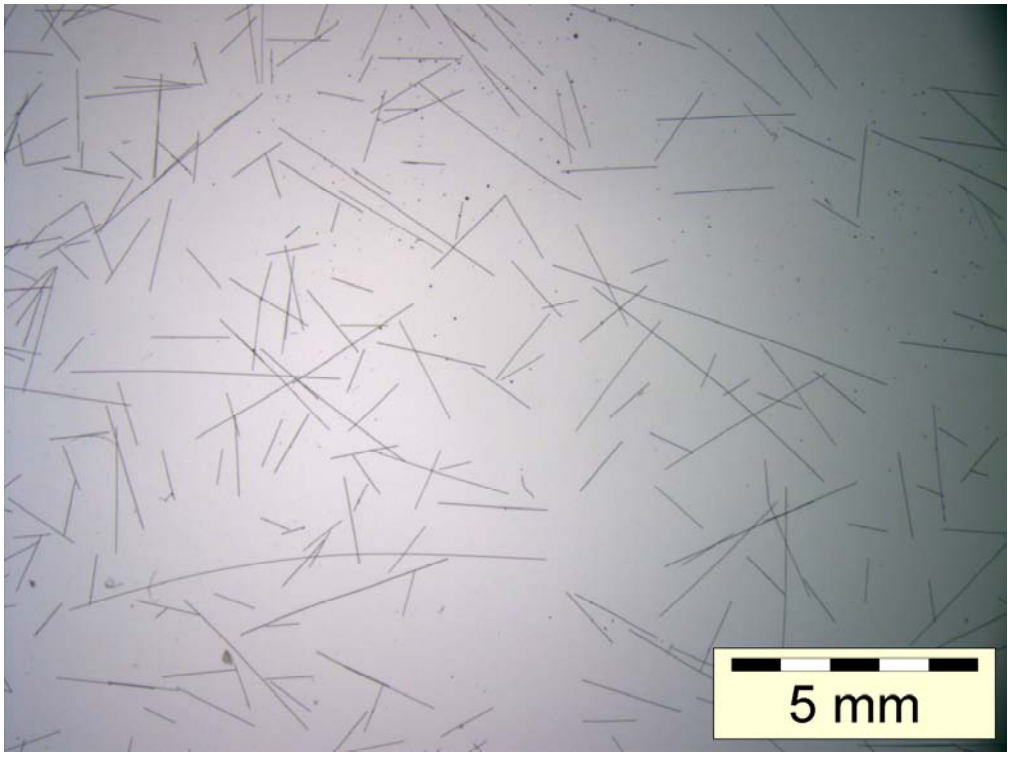

Figure C11c: Optical microscope photo taken with sample from GFL1-23

Appendix C12: Design of experiment GFL2

Material used: 50% Compel PP-GF30-0403P25/10 with Sasol PP 1100N

COOLING SYSTEM:

Chiller set at 12 °C, 3.3 bar
Plasticiser: 20
Piston: 180
Fixed Mould 1: 170
Fixed Mould 2: 180
Moving Mould Cooling Circuit Pressure: 2.9 bar

BATCH SETUP (Critical Packing Pressure Control)

Volume: 228 ml
Change over pt: 7 mm
Cooling Time: 90 s

SPEED PROFILE

Position B: 224 mm @ 140 mm/s
Position C: 15 mm @ 100 mm/s
Position D: 10 mm @ 50 mm/s
Position E: 7 mm @ 20 mm/s

PRESSURE PROFILE

Injection: 120 bar
Packing : 120 bar for 15 s
Post Injection Pressure: 80 bar for 90 s

OVERVIEW:

Ambient Temp: 25 °C
Humidity: 62%

TEMPERATURES during stabilisation

Engel Plasticiser 1:	Set 214 °C	Actual 214 °C
Engel Plasticiser 2:	Set 214 °C	Actual 214 °C
Engel Plasticiser 3:	Set 214 °C	Actual 214 °C
Engel Plasticiser 4:	Set 214 °C	Actual 213 °C
Infeed Valve:	Set 214 °C	Actual 211 °C
Infeed Nozzle:	Set 214 °C	Actual 212 °C
MTC Middle:	Set 214 °C	Actual 220 °C
MTC Bottom:	Set 0 °C	Actual 180 °C
Horizontal Hot Runner:	Set 214 °C	Actual 215 °C
Hot Runner Bend:	Set 214 °C	Actual 212 °C
Vertical Hot Runner	Set 214 °C	Actual 214 °C
Outfeed Valve:	Set 214 °C	Actual 216 °C
MLC Right:	Set 214 °C	Actual 215 °C
MLC Left:	Set 214 °C	Actual 213 °C

ENGEL SETPOINTS

Metering Plunger Rear Pressure: 34%
Metering Plunger Rear Volume : 100%
Hydraulic Pressure Actual Value PHx: 86 bar approx

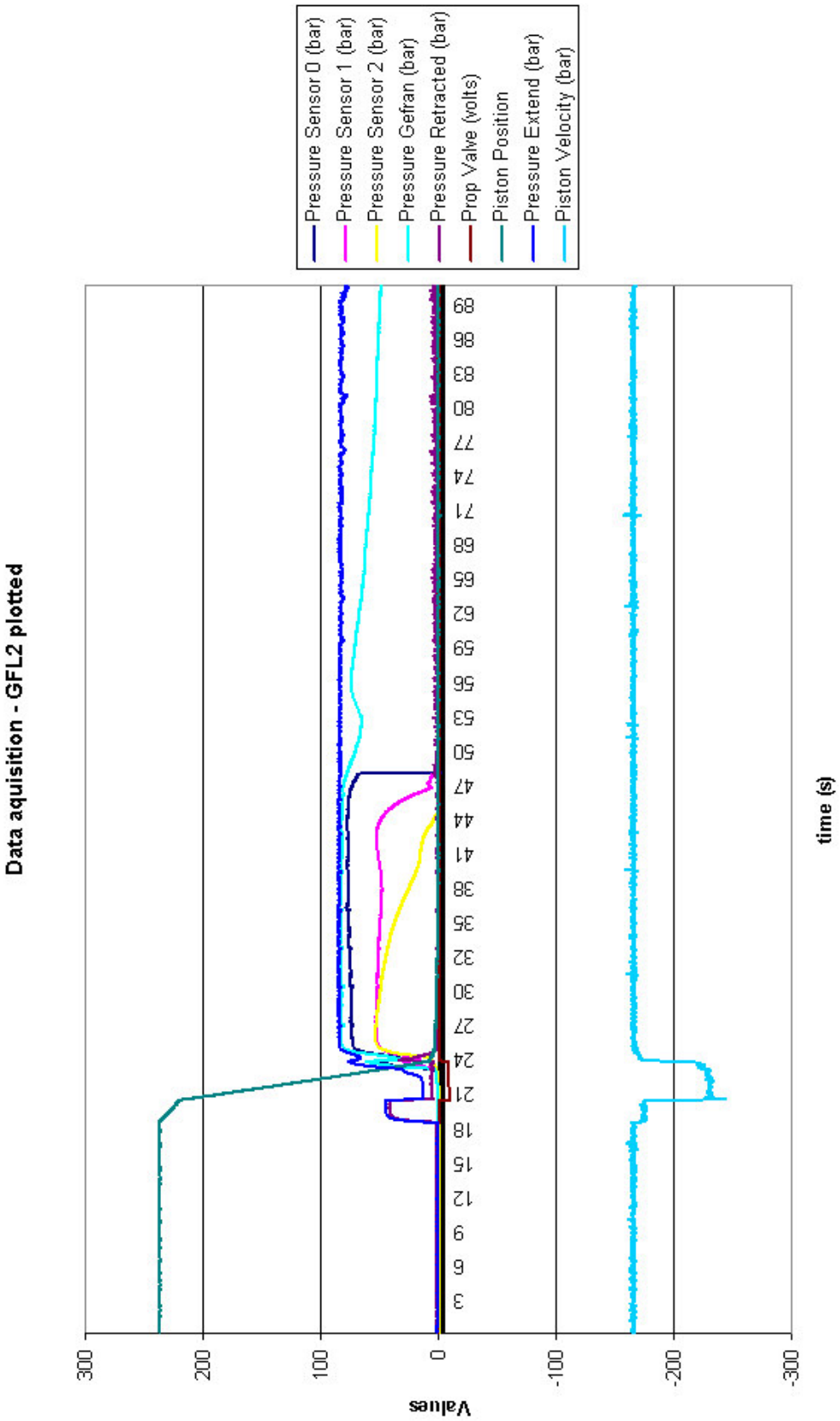

Figure C12a: Cavity pressures in lomolding DOE GFL2

Figure C12b: Fibre skeleton remaining after burn off of GFL2-27

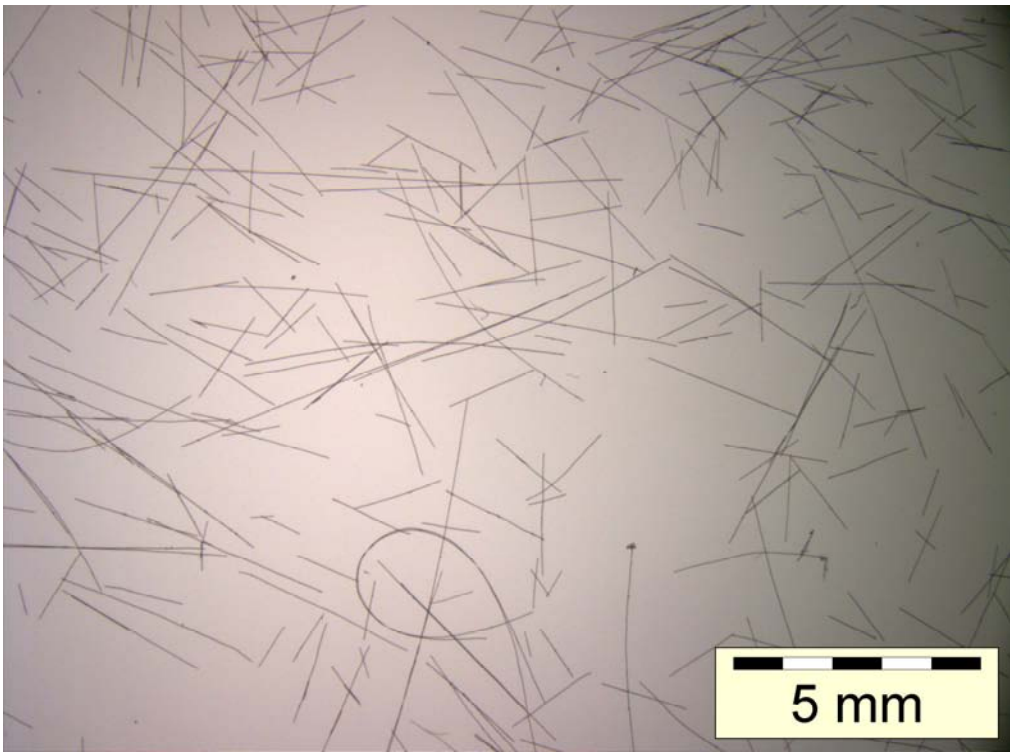

Figure C12c: Optical microscope photo taken with sample from GFL2-27

Appendix C13: Design of experiment GFL3

Material used: 50% Compel PP-GF30-0403P25/10 with Sasol PP 1100N

COOLING SYSTEM:

Chiller set at 12 °C, 3.3 bar
Plasticiser: 20
Piston: 180
Fixed Mould 1: 170
Fixed Mould 2: 180
Moving Mould Cooling Circuit Pressure: 2.9 bar

BATCH SETUP (Critical Packing Pressure Control)

Volume: 230 ml
Change over pt: 7 mm
Cooling Time: 90 s

SPEED PROFILE

Position B: 224 mm @ 140 mm/s
Position C: 15 mm @ 100 mm/s
Position D: 10 mm @ 50 mm/s
Position E: 7 mm @ 20 mm/s

PRESSURE PROFILE

Injection: 120 bar
Packing: 120 bar for 15 s
Post Injection Pressure: 80 bar for 90 s

OVERVIEW:

Ambient Temp: 23 °C
Humidity: 58%

TEMPERATURES during stabilisation

Engel Plasticiser 1:	Set 220 °C	Actual 220 °C
Engel Plasticiser 2:	Set 220 °C	Actual 220 °C
Engel Plasticiser 3:	Set 220 °C	Actual 220 °C
Engel Plasticiser 4:	Set 220 °C	Actual 219 °C
Infeed Valve:	Set 220 °C	Actual 219 °C
Infeed Nozzle:	Set 220 °C	Actual 216 °C
MTC Middle:	Set 220 °C	Actual 224 °C
MTC Bottom:	Set 0 °C	Actual 183 °C
Horizontal Hot Runner:	Set 220 °C	Actual 221 °C
Hot Runner Bend:	Set 220 °C	Actual 219 °C
Vertical Hot Runner	Set 220 °C	Actual 222 °C
Outfeed Valve:	Set 220 °C	Actual 225 °C
MLC Right:	Set 220 °C	Actual 213 °C
MLC Left:	Set 220 °C	Actual 209 °C

ENGEL SETPOINTS

Metering Plunger Rear Pressure: 40%
Metering Plunger Rear Volume : 100%
Hydraulic Pressure Actual Value PHx: 100 bar approx

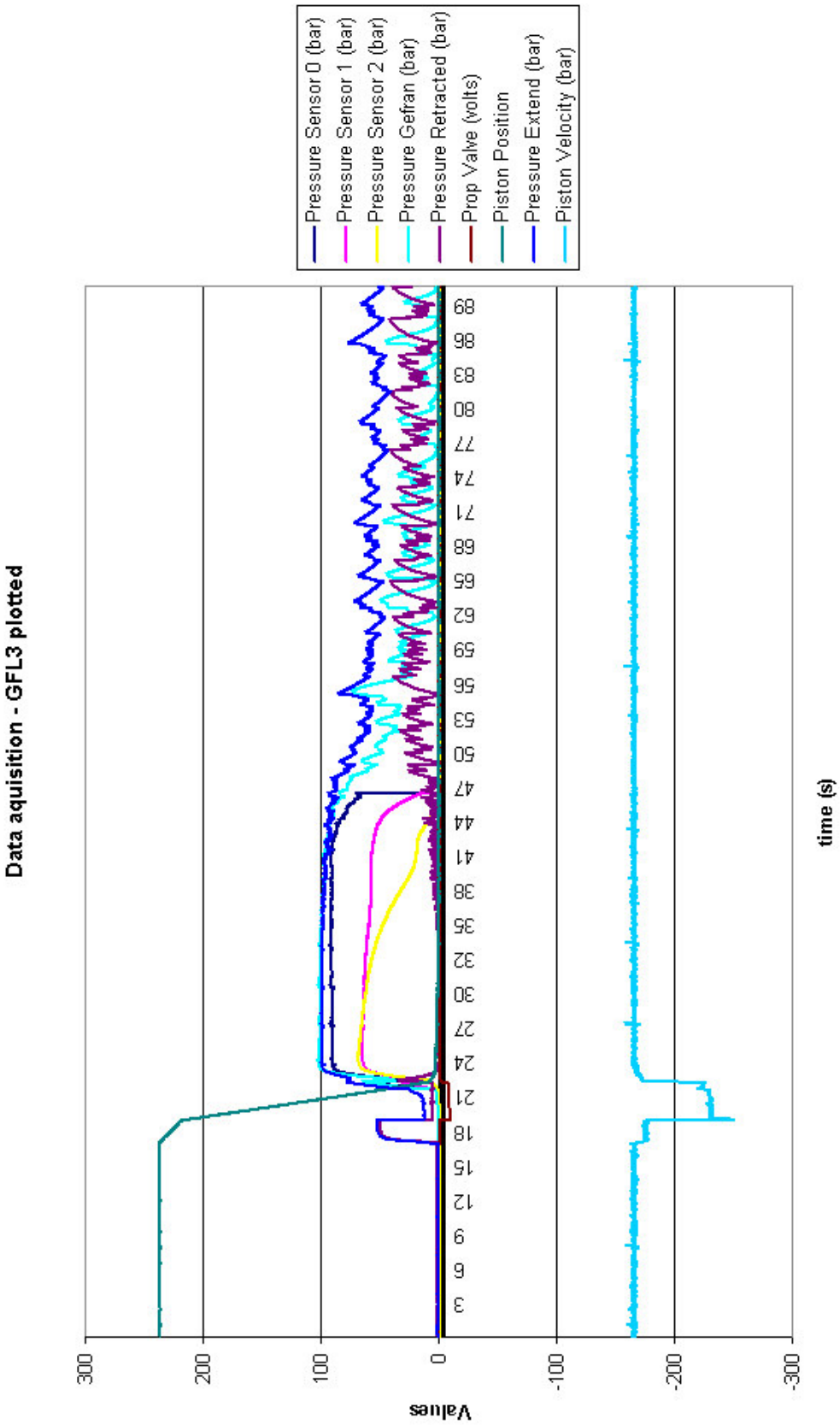

Figure C13a: Cavity pressures in lomolding DOE GFL3

Figure C13b: Fibre skeleton remaining after burn off of GFL3-27

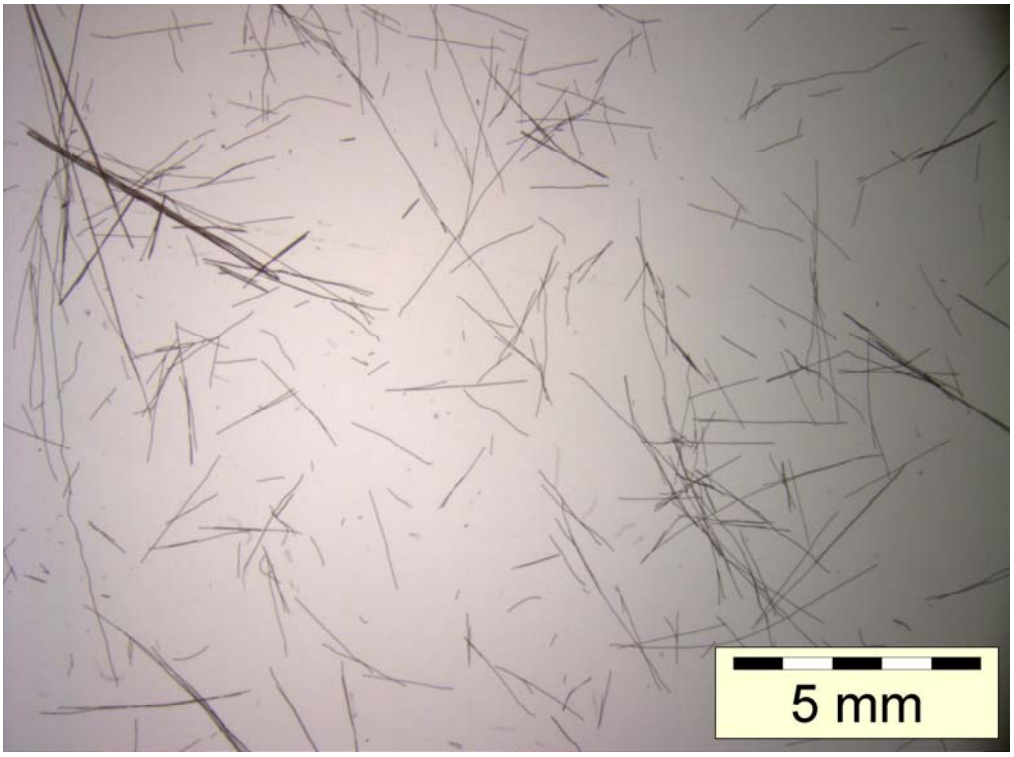

Figure C13c: Optical microscope photo taken with sample from GFL3-27

Appendix C14: Design of experiment GFL4

Material used: 50% Compel PP-GF30-0403P25/10 with Sasol PP1100N

COOLING SYSTEM:

Chiller set at 12 °C, 3.3 bar
Plasticiser: 20
Piston: 180
Fixed Mould 1: 170
Fixed Mould 2: 180
Moving Mould Cooling Circuit Pressure: 2.9 bar

BATCH SETUP (Critical Packing Pressure Control)

Volume: 224 ml
Change over pt: 7 mm
Cooling Time: 90 s

SPEED PROFILE

Position B: 224 mm @ 140 mm/s
Position C: 15 mm @ 100 mm/s
Position D: 10 mm @ 50 mm/s
Position E: 7 mm @ 20 mm/s

PRESSURE PROFILE

Injection: 120 bar
Packing : 120 bar for 15 s
Post Injection Pressure: 80 bar for 90 s

OVERVIEW:

Ambient Temp: 23 °C
Humidity: 59%

TEMPERATURES during stabilisation

Engel Plasticiser 1:	Set 180 °C	Actual 180 °C
Engel Plasticiser 2:	Set 180 °C	Actual 180 °C
Engel Plasticiser 3:	Set 180 °C	Actual 180 °C
Engel Plasticiser 4:	Set 180 °C	Actual 179 °C
Infeed Valve:	Set 180 °C	Actual 181 °C
Infeed Nozzle:	Set 180 °C	Actual 180 °C
MTC Middle:	Set 180 °C	Actual 184 °C
MTC Bottom:	Set 0 °C	Actual 153 °C
Horizontal Hot Runner:	Set 180 °C	Actual 182 °C
Hot Runner Bend:	Set 180 °C	Actual 178 °C
Vertical Hot Runner	Set 180 °C	Actual 181 °C
Outfeed Valve:	Set 180 °C	Actual 185 °C
MLC Right:	Set 180 °C	Actual 185 °C
MLC Left:	Set 180 °C	Actual 179 °C

ENGEL SETPOINTS

Metering Plunger Rear Pressure: 40%
Metering Plunger Rear Volume : 100%
Hydraulic Pressure Actual Value PHx: 100 bar approx

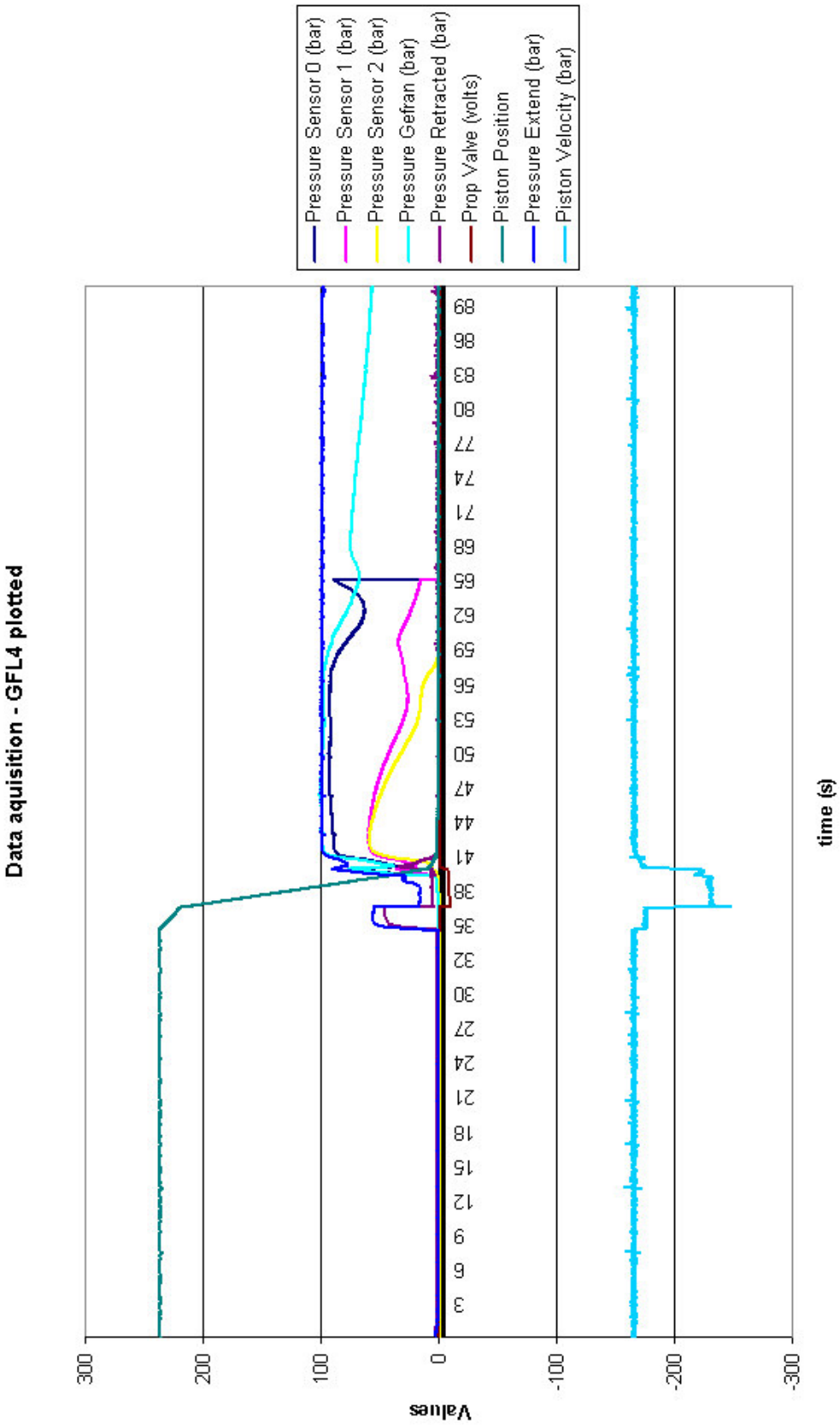

Figure C14a: Cavity pressures in lomolding DOE GFL4

Figure C14b: Fibre skeleton remaining after burn off of GFL4-28

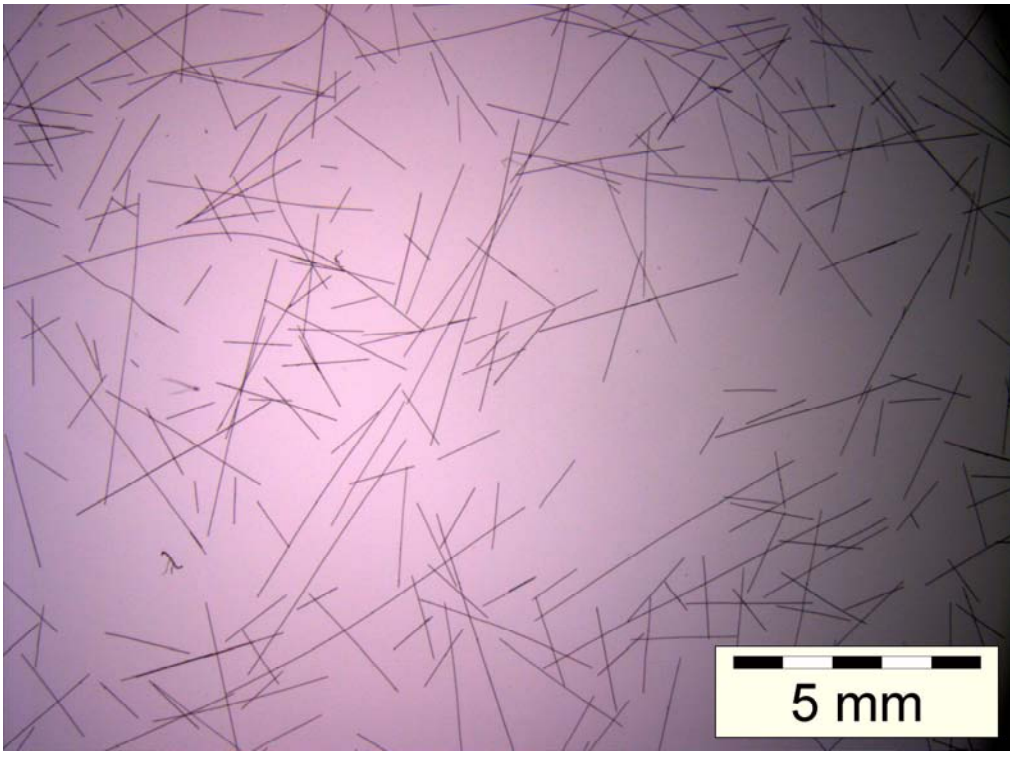

Figure C14c: Optical microscope photo taken with sample from GFL4-28

Appendix C15: Design of experiment GFL5

Material used: 50% Compel PP-GF30-0403P25/10 with Sasol PP1100N

COOLING SYSTEM:

Chiller set at 12 °C, 3.3 bar
Plasticiser: 20
Piston: 180
Fixed Mould 1: 170
Fixed Mould 2: 180
Moving Mould Cooling Circuit Pressure: 2.9 bar

BATCH SETUP (Critical Packing Pressure Control)

Volume: 225 ml
Change over pt: 7 mm
Cooling Time: 90 s

SPEED PROFILE

Position B: 224 mm @ 140 mm/s
Position C: 15 mm @ 100 mm/s
Position D: 10 mm @ 50 mm/s
Position E: 7 mm @ 20 mm/s

PRESSURE PROFILE

Injection: 120 bar
Packing : 120 bar for 15 s
Post Injection Pressure: 80 bar for 90 s

OVERVIEW:

Ambient Temp: 23 °C
Humidity: 58%

TEMPERATURES during stabilisation

Engel Plasticiser 1:	S200 A200
Engel Plasticiser 2:	S200 A200
Engel Plasticiser 3:	S200 A199
Engel Plasticiser 4:	S200 A198
Infeed Valve:	S200 A200
Infeed Nozzle:	S200 A195
MTC Middle:	S200 A208
MTC Bottom:	S0 A168
Horizontal Hot Runner:	S200 A202
Hot Runner Bend:	S200 A201
Vertical Hot Runner	S200 A203
Outfeed Valve:	S200 A204
MLC Right:	S200 A194
MLC Left:	S200 A195

ENGEL SETPOINTS

Metering Plunger Rear Pressure: 32%
Metering Plunger Rear Volume : 100%
Hydraulic Pressure Actual Value PHx: 80 bar approx

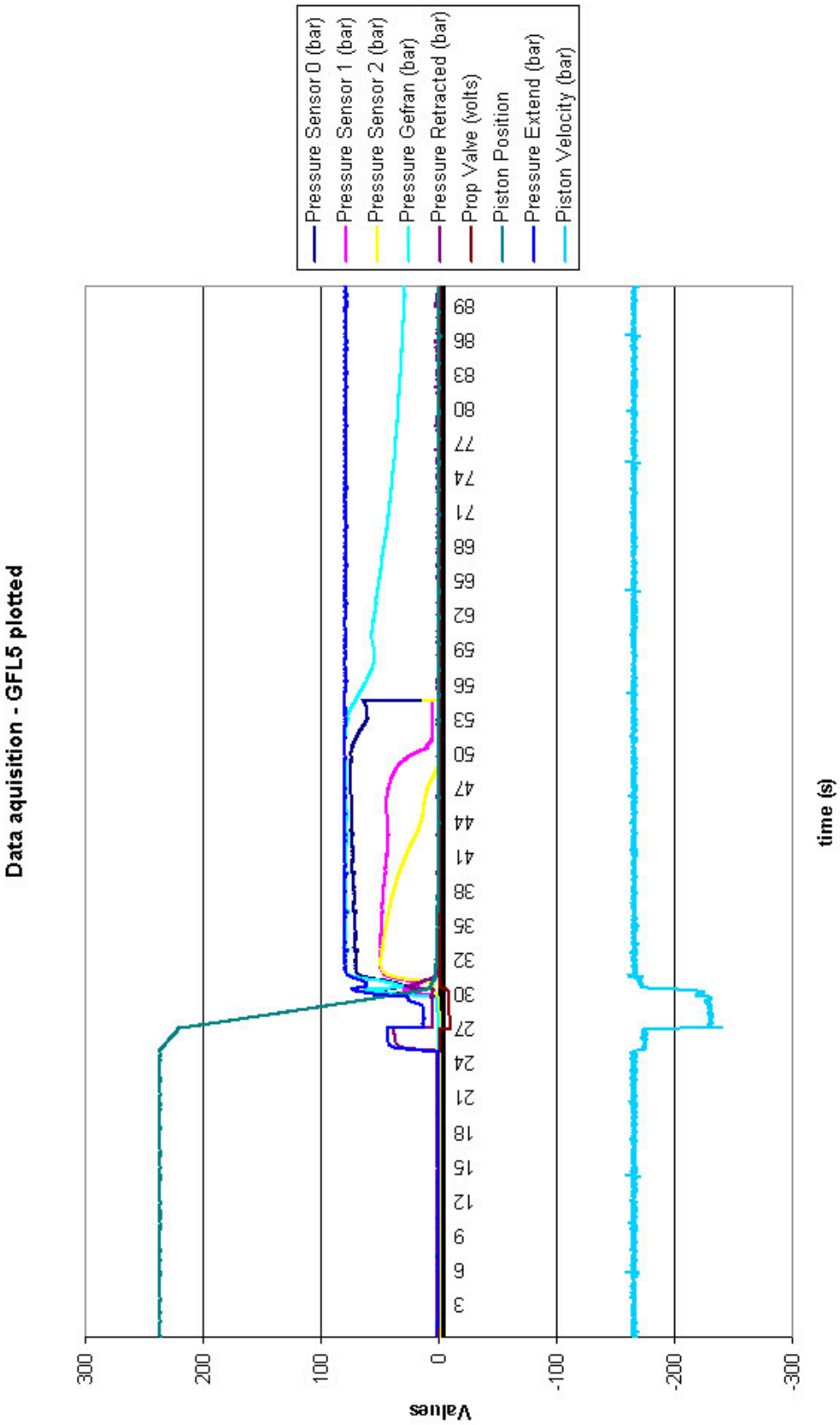

Figure C15a: Cavity pressures in lomolding DOE GFL5

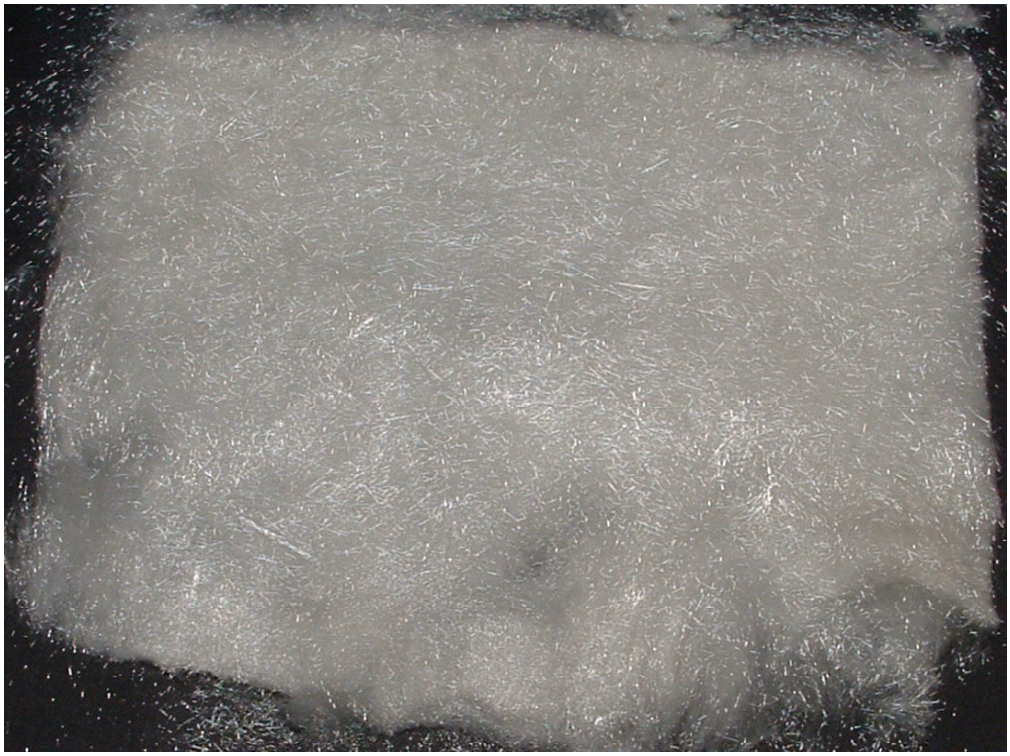

Figure C15b: Fibre skeleton remaining after burn off of GFL5-28

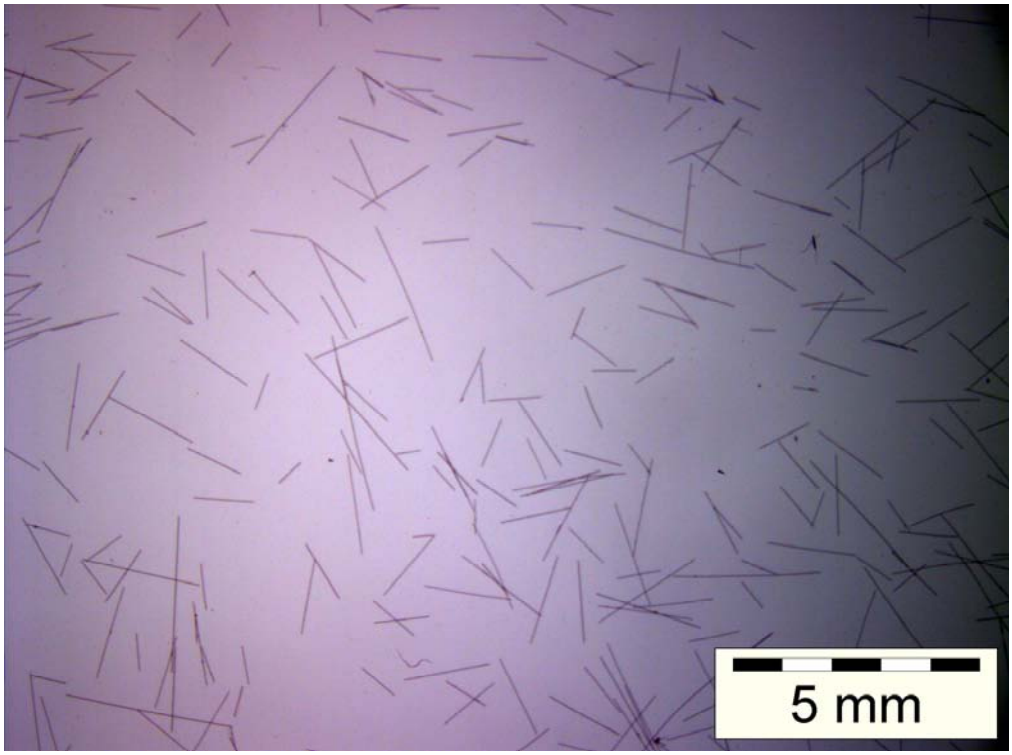

Figure C15c: Optical microscope photo taken with sample from GFL5-28

Appendix C16: Design of experiment GFL6

Material used: 50% Compel PP-GF30-0403P25/10 with Sasol PP1100N

COOLING SYSTEM:

Chiller set at 12 °C, 3.3 bar
Plasticiser: 20
Piston: 180
Fixed Mould 1: 170
Fixed Mould 2: 180
Moving Mould Cooling Circuit Pressure: 2.9 bar

BATCH SETUP (Critical Packing Pressure Control)

Volume: 225 ml
Change over pt: 7 mm
Cooling Time: 90 s

SPEED PROFILE

Position B: 224 mm @ 140 mm/s
Position C: 15 mm @ 100 mm/s
Position D: 10 mm @ 50 mm/s
Position E: 7 mm @ 20 mm/s

PRESSURE PROFILE

Injection: 120 bar
Packing : 120 bar for 15 s
Post Injection Pressure: 80 bar for 90 s

OVERVIEW:

Ambient Temp: 23 °C
Humidity: 58%

TEMPERATURES during stabilisation

Engel Plasticiser 1:	S200 A200
Engel Plasticiser 2:	S200 A200
Engel Plasticiser 3:	S200 A199
Engel Plasticiser 4:	S200 A198
Infeed Valve:	S200 A200
Infeed Nozzle:	S200 A195
MTC Middle:	S200 A208
MTC Bottom:	S0 A168
Horizontal Hot Runner:	S200 A202
Hot Runner Bend:	S200 A201
Vertical Hot Runner	S200 A203
Outfeed Valve:	S200 A204
MLC Right:	S200 A194
MLC Left:	S200 A195

ENGEL SETPOINTS

Metering Plunger Rear Pressure: 32%
Metering Plunger Rear Volume : 100%
Hydraulic Pressure Actual Value PHx: 80 bar approx

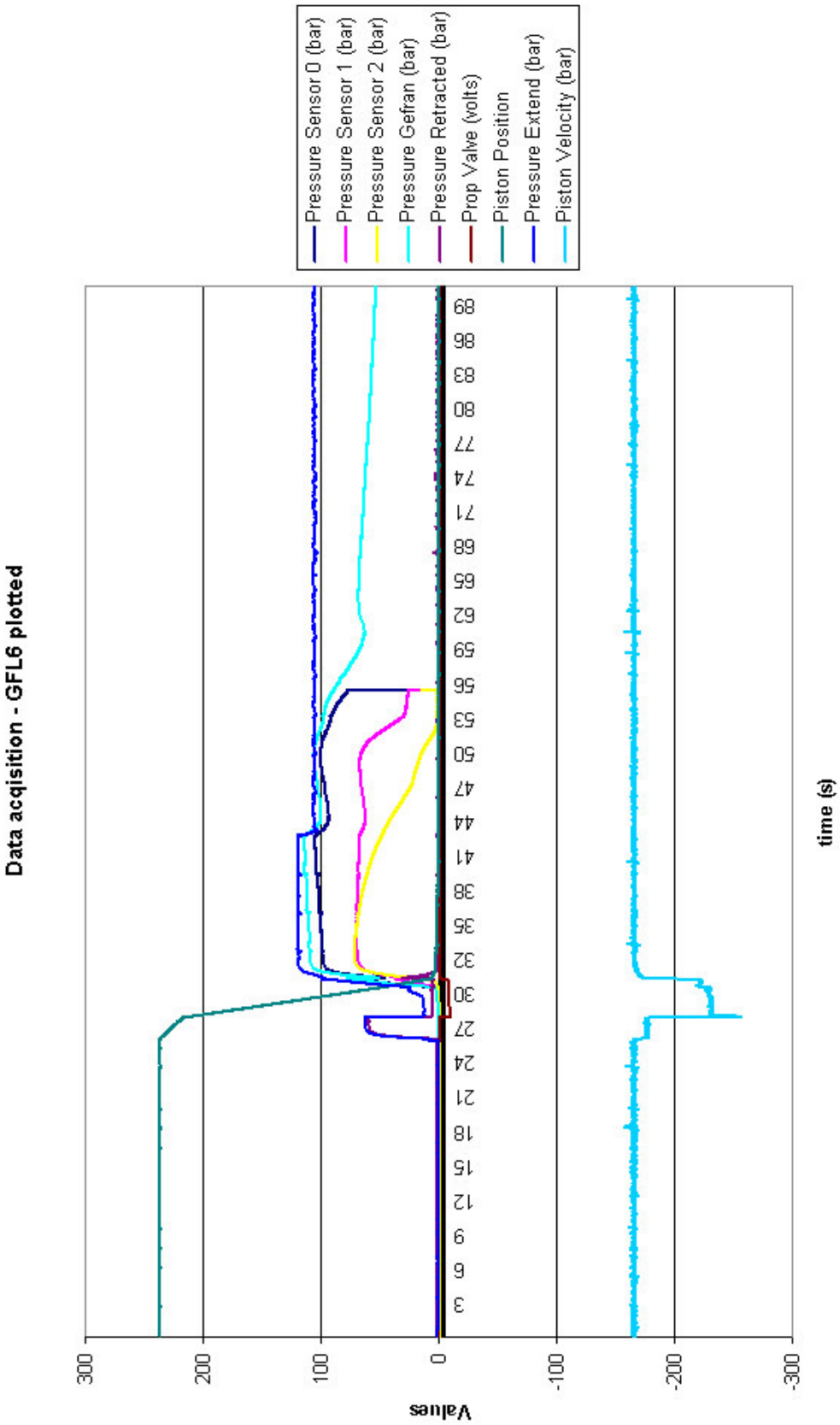

Figure C16a: Cavity pressures in lomolding DOE GFL6

Figure C16b: Fibre skeleton remaining after burn off of GFL6-27

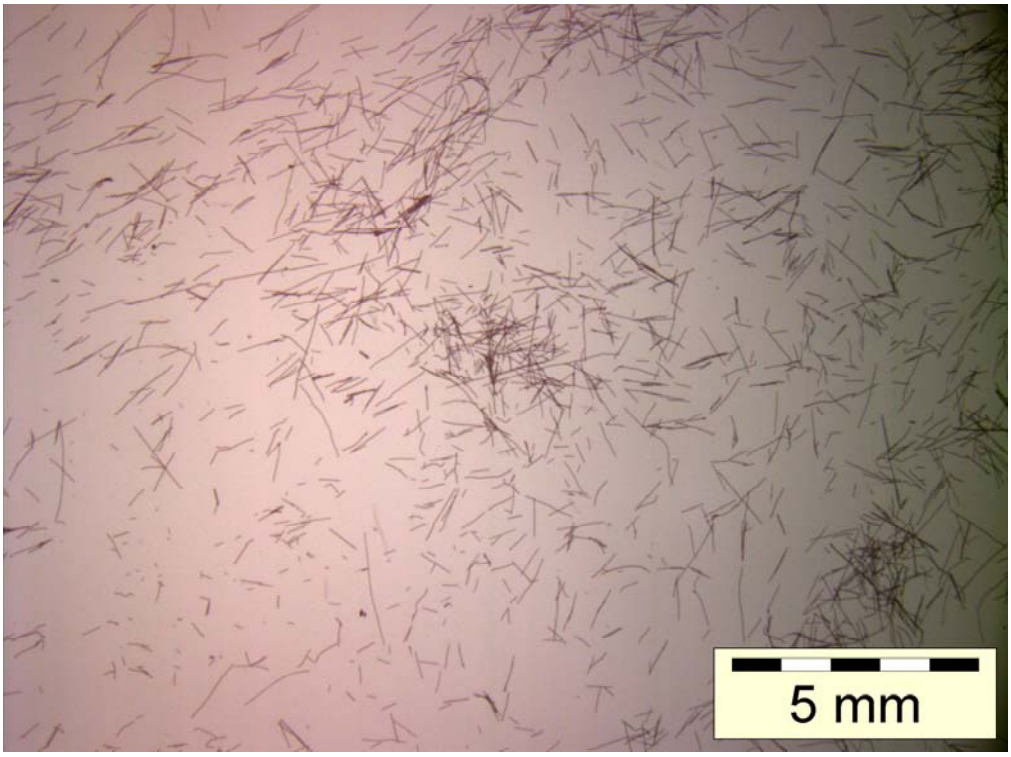

Figure C16c: Optical microscope photo taken with sample from GFL6-27

Appendix C17: Design of experiment GFL7

Material used: 50% Compel PP-GF30-0403P25/10 with Sasol PP1100N

COOLING SYSTEM:

Chiller set at 12 °C, 3.3 bar
Plasticiser: 30
Piston: 180
Fixed Mould 1: 170
Fixed Mould 2: 180
Moving Mould Cooling Circuit Pressure: 2.9 bar

BATCH SETUP (Critical Packing Pressure Control)

Volume: 231 ml
Change over pt: 7 mm
Cooling Time: 90 s

SPEED PROFILE

Position B: 224 mm @ 140 mm/s
Position C: 15 mm @ 100 mm/s
Position D: 10 mm @ 50 mm/s
Position E: 7 mm @ 20 mm/s

PRESSURE PROFILE

Injection: 120 bar
Packing : 120 bar for 15 s
Post Injection Pressure: 80 bar for 90 s

OVERVIEW:

Ambient Temp: 21 °C
Humidity: 52%

TEMPERATURES during stabilisation

Engel Plasticiser 1:	Set 214 °C	Actual 214 °C
Engel Plasticiser 2:	Set 214 °C	Actual 214 °C
Engel Plasticiser 3:	Set 214 °C	Actual 213 °C
Engel Plasticiser 4:	Set 214 °C	Actual 112 °C
Infeed Valve:	Set 214 °C	Actual 212 °C
Infeed Nozzle:	Set 214 °C	Actual 210 °C
MTC Middle:	Set 214 °C	Actual 219 °C
MTC Bottom:	Set 0 °C	Actual 180 °C
Horizontal Hot Runner:	Set 214 °C	Actual 214 °C
Hot Runner Bend:	Set 214 °C	Actual 213 °C
Vertical Hot Runner	Set 214 °C	Actual 215 °C
Outfeed Valve:	Set 214 °C	Actual 216 °C
MLC Right:	Set 214 °C	Actual 217 °C
MLC Left:	Set 214 °C	Actual 219 °C

ENGEL SETPOINTS

Metering Plunger Rear Pressure: 45%
Metering Plunger Rear Volume : 100%
Hydraulic Pressure Actual Value PHx: 114 bar approx

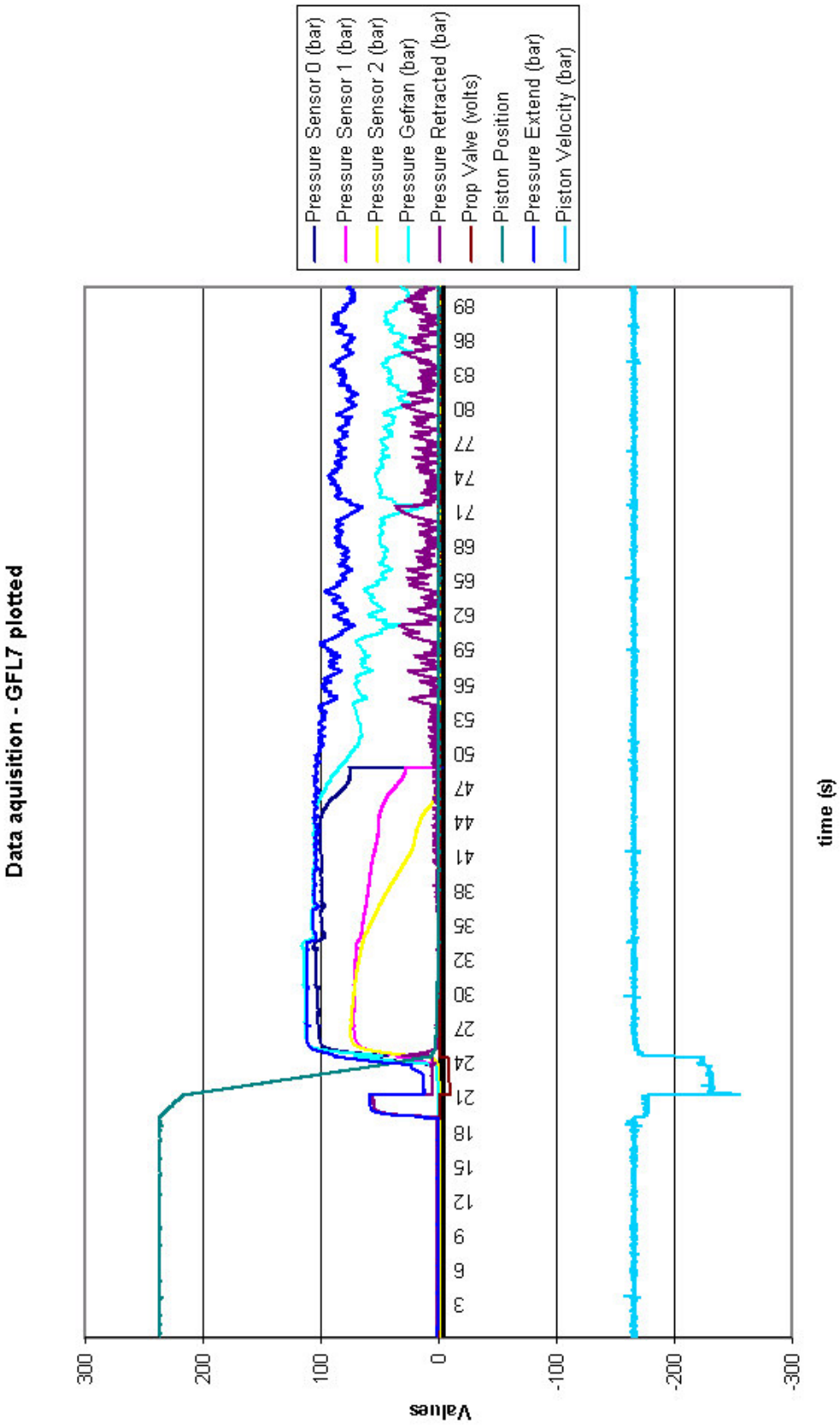

Figure C17a: Cavity pressures in lomolding DOE GFL7

Figure C17b: Fibre skeleton remaining after burn off of GFL1-23

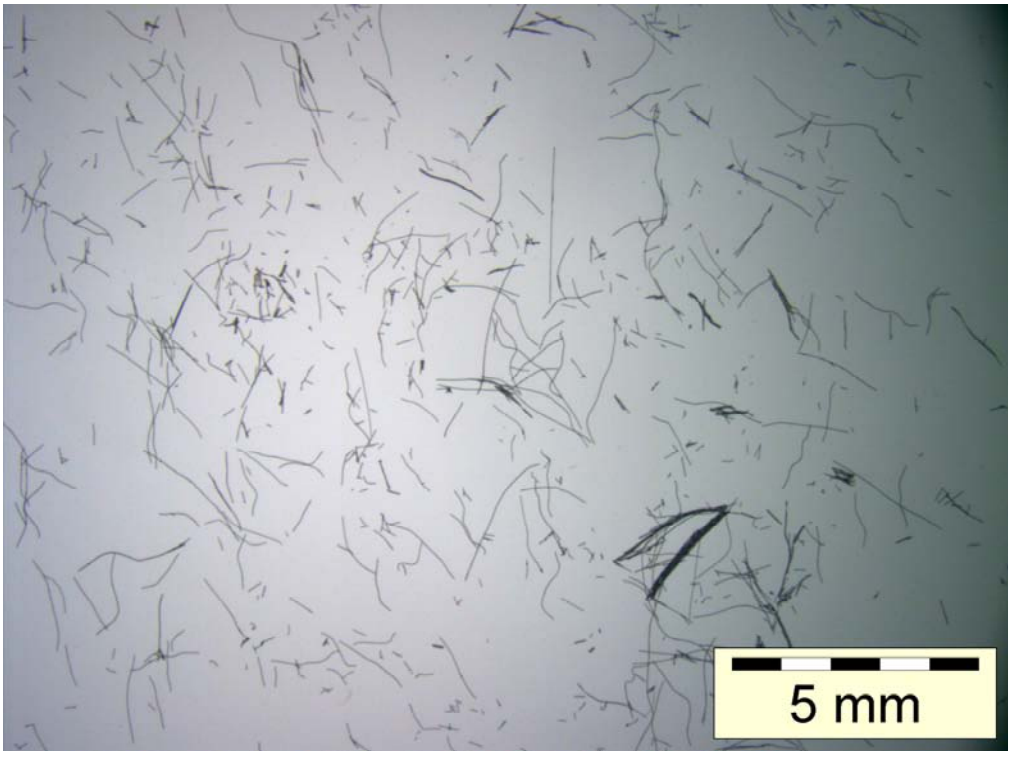

Figure C17c: Optical microscope photo taken with sample from GFL1-23

Appendix C18: Design of experiment GFL8

Material used: 50% Compel PP-GF30-0403P25/10 with Sasol PP1100N

COOLING SYSTEM:

Chiller set at 12 °C, 3.3 bar
Plasticiser: 40
Piston: 180
Fixed Mould 1: 170
Fixed Mould 2: 180
Moving Mould Cooling Circuit Pressure: 2.9 bar

BATCH SETUP (Critical Packing Pressure Control)

Volume: 224 ml
Change over pt: 7 mm
Cooling Time: 90 s

SPEED PROFILE

Position B: 224 mm @ 140 mm/s
Position C: 15 mm @ 100 mm/s
Position D: 10 mm @ 50 mm/s
Position E: 7 mm @ 20 mm/s

PRESSURE PROFILE

Injection: 120 bar
Packing : 120 bar for 15 s
Post Injection Pressure: 80 bar for 90 s

OVERVIEW:

Ambient Temp: 23 °C
Humidity: 59%

TEMPERATURES during stabilisation

Engel Plasticiser 1:	Set 186 °C	Actual 186 °C
Engel Plasticiser 2:	Set 186 °C	Actual 186 °C
Engel Plasticiser 3:	Set 186 °C	Actual 185 °C
Engel Plasticiser 4:	Set 186 °C	Actual 184 °C
Infeed Valve:	Set 186 °C	Actual 187 °C
Infeed Nozzle:	Set 186 °C	Actual 183 °C
MTC Middle:	Set 186 °C	Actual 190 °C
MTC Bottom:	Set 0 °C	Actual 156 °C
Horizontal Hot Runner:	Set 186 °C	Actual 185 °C
Hot Runner Bend:	Set 186 °C	Actual 186 °C
Vertical Hot Runner	Set 186 °C	Actual 187 °C
Outfeed Valve:	Set 186 °C	Actual 189 °C
MLC Right:	Set 186 °C	Actual 179 °C
MLC Left:	Set 186 °C	Actual 177 °C

ENGEL SETPOINTS

Metering Plunger Rear Pressure: 34%
Metering Plunger Rear Volume : 100%
Hydr Pressure Actual Value PHx: 86 bar approx

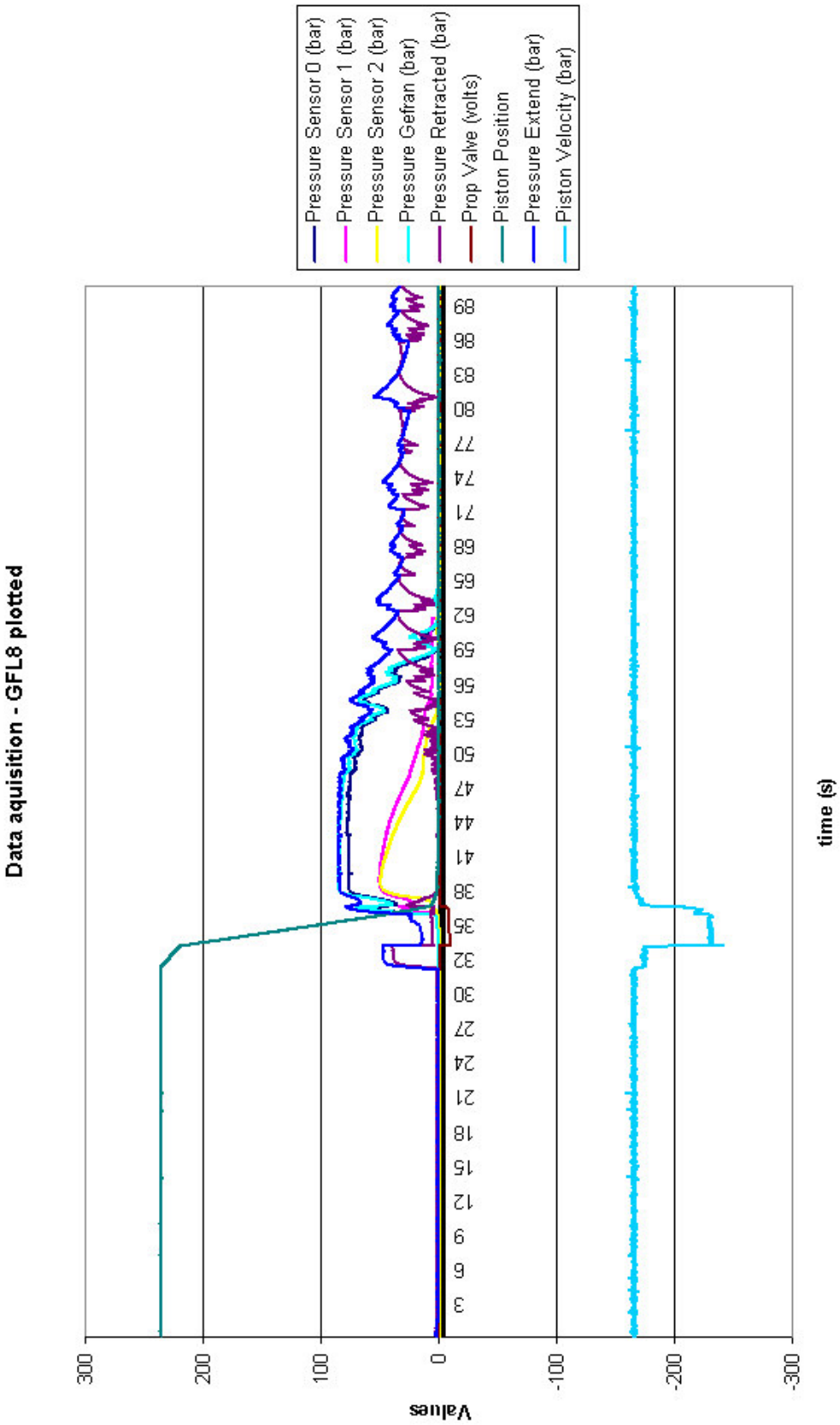

Figure C18a: Cavity pressures in lomolding GFL8

Figure C18b: Fibre skeleton remaining after burn off of GFL8-27

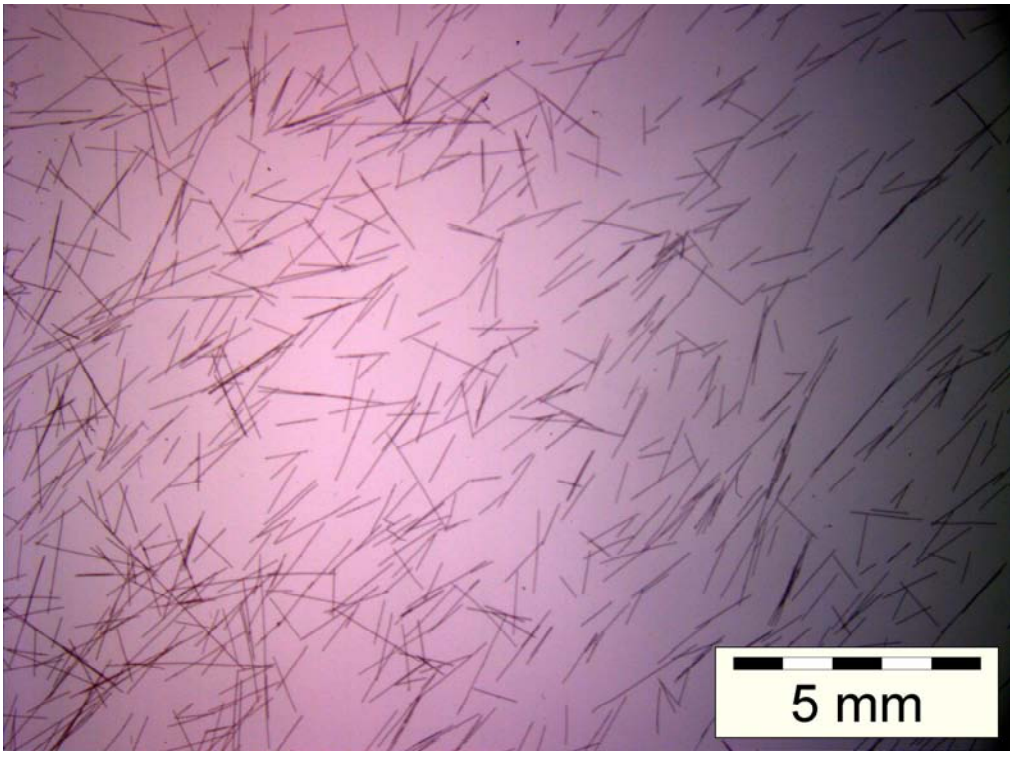

Figure C18c: Optical microscope photo taken with sample from GFL8-27

Appendix C19: Design of experiment GFL9

Material used: 50% Compel PP-GF30-0403P25/10 with Sasol PP1100N

COOLING SYSTEM:

Chiller set at 12 °C, 3.3 bar
Plasticiser: 40
Piston: 180
Fixed Mould 1: 170
Fixed Mould 2: 180
Moving Mould Cooling Circuit Pressure: 2.9 bar

BATCH SETUP (Critical Packing Pressure Control)

Volume: 229 ml
Change over pt: 7 mm
Cooling Time: 90 s

SPEED PROFILE

Position B: 224 mm @ 140 mm/s
Position C: 15 mm @ 100 mm/s
Position D: 10 mm @ 50 mm/s
Position E: 7 mm @ 20 mm/s

PRESSURE PROFILE

Injection: 120 bar
Packing: 120 bar for 15 s
Post Injection Pressure: 80 bar for 90 s

OVERVIEW:

Ambient Temp: 23 °C
Humidity: 58%

TEMPERATURES during stabilisation

Engel Plasticiser 1:	Set 200 °C	Actual 200 °C
Engel Plasticiser 2:	Set 200 °C	Actual 200 °C
Engel Plasticiser 3:	Set 200 °C	Actual 200 °C
Engel Plasticiser 4:	Set 200 °C	Actual 199 °C
Infeed Valve:	Set 200 °C	Actual 201 °C
Infeed Nozzle:	Set 200 °C	Actual 199 °C
MTC Middle:	Set 200 °C	Actual 207 °C
MTC Bottom:	Set 0 °C	Actual 168 °C
Horizontal Hot Runner:	Set 200 °C	Actual 202 °C
Hot Runner Bend:	Set 200 °C	Actual 198 °C
Vertical Hot Runner	Set 200 °C	Actual 200 °C
Outfeed Valve:	Set 200 °C	Actual 202 °C
MLC Right:	Set 200 °C	Actual 196 °C
MLC Left:	Set 200 °C	Actual 199 °C

ENGEL SETPOINTS

Metering Plunger Rear Pressure: 45%
Metering Plunger Rear Volume : 100%
Hydraulic Pressure Actual Value PHx: 100 bar approx

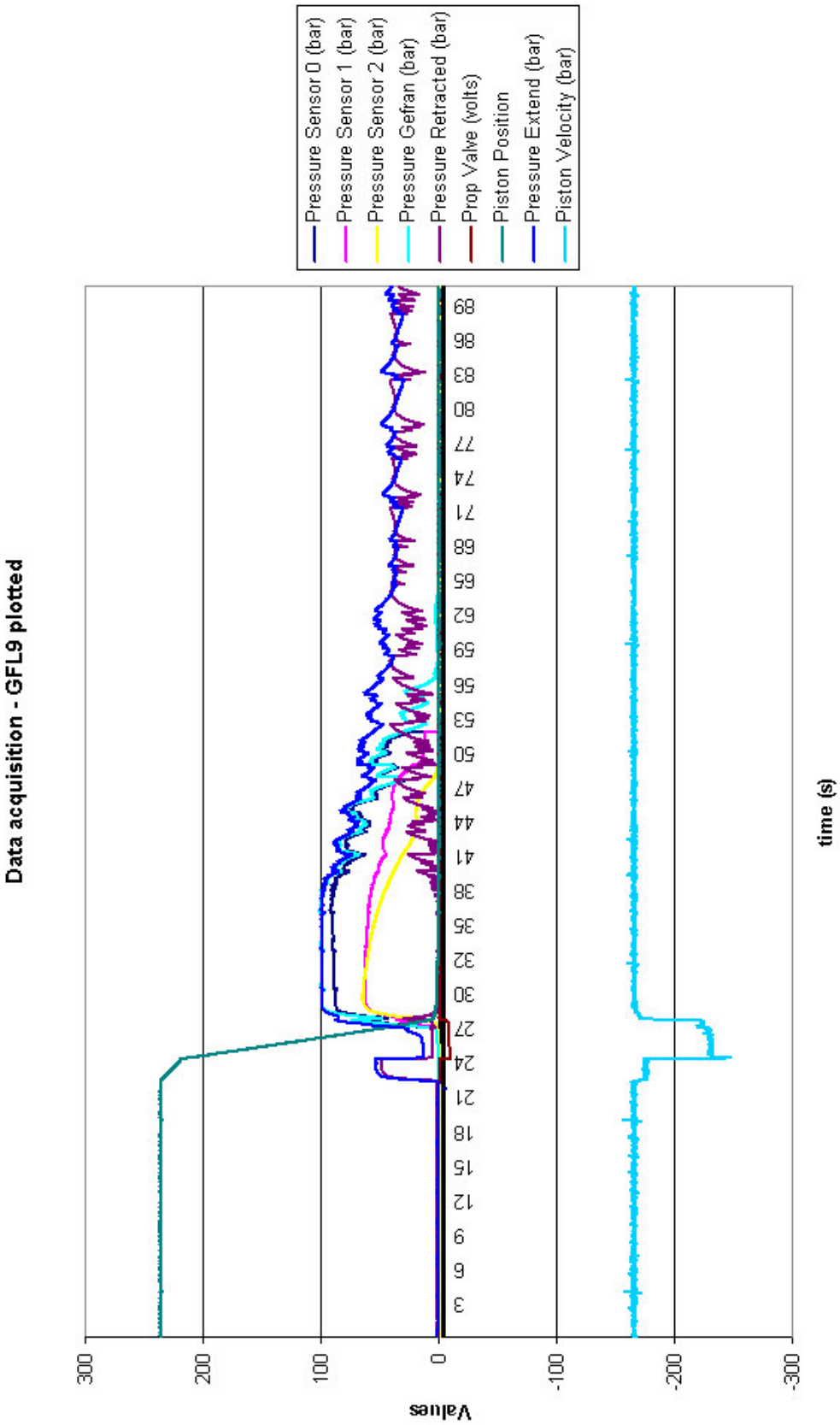

Figure C19a: Cavity pressure in lomolding DOE GFL9pressures in lomolding

Figure C19b: Fibre skeleton remaining after burn off of GFL9-22

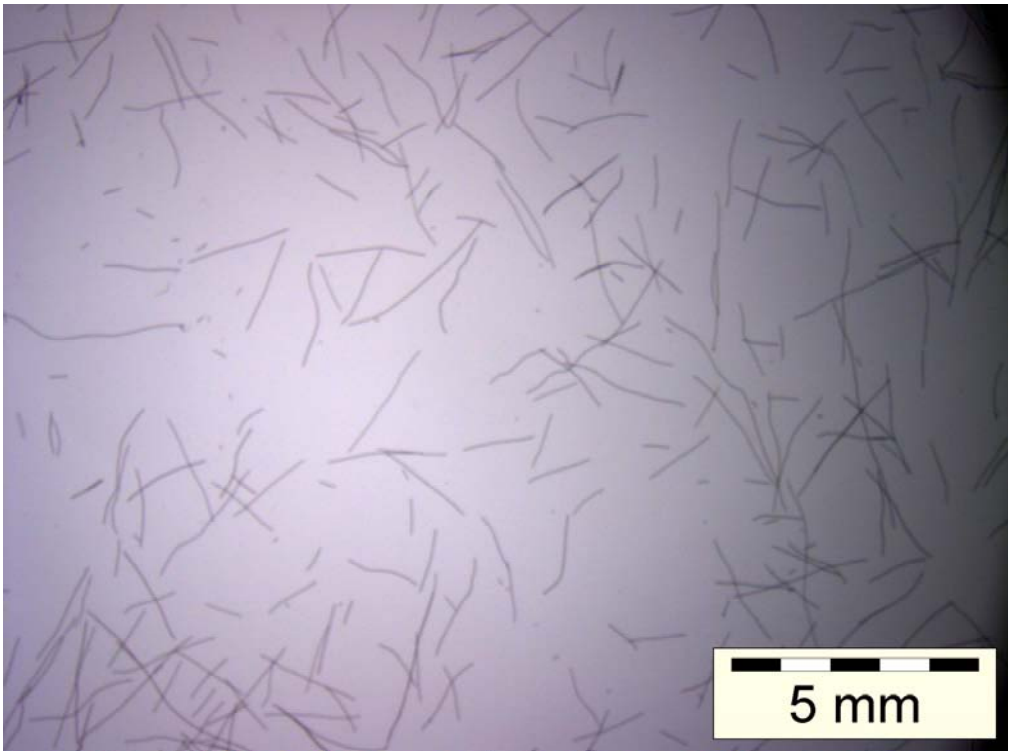

Figure C19c: Optical microscope photo taken with sample from GFL9-22

Appendix C20: Design of experiment GFL10

Material used: 50% Compel PP-GF30-0403P25/10 with Sasol PP1100N

COOLING SYSTEM:

Chiller set at 12 °C, 3.3 bar
Plasticiser: 40
Piston: 180
Fixed Mould 1: 170
Fixed Mould 2: 180
Moving Mould Cooling Circuit Pressure: 2.9 bar

BATCH SETUP (Critical Packing Pressure Control)

Volume: 229 ml
Change over pt: 7 mm
Cooling Time: 90 s

SPEED PROFILE

Position B: 224 mm @ 140 mm/s
Position C: 15 mm @ 100 mm/s
Position D: 10 mm @ 50 mm/s
Position E: 7 mm @ 20 mm/s

PRESSURE PROFILE

Injection: 120 bar
Packing : 120 bar for 15 s
Post Injection Pressure: 80 bar for 90 s

OVERVIEW:

Ambient Temp: 25 °C
Humidity: 64%

TEMPERATURES during stabilisation

Engel Plasticiser 1:	Set 186 °C	Actual 186 °C
Engel Plasticiser 2:	Set 186 °C	Actual 186 °C
Engel Plasticiser 3:	Set 186 °C	Actual 186 °C
Engel Plasticiser 4:	Set 186 °C	Actual 186 °C
Infeed Valve:	Set 186 °C	Actual 186 °C
Infeed Nozzle:	Set 186 °C	Actual 185 °C
MTC Middle:	Set 186 °C	Actual 193 °C
MTC Bottom:	Set 0 °C	Actual 158 °C
Horizontal Hot Runner:	Set 186 °C	Actual 184 °C
Hot Runner Bend:	Set 186 °C	Actual 184 °C
Vertical Hot Runner	Set 186 °C	Actual 187 °C
Outfeed Valve:	Set 186 °C	Actual 189 °C
MLC Right:	Set 186 °C	Actual 184 °C
MLC Left:	Set 186 °C	Actual 174 °C

ENGEL SETPOINTS

Metering Plunger Rear Pressure: 46%
Metering Plunger Rear Volume : 100%
Hydraulic Pressure Actual Value PHx: 114 bar approx

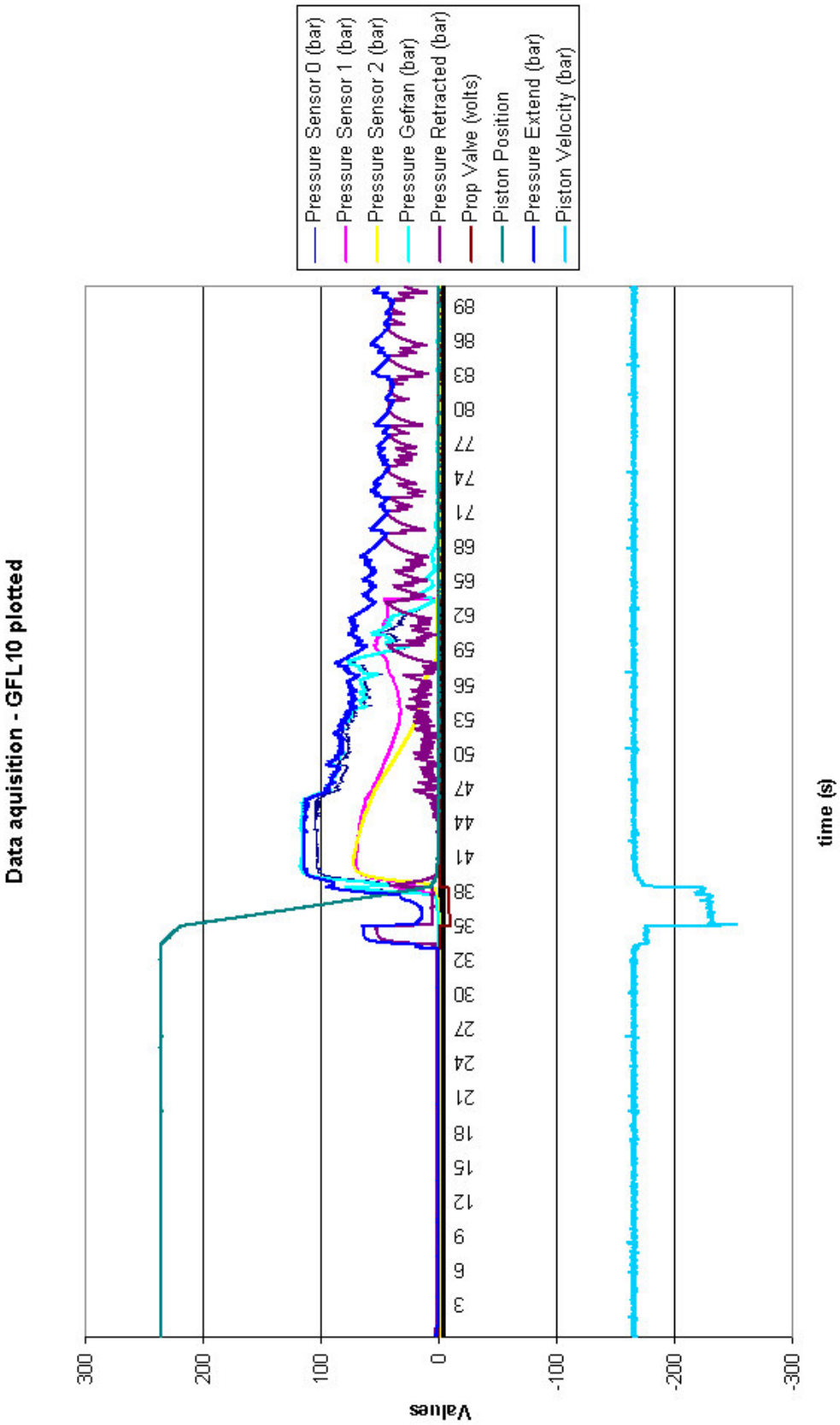

Figure C20a: Cavity pressure in lomolding DOE GFL10

Figure C20b: Fibre skeleton remaining after burn off of GFL10-28

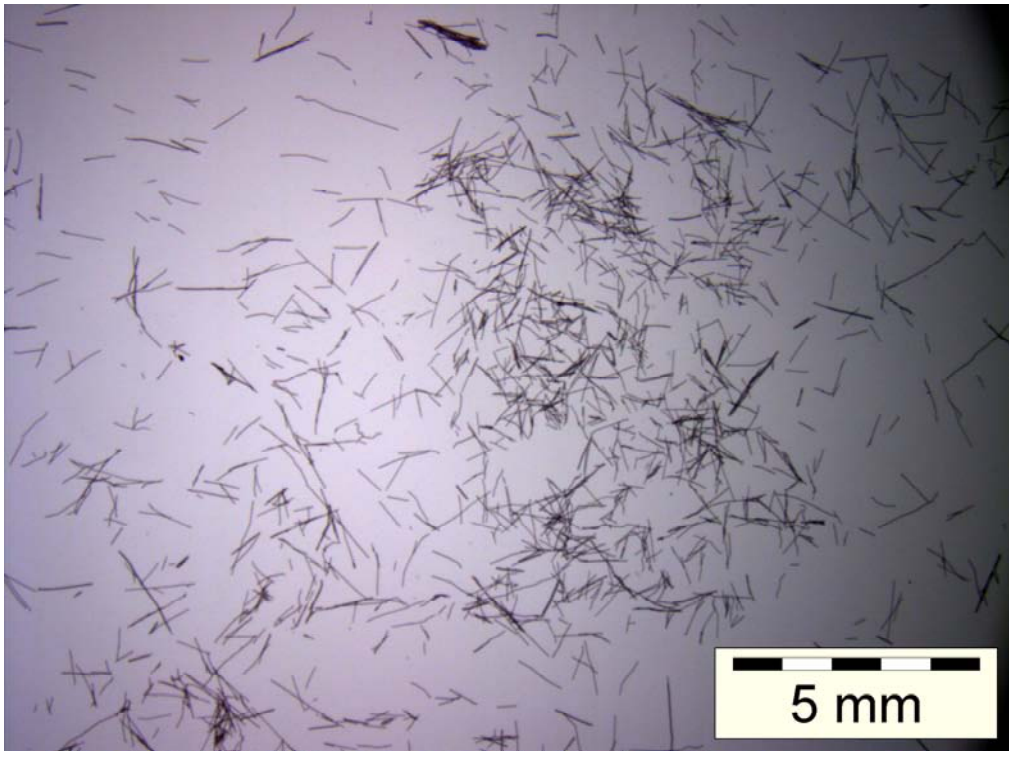

Figure C20c: Optical microscope photo taken with sample from GFL10-28

Appendix D: Statistical Results for DOE

Appendix D1: Tensile strength

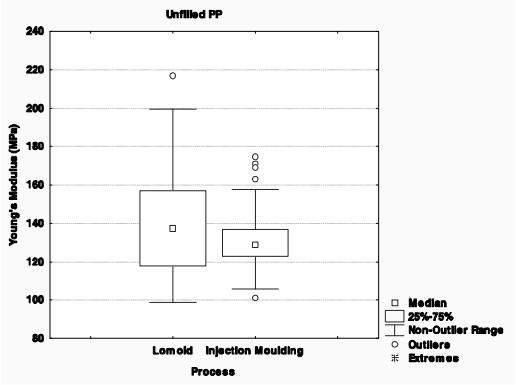

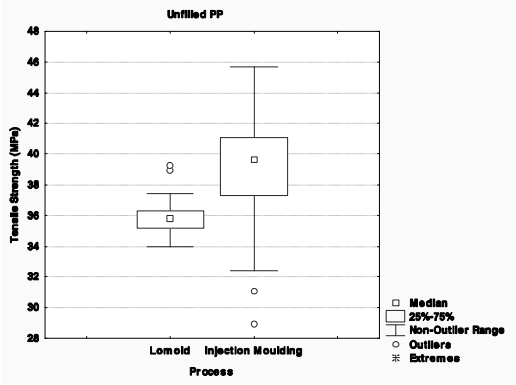

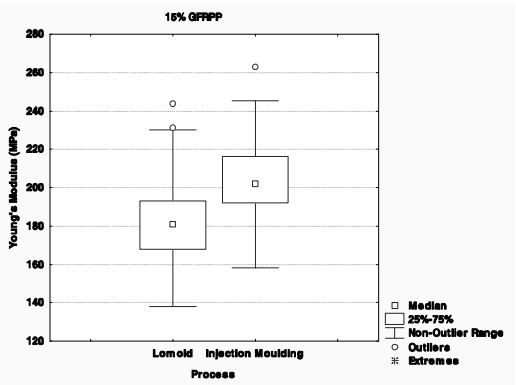

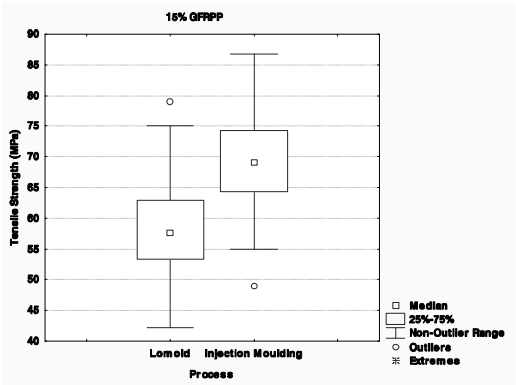

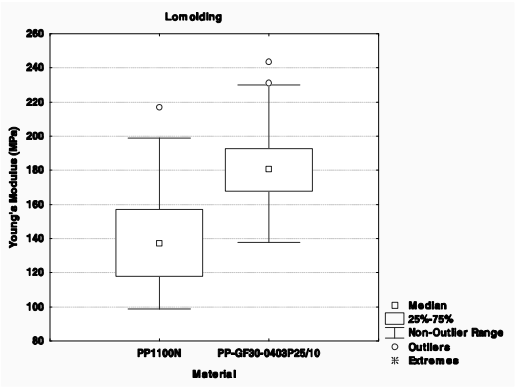

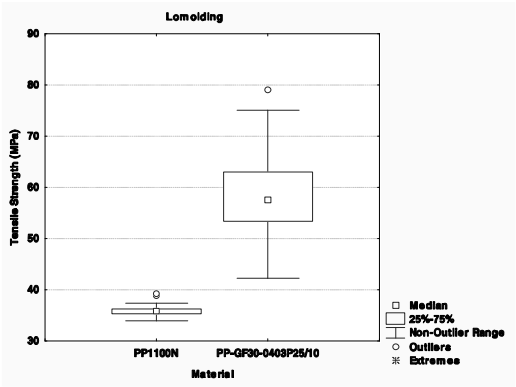

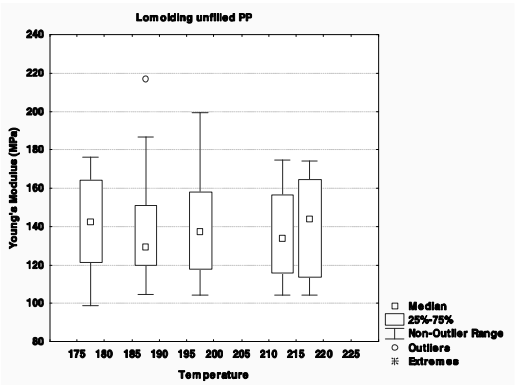

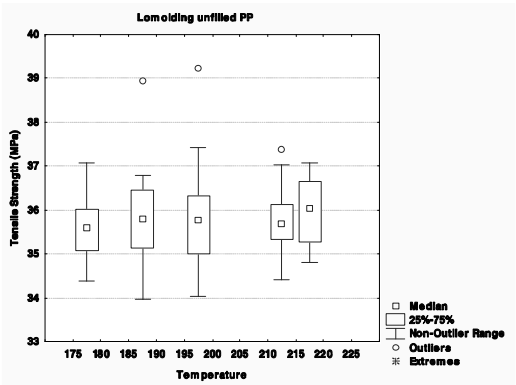

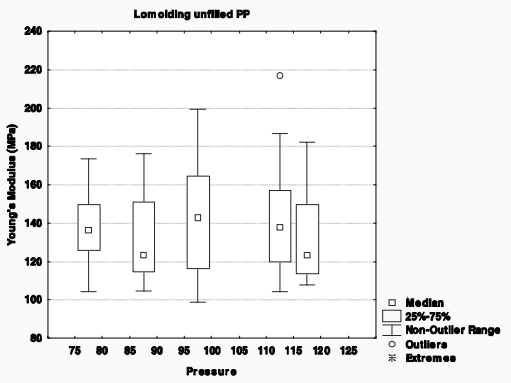
Lomolding unfilled PP
Young's Modulus (MPa)
240
220
200
180
160
140
120
100
80
75 80 85 90 95 100 105 110 115 120 125
Pressure
Median
25%-75%
Non-Outlier Range
Outliers
Extremes

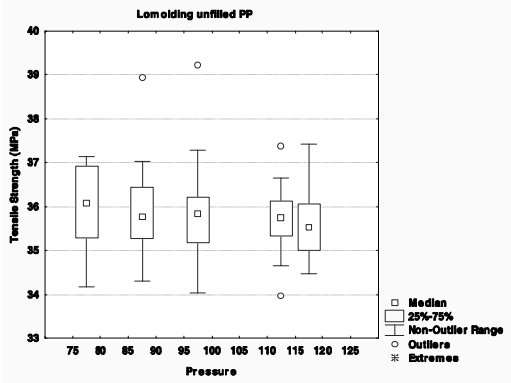
Lomolding unfilled PP
Tensile Strength (MPa)
40
39
38
37
36
35
34
33
75 80 85 90 95 100 105 110 115 120 125
Pressure
Median
25%-75%
Non-Outlier Range
Outliers
Extremes

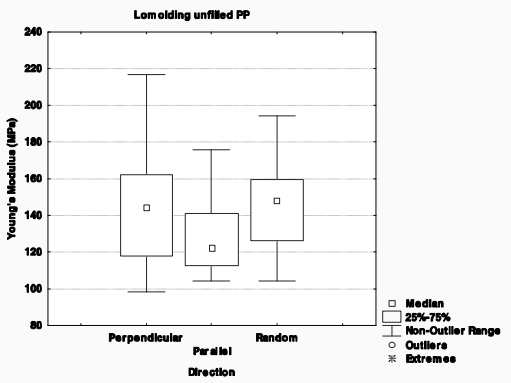
Lomolding unfilled PP
Young's Modulus (MPa)
240
220
200
180
160
140
120
100
80
Perpendicular
Parallel
Random
Direction
Median
25%-75%
Non-Outlier Range
Outliers
Extremes

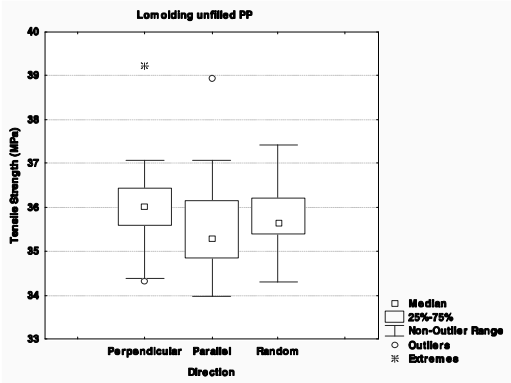
Lomolding unfilled PP
Tensile Strength (MPa)
40
39
38
37
36
35
34
33
Perpendicular
Parallel
Random
Direction
Median
25%-75%
Non-Outlier Range
Outliers
Extremes

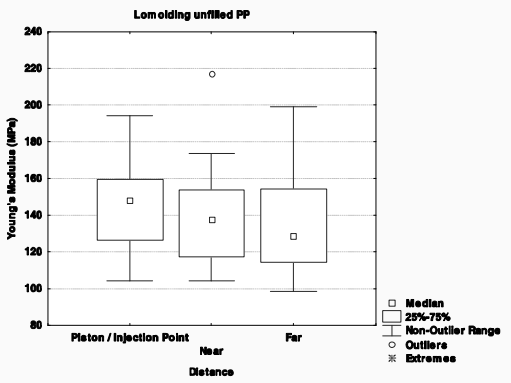
Lomolding unfilled PP
Young's Modulus (MPa)
240
220
200
180
160
140
120
100
80
Piston / Injection Point
Near
Far
Distance
Median
25%-75%
Non-Outlier Range
Outliers
Extremes

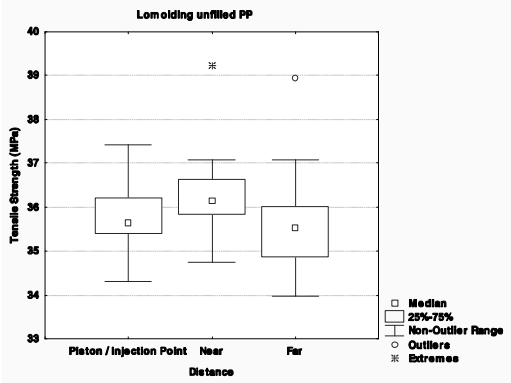
Lomolding unfilled PP
Tensile Strength (MPa)
40
39
38
37
36
35
34
33
Piston / Injection Point
Near
Far
Distance
Median
25%-75%
Non-Outlier Range
Outliers
Extremes

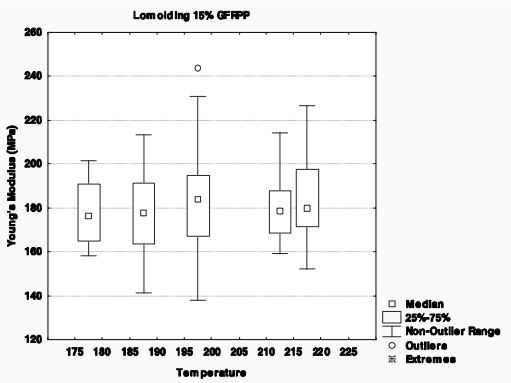
Lomolding 15% GFRPP
Young's Modulus (MPa)
260
240
220
200
180
160
140
120
175 180 185 190 195 200 205 210 215 220 225
Temperature
Median
25%-75%
Non-Outlier Range
Outliers
Extremes

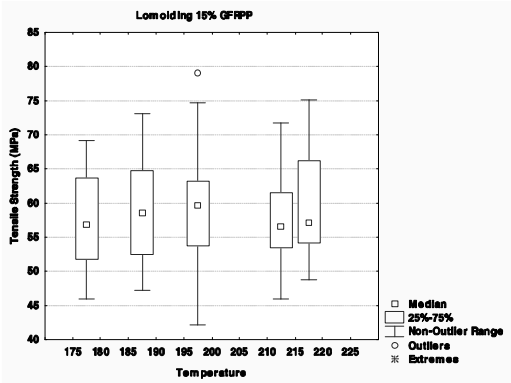
Lomolding 15% GFRPP
Tensile Strength (MPa)
85
80
75
70
65
60
55
50
45
40
175 180 185 190 195 200 205 210 215 220 225
Temperature
Median
25%-75%
Non-Outlier Range
Outliers
Extremes

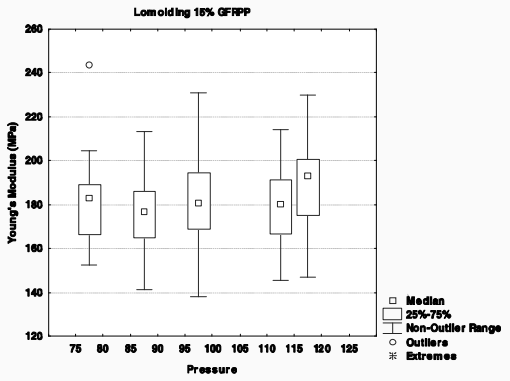
Lomolding 15% GFRPP
Young's Modulus (MPa)
Pressure
Median
25%-75%
Non-Outlier Range
Outliers
Extremes

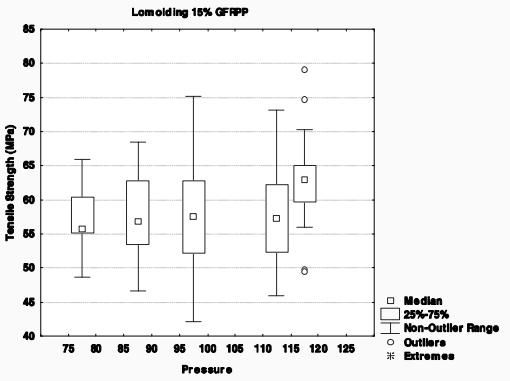
Lomolding 15% GFRPP
Tensile Strength (MPa)
Pressure
Median
25%-75%
Non-Outlier Range
Outliers
Extremes

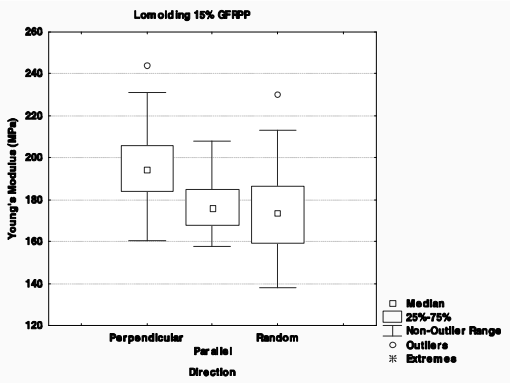
Lomolding 15% GFRPP
Young's Modulus (MPa)
Perpendicular
Parallel
Random
Direction
Median
25%-75%
Non-Outlier Range
Outliers
Extremes

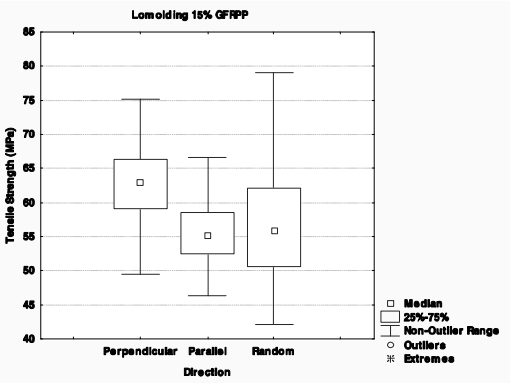
Lomolding 15% GFRPP
Tensile Strength (MPa)
Perpendicular
Parallel
Random
Direction
Median
25%-75%
Non-Outlier Range
Outliers
Extremes

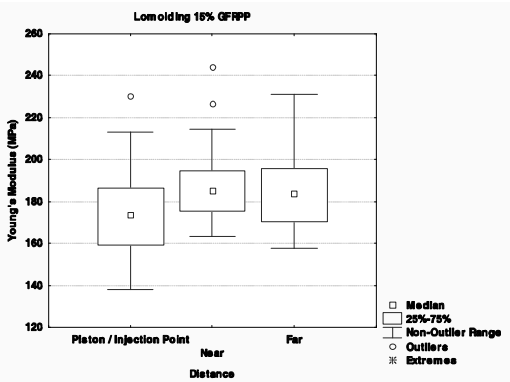
Lomolding 15% GFRPP
Young's Modulus (MPa)
Piston / Injection Point
Near
Far
Distance
Median
25%-75%
Non-Outlier Range
Outliers
Extremes

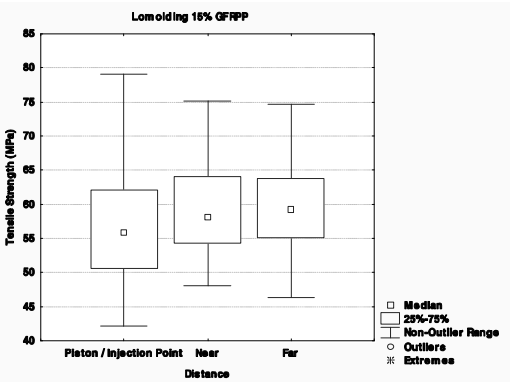
Lomolding 15% GFRPP
Tensile Strength (MPa)
Piston / Injection Point
Near
Far
Distance
Median
25%-75%
Non-Outlier Range
Outliers
Extremes

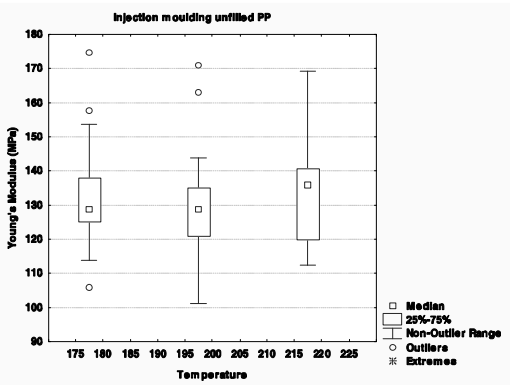
Injection moulding unfilled PP
Young's Modulus (MPa)
Temperature
Median
25%-75%
Non-Outlier Range
Outliers
Extremes

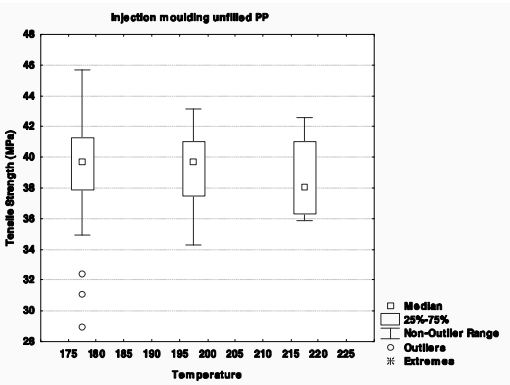
Injection moulding unfilled PP
Tensile Strength (MPa)
Temperature
Median
25%-75%
Non-Outlier Range
Outliers
Extremes

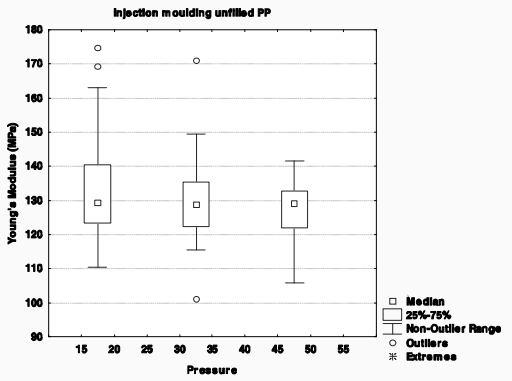
Injection moulding unfilled PP
Young's Modulus (MPa)
Pressure
Median
25%-75%
Non-Outlier Range
Outliers
Extremes

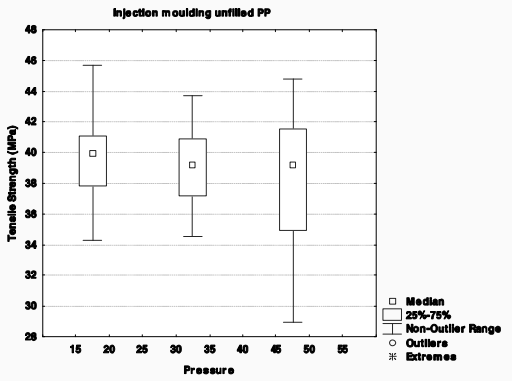
Injection moulding unfilled PP
Tensile Strength (MPa)
Pressure
Median
25%-75%
Non-Outlier Range
Outliers
Extremes

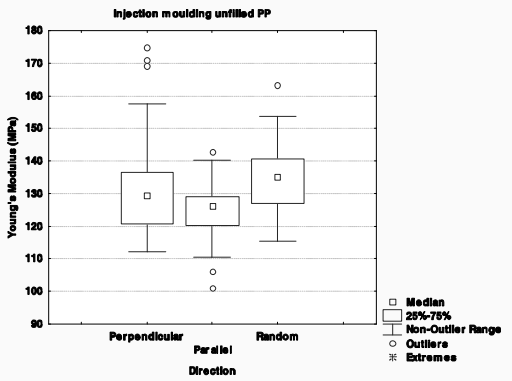
Injection moulding unfilled PP
Young's Modulus (MPa)
Perpendicular
Parallel
Random
Direction
Median
25%-75%
Non-Outlier Range
Outliers
Extremes

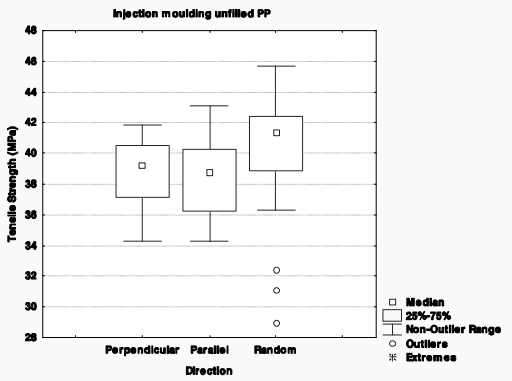
Injection moulding unfilled PP
Tensile Strength (MPa)
Perpendicular
Parallel
Random
Direction
Median
25%-75%
Non-Outlier Range
Outliers
Extremes

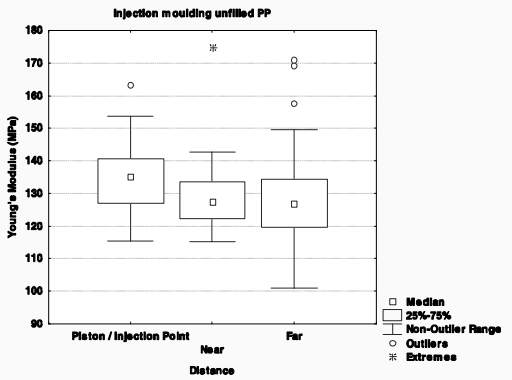
Injection moulding unfilled PP
Young's Modulus (MPa)
Piston / Injection Point
Near
Far
Distance
Median
25%-75%
Non-Outlier Range
Outliers
Extremes

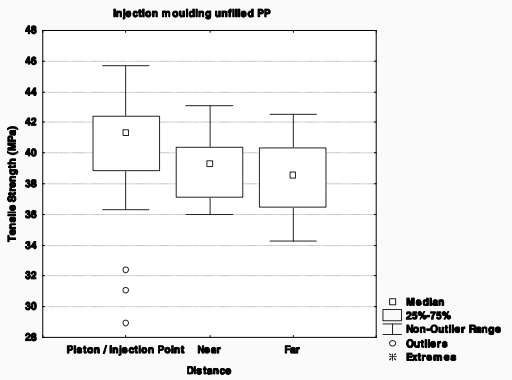
Injection moulding unfilled PP
Tensile Strength (MPa)
Piston / Injection Point
Near
Far
Distance
Median
25%-75%
Non-Outlier Range
Outliers
Extremes

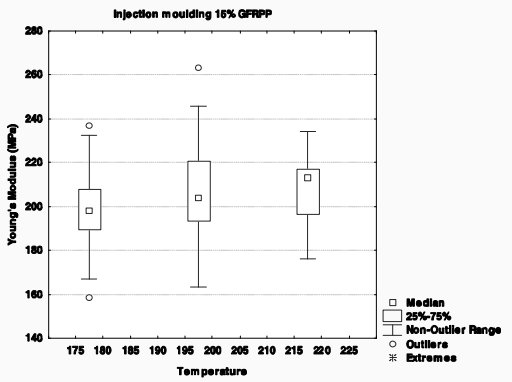
Injection moulding 15% GFRPP
Young's Modulus (MPa)
Temperature
Median
25%-75%
Non-Outlier Range
Outliers
Extremes

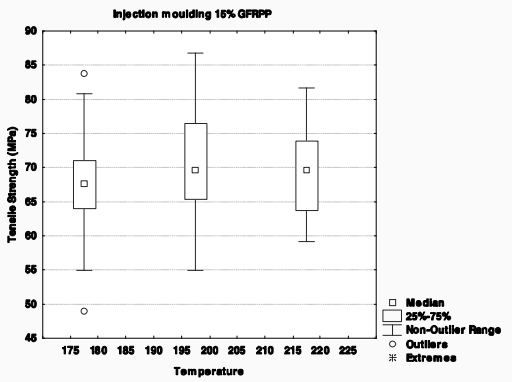
Injection moulding 15% GFRPP
Tensile Strength (MPa)
Temperature
Median
25%-75%
Non-Outlier Range
Outliers
Extremes

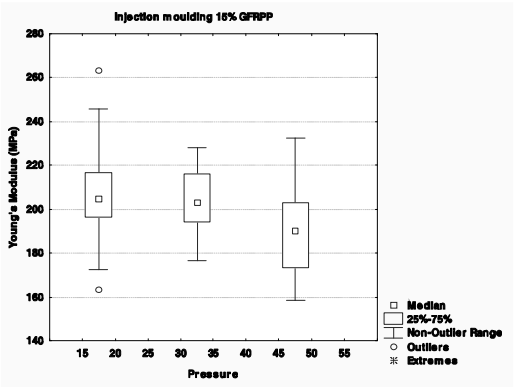
Injection moulding 15% GFRPP
Young's Modulus (MPa)
Pressure
Median
25%-75%
Non-Outlier Range
Outliers
Extremes

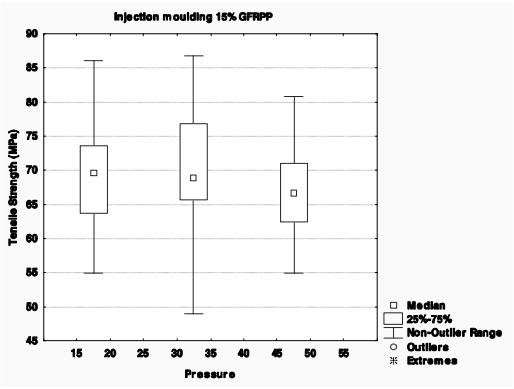
Injection moulding 15% GFRPP
Tensile Strength (MPa)
Pressure
Median
25%-75%
Non-Outlier Range
Outliers
Extremes

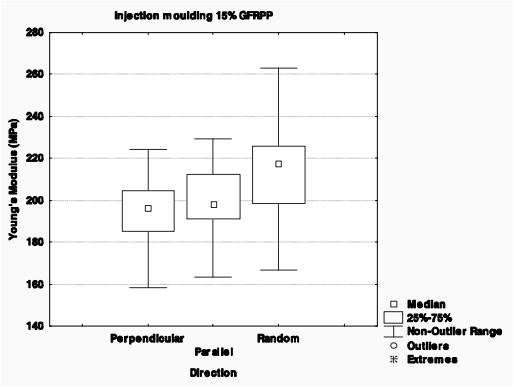
Injection moulding 15% GFRPP
Young's Modulus (MPa)
Perpendicular
Parallel
Random
Direction
Median
25%-75%
Non-Outlier Range
Outliers
Extremes

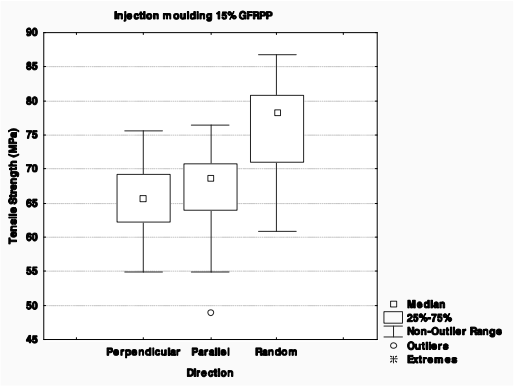
Injection moulding 15% GFRPP
Tensile Strength (MPa)
Perpendicular
Parallel
Random
Direction
Median
25%-75%
Non-Outlier Range
Outliers
Extremes

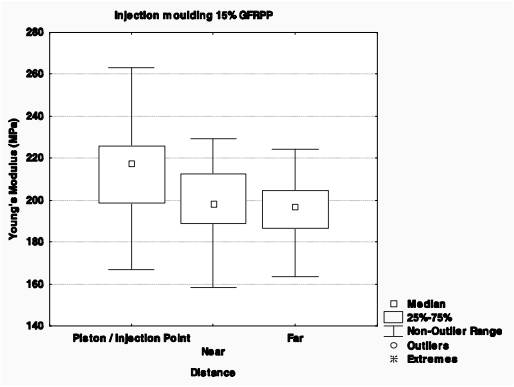
Injection moulding 15% GFRPP
Young's Modulus (MPa)
Piston / Injection Point
Near
Far
Distance
Median
25%-75%
Non-Outlier Range
Outliers
Extremes

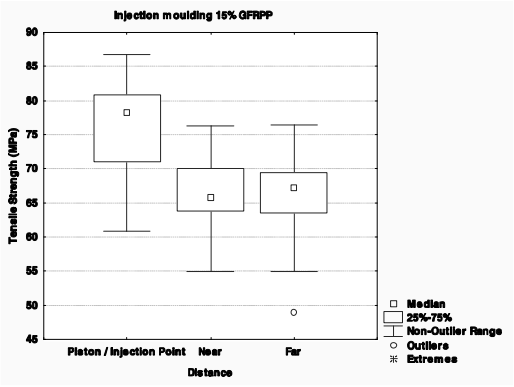
Injection moulding 15% GFRPP
Tensile Strength (MPa)
Piston / Injection Point
Near
Far
Distance
Median
25%-75%
Non-Outlier Range
Outliers
Extremes

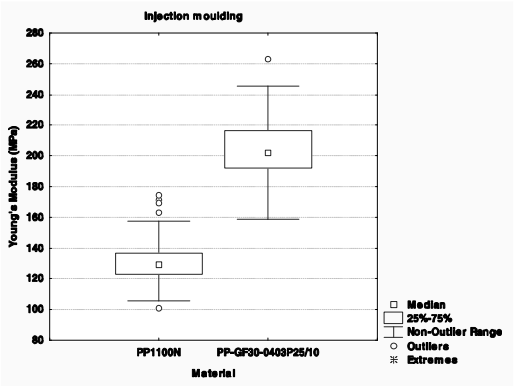
Injection moulding
Young's Modulus (MPa)
PP1100N
PP-GF30-0403P25/10
Material
Median
25%-75%
Non-Outlier Range
Outliers
Extremes

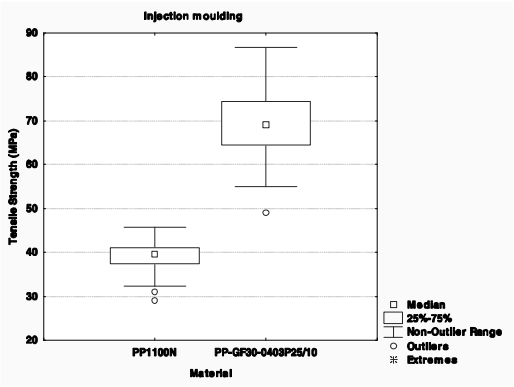
Injection moulding
Tensile Strength (MPa)
PP1100N
PP-GF30-0403P25/10
Material
Median
25%-75%
Non-Outlier Range
Outliers
Extremes

Appendix D2: Flexural modulus

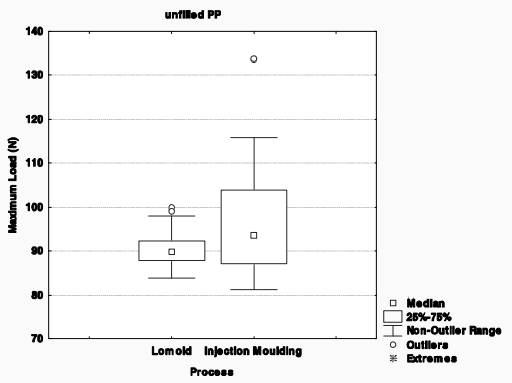

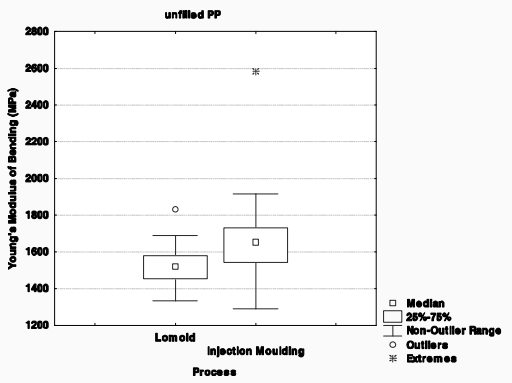

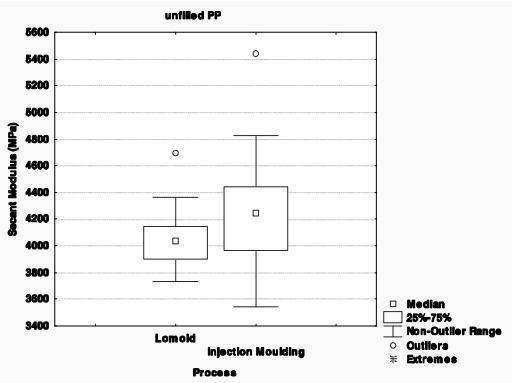

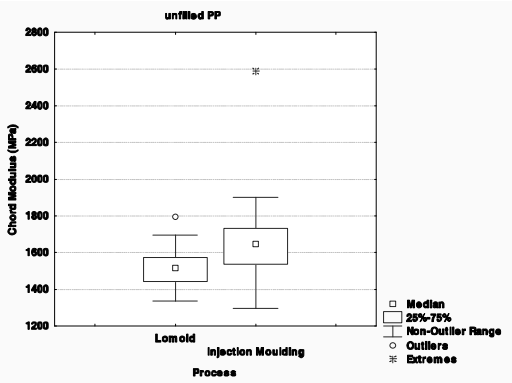

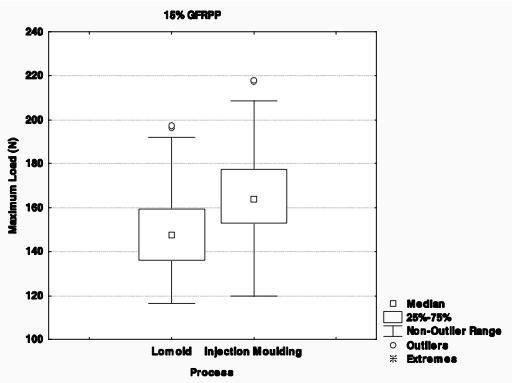

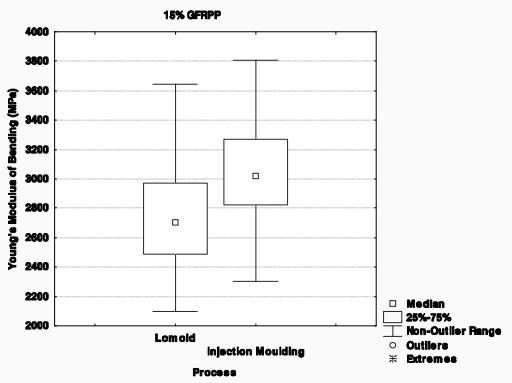

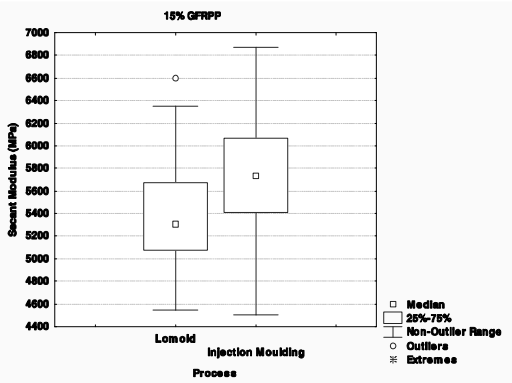

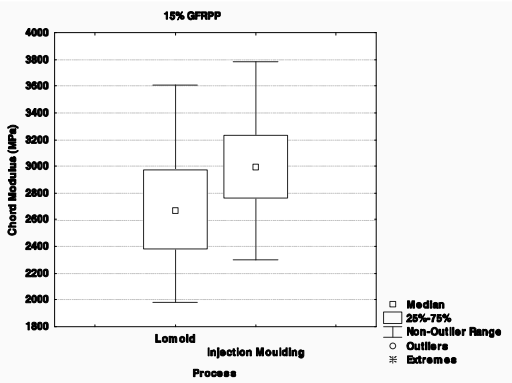

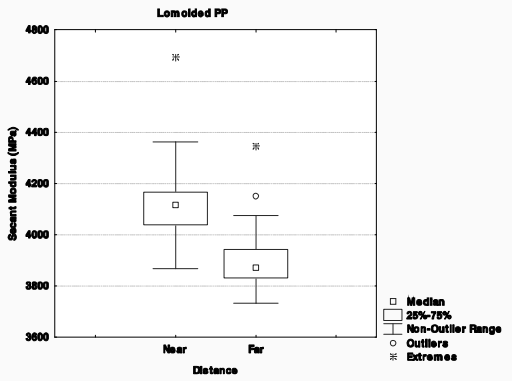
Lomolded PP
Secant Modulus (MPa)
4800
4600
4400
4200
4000
3800
3600
Near
Far
Distance
Median
25%-75%
Non-Outlier Range
Outliers
Extremes

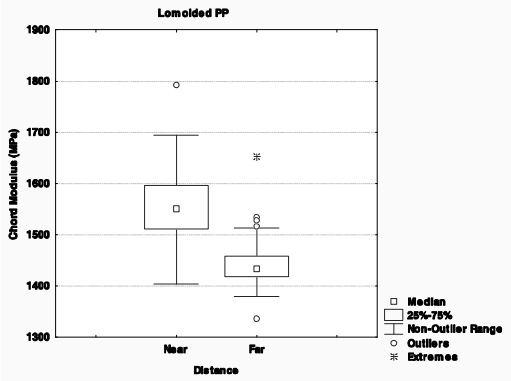
Lomolded PP
Chord Modulus (MPa)
1900
1800
1700
1600
1500
1400
1300
Near
Far
Distance
Median
25%-75%
Non-Outlier Range
Outliers
Extremes

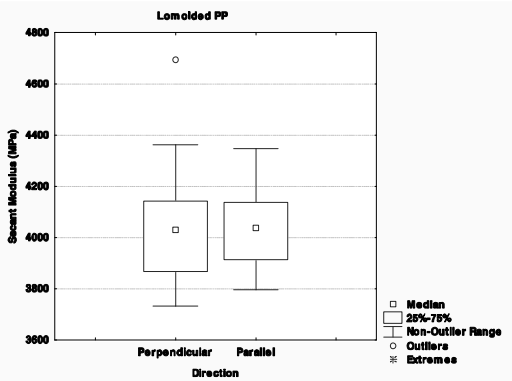
Lomolded PP
Secant Modulus (MPa)
4800
4600
4400
4200
4000
3800
3600
Perpendicular
Parallel
Direction
Median
25%-75%
Non-Outlier Range
Outliers
Extremes

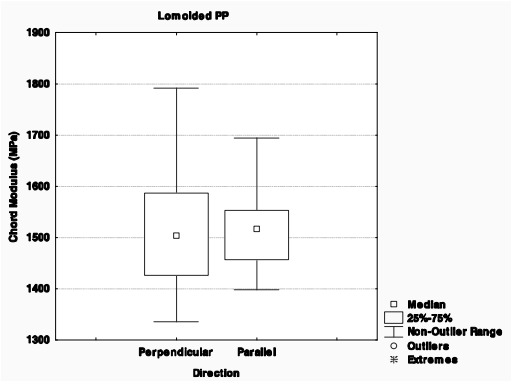
Lomolded PP
Chord Modulus (MPa)
1900
1800
1700
1600
1500
1400
1300
Perpendicular
Parallel
Direction
Median
25%-75%
Non-Outlier Range
Outliers
Extremes

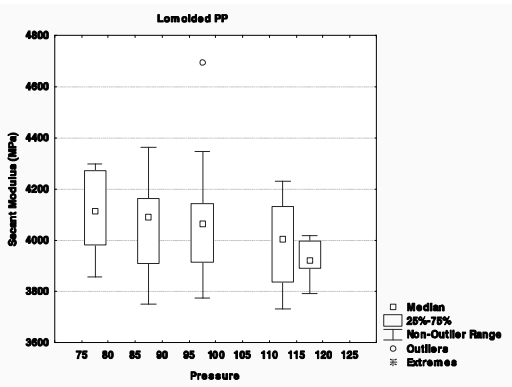
Lomolded PP
Secant Modulus (MPa)
4800
4600
4400
4200
4000
3800
3600
75 80 85 90 95 100 105 110 115 120 125
Pressure
Median
25%-75%
Non-Outlier Range
Outliers
Extremes

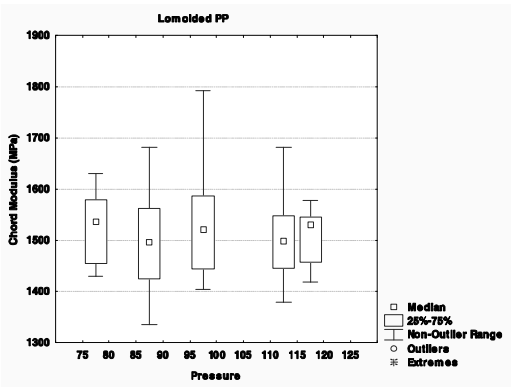
Lomolded PP
Chord Modulus (MPa)
1900
1800
1700
1600
1500
1400
1300
75 80 85 90 95 100 105 110 115 120 125
Pressure
Median
25%-75%
Non-Outlier Range
Outliers
Extremes

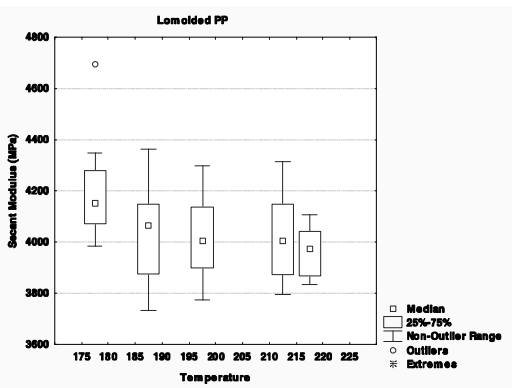
Lomolded PP
Secant Modulus (MPa)
4800
4600
4400
4200
4000
3800
3600
175 180 185 190 195 200 205 210 215 220 225
Temperature
Median
25%-75%
Non-Outlier Range
Outliers
Extremes

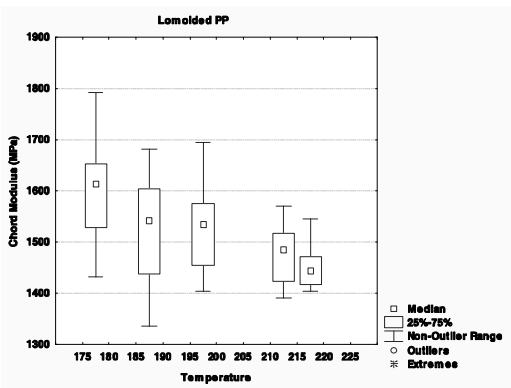
Lomolded PP
Chord Modulus (MPa)
1900
1800
1700
1600
1500
1400
1300
175 180 185 190 195 200 205 210 215 220 225
Temperature
Median
25%-75%
Non-Outlier Range
Outliers
Extremes

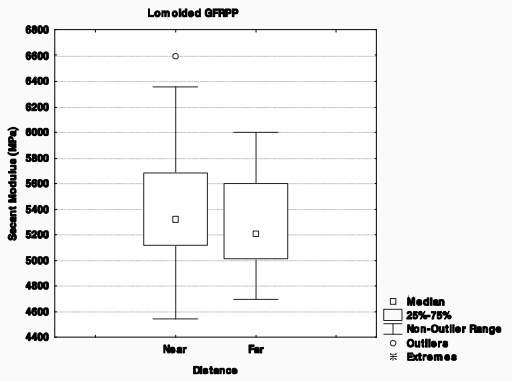
Lomolded GFRPP
Secant Modulus (MPa)
Near
Far
Distance
Median
25%-75%
Non-Outlier Range
Outliers
Extremes

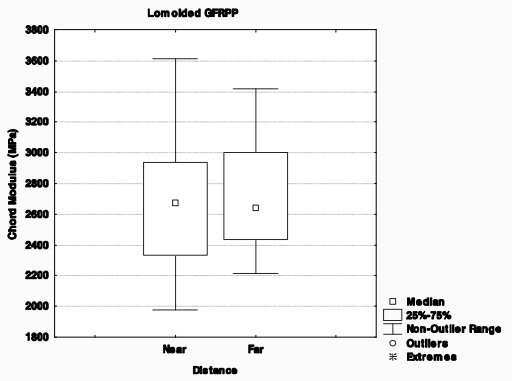
Lomolded GFRPP
Chord Modulus (MPa)
Near
Far
Distance
Median
25%-75%
Non-Outlier Range
Outliers
Extremes

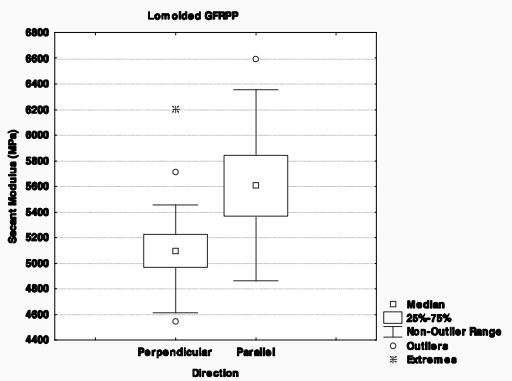
Lomolded GFRPP
Secant Modulus (MPa)
Perpendicular
Parallel
Direction
Median
25%-75%
Non-Outlier Range
Outliers
Extremes

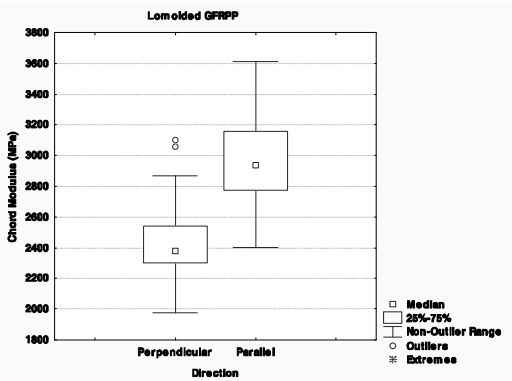
Lomolded GFRPP
Chord Modulus (MPa)
Perpendicular
Parallel
Direction
Median
25%-75%
Non-Outlier Range
Outliers
Extremes

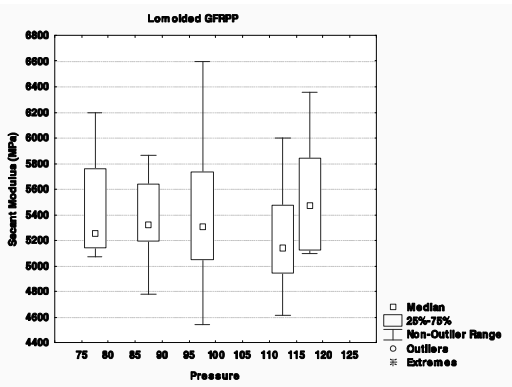
Lomolded GFRPP
Secant Modulus (MPa)
75 80 85 90 95 100 105 110 115 120 125
Pressure
Median
25%-75%
Non-Outlier Range
Outliers
Extremes

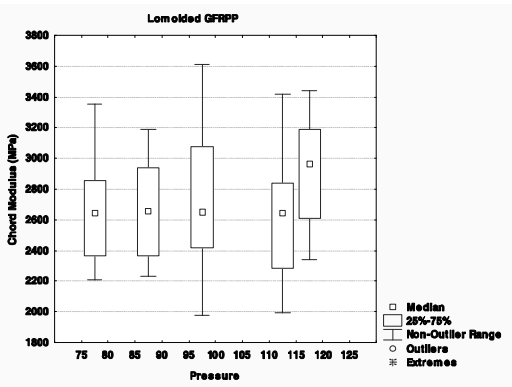
Lomolded GFRPP
Chord Modulus (MPa)
75 80 85 90 95 100 105 110 115 120 125
Pressure
Median
25%-75%
Non-Outlier Range
Outliers
Extremes

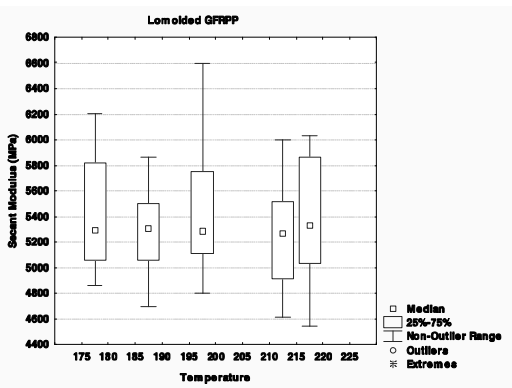
Lomolded GFRPP
Secant Modulus (MPa)
175 180 185 190 195 200 205 210 215 220 225
Temperature
Median
25%-75%
Non-Outlier Range
Outliers
Extremes

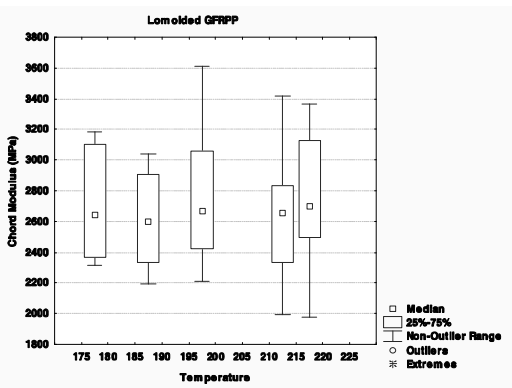
Lomolded GFRPP
Chord Modulus (MPa)
175 180 185 190 195 200 205 210 215 220 225
Temperature
Median
25%-75%
Non-Outlier Range
Outliers
Extremes

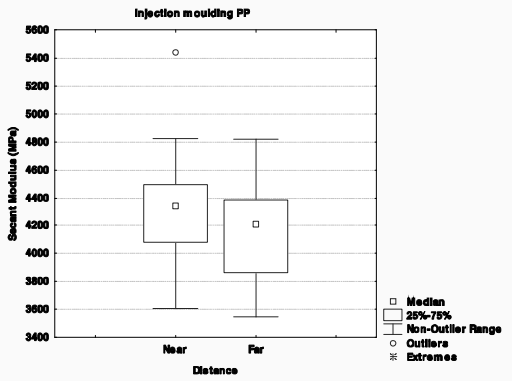
Injection moulding PP
Secant Modulus (MPa)
Near
Far
Distance
Median
25%-75%
Non-Outlier Range
Outliers
Extremes


Injection moulding PP
Chord Modulus (MPa)
Near
Far
Distance
Median
25%-75%
Non-Outlier Range
Outliers
Extremes

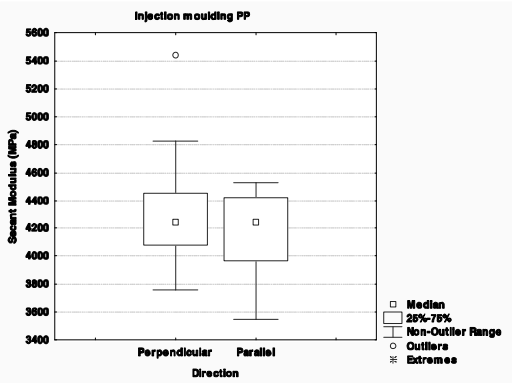
Injection moulding PP
Secant Modulus (MPa)
Perpendicular
Parallel
Direction
Median
25%-75%
Non-Outlier Range
Outliers
Extremes

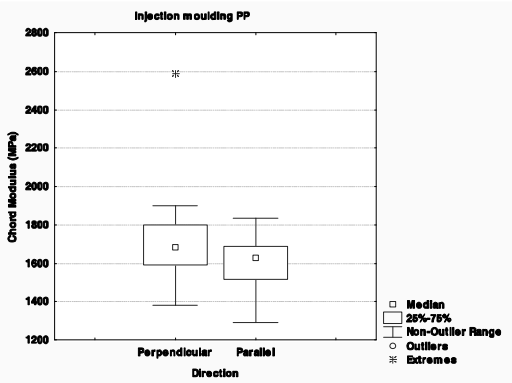
Injection moulding PP
Chord Modulus (MPa)
Perpendicular
Parallel
Direction
Median
25%-75%
Non-Outlier Range
Outliers
Extremes

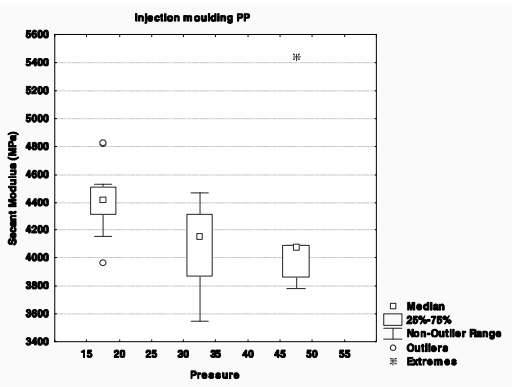
Injection moulding PP
Secant Modulus (MPa)
Pressure
Median
25%-75%
Non-Outlier Range
Outliers
Extremes

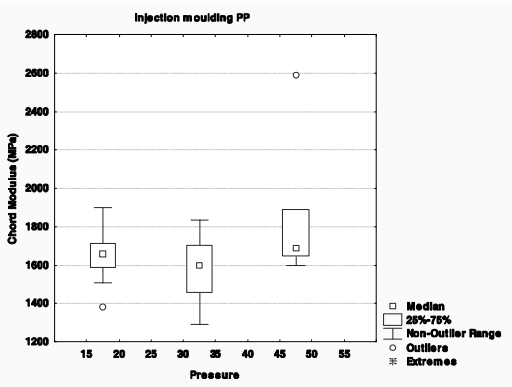
Injection moulding PP
Chord Modulus (MPa)
Pressure
Median
25%-75%
Non-Outlier Range
Outliers
Extremes

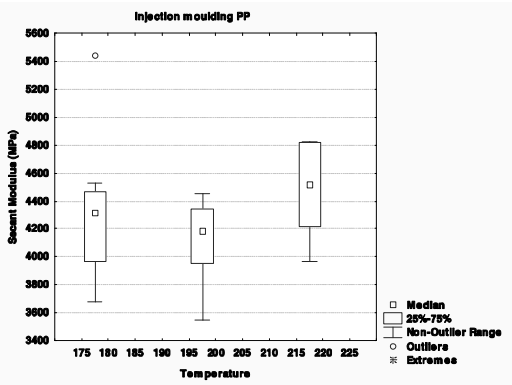
Injection moulding PP
Secant Modulus (MPa)
Temperature
Median
25%-75%
Non-Outlier Range
Outliers
Extremes

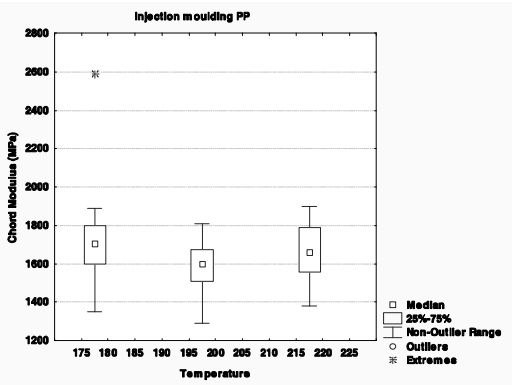
Injection moulding PP
Chord Modulus (MPa)
Temperature
Median
25%-75%
Non-Outlier Range
Outliers
Extremes

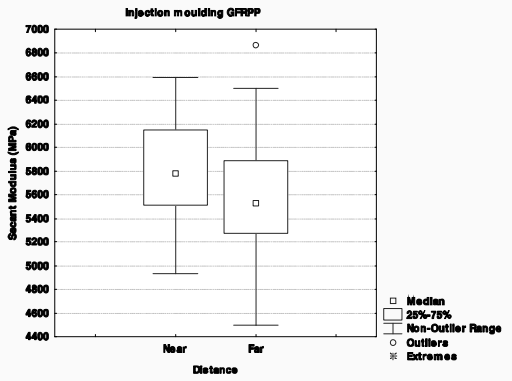
Injection moulding GFRPP
Secant Modulus (MPa)
Near
Far
Distance
Median
25%-75%
Non-Outlier Range
Outliers
Extremes

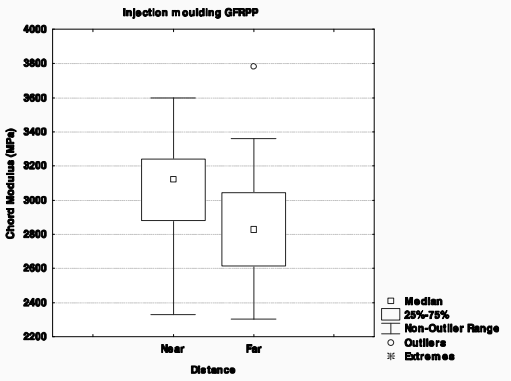
Injection moulding GFRPP
Chord Modulus (MPa)
Near
Far
Distance
Median
25%-75%
Non-Outlier Range
Outliers
Extremes

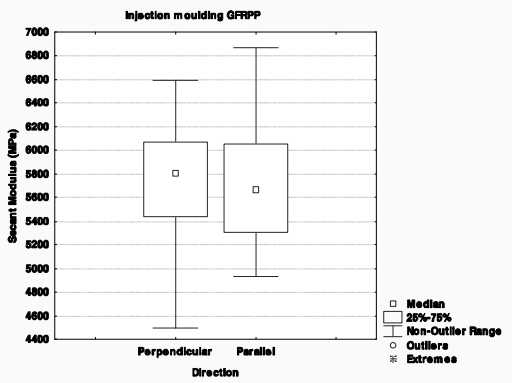
Injection moulding GFRPP
Secant Modulus (MPa)
Perpendicular
Parallel
Direction
Median
25%-75%
Non-Outlier Range
Outliers
Extremes

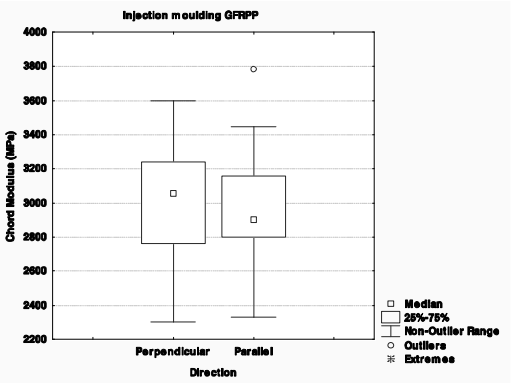
Injection moulding GFRPP
Chord Modulus (MPa)
Perpendicular
Parallel
Direction
Median
25%-75%
Non-Outlier Range
Outliers
Extremes

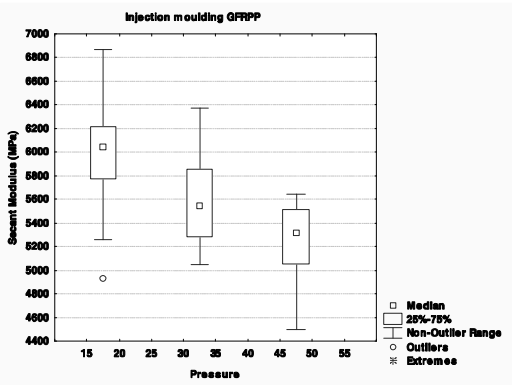
Injection moulding GFRPP
Secant Modulus (MPa)
Pressure
Median
25%-75%
Non-Outlier Range
Outliers
Extremes

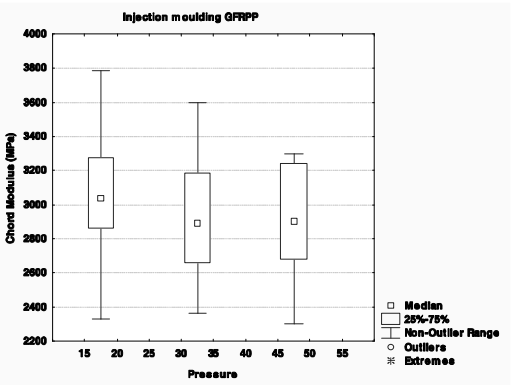
Injection moulding GFRPP
Chord Modulus (MPa)
Pressure
Median
25%-75%
Non-Outlier Range
Outliers
Extremes

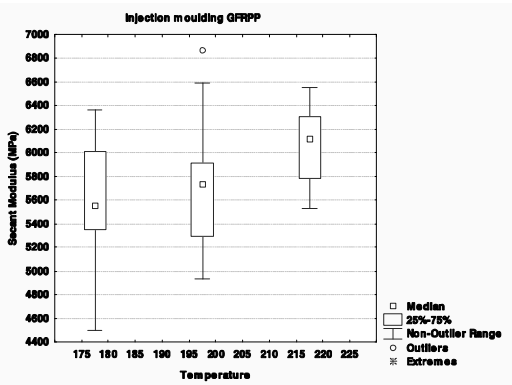
Injection moulding GFRPP
Secant Modulus (MPa)
Temperature
Median
25%-75%
Non-Outlier Range
Outliers
Extremes

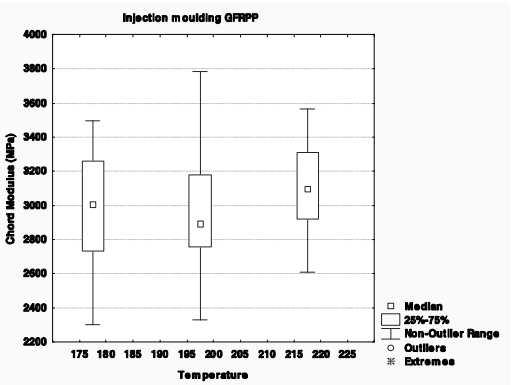
Injection moulding GFRPP
Chord Modulus (MPa)
Temperature
Median
25%-75%
Non-Outlier Range
Outliers
Extremes

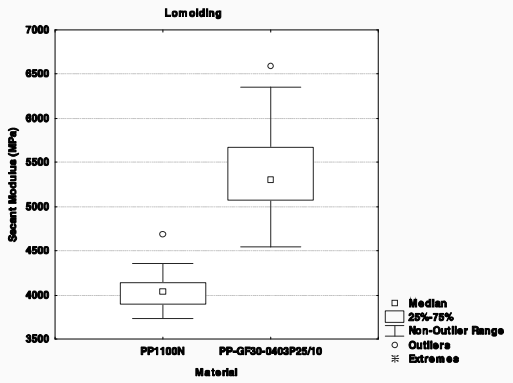
Lomolding
Secant Modulus (MPa)
7000
6500
6000
5500
5000
4500
4000
3500
PP1100N
PP-GF30-0403P25/10
Material
Median
25%-75%
Non-Outlier Range
Outliers
Extremes

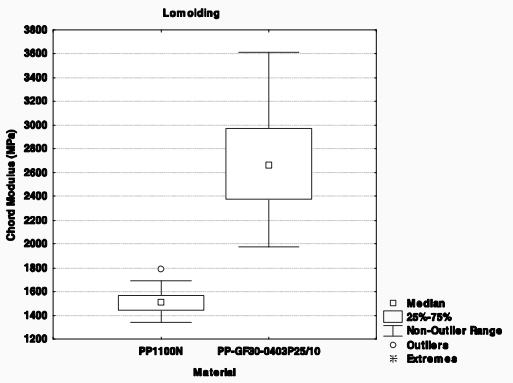
Lomolding
Chord Modulus (MPa)
3800
3600
3400
3200
3000
2800
2600
2400
2200
2000
1800
1600
1400
1200
PP1100N
PP-GF30-0403P25/10
Material
Median
25%-75%
Non-Outlier Range
Outliers
Extremes

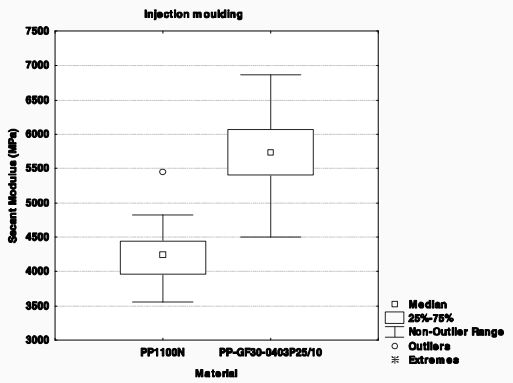
Injection moulding
Secant Modulus (MPa)
7500
7000
6500
6000
5500
5000
4500
4000
3500
3000
PP1100N
PP-GF30-0403P25/10
Material
Median
25%-75%
Non-Outlier Range
Outliers
Extremes

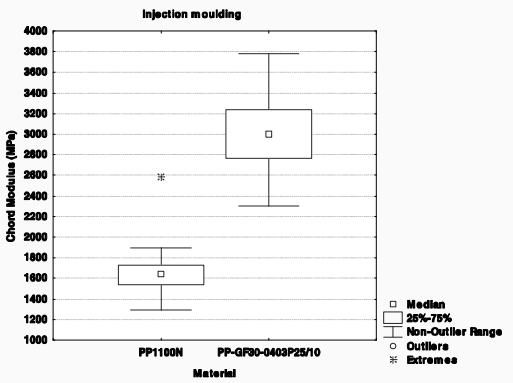
Injection moulding
Chord Modulus (MPa)
4000
3800
3600
3400
3200
3000
2800
2600
2400
2200
2000
1800
1600
1400
1200
1000
PP1100N
PP-GF30-0403P25/10
Material
Median
25%-75%
Non-Outlier Range
Outliers
Extremes

Appendix D3: Impact resistance

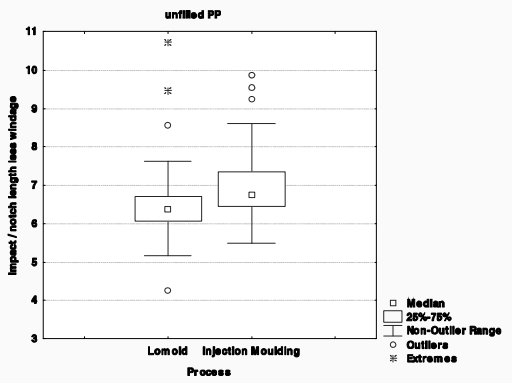

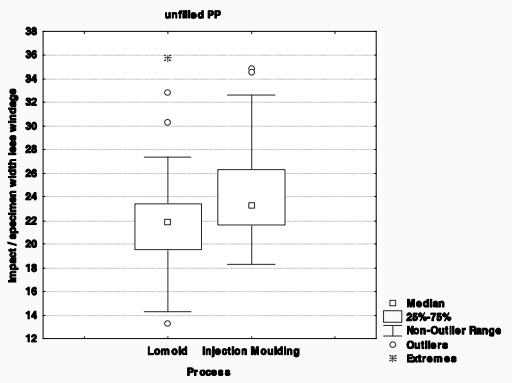

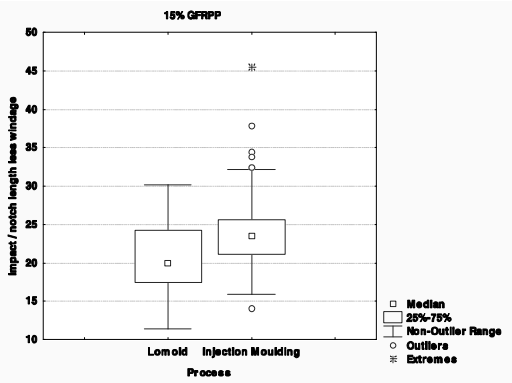

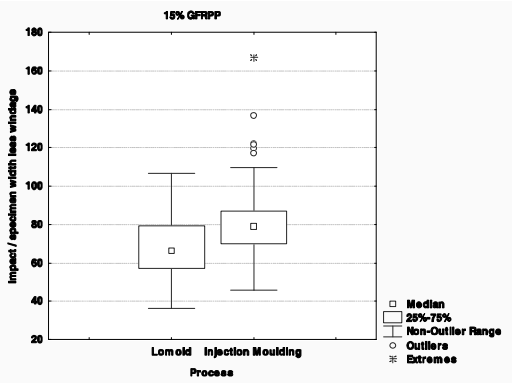

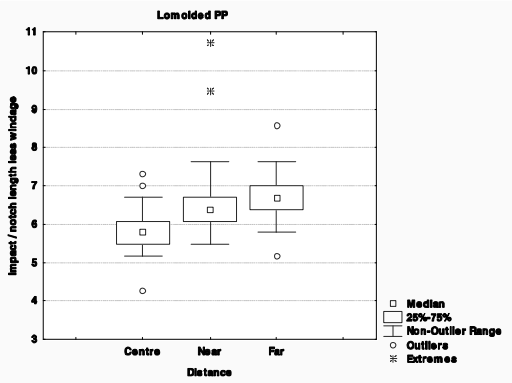

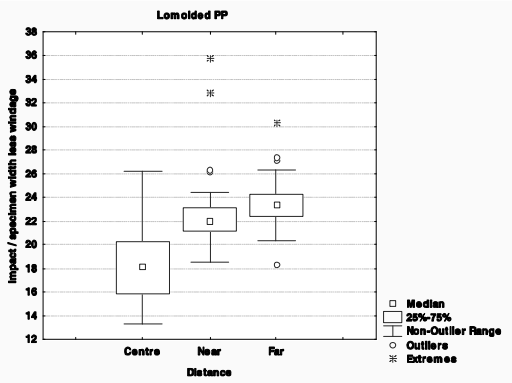

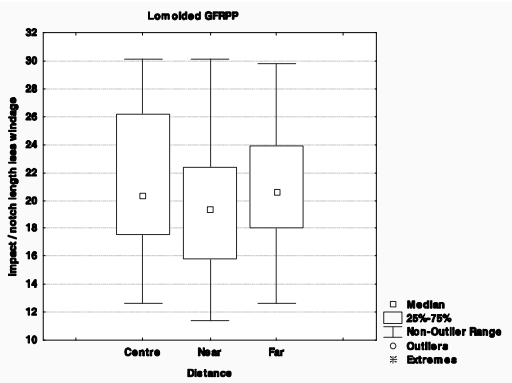

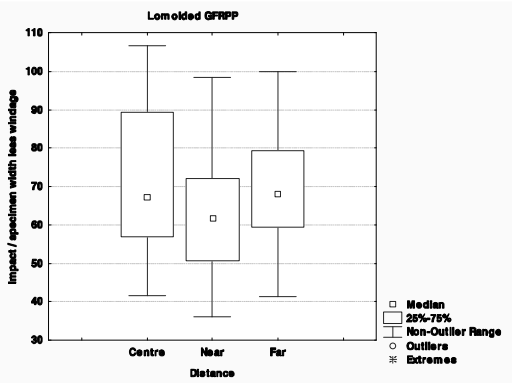

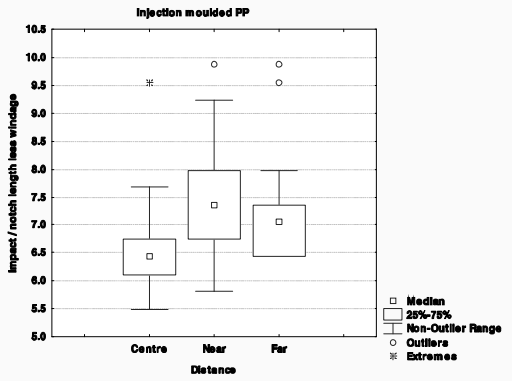
Injection moulded PP
Impact / notch length less windage
Centre
Near
Far
Distance
Median
25%-75%
Non-Outlier Range
Outliers
Extremes

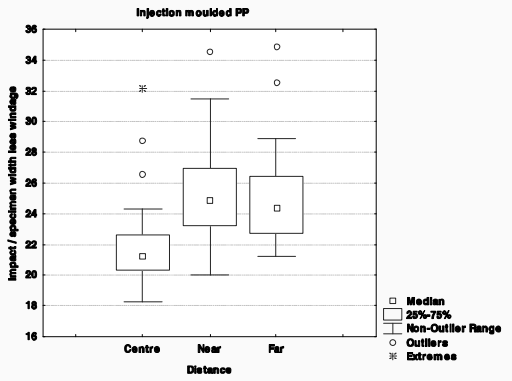
Injection moulded PP
Impact / specimen width less windage
Centre
Near
Far
Distance
Median
25%-75%
Non-Outlier Range
Outliers
Extremes

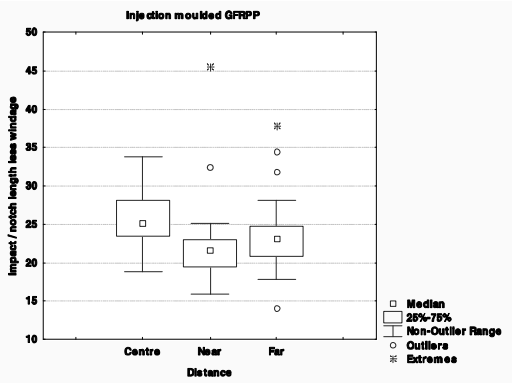
Injection moulded GFRPP
Impact / notch length less windage
Centre
Near
Far
Distance
Median
25%-75%
Non-Outlier Range
Outliers
Extremes

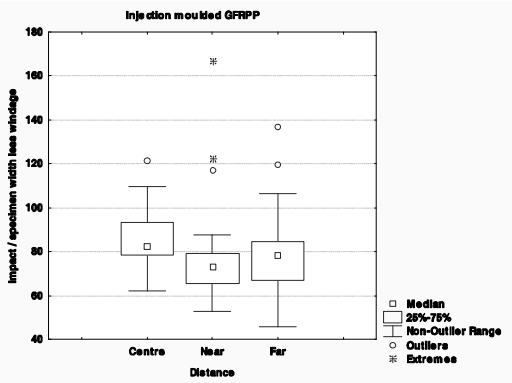
Injection moulded GFRPP
Impact / specimen width less windage
Centre
Near
Far
Distance
Median
25%-75%
Non-Outlier Range
Outliers
Extremes

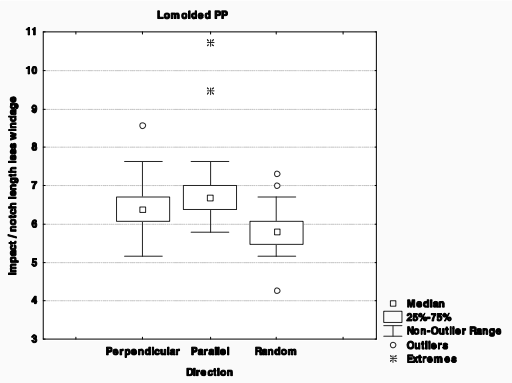
Lomolded PP
Impact / notch length less windage
Perpendicular
Parallel
Random
Direction
Median
25%-75%
Non-Outlier Range
Outliers
Extremes

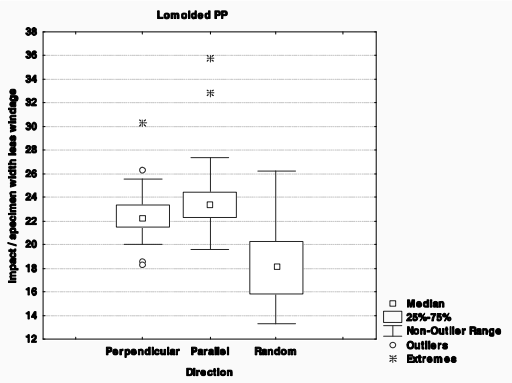
Lomolded PP
Impact / specimen width less windage
Perpendicular
Parallel
Random
Direction
Median
25%-75%
Non-Outlier Range
Outliers
Extremes

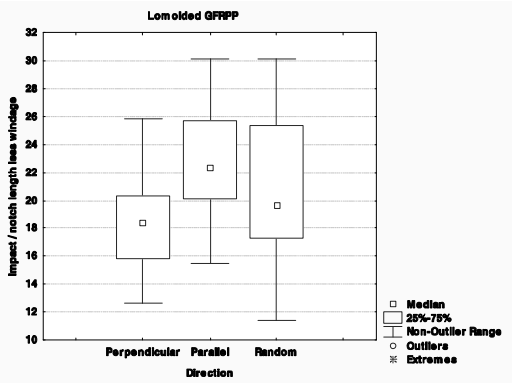
Lomolded GFRPP
Impact / notch length less windage
Perpendicular
Parallel
Random
Direction
Median
25%-75%
Non-Outlier Range
Outliers
Extremes

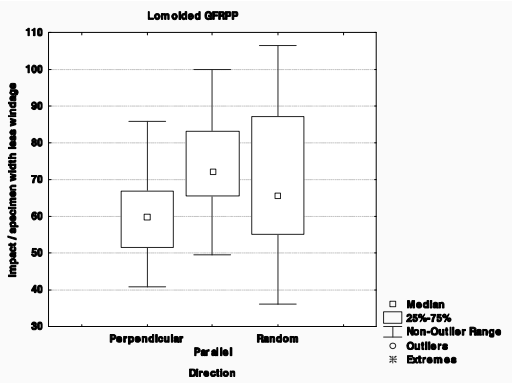
Lomolded GFRPP
Impact / specimen width less windage
Perpendicular
Parallel
Random
Direction
Median
25%-75%
Non-Outlier Range
Outliers
Extremes

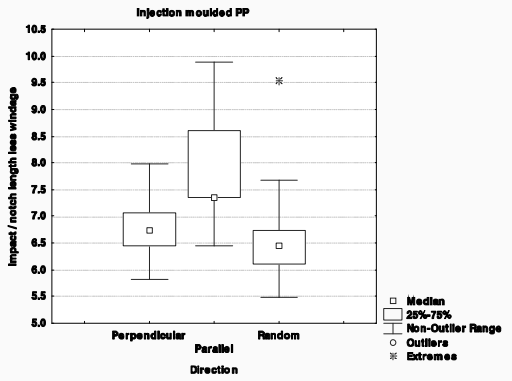
Injection moulded PP
Impact / notch length less windage
Perpendicular
Parallel
Random
Direction
Median
25%-75%
Non-Outlier Range
Outliers
Extremes

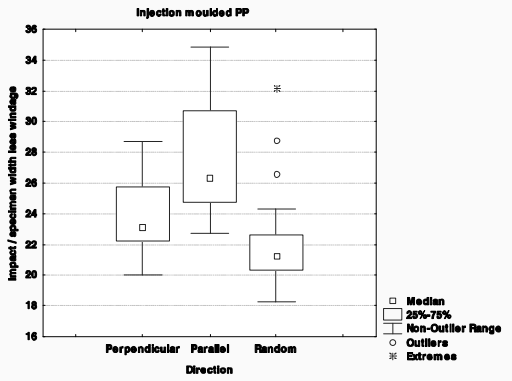
Injection moulded PP
Impact / specimen width less windage
Perpendicular
Parallel
Random
Direction
Median
25%-75%
Non-Outlier Range
Outliers
Extremes

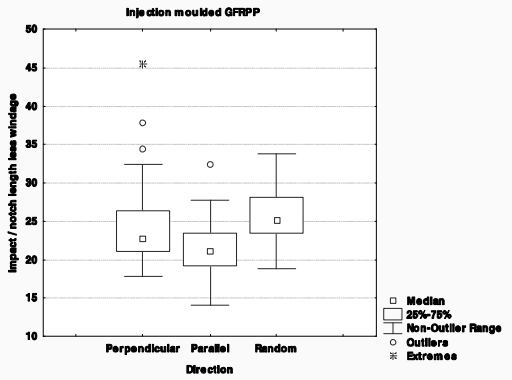
Injection moulded GFRPP
Impact / notch length less windage
Perpendicular
Parallel
Random
Direction
Median
25%-75%
Non-Outlier Range
Outliers
Extremes

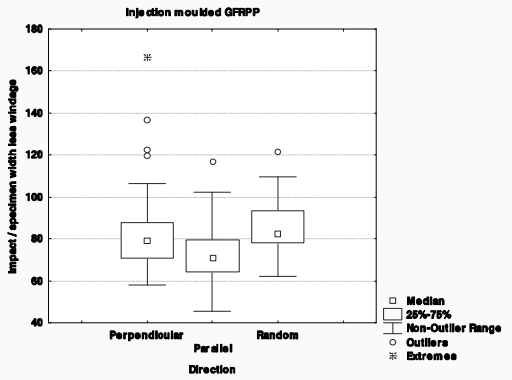
Injection moulded GFRPP
Impact / specimen width less windage
Perpendicular
Parallel
Random
Direction
Median
25%-75%
Non-Outlier Range
Outliers
Extremes

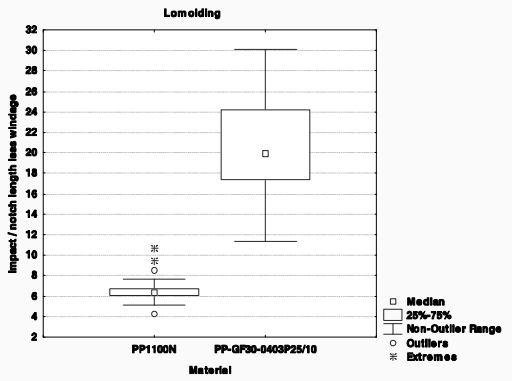
Lomolding
Impact / notch length less windage
PP1100N
PP-GF30-0403P25/10
Material
Median
25%-75%
Non-Outlier Range
Outliers
Extremes

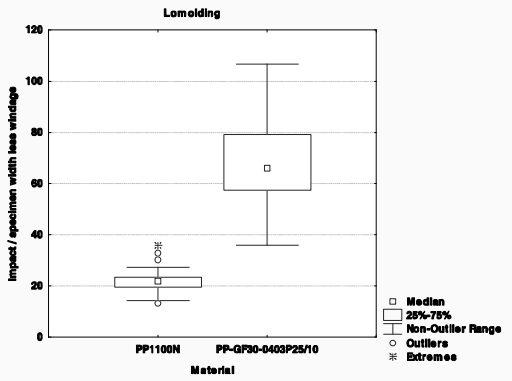
Lomolding
Impact / specimen width less windage
PP1100N
PP-GF30-0403P25/10
Material
Median
25%-75%
Non-Outlier Range
Outliers
Extremes

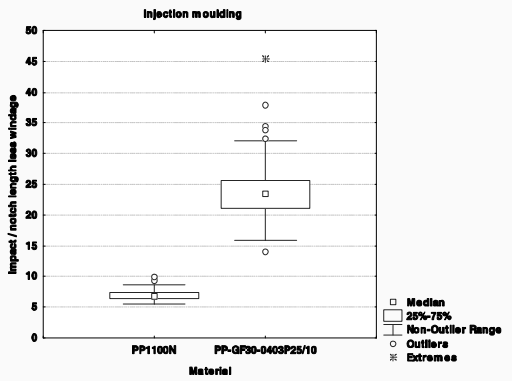
Injection moulding
Impact / notch length less windage
PP1100N
PP-GF30-0403P25/10
Material
Median
25%-75%
Non-Outlier Range
Outliers
Extremes

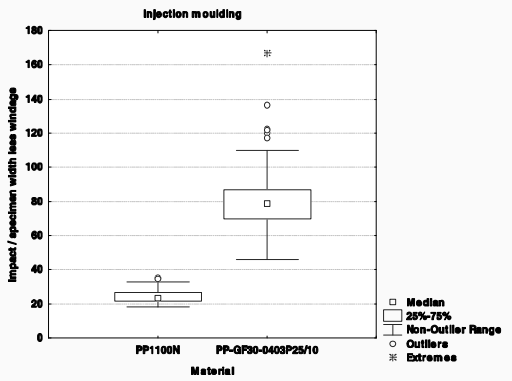
Injection moulding
Impact / specimen width less windage
PP1100N
PP-GF30-0403P25/10
Material
Median
25%-75%
Non-Outlier Range
Outliers
Extremes

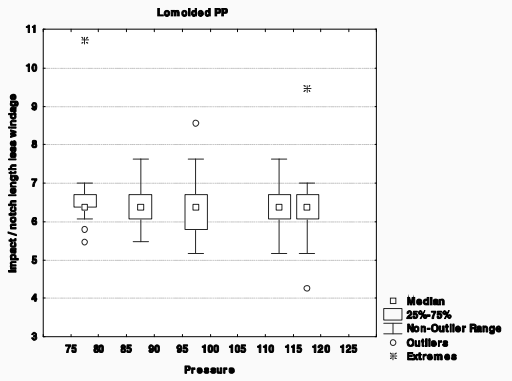
Lomolded PP
Impact / notch length less windage
Pressure
Median
25%-75%
Non-Outlier Range
Outliers
Extremes

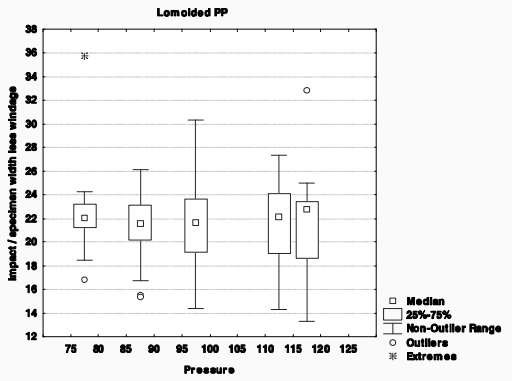
Lomolded PP
Impact / specimen width less windage
Pressure
Median
25%-75%
Non-Outlier Range
Outliers
Extremes

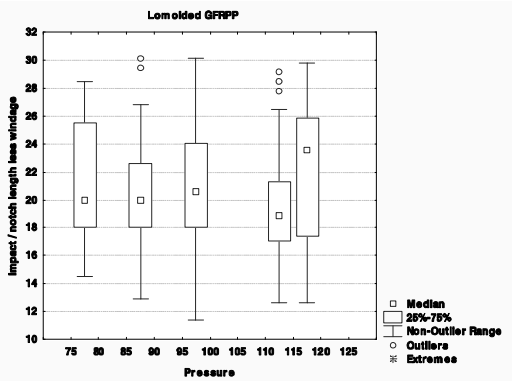
Lomolded GFRPP
Impact / notch length less windage
Pressure
Median
25%-75%
Non-Outlier Range
Outliers
Extremes

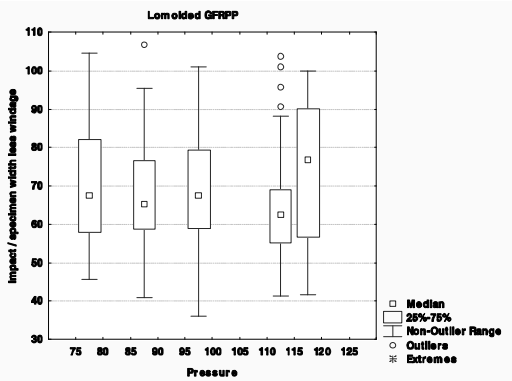
Lomolded GFRPP
Impact / specimen width less windage
Pressure
Median
25%-75%
Non-Outlier Range
Outliers
Extremes

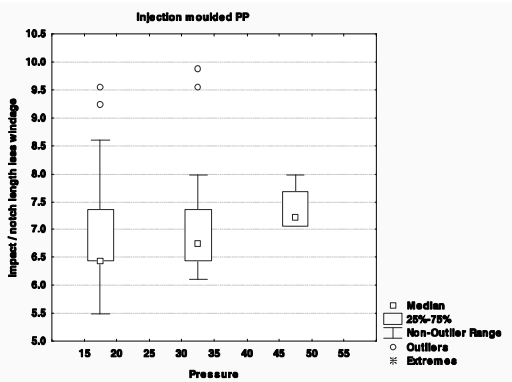
Injection moulded PP
Impact / notch length less windage
Pressure
Median
25%-75%
Non-Outlier Range
Outliers
Extremes

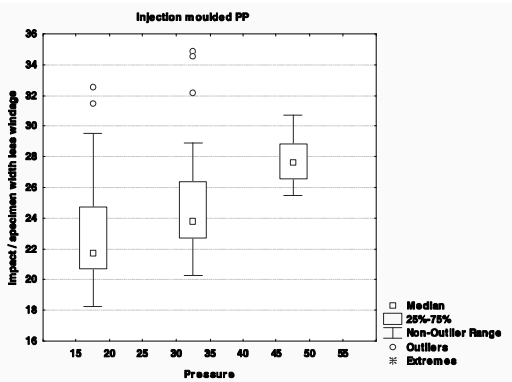
Injection moulded PP
Impact / specimen width less windage
Pressure
Median
25%-75%
Non-Outlier Range
Outliers
Extremes

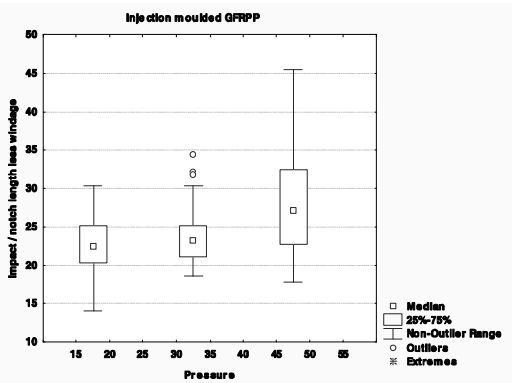
Injection moulded GFRPP
Impact / notch length less windage
Pressure
Median
25%-75%
Non-Outlier Range
Outliers
Extremes

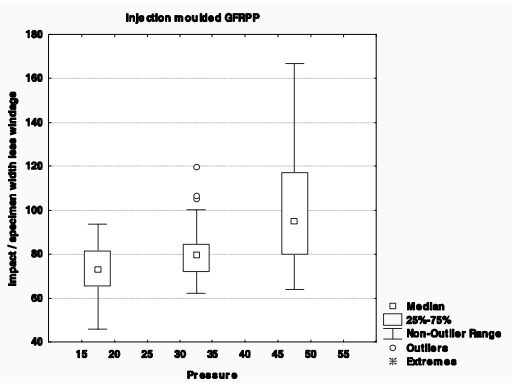
Injection moulded GFRPP
Impact / specimen width less windage
Pressure
Median
25%-75%
Non-Outlier Range
Outliers
Extremes

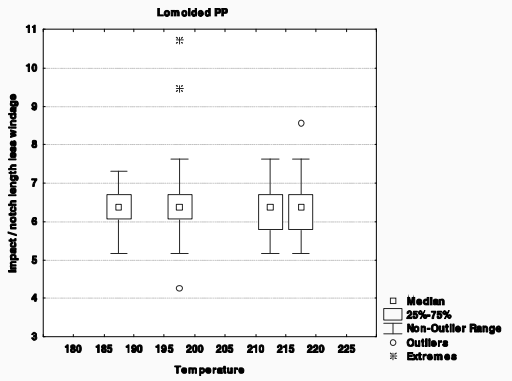
Lomolded PP
Impact / notch length less windage
Temperature
Median
25%-75%
Non-Outlier Range
Outliers
Extremes

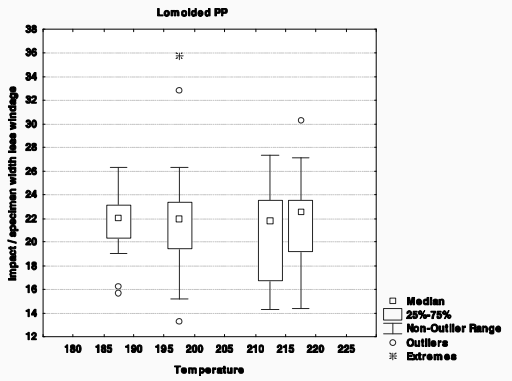
Lomolded PP
Impact / specimen width less windage
Temperature
Median
25%-75%
Non-Outlier Range
Outliers
Extremes

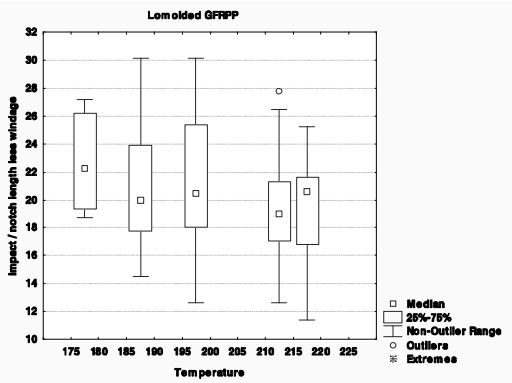
Lomolded GFRPP
Impact / notch length less windage
Temperature
Median
25%-75%
Non-Outlier Range
Outliers
Extremes

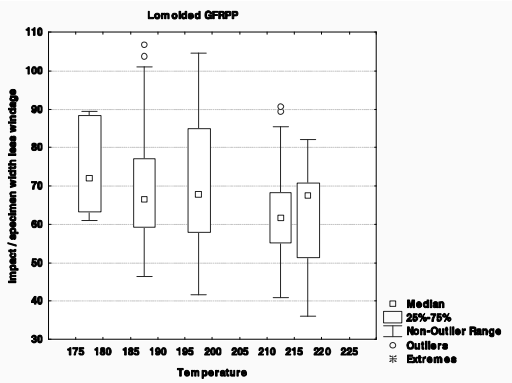
Lomolded GFRPP
Impact / specimen width less windage
Temperature
Median
25%-75%
Non-Outlier Range
Outliers
Extremes

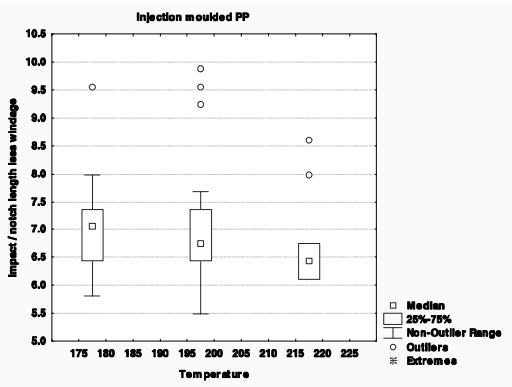
Injection moulded PP
Impact / notch length less windage
Temperature
Median
25%-75%
Non-Outlier Range
Outliers
Extremes

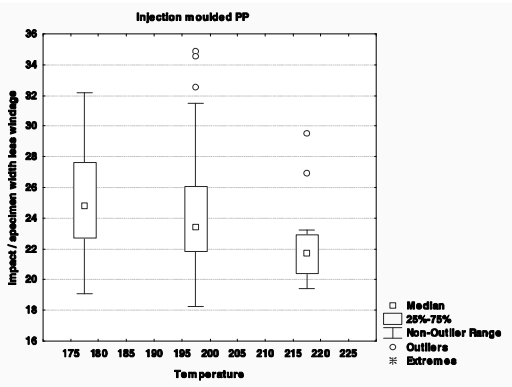
Injection moulded PP
Impact / specimen width less windage
Temperature
Median
25%-75%
Non-Outlier Range
Outliers
Extremes

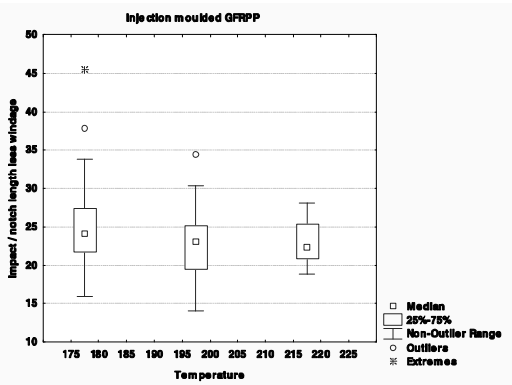
Injection moulded GFRPP
Impact / notch length less windage
Temperature
Median
25%-75%
Non-Outlier Range
Outliers
Extremes

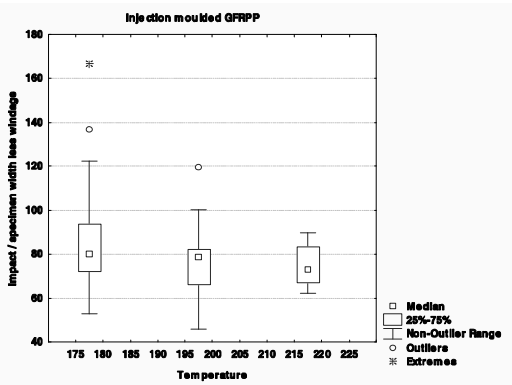
Injection moulded GFRPP
Impact / specimen width less windage
Temperature
Median
25%-75%
Non-Outlier Range
Outliers
Extremes

Appendix D4: Specimen warpage

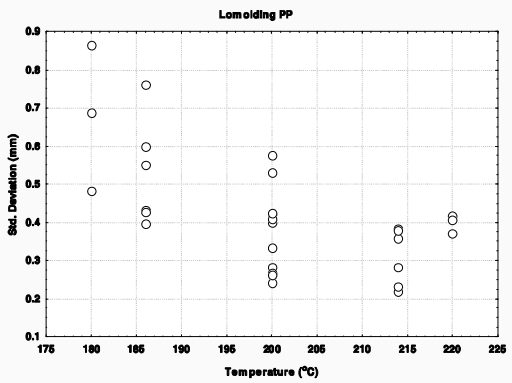

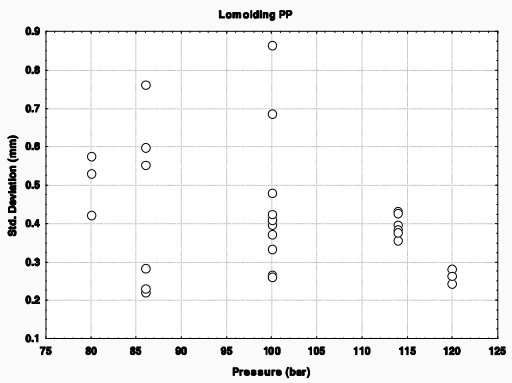

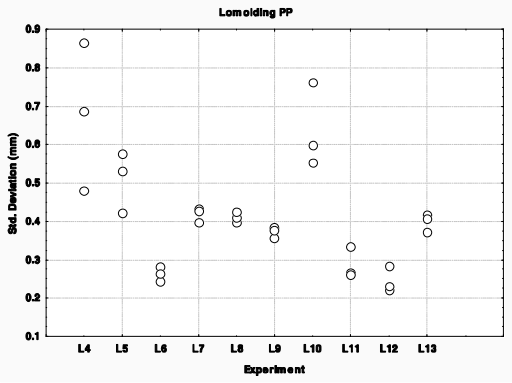

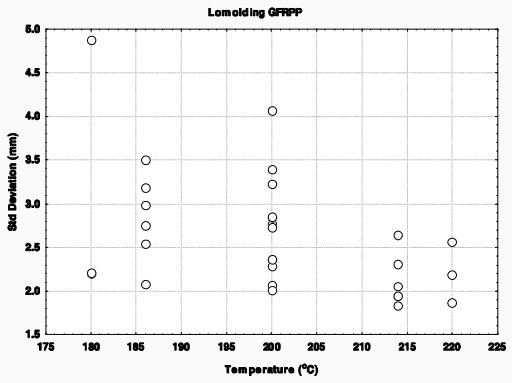

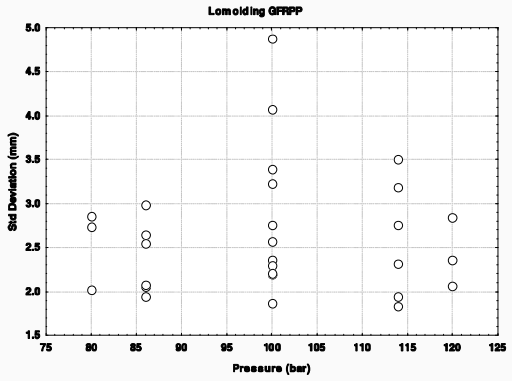

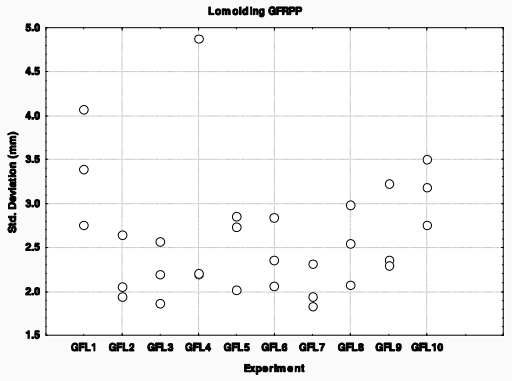

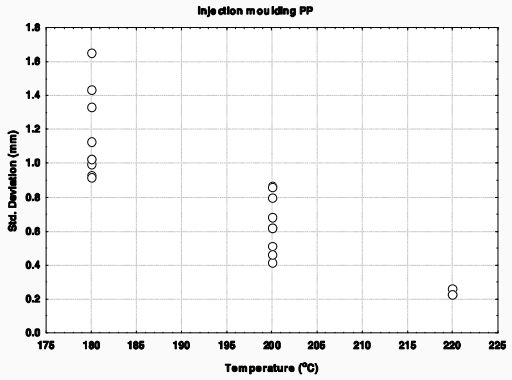

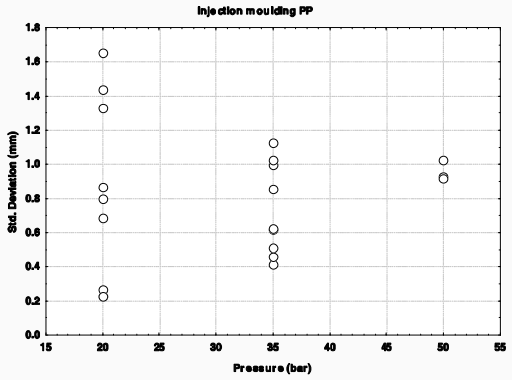

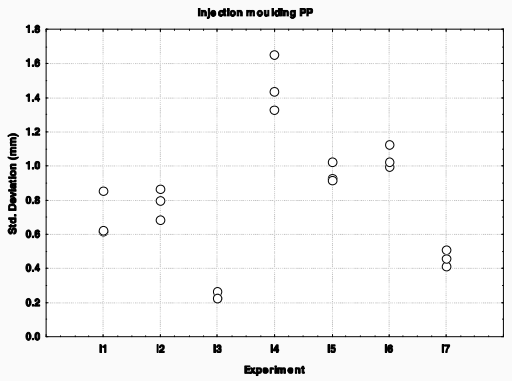
Injection moulding PP
Std. Deviation (mm)
Experiment
I1
I2
I3
I4
I5
I6
I7

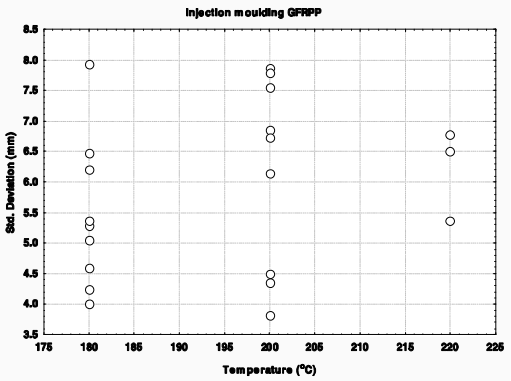
Injection moulding GFRPP
Std. Deviation (mm)
Temperature (°C)

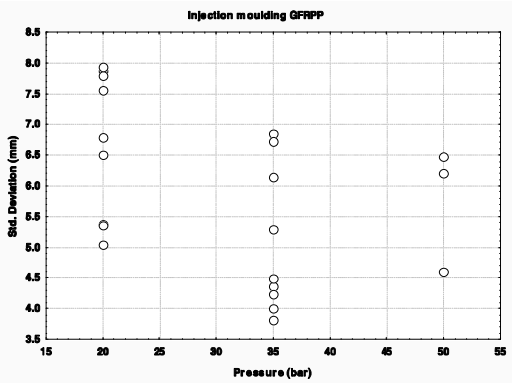
Injection moulding GFRPP
Std. Deviation (mm)
Pressure (bar)

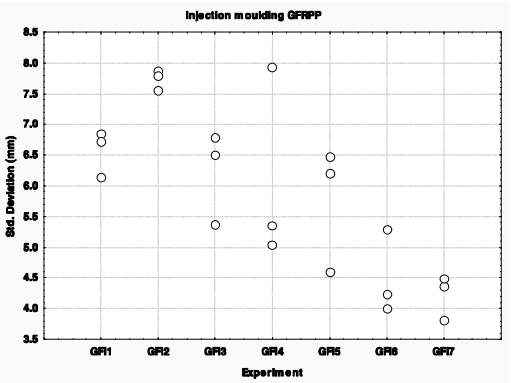
Injection moulding GFRPP
Std. Deviation (mm)
Experiment
GFI1
GFI2
GFI3
GFI4
GFI5
GFI6
GFI7

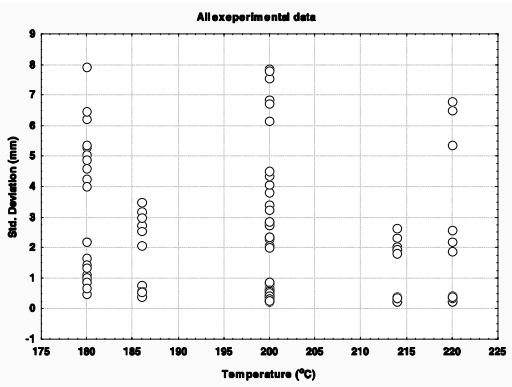
All exeperimental data
Std. Deviation (mm)
Temperature (°C)

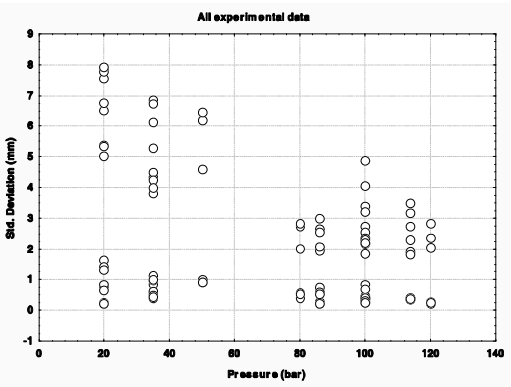
All experimental data
Std. Deviation (mm)
Pressure (bar)

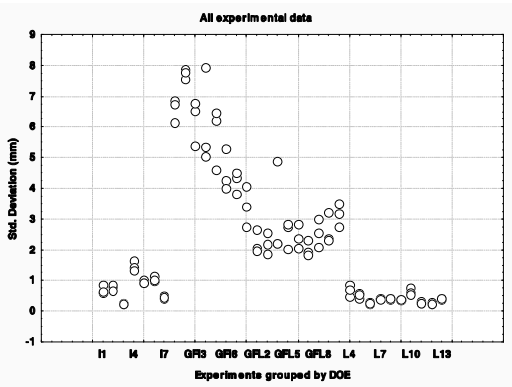
All experimental data
Std. Deviation (mm)
Experiments grouped by DOE
I1
I4
I7
GFI3
GFI6
GFL2
GFL5
GFL8
L4
L7
L10
L13

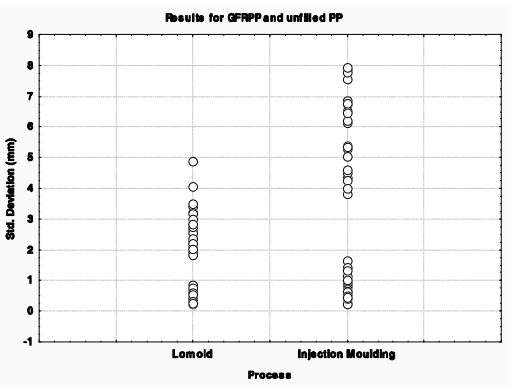
Results for GFRPP and unfilled PP
Std. Deviation (mm)
Process
Lomold
Injection Moulding

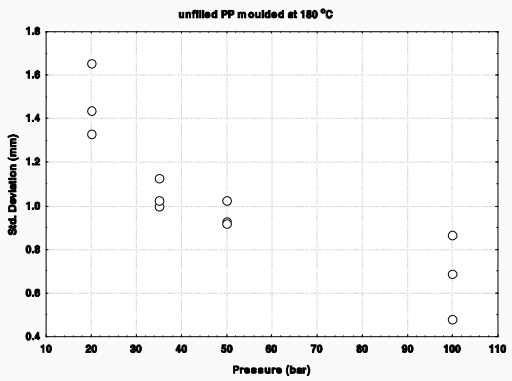
unfilled PP moulded at 180 °C
Std. Deviation (mm)
Pressure (bar)

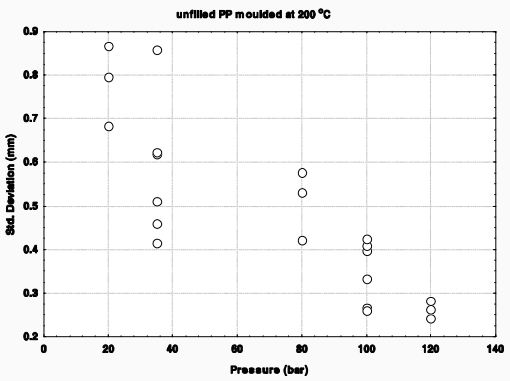
unfilled PP moulded at 200 °C
Std. Deviation (mm)
Pressure (bar)

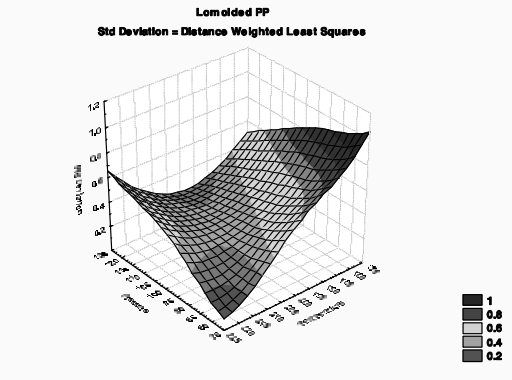
Lomolded PP
Std Deviation = Distance Weighted Least Squares
Pressure
Temperature

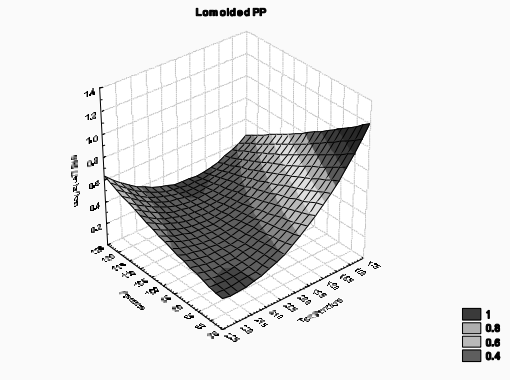
Lomolded PP
Pressure
Temperature

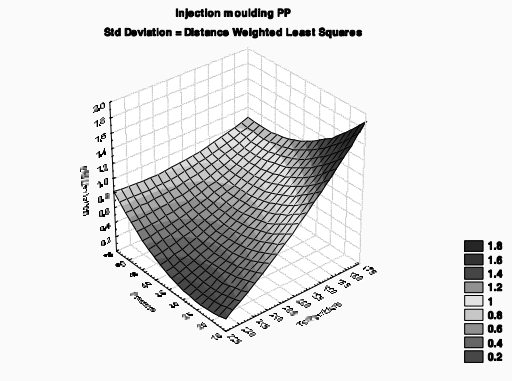
Injection moulding PP
Std Deviation = Distance Weighted Least Squares
Pressure
Temperature

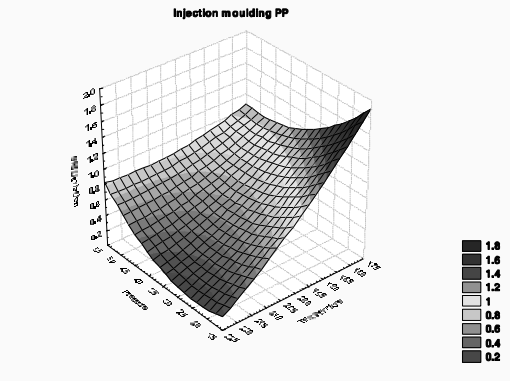
Injection moulding PP
Pressure
Temperature

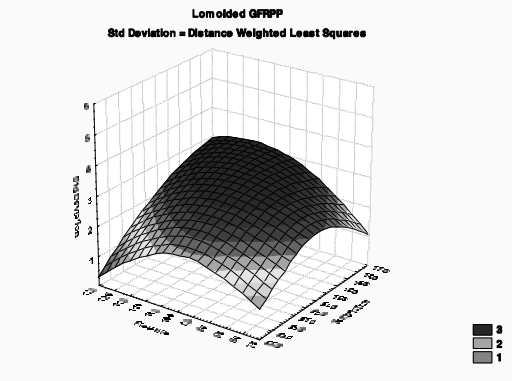
Lomolded GFRPP
Std Deviation = Distance Weighted Least Squares
Pressure
Temperature

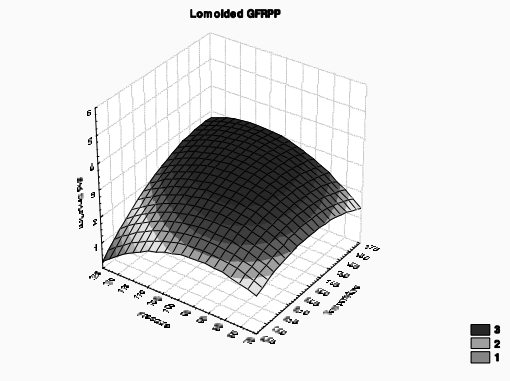
Lomolded GFRPP
Pressure
Temperature

Radii of curvature for injection moulded components

Board Number	Y1 (L) @ X=30.78	Y2 (L) @ X=150.20	Y3 (L) @ X=269.27	(1/R (L)) Exp 8	Y1 (W) @ X=37.86	Y2 (W) @ Y=86.36	Y3 (W) @ X=171.48	(1/R (W)) Exp 8
GFI1-2	26.02	21.85	25.34	**849**	13.22	19.16	26.10	**14926**
GFI1-15	26.03	22.03	25.47	**801**	14.44	19.69	25.65	**11367**
GFI1-22	25.87	21.76	25.42	**877**	13.54	19.17	25.71	**13363**
GFI2-16	23.43	27.08	23.87	**700**	19.87	23.89	35.83	**16734**
GFI2-19	24.91	26.10	24.02	**146**	19.59	23.30	33.31	**13088**
GFI2-20	24.19	25.09	24.19	**48**	17.01	21.88	32.67	**18534**
GFI3-15	24.16	26.45	24.06	**325**	20.44	23.82	33.49	**11529**
GFI3-19	26.83	20.15	27.15	**2702**	24.11	22.01	14.70	**5596**
GFI3-23	26.07	18.57	27.87	**4014**	23.71	20.78	12.60	**8691**
GFI7-14	27.17	18.34	26.97	**4379**	14.19	17.62	17.01	**773**
GFI7-19	26.87	18.61	26.79	**3890**	13.69	17.50	18.14	**898**
GFI7-23	27.02	19.86	26.38	**2692**	15.61	18.97	19.50	**662**
GFI6-12	27.13	18.28	27.33	**4600**	17.80	18.83	14.36	**1703**
GFI6-18	26.98	18.20	27.25	**4558**	16.31	18.23	15.82	**1697**
GFI6-25	26.68	18.90	26.52	**3418**	12.74	17.36	19.77	**4087**
GFI5-16	26.67	20.16	26.17	**2259**	12.64	17.98	22.74	**9267**
GFI5-21	25.88	22.85	25.43	**457**	15.03	20.20	27.27	**13198**
GFI5-22	25.16	23.42	25.47	**210**	18.04	21.54	26.99	**6895**
GFI4-14	22.53	29.26	23.58	**2305**	27.33	27.47	36.77	**443**
GFI4-18	21.95	28.31	23.42	**1869**	22.54	25.21	38.28	**11956**
GFI4-25	21.73	29.09	23.67	**2408**	26.99	27.13	37.16	**469**
I3-22	25.06	24.85	25.51	**8**	25.59	25.00	25.39	**81**
I3-26	25.22	24.77	25.52	**20**	25.31	24.91	25.25	**50**
I3-30	25.03	25.17	25.42	**2**	25.84	25.28	25.82	**108**
I2-15	25.00	26.45	25.12	**114**	27.20	26.53	27.53	**242**
I2-20	24.92	26.56	25.08	**145**	27.51	26.69	27.56	**255**
I2-26	25.09	26.23	25.14	**73**	26.93	26.32	27.23	**198**
I1-15	25.11	26.39	25.18	**92**	26.63	26.32	26.94	**69**
I1-22	25.05	26.59	25.06	**140**	26.39	24.43	27.48	**2101**
I1-25	25.13	26.29	25.30	**68**	26.79	26.36	26.44	**12**
I7-19	25.24	26.04	25.26	**38**	25.94	25.96	26.40	**3**
I7-21	25.32	25.96	25.29	**25**	25.38	25.74	26.45	**91**
I7-25	25.27	26.12	25.25	**43**	26.12	26.09	26.33	**3**
I5-21	25.92	27.35	25.39	**166**	27.89	27.53	27.07	**61**
I5-22	25.87	27.24	25.37	**153**	27.62	27.36	27.23	**12**
I5-27	25.84	27.20	25.35	**151**	27.65	27.26	27.29	**3**
I6-23	25.43	27.32	24.92	**269**	27.11	27.22	27.74	**19**
I6-24	25.56	27.24	25.05	**218**	27.06	27.20	27.19	**1**
I6-29	25.57	27.24	25.00	**223**	27.15	27.16	27.37	**1**
I4-24	24.74	27.80	24.54	**596**	27.32	27.40	29.34	**56**
I4-29	24.62	27.72	24.71	**558**	28.21	27.65	28.76	**221**
I4-30	24.61	27.37	24.71	**437**	27.81	27.24	28.70	**301**

Radii of curvature for lomolded polyproplene

Board Number	Y1 (L) @ X=30.78	Y2 (L) @ X=150.20	Y3 (L) @ X=269.27	(1/R (L)) Exp 8	Y1 (W) @ X=37.86	Y2 (W) @ Y=86.36	Y3 (W) @ X=171.48	(1/R (W)) Exp 8
L4-12	25.50	25.47	25.03	**1**	26.31	25.55	25.50	**13**
L4-28	25.53	27.06	24.85	**202**	26.62	27.06	26.31	**120**
L4-26	25.52	26.15	24.87	**48**	26.52	26.07	26.33	**43**
L5-27	25.47	26.14	25.06	**43**	26.33	26.27	25.38	**21**
L5-22	25.45	25.73	25.11	**10**	25.92	25.81	25.20	**24**
L5-19	25.39	26.02	25.07	**35**	26.26	26.12	25.19	**47**
L6-28	25.52	25.45	25.21	**1**	25.81	25.44	25.42	**3**
L6-22	25.54	25.19	25.25	**1**	25.54	25.11	25.31	**31**
L6-17	25.51	24.99	25.24	**8**	25.53	24.93	25.22	**63**
L7-23	25.50	25.63	25.10	**4**	26.28	25.62	25.61	**1**
L7-19	25.48	25.65	25.12	**5**	26.20	25.68	25.55	**24**
L7-15	25.52	25.62	25.11	**3**	26.12	25.65	25.49	**27**
L12-24	25.41	24.99	25.14	**4**	25.49	24.96	25.02	**12**
L12-19	25.41	25.01	25.22	**5**	25.44	24.92	25.07	**29**
L12-17	25.38	24.84	25.23	**12**	25.38	24.81	25.00	**40**
L13-13	25.40	24.31	25.30	**63**	25.01	24.19	25.00	**241**
L13-23	25.35	24.18	25.30	**77**	24.88	24.02	25.02	**312**
L13-30	25.34	24.26	25.32	**68**	25.06	24.06	25.18	**398**
L8-14	25.55	25.59	25.19	**1**	26.05	25.66	25.15	**72**
L8-19	25.47	25.75	25.17	**10**	26.04	25.81	25.27	**43**
L8-27	25.49	25.62	25.17	**3**	26.09	25.68	25.30	**56**
L9-26	25.39	24.30	25.32	**66**	25.49	24.32	24.96	**271**
L9-23	25.37	24.34	25.31	**58**	25.34	24.31	24.98	**248**
L9-17	25.36	24.29	25.32	**65**	25.29	24.21	25.02	**315**
L10-27	25.53	26.84	24.96	**147**	26.38	26.76	26.04	**98**
L10-20	25.52	26.34	25.04	**62**	26.13	26.28	25.60	**39**
L10-14	25.51	26.18	25.07	**45**	26.12	26.15	25.48	**7**
L11-27	25.48	25.35	25.17	**1**	25.76	25.30	25.34	**7**
L11-24	25.43	25.30	25.20	**1**	25.60	25.24	25.38	**18**
L11-18	25.52	25.39	25.21	**1**	25.56	25.26	25.22	**4**

Radii of curvature for lomolded GFRPP

Board Number	Y1 (L) @ X=30.78	Y2 (L) @ X=150.20	Y3 (L) @ X=269.27	(1/R (L)) Exp 8	Y1 (W) @ X=37.86	Y2 (W) @ Y=86.36	Y3 (W) @ X=171.48	(1/R (W)) Exp 8
GFL1-18	22.67	27.75	23.92	**1169**	27.94	26.83	32.52	**2205**
GFL1-17	23.08	27.59	23.82	**1017**	26.19	25.99	33.76	**546**
GFL1-26	22.87	27.67	23.63	**1164**	25.87	25.65	34.98	**711**
GFL2-29	22.82	26.57	24.41	**484**	29.19	26.56	31.27	**4307**
GFL2-23	22.81	26.62	24.20	**551**	29.91	26.41	30.23	**4624**
GFL2-16	23.29	26.77	24.56	**458**	32.38	28.10	27.91	**289**
GFL3-16	22.94	25.60	24.41	**187**	30.13	26.01	29.56	**5042**
GFL3-21	22.85	26.91	24.11	**680**	26.99	25.76	32.20	**2760**
GFL9-16	22.60	27.70	24.24	**1059**	31.00	27.79	31.15	**3746**
GFL9-23	22.78	27.06	24.02	**780**	29.58	26.91	32.14	**4826**
GFL10-26	23.11	28.11	23.53	**1376**	27.57	26.78	34.07	**1978**
GFL10-21	22.65	27.59	24.05	**1047**	27.75	26.75	32.98	**2189**
GFL10-16	23.21	28.02	23.77	**1227**	26.72	26.68	33.22	**78**
GFL7-16	22.93	26.12	24.26	**351**	29.57	26.28	30.58	**4892**
GFL7-14	22.75	26.08	24.57	**299**	28.36	25.56	30.77	**5044**
GFL8-14	22.75	27.80	23.90	**1180**	29.02	27.20	32.46	**3326**
GFL8-29	22.73	26.88	24.43	**607**	30.31	27.16	29.59	**2661**
GFL8-23	22.68	27.61	23.90	**1095**	26.80	26.18	33.17	**1524**
GFL9-24	22.69	27.99	23.82	**1327**	27.77	26.80	33.39	**2205**
GFL6-23	23.00	26.77	24.34	**546**	30.45	26.69	30.54	**4997**
GFL6-17	23.10	27.82	23.86	**1123**	27.35	26.45	32.90	**2026**
GFL6-12	22.78	26.73	23.99	**646**	29.33	26.27	31.96	**6006**
GFL7-18	22.69	26.42	24.48	**432**	31.27	26.83	30.82	**6067**
GFL3-25	22.16	26.20	24.28	**462**	29.33	25.70	31.40	**7110**
GFL4-29	22.40	24.36	25.40	**120**	33.45	26.60	23.94	**6269**
GFL4-24	22.76	27.00	24.06	**744**	28.97	26.50	31.58	**4341**
GFL4-23	22.52	29.93	24.23	**2550**	28.98	26.65	31.58	**3991**
GFL5-25	22.35	26.56	24.18	**600**	28.13	25.63	30.82	**4513**
GFL5-21	22.93	26.80	24.06	**632**	26.67	25.54	32.93	**2887**
GFL5-20	22.88	26.49	23.99	**539**	26.80	25.35	31.63	**3166**